INTERIM SCIENTIFIC REPORT

on

DEVELOPMENT OF AN EVALUATION TECHNIQUE FOR STRAPDOWN GUIDANCE SYSTEMS

Submitted to

NATIONAL AERONAUTICS AND SPACE ADMINISTRATION
ELECTRONICS RESEARCH CENTER
Cambridge, Massachusetts

February 13, 1968

Contract No. NAS 12-550

E. F. Hitt
AUTHOR - E. F. HITT

F. G. Rea
AUTHOR - F. G. REA

BATTELLE MEMORIAL INSTITUTE
Columbus Laboratories
505 King Avenue
Columbus, Ohio 43201

FOREWORD

This interim scientific report presents the results of a nine month study conducted by Battelle Memorial Institute, Columbus Laboratories, for NASA/ Electronics Research Center, Contract NAS 12-550.

The objective of this study was to develop an evaluation technique for strapdown guidance system performance utilizing performance parameters generated by both testing and analysis of the inertial sensors and guidance computer and by system simulation. This objective was accomplished by as follows:

(1) A penalty function was defined which expresses a functional relationship between the system parameters describing reliability, power, weight, and accuracy.

(2) Techniques were developed to estimate the system parameters used in the penalty function.

(3) Digital computer programs were developed implementing the first and second items. These programs are used as the basis for (a) system performance evaluation, (b) system design aids, and (c) system trade studies.

(4) The computer programs developed were exercised on a Jupiter flyby mission performed with a specific vehicle strapdown guidance system.

(5) The digital computer program decks, test cases, and documentation were delivered and an ERC employee instructed in their use.

This volume presents a summary of the study results, detailed technical discussion, recommendations, and conclusions.

TABLE OF CONTENTS

TABLE OF CONTENTS (Continued)

TABLE OF CONTENTS (Continued)

TABLE OF CONTENTS (Continued)

LIST OF FIGURES

TABLE OF CONTENTS (Continued)

TABLE OF CONTENTS (Continued)

LIST OF SYMBOLS AND DEFINITIONS

C_3	Hyperbolic excess velocity squared
D_T	Target miss degrees-of-freedom
D_V	Midcourse correction velocity degrees-of-freedom
Ig	Midcourse correction system specific impulse times gravity
K_{DC}	Midcourse correction system constant weight
K_{DV}	Midcourse correction system tankage factor
K_{P1}	Power source constant weight (lbs)
K_{P2}	Power source variable weight (lbs/watt)
MTBF	Mean time between failures
MTTF	Mean time to failure
P_{FG}	Probability of mission failure attributable to the guidance
P_{FR}	Probability of failure attributable to hardware reliability
P_{FT}	Probability of failure attributable to target miss
P_{FTR}	Probability of failure attributable to hardware reliability or target target miss
P_{FV}	Probability of failure attributable to insufficient midcourse fuel
R_V	The square root of the trace of the midcourse correction velocity covariance matrix
R_T	The square root of the trace of the target miss covariance matrix
W_{DV}	Midcourse correction system weight
W_F	Midcourse correction system fuel weight
W_{GS}	Combined guidance system weight
W_{ICP}	Inertial measurement unit + computer + electrical energy source weight
W_{NG}	Nonguidance spacecraft weight
W_P	Electrical energy source weight

LIST OF SYMBOLS AND DEFINITIONS (Continued)

W_T	Total spacecraft weight
V_∞	Hyperbolic excess velocity
ΔV	Midcourse correction velocity
μ	Spacecraft midcourse correction mass ratio
ψ_T	Allowed target miss distance divided by the square root of the trace of the target miss covariance matrix
ψ_V	Spacecraft delta-V capability divided by the square root of the trace of the midcourse correction velocity covariance matrix

DEVELOPMENT OF AN EVALUATION TECHNIQUE FOR STRAPDOWN GUIDANCE SYSTEMS

By Ellis F. Hitt and F. G. Rea

BATTELLE MEMORIAL INSTITUTE
Columbus Laboratories
Columbus, Ohio 43201

INTRODUCTION

This report presents the results of a nine-month study on "Development of an Evaluation Technique for Strapdown Guidance Systems" for future NASA unmanned interplanetary probe missions, conducted by Battelle Memorial Institute for NASA/Electronics Research Center. This volume presents a summary of the study results, detailed technical discussion, recommendations, and conclusions.

Study Objectives

The overall objective of this study was to develop an evaluation technique for automated interplanetary probe mission strapdown guidance systems. This technique was to be designed to provide a measure or index of guidance system performance for this class of missions. The technique was to utilize system parameters describing the reliability, power, weight, and accuracy. In addition, techniques were to be developed to estimate the system parameters using analytical methods as well as available test data.

Summary of Study Elements

To accomplish the study objectives, the project was carried out in the following five major steps:

(1) A system performance index or penalty function was defined which expresses a functional relation between system parameters describing the reliability, power, weight, and accuracy. In performance of this task, consideration was given to existing "cost-effectiveness" models.

(2) Techniques were developed to estimate the system parameters used in the system performance index. These techniques use analytical methods as well as available test data as the basis of the estimates.

(3) Digital computer programs were developed which:

(a) Calculate the system penalty given the system parameters, or select a quasi-optimum system configuration from various subsystem alternatives.

(b) Calculate estimates of the system parameters for use in determining the system penalty.

(4) A boost trajectory for the conceptual 260(3.7)/SIVB/Centaur I/Kick launch vehicle was generated for a Jupiter flyby mission. The interplanetary trajectory and state transition matrices were generated with the Lewis Research Center n-body program. The ERC Strapdown Error Analysis Program (SEAP) was used with the boost trajectory data to generate the inertial sensor error sensitivity coefficients. The computer programs developed under the previous step were exercised on the Jupiter flyby mission for a NASA/ERC specified guidance system.

(5) The digital computer program decks, test cases, and documentation were delivered and a NASA/ERC employee was instructed in the use of these programs.

Major Assumptions for Exercising the Programs

It was necessary to assume specific mission, launch vehicle, spacecraft, inertial sensors, strapdown guidance computers, and other data required for exercising the computer programs developed under this study.

Mission and Spacecraft.--The mission used in exercising of the computer programs was a Jupiter flyby mission with launch to occur during 1972. This mission, or variations, thereof has been studied previously (References 1,2, 3, and 4).

The midcourse propulsion system was assumed to be a gas-pressure-regulated monopropellant hydrazine unit using a Shell 405-type catalyst (Reference 1).

Guidance system electrical power was assumed to be supplied by a RTG (radioisotope thermoelectric generator)(References 1 and 2).

Perfect update of velocity, position, and attitude were assumed to occur during the parking orbit. Hence, the boost analysis considers errors during the burn from the parking orbit to the final velocity as the only contributors to injection errors.

Prior to the midcourse correction, an attitude update was assumed with a 10 arc second uncertainty about each of the principal axes. Error in the midcourse correction magnitude was assumed to be solely attributable to the roll axis accelerometer.

Launch Vehicle.--For the purpose of exercising the computer programs, the conceptual 260(3.7)/SIVB Centaur I/Kick launch vehicle was assumed to be suitable for this mission. Data on this conceptual vehicle are contained in the subsequent section of this report describing the boost trajectory. Guidance and navigation of this vehicle were assumed to be under control of the strapdown guidance system located above the Kick stage. It was assumed that the weight of the strapdown guidance system was included in the final payload weight injected on the escape trajectory.

Candidate Components.--The major portion of the data assumed for candidate gyroscopes and accelerometers was based on manufacturers' data and government agency test reports. Reliabilities for the inertial sensors and computers were assumed for purposes of exercising the computer programs, and thus, results involving these data should not be considered conclusive.

Weight and power for the conceptual SRT computer (an assumed computer for the specified system A) were estimated using simple techniques described in a subsequent section of this report.

SUMMARY

An evaluation technique for strapdown guidance systems designed for unmanned interplanetary missions has been developed. This technique provides a measure of system performance on each mission being examined. In addition, the technique is useful in evaluation of competitive systems, as an aid in preliminary design of conceptual systems, and for determination of research needed to improve system performance.

Cost-effectiveness for the problem is defined with cost equal to the weight of the guidance system and effectiveness equal to the probability of the guidance system operating correctly. Weight is defined to be the sum of the weights of the inertial measurement unit (IMU), computer, midcourse correction propulsion system, and guidance electrical energy source. The effectiveness probability is defined to be the appropriate combination of the probabilities of failure due to guidance system unreliability, failure due to insufficient midcourse fuel, and failure due to missing the target by more than a prescribed distance. Using this cost-(or weight-)effectiveness model, several penalty functions have been developed. These may be broken into two categories: those which hold effectiveness or probability constant and consider weight as the penalty and those which hold weight constant and consider the ineffectiveness or probability of failure as a penalty. This eliminates dollar cost as a parameter but combines power, reliability, and accuracy by considering their effects on total guidance system weight. These penalty functions provide meaningful and useful information.

Penalty Functions

Three different penalty functions were developed. The need for three penalty functions (indicated by three modes) became apparent when "real world"

launch vehicle and mission considerations were investigated. The three modes are as follows:

Mode 1: The probability of mission failure due to lack of guidance reliability and accuracy (P_{FG}) is a user specified constant. Another user specified constant is all nonguidance weight (W_{NG}). The penalty function is the combined guidance system weight (W_{GS}) which consists of the sum of guidance system hardware weight plus electrical power source weight (W_{ICP}) and midcourse propulsion system weight (W_{DV}). An increase in the combined guidance system weight necessary to assure a given influence, by the guidance system, on probability of mission success is reflected in an increased launch weight (W_T).

Mode 2: The total launch weight, equal to the sum of the nonguidance weight plus the combined guidance system weight, is a user specified constant. In addition, the nonguidance weight is specified as is the combined guidance system weight. Any decrease in guidance system hardware or power source weight is offset with an increase in midcourse propulsion system weight or vice-versa. The probability of mission failure due to lack of reliability or accuracy is the penalty function.

Mode 3: The third mode involves user specified total launch weight and probability of mission failure due to lack of guidance reliability and accuracy. The combined guidance system weight is the penalty function. In this mode the nonguidance weight (useful payload) is the difference between the launch weight and combined guidance system weight. Thus, for increasing W_{GS}, W_{NG} is reduced.

The three penalty functions are shown in Table I for comparison.

TABLE I
THREE PENALTY FUNCTIONS FOR
EVALUATION OF STRAPDOWN GUIDANCE SYSTEMS*

Mode	W_T	W_{NG}	W_{GS}	P_{FG}	Remarks
1	V	F	P	F	Fixed Nonguidance Weight and Probability of Guidance Failure
2	F	F	F	P	Fixed Total Weight and Guidance System Weight
3	F	V	P	F	Fixed Total Weight and Probability of Guidance Failure

* V$\triangleq$ Variable with System
F$\triangleq$ Constant
P$\triangleq$ Penalty Function

For each of the modes, the minimum value of the penalty function defines the best system.

Sensitivity of each penalty function with respect to specific system hardware parameters is expressed as the percent change in penalty per percent change in data. These sensitivities allow easy determination of the system parameters and components which affect the penalty function most directly (large sensitivity magnitude). The algebraic sign indicates which direction the penalty changes for an increase in the system parameter. Further explanation of the penalty functions and sensitivities is contained in the technical discussion section of this report.

System Parameters Estimation

The strapdown inertial measurement unit (IMU)(also referred to as the inertial sensing unit (ISU)) weight is estimated by evaluating analytic expressions approximating the design of an IMU. Nine designs, of which any six are evaluated in the computer subroutine MECHDS, have been described analytically for the case where the base of the IMU is mounted horizontally in the vehicle. Similarly, six designs have been developed for the case where the base of the IMU is mounted vertically in the vehicle. The current designs and their analytic expressions are described further in the technical discussion section of this report. Other designs for which analytical expressions can be developed may be added to or substituted for designs now in the program.

The strapdown inertial guidance system (IGS) computer weight can be estimated should such an estimate be required. The recommended means of doing this requires input of specific values for the weights of each module of the computer. This assumes the computer would be assembled from trays containing these modules. The weight factors contained in the technical discussion section of this report were estimated based upon a computer organized in a modular fashion in which the tray structure of the modules is assumed to form four sides of the computer case. Since this technique is quite simple and the computer requirements vary little from one strapdown IMU to another for the same interplanetary mission, a computer subroutine was not written to calculate the IGS computer weight.

Estimation of the system power requirements is dependent upon the thermal design of the IMU as well as the IGS computer. The primary concern in thermal control of the IMU should be to minimize the total system power required. The IMU power is estimated by solution of heat transfer equations presented in the technical discussion following this summary. Since many possible tradeoffs exist in thermal control of the IMU, this should by no means be considered as other than a tool for estimating the IMU power.

Computer prime power can be estimated by summation of the estimated power required by the input/output (I/O), memory, and processor modules and division of this summation by the efficiency of the proposed computer power supply. Since the I/O module power depends upon the electrical interfaces of the IMU, telemetry, etc. with the computer, precise power estimates cannot be made until

this information is available. Therefore, a subroutine to calculate computer power was not written.

System reliability is predicted assuming there are no redundant components. Several possible reliability descriptions were examined. The Weibull distribution was chosen to allow more realistic estimation of failure probabilities without the large amounts of data needed for more complex distributions such as the Markovian. The Weibull distribution contains the more commonly used exponential model if the exponent α is set equal to one. The mean time to failure (MTTF) and α are input data for the candidate gyroscopes, accelerometers, and computers. The mean times between failure (MTBF) are input data for the guidance electrical power source and IMU electronics. The probability of failure of the midcourse propulsion system to ignite is also input data. Using these data, the program calculates the reliability of the strapdown guidance system.

Computer Programs

The calculation of the three penalty functions and the necessary estimation of the system parameters have been coded into a deck of FORTRAN subroutines. The subroutines, with a short, simple, main program calculate the necessary system parameters and evaluate them according to the specified penalty function.

Data needed to run the program are divided into four categories. The first three involve data describing the mission and spacecraft and include: (1) injection error sensitivities as computed by the Strapdown Error Analysis Program (SEAP); (2) state transition matrices generated by the n-body program; and (3) data describing mission values, IMU design values, and spacecraft subsystems. The fourth category is data describing candidate components (accelerometers, gyroscopes, and computers) and includes: component (1) weight, (2) dimensions, (3) excitation power, (4) reliability, and (5) error coefficients. Computer data required is similar to that for gyros and accelerometers except that the number of bits used to store each element of the attitude matrix, attitude update integration frequency, and integration scheme (rectangular, Runge-Kutta second order, or Runge-Kutta fourth order) are used in the error determination.

The program and its subroutines operate in one of two ways. A specific set of candidate components may be evaluated, or, by a searching technique (similar to steepest descent), a combination of the candidate components may be found which yields the minimum penalty. Energy source and midcourse correction subsystems as well as the IMU block, base, and cover design are modelled internally. Options are provided to allow specification of the type of midcourse correction (zeroing all position or any one component of miss at the target), mechanical orientation (horizontal or vertical), mechanical configuration (one of the stored designs or the one yielding minimum weight), midcourse correction accuracy (specified or computed), and an option which indicates if the gyros and accelerometers must be identical or may be non-identical along the three axes when the searching technique is selected. After selection of the desired options and a set of candidate components, either arbitrarily or by the searching technique, all other system characteristics are calculated and the penalty obtained. The program output consists of a four-page report listing

the selected components and their data, mission and subsystem characteristics, and the penalty function value. In addition, normalized derivatives or sensitivities of the penalty to each piece of data is printed. This allows the designer to evaluate the relative importance of the data on the penalty function value. Furthermore, outputs in the form of tables or curves may be obtained to show the behavior of the penalty function as any piece of hardware or mission data is swept over a wide range of values.

Mission Characteristics

Launch Vehicle Characteristics.--The conceptual 260(3.7)/SIVB/Centaur I/Kick launch vehicle was assumed to be suitable for the Jupiter flyby mission. A version of this vehicle has been studied extensively (References 5 and 6) by Battelle Memorial Institute, NASA Launch Vehicle Planning Project under Contract NASw-1146. Selected characteristics of this vehicle are given in Table II. The 260(3.7) first stage is a solid propellant, single engine stage and is described in detail in Reference 7. The SIVB second stage is the same as the SIVB utilized by the Saturn IB and Saturn V launch vehicles. The Centaur I third stage is bas based on design evolution and concentrated development effort to employ hydrogen-flourine propellants (Reference 8). The "Kick" fourth stage is a small high energy stage originally proposed for use with the SLV3C and SLV3C/Centaur (Reference 8).

TABLE II
SELECTED CHARACTERISTICS OF 260(3.7)/SIVB/CENTAUR I/KICK LAUNCH VEHICLE

Stage	260(3.7)	SIVB	Centaur I	Kick
Initial Total Gross Weight (lb)*	4,019,302	315,303***	54,202	12,410
Final Total Gross Weight (lb)*	720,302	85,303	17,602	6,460
Vacuum Thrust (lb)	6,430,000**	205,000	31,000	7,500
Propellant Weight Flow (lb/sec)	24,300**	482	68.20	16.47
Exit Area (ft^2)	376	35.8	16.58	4.14

* All weights include 5,410 lb payload.
** Initial value only for time history, see Appendix A, Figure A-2.
*** Includes 5,600 lb shroud which is ejected 26 seconds after SIVB ignition.

This launch vehicle was simulated using the Battelle three-degree-of-freedom computer program. The simulated boost trajectory was used in the guidance error analysis. Further discussion of the launch vehicle simulation and boost trajectory are contained in Appendix A of this report.

Trajectory Characteristics.--The boost trajectory was assumed to start with a vertical rise from Cape Kennedy until a relative velocity of 150 ft/sec was attained. The vehicle was subjected to an instantaneous deflection of the flight path through a selected kick angle of 1.83 degrees from the vertical along an initial azimuth of 90 degrees from true north. The vehicle then flew a gravity turn until first stage burnout. A linear time dependent pitch steering profile was used to steer the second stage into a nearly circular 100 nm parking orbit. It was assumed that the SIVB stage was restarted at the correct time to begin the final injection phase of the launch trajectory.

Characteristics of the interplanetary trajectory are tabulated in Table III. The Lewis Research Center n-body computer program was modified to calculate n-body state transition matrices. The state transition matrices used in exercising of these computer programs were obtained by running the Lewis n-body program for the trajectory summarized in Table III. Further discussion of the interplanetary trajectory and state transition matrices is contained in a subsequent section of this report.

TABLE III
CHARACTERISTICS OF 1972 JUPITER FLYBY MISSION INTERPLANETARY TRAJECTORY

Launch date	March 4, 1972
Arrival date	April 18, 1973
Time of flight	410 days
Departure asymptote (from Earth)	
V_∞	12.195 km/sec
C_3	147.718 km^2/sec^2
Declination	-25.3 deg
Angle to Sun-Earth line	93.0 deg
Approach asymptote (to Jupiter)	
V_∞	17.53 km/sec
Declination to plane of Jupiter	1.64 deg
Angle to Jupiter-Sun line	153.2 deg
Interplanetary Orbit	
True anomaly at launch	-6 deg
True anomaly at arrival	129.3 deg
Heliocentric central angle	135.3 deg
Inclination to ecliptic	-0.57 deg
Perihelion	0.989 AU
Aphelion*	650 AU
Eccentricity**	0.972 - 0.976
Earth-Jupiter distance at encounter	7.67989×10^{11} meters

* Does not pass aphelion on way to Jupiter.
** Varies due to n-body effects.

Spacecraft.--The spacecraft weight derived from the reference trajectory is 5410 pounds. No assumptions about the spacecraft scientific payload or structure were made since these have been studied previously (References 1, 2, and 4). The midcourse propulsion system was assumed to be a monopropellant hydrazine unit using a Shell 405-type catalyst. The guidance system electrical power source was assumed to be part of the spacecraft total weight as was the midcourse propulsion system. The strapdown guidance system onboard the spacecraft was assumed to provide the primary guidance and control functions for all launch vehicle stages as well as the midcourse correction.

Guidance System A.--The strapdown guidance system being assembled in breadboard form at ERC was used in the exercising of the computer programs developed under this contract. This system is made up of the Honeywell GG 334A gyroscope (three units orthogonally mounted) and the Arma D4E accelerometer (three units orthogonally mounted) and is referred to as system A. Estimates of the weight of the conceptual IMU containing these instruments have been made. In addition, estimates of the characteristics of a conceptual computer, referred to as SRT, were made for purposes of exercising of the computer programs.

Mission Results Using System A

The computer programs developed as part of this study were exercised on the Jupiter flyby mission for the specified strapdown guidance system described in the foregoing section. Figure 1a presents the penalty for the mode being evaluated (mode 3 penalty is weight), lists descriptive information about the launch vehicle and mission, and presents the hardware data for each instrument used in the IMU. In addition, data describing the conceptual SRT computer are presented. The notation RUK - 2 denotes that a Runge-Kutta second order algorithm was used to update the direction cosine matrix.

Figure 1b presents the results of the penalty function and the estimation techniques incorporated in the program. For example, all horizontal designs were evaluated and design number 4 was found to be optimum (yielding minimum weight). The dimensions of the case of the IMU containing the inertial sensors are presented for that design. In addition, the calculated weights of the block, base, cover, and insulation are presented. The electronics weight was a specified value. The components weight is the summation of the weights of the inertial sensors and computer. The total estimated weight for the system A IMU and computer is calculated to be 69.46 pounds for IMU design 4.

The thermal analysis presented indicates that the thermal conductance for the IMU was calculated to be 2.17 watts/^{o}F on the basis that no heater power or cooling was to be required at the maximum ambient temperature. The peak watts listed are the total power (IMU plus computer) required at the minimum ambient temperature for the calculated thermal conductance. The average watts listed are the total power required at the average ambient temperature. The energy source weight is the weight of the radioisotope thermoelectric generator (RTG) needed to supply the average power required. This assumes that the peak power is required for a short time and would be drawn from a small secondary energy source as well as the RTG.

PENALTY(MODE 3)= 222.03808 PAGE 1

ZERO OR POS. ERRORS AT TARGET 260/S-IVB/CENTAUR-I/KICK JUPITER FLY BY
WITH MID COURSE AT 25.0 HOURS ZERO ALL ERRORS BEFORE SECOND BURN

HARDWARE DATA (ARBITRARY)

ACCELEROMETERS	WEIGHT	POWER	MTTF	ALPHA	LENGTH	DIAMETER	WIDTH	AXIS
ARMA D-4E	.35	1.50	100000.00	1.00	1.30	2.70	-0.00	YAW
CONSTANT	67.00E-07	10.00E-06	90.00E-08	10.00E-08	-0.	-0.	56.00E-07	56.00E-07	20.00E+00	20.00E+00
PER DEG-F	-0.	-0.	-0.	-0.	-0.	-0.	-0.	-0.	-0.	-0.
	K0	K1	K2	K3	M0	N0	M1	N1	IP	IN
	G	G/G	G/G**2	G/G**3	G/G	G/G	G/G**2	G/G**2	ARC SEC	ARC SEC
ARMA D-4E	.35	1.50	100000.00	1.00	1.30	2.70	-0.00	PITCH
CONSTANT	67.00E-07	10.00E-06	90.00E-08	10.00E-08	-0.	-0.	56.00E-07	56.00E-07	20.00E+00	20.00E+00
PER DEG-F	-0.	-0.	-0.	-0.	-0.	-0.	-0.	-0.	-0.	-0.
	K0	K1	K2	K3	M0	N0	M1	N1	IP	IN
	G	G/G	G/G**2	G/G**3	G/G	G/G	G/G**2	G/G**2	ARC SEC	ARC SEC
ARMA D-4E	.35	1.50	100000.00	1.00	1.30	2.70	-0.00	ROLL
CONSTANT	67.00E-07	10.00E-06	90.00E-08	10.00E-08	-0.	-0.	56.00E-07	56.00E-07	20.00E+00	20.00E+00
PER DEG-F	-0.	-0.	-0.	-0.	-0.	-0.	-0.	-0.	-0.	-0.
	K0	K1	K2	K3	M0	N0	M1	N1	IP	IN
	G	G/G	G/G**2	G/G**3	G/G	G/G	G/G**2	G/G**2	ARC SEC	ARC SEC

GYROSCOPES	WEIGHT	POWER	MTTF	ALPHA	LENGTH	DIAMETER	WIDTH	AXIS
GG 334-A	1.65	3.00	25000.00	1.00	4.70	2.50	-0.00	YAW
CONSTANT	10.00E-02	15.00E-02	15.00E-02	40.00E-03	60.00E-01	70.00E-01	10.00E-05	-0.	-0.	-0.
PER DEG-F	-0.	-0.	-0.	-0.	-0.	-0.	-0.	-0.	-0.	-0.
	R	UI	US	S	IS	IO	T			
	DEG/HOUR	DEG/HR/G	DEG/HR/G	DEG/H/G**2	ARC-SEC	ARC-SEC	UNITY			
GG 334-A	1.65	3.00	25000.00	1.00	4.70	2.50	-0.00	PITCH
CONSTANT	10.00E-02	15.00E-02	15.00E-02	40.00E-03	60.00E-01	70.00E-01	10.00E-05	-0.	-0.	-0.
PER DEG-F	-0.	-0.	-0.	-0.	-0.	-0.	-0.	-0.	-0.	-0.
	R	UI	US	S	IS	IO	T			
	DEG/HOUR	DEG/HR/G	DEG/HR/G	DEG/H/G**2	ARC-SEC	ARC-SEC	UNITY			
GG 334-A	1.65	3.00	25000.00	1.00	4.70	2.50	-0.00	ROLL
CONSTANT	10.00E-02	15.00E-02	15.00E-02	40.00E-03	60.00E-01	70.00E-01	10.00E-05	-0.	-0.	-0.
PER DEG-F	-0.	-0.	-0.	-0.	-0.	-0.	-0.	-0.	-0.	-0.
	R	UI	US	S	IS	IO	T			
	DEG/HOUR	DEG/HR/G	DEG/HR/G	DEG/H/G**2	ARC-SEC	ARC-SEC	UNITY			

COMPUTER	WEIGHT	POWER	MTTF	ALPHA	BITS	COMP.FREQ.	INT.SCH.
SRT RUK-2	36.00	90.00	6000.00	1.00	32	128	2

FIGURE 1a. PENALTY, MODE 3, REPORT ON SYSTEM A

IMU MECHANICAL DATA(HORIZONTAL DESIGN NUMBER 4 OPTIMUM) PAGE 2

OUTSIDE DIMENSIONS		WEIGHT	
LENGTH=	9.35000	BLOCK=	8.70314
WIDTH=	10.45000	BASE=	4.54869
HEIGHT=	5.45000	COVER=	2.86681
		INSULATION=	1.34474
		ELECTRONICS=	10.00000
		COMPONENTS=	42.00000

TOTAL(IMU+COMPUTER)WEIGHT= 69.46339

THERMAL ANALYSIS

AVERAGE WATTS = 307.5 MIN.HEATER WATTS = -.0
PEAK WATTS = 372.7 THERMAL COND. = 2.17(W/D-F)

ENERGY SOURCE WEIGHT= 119.28750

ERROR ANALYSIS

		DR	CR	OP	RMS	DOF
INJECTION	POSITION	41.9901E+01	29.7034E+02	27.1399E+02	40.4537E+02	1.992334
	VELOCITY	39.5908E-02	81.8120E-01	73.8946E-01	11.0315E+00	1.984135
	ATTITUDE	78.3763E-05	46.1650E-05	46.1627E-05	10.2005E-04	2.276002
MID COURSE	POSITION	13.8155E+04	85.1262E+04	61.2611E+04	10.5784E+05	1.680602
	VELOCITY	15.8048E-01	96.1112E-01	68.3294E-01	11.8979E+00	1.658041
	ATTITUDE	43.7641E-03	42.8659E-03	42.8547E-03	74.7616E-03	2.998805
CORRECTION DELTA VEL.		43.0115E-01	81.9120E-01	26.6370E-01	96.2761E-01	1.000000
AT TARGET						
NO MID COR	POSITION	42.9655E+06	11.6450E+08	10.2767E+07	11.6982E+08	1.007496
	VELOCITY	10.3071E+02	16.2465E+02	20.5677E+03	20.6575E+03	1.008347
PERFECT MC	POSITION	60.2516E+06	32.8081E-07	71.4959E+06	93.4982E+06	1.937559
	VELOCITY	58.2382E+01	15.0162E+02	93.7736E+01	18.6370E+02	1.210988
IMPERFECT	POSITION	60.2524E+06	84.3593E+04	71.4965E+06	93.5030E+06	1.937878
	VELOCITY	58.2419E+01	15.0163E+02	93.7866E+01	18.6378E+02	1.211131

MIDCOURSE SYSTEM

RELATIVE ACCURACY		WEIGHT			
MAGNITUDE=	.00072442	FUEL=	11.84962	DELTA-V CAPABILITY=	16.45111
ANGLE=	.00291000	TANKAGE=	1.13756	EXPECTED BURN TIME=	32.35117
		CONSTANT=	20.30000		

TOTAL MIDCOURSE WEIGHT= 33.28719

PENALTY ANALYSIS

PROBABILITIES OF FAILURE		WEIGHT	
RELIABILITY=	.01308678	NON-GUIDANCE=	5187.96
SUFFICIENT FUEL=	.08806572	GUIDANCE=	222.04 (PENALTY)
MISS AT TARGET=0	.00000000		
SYSTEM=	.10000000 (FIXED)	TOTAL=	5410.00 (FIXED)

FIGURE 1b. PENALTY, MODE 3, REPORT ON SYSTEM A (Continued)

Figure 1b also presents the results of the navigation error analysis at various times along the trajectory. For instance, the velocity errors at injection are given in down range (DR), cross range (CR), and out of plane (OP) components. The root mean square (RMS) of these components is 11.03 ft/sec at injection with the degree of freedom (DOF) of 1.984. The injection errors propagated to the target with no midcourse correction are seen to result in a CR position error of 11.6450×10^8 ft. If a single perfect midcourse delta-velocity correction is made to null the CR position error, the correction delta-velocity required has an RMS value of 9.6276 ft/sec. If an imperfect midcourse is made with the relative accuracy shown, the CR position error at the target is seen to be 84.3593×10^4 ft. Data describing the midcourse propulsion system are also presented. It can be seen that the delta-V capability is 16.45111 ft/sec and the expected burn time for the 9.6276 ft/sec velocity correction is 32.35 sec. The total midcourse propulsion system weight was calculated to be 33.287 lb.

The penalty analysis for this mode, mode 3, is presented. The probability of failure due to hardware reliability was calculated to be 0.013. For the specified (fixed) probability of system failure, 0.1000000, and the probability of failure due to hardware reliability, it is seen that the probability of failure due to not having sufficient fuel was calculated to be 0.088. The total weight of the spacecraft and guidance system was specified (fixed) at 5,410 lb. The penalty for this mode is shown to be a guidance system weight of 222.04 lb. It should be recalled that this weight is the summation of the IMU + computer + energy source + midcourse propulsion system weights. The resultant non-guidance weight is seen to be 5,187.96 lb.

Figure 1c lists the mission and spacecraft data used in the computation of the results presented in Figure 1b. A short phrase describing the item of data and the value used in the computation is followed by the sensitivity of the penalty to that value. This sensitivity, as noted in Figure 1c, is the percent change in the penalty to a one percent change in the data value. For example, a one percent change in ID 23, the IMU electronics power, would result in a 0.233 percent change in the penalty for this case. A negative value of sensitivity indicates that the penalty will decrease if the data value is increased and vice versa.

Sensitivity of the penalty to inertial sensor and computer data is presented in Figure 1d. A zero value of sensitivity indicates that a one percent change in the data value presented in Figure 1a for the item of interest results in no change in the penalty out to the number of significant figures printed, or that the data value was zero. The sensitivity to the number of bits of the computer and integration scheme is not the sensitivity to a percent change in the data value but is the percent change in penalty due to the change noted for these items. For example, an increase of one bit results in a 0.00199 percent decrease in the penalty. It is interesting to note that the pitch gyro fixed restraint drift uncertainty, R, affects the penalty much more than any of the other error coefficients of the inertial sensors. The sensitivity analysis presented in Figure 1d indicates that hardware design effort might be better directed toward decreasing the weight of the computer by a percent than decreasing the pitch gyro fixed restraint drift by a percent since the penalty decrease would be nearly five times greater.

MISSION AND SPACE CRAFT DATA

IC=0

ID	DESCRIPTION		VALUE	SENSITIVITY		ID	DESCRIPTION		VALUE	SENSITIVITY
1	TIME TO MID COURSE	(HOURS)	25.00000	.0019055		20	VIBRATION UPPER FREQ.	(CPS)	100.00000	0.0000000
2	PROBABILITY OF GUIDANCE FAIL.		.10000	-.0188316		21	INSULATION THICKNESS	(IN)	.05000	.0060564
3	MID COURSE SYSTEM CON.	(LB/LB)	1.09600	.0584908		22	INSULATION DENSITY	(IN)	.09100	.0060564
4	SPECIFIC IMPULSE	(SEC.)	233.00000	-.0578488		23	ELECTRONICS POWER	(WATTS)	30.00000	.2330681
C 5	NONGUIDANCE WEIGHT	(LB)	5000.00000	0.0000000		24	MID COURSE SYSTEM	(LB)	20.30000	.0914258
6	TOTAL WEIGHT	(LB)	5410.00000	.0584908		25	BOOST TIME	(HOURS)	.20000	.0000010
7	ENERGY SOURCE CONSTANT	(LB)	13.20000	.0594493		26	OPERATING TEMPERATURE	(DEG-F)	160.00000	-2.0026595
8	ENERGY SOURCE CONSTANT	(LB/W)	.34500	.4777897		27	MAX.AMBIENT TEMPERATURE	(DEG-F)	140.00000	2.5437006
9	BLOCK DENSITY	(LB/IN**3)	.09700	.0391966		28	AVE.AMBIENT TEMPERATURE	(DEG-F)	60.00000	-.2027693
10	BASE DENSITY	(LB/IN**3)	.09700	.0204861		29	MIN.AMBIENT TEMPERATURE	(DEG-F)	30.00000	0.0000000
11	COVER DENSITY	(LB/IN**3)	.09700	.0129113		30	OPERATING TEMP.UNCER.	(DEG-F)	.10000	0.0000000
12	IMU COMPONENT SEPARATION	(IN)	.25000	.0380460	A	31	THERMAL CONDUCTIVITY	(W/DEG-F)	0.00000	0.0000000
13	BASE OFFSET	(IN)	1.50000	.0204780	B	32	REL.UNC.IN MID COURSE MAG.		-1.00000	0.0000000
14	BASE THICKNESS	(IN)	.50000	.0204961	B	33	REL.UNC.IN MID COURSE ANGLE		.00291	0.0000000
15	COVER CLEARANCE	(IN)	.25000	.0006225		34	TARGET MISS DISTANCE	(FT)	100000000.00000	0.0000000
16	COVER THICKNESS	(IN)	.10000	.0129113		35	MID COURSE THRUST	(LB)	50.00000	0.0000000
17	ELECTRONICS WEIGHT	(LB)	10.00000	.0450373		36	MIDCOURSE ENGINE RELIABILTY		.00100	.0001704
18	ELECTRONICS MTBF	(HR)	10000.00000	-.0004212		37	ENERGY SOURCE MTBF	(HRS)	10000.00000	-.0004212
19	VIBRATION(MILLARAD/SEC)**2/CPS		.30457	0.0000000		38			0.00000	0.0000000

NOTES A=COMPUTED BY PROGRAM IF DATA SET TO ZERO
B=COMPUTED BY PROGRAM IF DATA SET TO LESS THAN ZERO
C=NOT USED BY THIS PENALTY FUNCTION

SENSITIVITY = PERCENT CHANGE IN PENALTY / PERCENT CHANGE IN DATA

FIGURE 1c. PENALTY, MODE 3, REPORT ON SYSTEM A

HARDWARE SENSITIVITY

ID		IC=	ARMA D-4E YAW ACC. 1	ARMA D-4E PITCH ACC. 1	ARMA D-4E ROLL ACC. 1		GG 334-A YAW GYRO 22	GG 334-A PITCH GYRO 22	GG 334-A ROLL GYRO 22
1	WEIGHT		.0015763	.0015763	.0015763		.0074312	.0074312	.0074312
2	POWER		.0116534	.0116534	.0116534		.0233068	.0233068	.0233068
3	MTTF		-.0000003	-.0000003	-.0000003		-.0001685	-.0001685	-.0001685
4	ALPHA		-.0000043	-.0000043	-.0000043		-.0011963	-.0011963	-.0011963
5	LENGTH		.0067932	.0025639	.0067932		.0084004	.0201039	.0201039
6	DIAMETER		.0148378	.0139984	.0148378		.0123136	.0204469	.0204469
7	WIDTH		0.0000000	0.0000000	0.0000000		0.0000000	0.0000000	0.0000000
CONSTANT						CONSTANT			
8	K0		.0000381	.0000044	.0000249	R	.0041645	.0362160	.0001969
9	K1		0.0000000	0.0000000	.0000523	UI	0.0000000	0.0000000	0.0000000
10	K2		0.0000000	0.0000000	.0000006	US	0.0000000	0.0000000	.0004372
11	K3		0.0000000	0.0000000	.0000000	S	0.0000000	0.0000000	0.0000000
12	M0		0.0000000	0.0000000	0.0000000	IS	.0000089	.0000001	.0000006
13	N0		0.0000000	0.0000000	0.0000000	I0	.0000000	.0000002	.0000000
14	M1		0.0000000	0.0000000	0.0000000	T	.0000001	.0009535	.0000000
15	N1		0.0000000	0.0000000	0.0000000		0.0000000	0.0000000	0.0000000
16	IP		.0073824	.0008395	.0008395		0.0000000	0.0000000	0.0000000
17	IN		0.0000000	0.0000000	.0073824		0.0000000	0.0000000	0.0000000
PER DEG-F						PER DEG-F			
18	K0		0.0000000	0.0000000	0.0000000	R	0.0000000	0.0000000	0.0000000
19	K1		0.0000000	0.0000000	0.0000000	UI	0.0000000	0.0000000	0.0000000
20	K2		0.0000000	0.0000000	0.0000000	US	0.0000000	0.0000000	0.0000000
21	K3		0.0000000	0.0000000	0.0000000	S	0.0000000	0.0000000	0.0000000
22	M0		0.0000000	0.0000000	0.0000000	IS	0.0000000	0.0000000	0.0000000
23	N0		0.0000000	0.0000000	0.0000000	I0	0.0000000	0.0000000	0.0000000
24	M1		0.0000000	0.0000000	0.0000000	T	0.0000000	0.0000000	0.0000000
25	N1		0.0000000	0.0000000	0.0000000		0.0000000	0.0000000	0.0000000
26	IP		0.0000000	0.0000000	0.0000000		0.0000000	0.0000000	0.0000000
27	IN		0.0000000	0.0000000	0.0000000		0.0000000	0.0000000	0.0000000

COMPUTER SENSITIVITY

SRT RUK=2

IC= 49

ID			ID			
1	WEIGHT	.1621344	8	NO.OF BITS	-.0019901	PER BIT
2	POWER	.1398409	9	COMP.FREQ.	.0000533	
3	MTTF	-.0007019	10	INT.SCHEME	.0191091	CHANGE TO RECT.
4	ALPHA	-.0040343	10	INT.SCHEME	0.0000000	CHANGE TO RUK-4

SENSITIVITY = PERCENT CHANGE IN PENALTY / PERCENT CHANGE IN DATA
EXCEPT AS NOTED FOR COMPUTER BITS AND INTEGRATION SCHEME

FIGURE 1d. PENALTY, MODE 3, REPORT ON SYSTEM A

Figure 2 presents a tabular listing of penalty for a range of values of K_0, bias, for the yaw, pitch, and roll accelerometers of system A. The value of the accelerometer bias was swept simultaneously for the three accelerometers. It can be seen that a one order of magnitude decrease from the original value made very little improvement in the penalty. An order of magnitude increase from the original value also made little difference although an increase of two orders of magnitude over the original value resulted in saturation of the penalty due to weight of the midcourse fuel required to correct the position error caused by the accelerometer bias coefficient listed.

Figure 3 presents four parameter plots, one of which is a plot of the tabular data presented in Figure 2. The computer plots the penalty for the mode being used (in this case mode 3 whose penalty is weight) versus the value of the parameter being swept. In this figure, a logarithmic sweep of the parameter was used. Plot 1 in Figure 3 is a plot of the data swept, K_0, for all three accelerometers simultaneously. This plot corresponds to the data in Figure 2. Plot 2 depicts the effect on the penalty if K_0 of the yaw accelerometer only is swept. Plot 3 presents similar information if the pitch accelerometer only is swept while plot 4 presents the penalty if the roll accelerometer only is swept while the other data values remain constant. From this plot it can be concluded, for example, that the bias of the pitch accelerometer could increase from 6.7 μg to 0.33 millig with no discernible increase in the penalty. It should be kept in mind that this is an example dependent upon the data used in the calculations. This example does illustrate the usefulness of the parameter sweeping and plotting routines of the computer program developed under this study.

Figure 4 presents parameter plots in which the fixed restraint drift, R, of the system A gyroscopes was swept logarithmically for penalty mode 3. Plot 1 presents the penalty versus R when all three gyroscopes are swept simultaneously. Plot 2 presents a sweep of the yaw gyro only, plot 3 a sweep of the pitch gyro only, and plot 4 a sweep of the roll gyro only. The normal value of R is 0.1°/hr. It can be concluded that for these data, little increase in the value of R for the pitch gyroscope can be tolerated as seen by the approximately 6 pound increase in the penalty when the value of R is increased from 0.1 to 0.199°/hr. The value of R for the roll gyrocope can be increased from 0.1 to 2.5°/hr before a discernible increase in the penalty occurs. Information such as this should prove useful in the design and selection of components for strapdown guidance systems.

Figure 5 presents a plot of the penalty versus the number of bits in a computer word for the conceptual SRT computer using a Runge-Kutta second order algorithm (RUK-2). A linear sweep of the parameter was used. It can be concluded that a word length greater than 27 bits does not result in an improvement in the penalty for mode 3. Use of a 23 bit word length would result in a 78 lb increase in the midcourse propulsion system fuel and tankage over that needed to perform the midcourse velocity correction required using a 27 bit or longer word. This is due to the increase in navigation errors the computer contributes in updating the direction cosine matrix and solving the guidance equations.

SWEEP FOR PENALTY MODE = 3

ARMA D-4E DATA NUMBER 8 ORIGINAL VALUE = 67.00000000E-07

YAW ACCEL. PITCH ACC. ROLL ACC. K0

ARBITRARY SYSTEM

VALUE	PENALTY	SYSTEM							SATURATION
67.00000000E-08	222.03070	1	1	1	22	22	22	49	
84.34800259E-08	222.03075	1	1	1	22	22	22	49	
10.61878439E-07	222.03082	1	1	1	22	22	22	49	
13.36825751E-07	222.03093	1	1	1	22	22	22	49	
16.82963909E-07	222.03110	1	1	1	22	22	22	49	
21.18726032E-07	222.03137	1	1	1	22	22	22	49	
26.67318043E-07	222.03181	1	1	1	22	22	22	49	
33.57954465E-07	222.03250	1	1	1	22	22	22	49	
42.27414208E-07	222.03359	1	1	1	22	22	22	49	
53.21999173E-07	222.03533	1	1	1	22	22	22	49	
67.00000000E-07	222.03808	1	1	1	22	22	22	49	
84.34800259E-07	222.04243	1	1	1	22	22	22	49	
10.61878439E-06	222.04932	1	1	1	22	22	22	49	
13.36825751E-06	222.06025	1	1	1	22	22	22	49	
16.82963909E-06	222.07754	1	1	1	22	22	22	49	
21.18726032E-06	222.10489	1	1	1	22	22	22	49	
26.67318043E-06	222.14814	1	1	1	22	22	22	49	
33.57954465E-06	222.21638	1	1	1	22	22	22	49	
42.27414208E-06	222.32381	1	1	1	22	22	22	49	
53.21999173E-06	222.49232	1	1	1	22	22	22	49	
67.00000000E-06	222.75512	1	1	1	22	22	22	49	
84.34800259E-06	223.16159	1	1	1	22	22	22	49	
10.61878439E-05	223.78275	1	1	1	22	22	22	49	
13.36825751E-05	224.71673	1	1	1	22	22	22	49	
16.82963909E-05	226.10805	1	1	1	22	22	22	49	
21.18726032E-05	228.68152	1	1	1	22	22	22	49	
26.67318043E-05	240.93967	1	1	1	22	22	22	49	
33.57954465E-05	1006138.40124	1	1	1	22	22	22	49	WEIGHT
42.27414208E-05	1006138.40124	1	1	1	22	22	22	49	WEIGHT
53.21999173E-05	1006138.40124	1	1	1	22	22	22	49	WEIGHT
67.00000000E-05	1006138.40124	1	1	1	22	22	22	49	WEIGHT

FIGURE 2. TABLE OF PENALTY, MODE 3, VARIATION WITH SYSTEM A ACCELEROMETER BIAS SWEEP

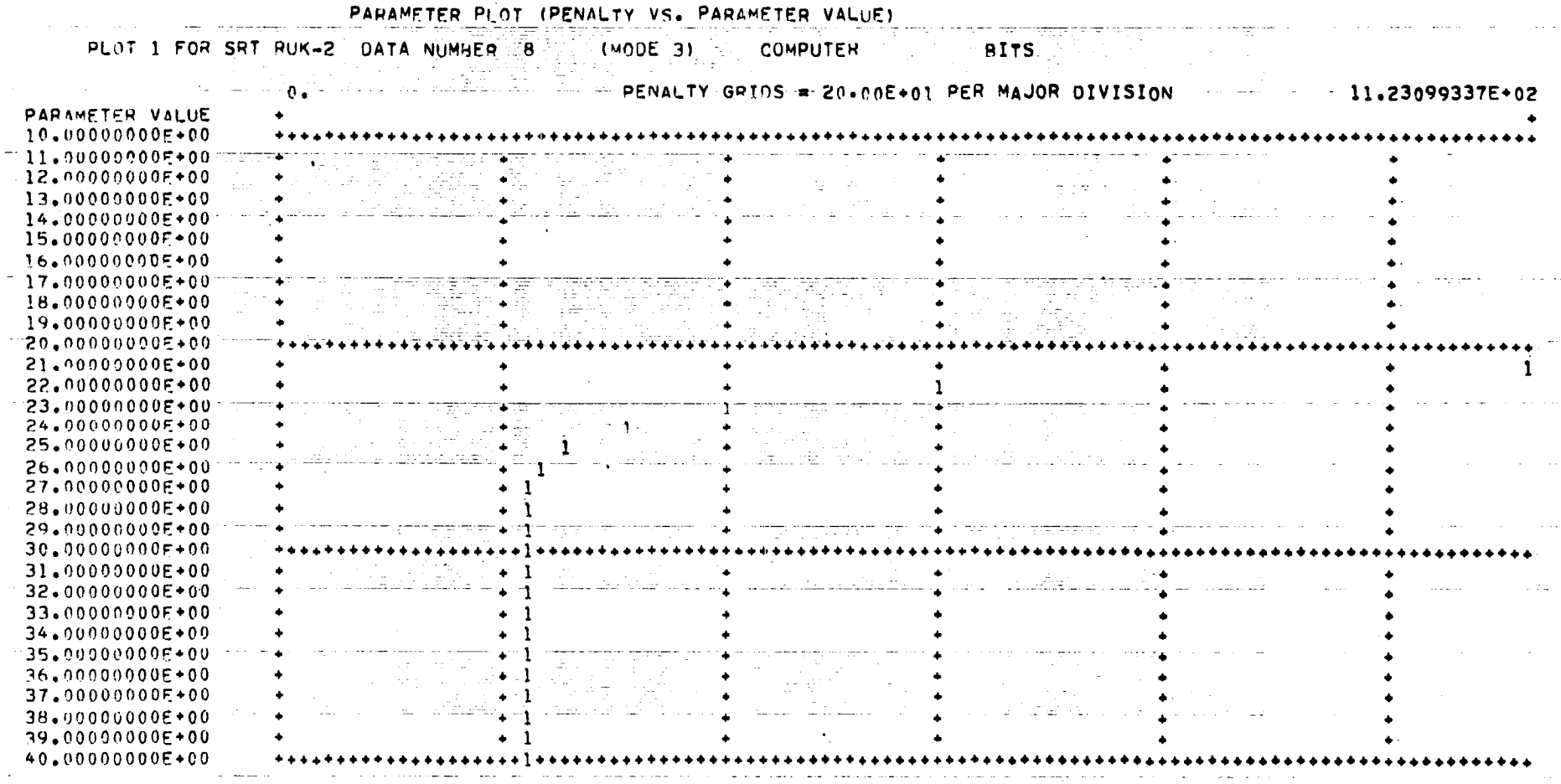

FIGURE 5. PLOT OF PENALTY, MODE 3, (SYSTEM A) VARIATION WITH NUMBER OF COMPUTER BITS SWEEP

The results presented in this summary section were meant to illustrate some of the features of the computer programs. Other results from the exercising of the computer programs developed under this study are presented in the technical discussion section of this report.

TECHNICAL DISCUSSION

Development of Performance Indices

Before starting to develop a performance index, four existing "cost-effectiveness" models were reviewed and evaluated. These models were developed for the USAF Space Systems Division (now Space and Missile Systems Organization) "Standardized Space Guidance System (SSGS) Study" and are discussed in Appendix B of this report. This appendix contains a review of each of the four models, lists the input data required, discusses the fundamental figure of merit utilized by each model, and presents an evaluation of the applicability of these models. This evaluation is summarized below.

Applicability of SSGS Cost Effectiveness Models.--Each of the "cost-effectiveness" models developed for evaluating competing guidance systems for the Standardized Space Guidance System (SSGS) may be useful if given the same requirement, i.e., determine for the national space mission model the SSGS which is most cost-effective. It can be stated that this was not the problem for which NASA/ERC was seeking a solution. NASA/ERC was concerned with development of a performance index which will trade off the system parameters of accuracy, weight, power, and reliability, and thereby serve as a design aid for selection of component subsystems of a strapdown guidance system.

All of the SSGS models require some of the same input data. Table IV lists some of the common input data. Some of the models required weight and power of the guidance system (inertial platform, computer, and aids) and others did not.

TABLE IV
COMMON INPUT DATA FOR SSGS COST-EFFECTIVENESS MODELS

(i)	Mission model
(ii)	Navigation accuracy requirement of each mission
(iii)	Probability of mission success
(iv)	Candidate guidance system error analysis
(v)	Candidate guidance system reliability
(vi)	Nonrecurring cost for launch vehicle and all other nonguidance items
(vii)	Recurring cost for launch vehicle and all other nonguidance items
(viii)	Nonrecurring guidance cost
(ix)	Recurring guidance cost

All of the models are heavily cost oriented. The cost data required is generally subject to doubt or not available. Two of the models make use of a figure of merit which can be expressed as dollars/pound of payload. For missions with quite heavy payloads, the figure of merit would appear much less sensitive to an increase in guidance system weight than a mission utilizing the same guidance system with a low payload weight. Two of the models are very much total mission cost oriented.

Greater length could be added to this report in providing additional rationale for non-use of the four SSGS models. It was apparent that a less complex and different type of cost function or performance index was required to aid in the design of strapdown guidance systems, be of use in evaluating competitive systems, and serve as a tool in the determination of research needed to improve system performance. It was decided that any model developed should be much less cost oriented than the SSGS models. The following section presents the models developed by Battelle.

Penalty Function Analysis.--The effectiveness of a guidance system on a specific spacecraft on a specific mission is evaluated by one of three penalty functions. The guidance system is described by the six system parameters shown in Table V.

TABLE V
GUIDANCE SYSTEM PARAMETERS

Symbol	Definition
P_{FR}	Probability of a failure due to hardware reliability.
R_V	Root-mean-square midcourse delta-V, the square-root of the trace of the midcourse delta-V covariance matrix.
D_V	The degrees-of-freedom of the midcourse delta-V covariance.
R_T	Root-mean-square target miss, the square root of the trace of the target miss covariance matrix.
D_T	Degrees-of-freedom of the target miss covariance.
W_{ICP}	Sum of inertial measurement unit, computer, and electrical energy source weights.

The penalty functions are calculated from the above system parameters and the mission and spacecraft parameters shown in Table VI.

TABLE VI
MISSION AND SPACECRAFT PARAMETERS

Symbol	
P_{FG}	Probability of mission failure attributable to the guidance system.
W_{NG}	Nonguidance spacecraft weight.
W_T	Total spacecraft weight.
X_{MISS}	Allowed miss distance at target.
K_{DV}	Midcourse correction system tankage factor (system weight/fuel weight).
K_{DC}	Midcourse correction system constant weight.
Ig	Specific impulse of the midcourse correction system times gravity.

The three penalty functions are defined in Table VII.

TABLE VII
PENALTY FUNCTION DEFINITION

Penalty Mode	P_{FG}	W_{NG}	W_{GS}	W_T
1	F	F	P	V
2	P	F	F	F
3	F	V	P	F

F = Fixed, used as a requirement
P = Variable, used as the penalty
V = Variable, used for information only

Penalty function, mode 1, assumes that a certain probability of mission failure attributable to guidance (P_{FG}) is reasonable and that nonguidance

spacecraft weight (W_{NG}) is fixed. The guidance system weight is calculated and used as the penalty function.

Penalty function, mode 2, assumes nonguidance, guidance system, and total spacecraft weights are constants with the probability of mission failure attributable to guidance (P_{FG}) variable and used as the penalty function.

Penalty function, mode 3, assumes that a certain probability of mission failure attributable to guidance (P_{FG}) is reasonable and that total spacecraft weight (W_T) is fixed. The guidance system weight (W_{GS}) is variable and used as the penalty function.

Calculation of the penalty function under any of the three modes will involve calculating the intermediate quantities defined in Table VIII.

TABLE VIII
INTERMEDIATE QUANTITIES USED IN
CALCULATING THE PENALTY FUNCTIONS

Symbol	Definition
P_{FV}	Probability of insufficient midcourse fuel
P_{FT}	Probability of excessive target miss
P_{FTR}	Probability of failure due to reliability or target miss
W_F	Weight of midcourse fuel
W_{DV}	Total weight of midcourse system
ΔV	Midcourse delta-V capability
μ	Spacecraft mass ratio
ψ_V	Midcourse delta-V capability divided by the square root of the trace of the delta-V covariance matrix (number of traces)
ψ_T	Allowed target miss distance divided by the square root of the trace of target miss covariance matrix (number of traces)

A detailed discussion of the steps used to calculate each penalty mode is given below.

Penalty Mode 1.--Probability of missing the target (P_{FT}) is calculated from the system parameters describing accuracy at the target by

$$P_{FT} = \text{Prob}(\psi_T, D_T)$$

with

$$\psi_T = X_{MISS}/R_T \quad .$$

The function Prob(ψ, D) is the probability distribution of the magnitude of a vector with normal, zero-mean, components as discussed in Appendix C. A table of this distribution is shown in Figure 6.

The combined probability of missing the target or failing due to reliability is obtained from

$$P_{FTR} = P_{FR} + P_{FT} - P_{FR}P_{FT} \quad .$$

With the probability of failure due to target miss or reliability known, the probability of failure due to insufficient fuel which will result in the specified P_{FG} is calculated by

$$P_{FV} = \frac{P_{FG} - P_{FTR}}{1 - P_{FTR}} \quad .$$

Note that if P_{FTR} exceeds P_{FG}, P_{FV} does not exist. In other words, if the probability of failure due to reliability or target miss is greater than P_{FG}, even a perfect system (zero probability of insufficient fuel) will not meet the required guidance system failure probability.

The delta-V capability required to achieve the required P_{FV} is now calculated by

$$\psi_V = \psi(P_{FV}, D_V)$$

and

$$\Delta V = R_V \psi_V$$

FIGURE 6. CUMULATIVE PROBABILITY DISTRIBUTION FUNCTION [Pr($|X| > \psi\sqrt{\text{TRACE}}$)] OF A VECTOR WITH NORMAL, ZERO MEAN, COMPONENTS

Magnitude/$\sqrt{\text{Trace}}$ = ψ

PROB.	D= 1.0	1.1	1.2	1.3	1.4	1.5	1.6	1.7	1.8	1.9	2.0	2.2	2.4	2.6	2.8	3.0
1.00E+00	0 0000X0	0000X0	0000X0	0000X0	0000X0	0000X0	0000X0	0000X0	0000X0	0000X0	0000X0	0000X0	0000X0	0000X0	0000X0	0000X
9.00E-01	.2072	.2182	.2297	.2358	.2464	.2577	.2696	.2822	.2955	.3097	.3237	.3522	.3770	.4004	.4218	.4398
8.00E-01	.3016	.3146	.3285	.3431	.3585	.3872	.4072	.4252	.4418	.4575	.4708	.4989	.5228	.5431	.5617	.5786
7.00E-01	.3866	.4020	.4506	.4748	.4967	.5182	.5371	.5539	.5695	.5840	.5972	.6209	.6411	.6591	.6746	.6887
6.00E-01	.5251	.5572	.5841	.6067	.6281	.6466	.6629	.6779	.6914	.7036	.7147	.7343	.7511	.7655	.7781	.7892
5.00E-01	.6753	.7026	.7255	.7459	.7631	.7783	.7918	.8036	.8143	.8239	.8326	.8476	.8602	.8708	.8800	.8880
4.00E-01	.8416	.8637	.8812	.8965	.9091	.9202	.9294	.9379	.9451	.9515	.9572	.9669	.9746	.9809	.9863	.9910
3.00E-01	1.0367	1.0560	1.0606	1.0690	1.0756	1.0814	1.0860	1.0897	1.0927	1.0952	1.0973	1.1004	1.1025	1.1039	1.1048	1.1053
2.00E-01	1.2819	1.2836	1.2841	1.2835	1.2822	1.2804	1.2784	1.2761	1.2737	1.2712	1.2686	1.2634	1.2583	1.2532	1.2483	1.2436
1.00E-01	1.6452	1.6284	1.6134	1.5982	1.5845	1.5716	1.5594	1.5480	1.5372	1.5270	1.5174	1.4997	1.4836	1.4689	1.4555	1.4433
9.00E-02	1.6955	1.6764	1.6586	1.6419	1.6263	1.6118	1.5982	1.5855	1.5736	1.5624	1.5518	1.5322	1.5146	1.4986	1.4841	1.4709
8.00E-02	1.7519	1.7288	1.7083	1.6894	1.6721	1.6559	1.6408	1.6267	1.6134	1.6010	1.5893	1.5678	1.5485	1.5312	1.5154	1.5009
7.00E-02	1.8120	1.7868	1.7637	1.7424	1.7228	1.7046	1.6878	1.6721	1.6574	1.6436	1.6307	1.6071	1.5860	1.5670	1.5497	1.5340
6.00E-02	1.8812	1.8522	1.8258	1.8017	1.7796	1.7593	1.7405	1.7230	1.7068	1.6916	1.6773	1.6513	1.6281	1.6073	1.5885	1.5712
5.00E-02	1.9600	1.9269	1.8970	1.8699	1.8456	1.8222	1.8011	1.7816	1.7635	1.7466	1.7308	1.7020	1.6764	1.6534	1.6326	1.6138
4.00E-02	2.0536	2.0157	1.9815	1.9506	1.9225	1.8967	1.8730	1.8511	1.8307	1.8118	1.7941	1.7620	1.7335	1.7081	1.6851	1.6643
3.00E-02	2.1704	2.1261	2.0865	2.0508	2.0185	1.9890	1.9619	1.9370	1.9139	1.8925	1.8726	1.8364	1.8044	1.7758	1.7501	1.7268
2.00E-02	2.3266	2.2740	2.2272	2.1852	2.1474	2.1129	2.0814	2.0525	2.0257	2.0009	1.9779	1.9362	1.8995	1.8668	1.8374	1.8108
1.00E-02	2.5760	2.5101	2.4518	2.3999	2.3531	2.3107	2.2721	2.2367	2.2041	2.1740	2.1460	2.0955	2.0511	2.0117	1.9764	1.9446
9.00E-03	2.6122	2.5444	2.4845	2.4311	2.3830	2.3395	2.2998	2.2635	2.2300	2.1991	2.1704	2.1186	2.0731	2.0327	1.9966	1.9640
8.00E-03	2.6521	2.5822	2.5205	2.4655	2.4160	2.3712	2.3304	2.2931	2.2587	2.2269	2.1973	2.1442	2.0975	2.0560	2.0189	1.9854
7.00E-03	2.6971	2.6247	2.5609	2.5040	2.4529	2.4067	2.3646	2.3261	2.2907	2.2579	2.2275	2.1728	2.1247	2.0821	2.0439	2.0095
6.00E-03	2.7482	2.6731	2.6069	2.5480	2.4951	2.4472	2.4037	2.3636	2.3272	2.2933	2.2619	2.2053	2.1557	2.1116	2.0723	2.0368
5.00E-03	2.8075	2.7293	2.6604	2.5991	2.5441	2.4943	2.4491	2.4077	2.3696	2.3344	2.3018	2.2431	2.1910	2.1460	2.1052	2.0685
4.00E-03	2.8784	2.7965	2.7244	2.6603	2.6027	2.5508	2.5035	2.4603	2.4205	2.3838	2.3498	2.2886	2.2349	2.1874	2.1449	2.1066
3.00E-03	2.9680	2.8812	2.8050	2.7372	2.6765	2.6217	2.5720	2.5264	2.4846	2.4460	2.4102	2.3459	2.2895	2.2395	2.1949	2.1547
2.00E-03	3.0905	2.9973	2.9155	2.8429	2.7778	2.7191	2.6658	2.6171	2.5724	2.5311	2.4929	2.4242	2.3641	2.3110	2.2635	2.2207
1.00E-03	3.2907	3.1871	3.0941	3.0154	2.9433	2.8783	2.8192	2.7654	2.7160	2.6704	2.6283	2.5525	2.4863	2.4277	2.3754	2.3284
9.00E-04	3.3202	3.2150	3.1227	3.0409	2.9677	2.9018	2.8419	2.7873	2.7372	2.6910	2.6482	2.5715	2.5043	2.4450	2.3920	2.3443
8.00E-04	3.3528	3.2460	3.1522	3.0691	2.9948	2.9278	2.8670	2.8116	2.7607	2.7138	2.6704	2.5925	2.5243	2.4641	2.4103	2.3620
7.00E-04	3.3897	3.2807	3.1854	3.1008	3.0252	2.9571	2.8953	2.8389	2.7871	2.7394	2.6953	2.6160	2.5468	2.4856	2.4310	2.3819
6.00E-04	3.4318	3.3206	3.2232	3.1370	3.0599	2.9905	2.9276	2.8700	2.8173	2.7687	2.7237	2.6430	2.5724	2.5101	2.4545	2.4045
5.00E-04	3.4804	3.3673	3.2677	3.1794	3.1006	3.0296	2.9652	2.9065	2.8526	2.8029	2.7570	2.6745	2.6025	2.5388	2.4820	2.4309
4.00E-04	3.5401	3.4235	3.3212	3.2306	3.1497	3.0768	3.0107	2.9505	2.8952	2.8442	2.7972	2.7126	2.6387	2.5734	2.5153	2.4629
3.00E-04	3.6154	3.4946	3.3890	3.2955	3.2120	3.1367	3.0685	3.0063	2.9493	2.8967	2.8481	2.7609	2.6846	2.6175	2.5575	2.5035
2.00E-04	3.7191	3.5931	3.4827	3.3850	3.2978	3.2192	3.1482	3.0833	3.0239	2.9691	2.9184	2.8276	2.7483	2.6782	2.6158	2.5597
1.00E-04	3.8907	3.7556	3.6376	3.5331	3.4399	3.3561	3.2801	3.2108	3.1473	3.0889	3.0348	2.9380	2.8535	2.7787	2.7122	2.6524
9.00E-05	3.9162	3.7800	3.6607	3.5551	3.4610	3.3765	3.2997	3.2298	3.1657	3.1067	3.0522	2.9544	2.8691	2.7936	2.7265	2.6662
8.00E-05	3.9445	3.8066	3.6863	3.5796	3.4845	3.3990	3.3215	3.2508	3.1861	3.1266	3.0714	2.9727	2.8865	2.8102	2.7425	2.6816
7.00E-05	3.9764	3.8376	3.7150	3.6072	3.5109	3.4245	3.3468	3.2765	3.2090	3.1489	3.0931	2.9932	2.9061	2.8290	2.7604	2.6989
6.00E-05	4.0130	3.8717	3.7480	3.6367	3.5412	3.4537	3.3742	3.3017	3.2353	3.1744	3.1179	3.0168	2.9285	2.8504	2.7810	2.7187
5.00E-05	4.0559	3.9123	3.7866	3.6757	3.5767	3.4878	3.4072	3.3336	3.2662	3.2044	3.1470	3.0444	2.9548	2.8756	2.8051	2.7419
4.00E-05	4.1077	3.9615	3.8334	3.7206	3.6196	3.5292	3.4471	3.3722	3.3037	3.2406	3.1822	3.0778	2.9867	2.9061	2.8343	2.7700
3.00E-05	4.1739	4.0240	3.8930	3.7778	3.6745	3.5818	3.4979	3.4213	3.3514	3.2867	3.2271	3.1203	3.0273	2.9449	2.8715	2.8058
2.00E-05	4.2655	4.1106	3.9756	3.8570	3.7505	3.6546	3.5680	3.4894	3.4176	3.3506	3.2893	3.1793	3.0832	2.9987	2.9231	2.8556
1.00E-05	4.4177X4	4.2546X4	4.1136X4	3.9877	3.8763	3.7756	3.6848	3.6028	3.5276	3.4573	3.3925	3.2779	3.1766	3.0884	3.0091	2.9378
9.00E-06	4.4404X4	4.2760X4	4.1342X4	4.0072	3.8950	3.7939	3.7024	3.6197	3.5440	3.4732	3.4079	3.2927	3.1900	3.1018	3.0220	2.9501
8.00E-06	4.4656X4	4.2995X4	4.1570X4	4.0288X3	3.9156	3.8140	3.7219	3.6385	3.5623	3.4909	3.4250	3.3091	3.2062	3.1165	3.0363	2.9638
7.00E-06	4.4940X4	4.3268X4	4.1828X4	4.0533X3	3.9393	3.8368	3.7443	3.6597	3.5829	3.5110	3.4443	3.3277	3.2237	3.1330	3.0525	2.9792
6.00E-06	4.5268X4	4.3577X4	4.2124X4	4.0813X3	3.9662X3	3.8628	3.7692	3.6840	3.6067	3.5342	3.4665	3.3490	3.2439	3.1520	3.0711	2.9969
5.00E-06	4.5645X4	4.3939X4	4.2471X4	4.1142X3	3.9978X3	3.8934X3	3.7980	3.7125	3.6345	3.5614	3.4934	3.3741	3.2675	3.1743	3.0930	3.0184
4.00E-06	4.6112X4	4.4378X4	4.2892X4	4.1541X4	4.0362X3	3.9305X3	3.8349X3	3.7471	3.6683	3.5945	3.5260	3.4036	3.2963	3.2014	3.1196	3.0446
3.00E-06	4.6703X4	4.4937X4	4.3429X4	4.2049X4	4.0851X3	3.9779X3	3.8809X3	3.7913X3	3.7114X3	3.6367	3.5676	3.4408	3.3326	3.2359	3.1536	3.0779
2.00E-06	4.7524X4	4.5715X4	4.4174X4	4.2756X4	4.1530X4	4.0436X3	3.9447X3	3.8527X3	3.7713X3	3.6954X3	3.6254X3	3.4925	3.3827	3.2840	3.2002	3.1243

X indicates extrapolation from Gamma Function Table

where $\psi(P, D)$ is obtained from function $Prob(\psi, D)$ by solving for ψ knowing P and D.

The familiar rocket equation,

$$\Delta V = Ig \log_e(\mu) \quad ,$$

is used to obtain the spacecraft mass ratio

$$\mu = e^{\Delta V/Ig} \quad .$$

The spacecraft mass ratio is the initial spacecraft weight divided by the final spacecraft weight or

$$\mu = \frac{W_T}{W_T - W_F} \quad .$$

The midcourse fuel weight required is then

$$W_F = W_T \frac{(\mu - 1)}{\mu} \quad .$$

Now

$$W_T = W_{ICP} + W_{NG} + W_{DV}$$

and since the midcourse correction system weight is estimated by

$$W_{DV} = W_F K_{DV} + K_{DC}$$

substitution into the equation for W_F in terms of W_T and μ yields

$$W_F = \frac{(\mu - 1)(W_{ICP} + W_{NG} + K_{DC})}{\mu - [\mu - 1] K_{DV}} \quad .$$

The effective weight of the complete guidance system is then calculated by

$$W_{GS} = W_{ICP} + W_F K_{DV} + K_{DC} \quad .$$

This is the desired penalty function. The above equations are shown in flow chart form in Figure 7.

Penalty Mode 2.--The probability of failing due to reliability or miss at the target (P_{FTR}) is calculated as in penalty mode 1. The combined guidance system probability of failure (P_{FG}), the penalty of mode 2, is calculated by including the probability of insufficient midcourse correction fuel (P_{FV}).

With a total spacecraft weight (W_T) and nonguidance spacecraft weight (W_{NG}) the total guidance system weight is fixed,

$$W_{GS} = W_T - W_{NG} \quad .$$

The midcourse system weight is assumed to be

$$W_{DV} = W_{GS} - W_{ICP} \quad .$$

Thus, the fuel weight is given by

$$W_F = \frac{W_{DV} - K_{DC}}{K_{DV}}$$

and the spacecraft mass ratio is

$$\mu = \frac{W_T}{W_T - W_F} \quad .$$

The delta-V capability is found by the rocket equation,

$$\Delta V = I g \log(\mu)$$

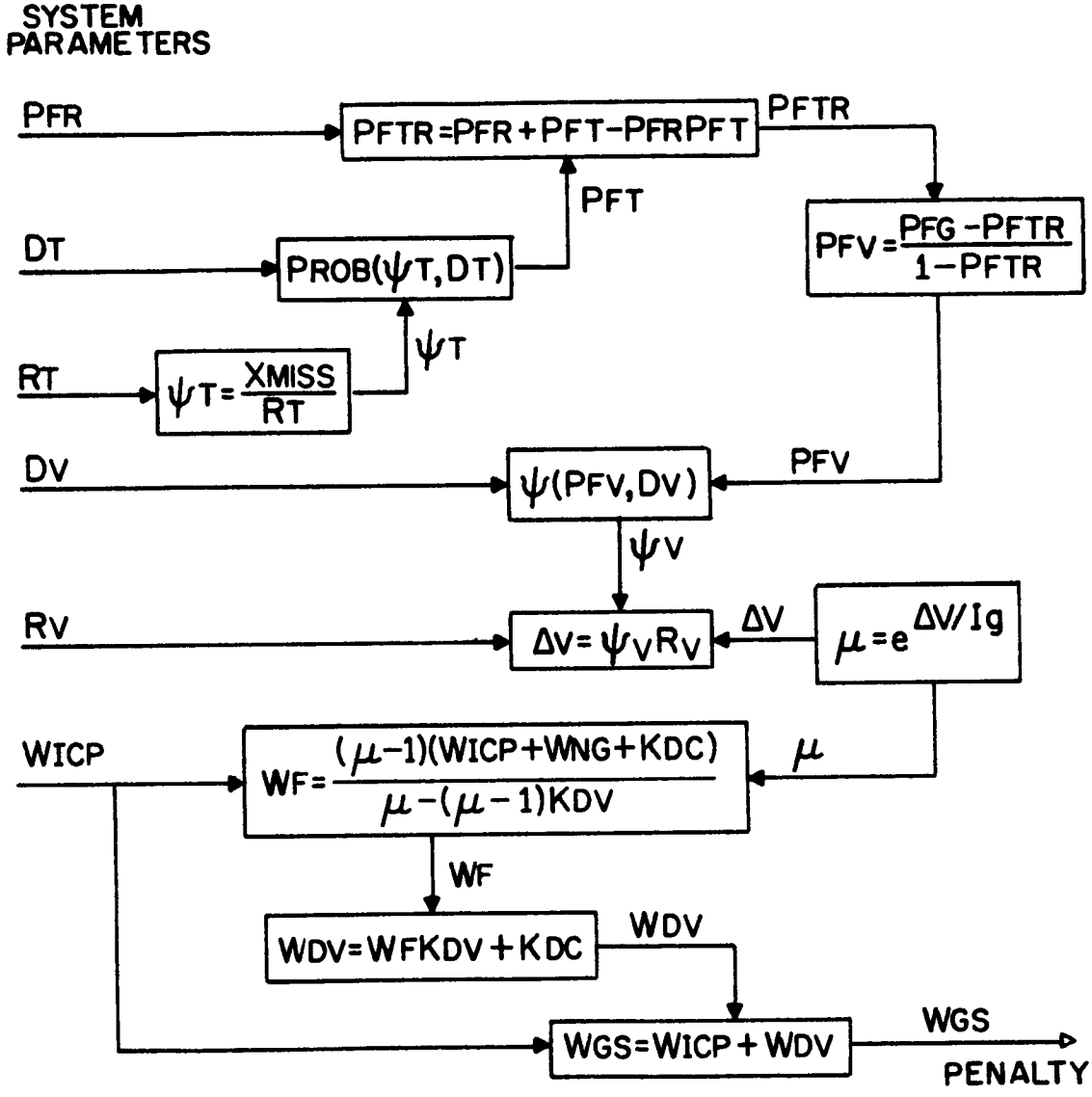

FIGURE 7. CALCULATION OF PENALTY, MODE 1

and the probability of insufficient fuel is

$$P_{FV} = \text{Prob}(\psi_V, D_V)$$

where

$$\psi_V = \frac{\Delta V}{R_V} \quad .$$

The combined probability of guidance system failure is found by

$$P_{FG} = P_{FTR} + P_{FV} - P_{FTR}P_{FV}$$

which is the desired penalty, mode 2. The above equations are shown in flow chart form in Figure 8.

Penalty Mode 3.--Penalty mode 3 is similar to penalty mode 1 in that the penalty is the effective weight of the guidance system (W_{GS}). However, the total spacecraft weight (W_T) is held constant under mode 3 unlike mode 1 where the nonguidance weight was held constant.

The probability of failing due to reliability or miss at the target (P_{FTR}) is calculated as under mode 1. Likewise, the probability of insufficient fuel is obtained from

$$P_{FV} = \frac{P_{FG} - P_{FTR}}{1 - P_{FTR}}$$

which is used to compute the required midcourse delta-V capability by

$$\Delta V = R_V \psi_V$$

where the number of traces (ψ_V) is obtained from the statistical distribution

$$\psi_V = \psi(P_{FV}, D_V) \quad .$$

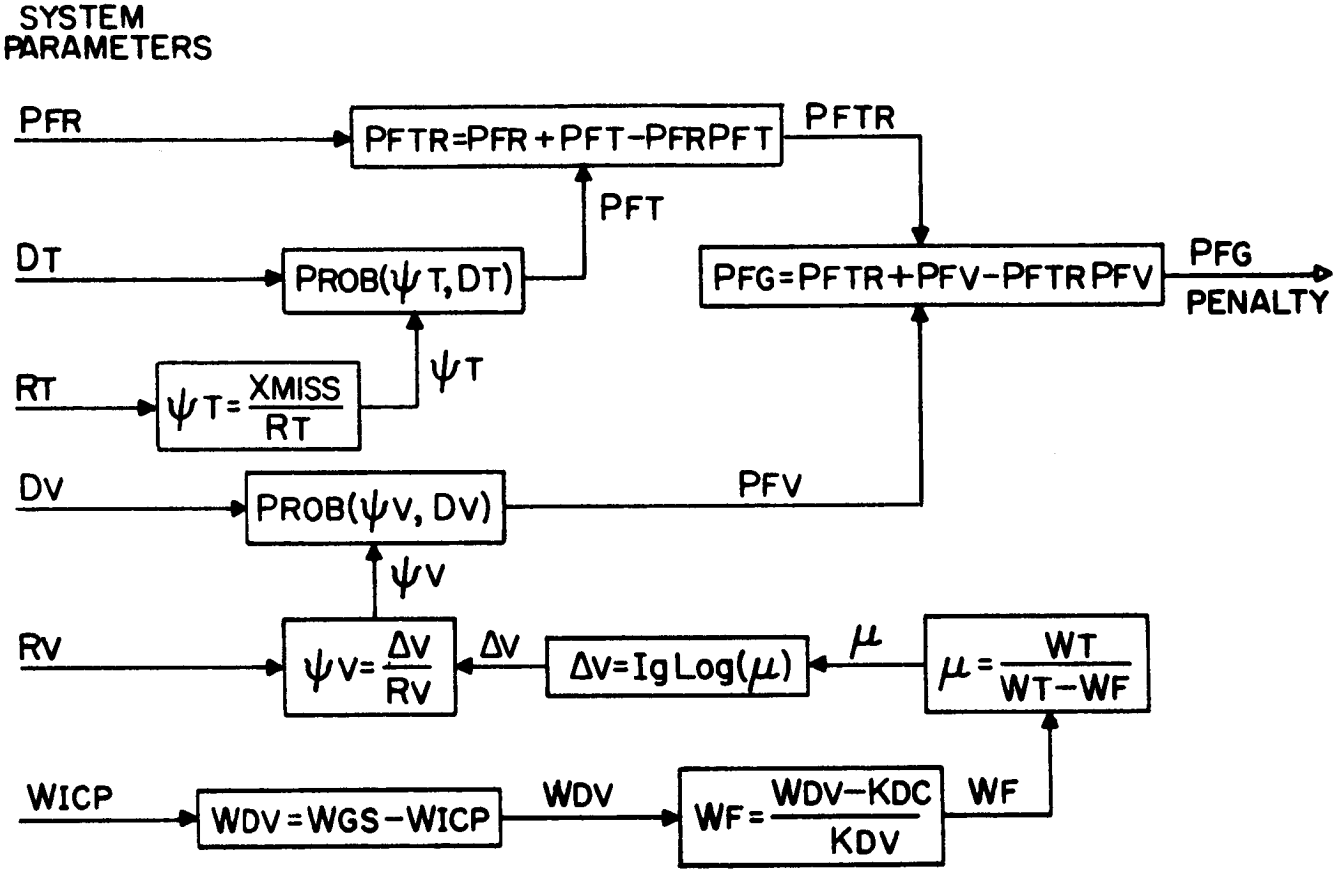

FIGURE 8. CALCULATION OF PENALTY, MODE 2

With the delta-V requirement known, the mass ratio is found by

$$\mu = e^{\Delta V/Ig} \quad .$$

Since the total spacecraft weight is known, the required fuel weight may be obtained directly from

$$W_F = W_T \frac{(\mu - 1)}{\mu} \quad .$$

The total effective guidance system weight is obtained by adding the midcourse system weight to the weight of the inertial measurement unit plus computer plus power source weight,

$$W_{GS} = W_{ICP} + W_F K_{DV} + K_{DC} \quad .$$

The equations for penalty mode 3 are shown in Figure 9.

Development of System Parameter Estimation Techniques

The system parameters which must be estimated for conceptual strapdown guidance systems are those used in the system performance indices (penalty functions). These parameters were discussed in the preceding section and are listed in Table V. This section describes the techniques developed to estimate the weight of (1) the inertial measurement unit, (2) the computer, and (3) the power source. In addition, the estimation of the system reliability and the accuracy analysis are discussed.

IMU Weight.--The strapdown IMU was broken down into the components shown in Table IX. Data shown is for the United Aircraft Corporate Systems Center (UACSC) strapdown IMU that was proposed for Centaur (Reference 9) and the Honeywell, Inc. SIGN III IMU (Reference 10). The electronics, wiring harness, etc., weigh 9.47 pounds for the UACSC design and 11.7 pounds for the Honeywell SIGN III IMU. Based upon this information, it was decided that the weight of the IMU electronics should be a user specified constant. A value of 10 pounds is believed representative of the state-of-the-art electronics weight for an IMU having three gyroscope and three accelerometer rebalance loops. It should be noted that the majority of the electronics weight is made up by the power supply, conditioning, and sequencing as shown in Table IX.

The weight of the sensor assembly block (SAB) is estimated as follows. Block weight is calculated by assuming each component (three gyroscopes and three accelerometers) is placed in a separate solid block of material as shown

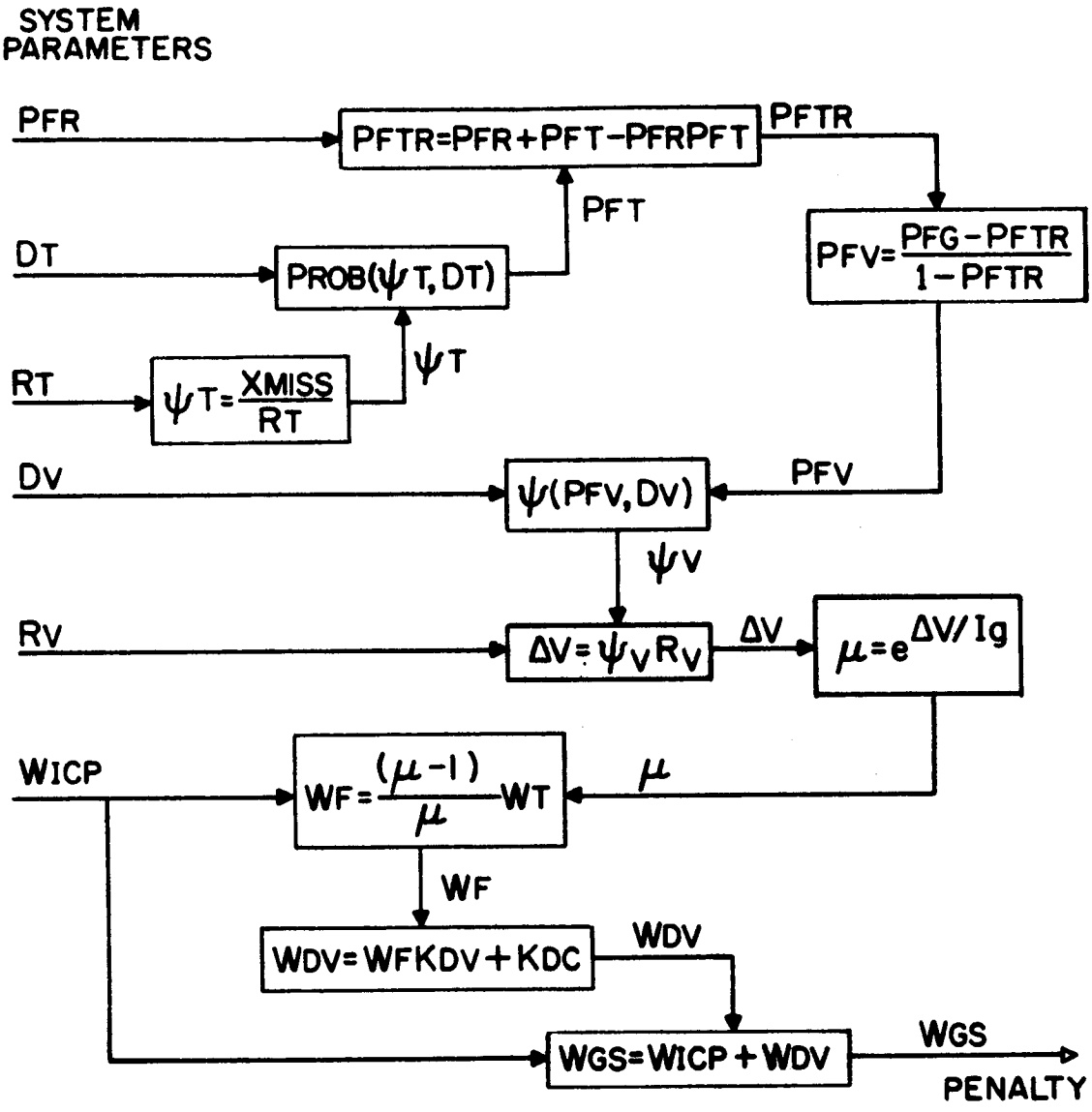

FIGURE 9. CALCULATION OF PENALTY, MODE 3

TABLE IX
STRAPDOWN IMU COMPONENTS AND WEIGHT

Component	UACSC CENTAUR IMU Weight	Honeywell SIGN III IMU Weight
Gyroscope(s)	4.89	4.95
Accelerometer(s)	1.14	1.50
Gyro(s) Torquing Loop Electronics	0.64	1.15
Accelerometer(s) Torquing Loop Electronics	0.61	0.56
Temperature Control Assembly	0.58	0.24
IMU Power Supply, Conditioning and Sequencing	4.32	8.00
Timing (Oscillator and Frequency Countdown)	0.20	0.16
Sensor Assembly Block	7.60	5.51
Base Plate	6.70	6.10
Cover(s) and Insulation	8.77	5.85
Calibration and Alignment Optical Components	0.51	0.10
Interface Electronics	3.12	0.15
Wiring Harness		1.20
Connectors		0.25
Vibration Isolators	----	0.46
Vertical Sensing Element (Option)	0.20	----
Telemetry (Option)	----	----
Other	----	0.05
TOTAL WEIGHT	39.28	36.23

in Figure 10 for cylindrical components and Figure 11 for rectangular components. The volume of the solid block of material is calculated. From this volume is subtracted the volume of the component in the block. The remaining volume of material is multiplied by the density of the material making up the block to find the weight of the block holding that component. The weight of the SAB is the summation of the weight of each of the individual component blocks.

For rectangular components, the equation for finding the volume of the component block can be written as

$$VBLK = (FL[I] + SEP) \times (D[I] + S2) \times (W[I] + S2) - W(I) \times FL(I) \times D(I)$$

where:

VBLK = Volume of the individual component block
D(I) = Dimension along the I^{th} sensor input axis
FL(I) = Dimension along the I^{th} sensor output axis
W(I) = Dimension perpendicular to D(I) and FL(I) of I^{th} sensor
SEP = Separation between sensors in assembled block
S2 = Twice the separation (SEP) between sensors.

For cylindrical components, the equation for finding the volume of the component block can be written as

$$VBLK = (D[I] + S2)^2 \times (FL[I] + SEP) - \frac{\pi}{4} D(I)^2 \times FL(I) \quad .$$

The weight of the block in either case can then be expressed as

$$WBLK = VBLK \times RHOBLK$$

where:

WBLK = Weight of the individual component block
VBLK = Volume of the individual component block
RHOBLK = Density of the material comprising the block.

For a given set of components, the block weight will always be estimated as the same value no matter which mechanical design is used.

The weight of the base, cover, and insulation is estimated as follows. Analytic expressions are written which describe each of the possible critical paths along each of the three dimensions which are used in calculation of the volume of the complete IMU. Each critical path length is calculated and the longest critical path in each direction establishes the dimensions of the IMU. These dimensions are used in calculation of the area of the base, sides, and top.

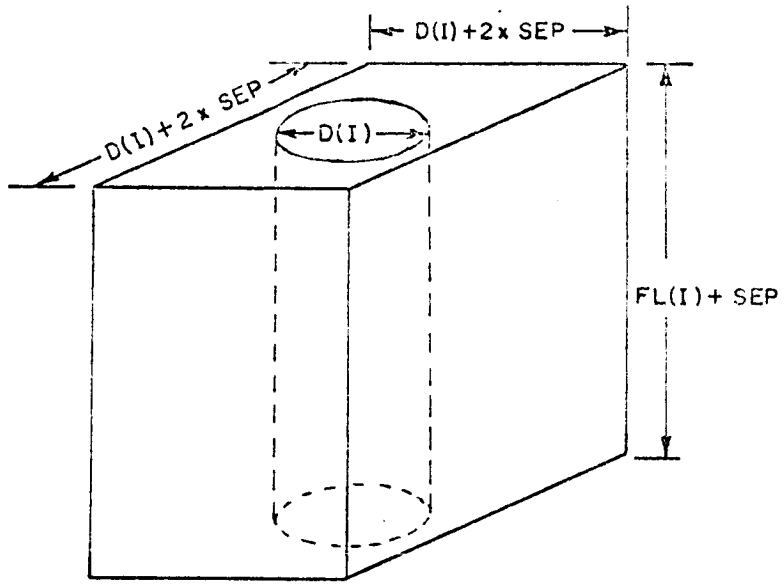

FIGURE 10. SKETCH OF CYLINDRICAL COMPONENT IN BLOCK

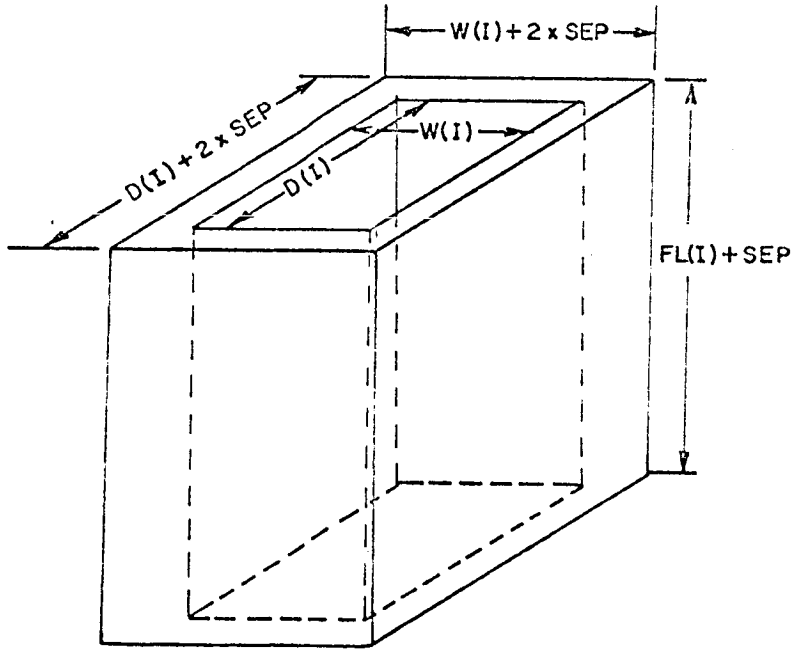

FIGURE 11. SKETCH OF RECTANGULAR COMPONENT IN BLOCK

The thickness of the base, sides, top, and insulation are used with the appropriate area to determine the volume of the base, cover, and insulation materials. These volumes are then multiplied by the density of the material used in each item to find the estimated weight of that item.

Figures D-1 through D-9 in Appendix D depict nine designs for the case where the base of the IMU is mounted horizontally in the vehicle. The analytic expressions which are solved to determine the dimensions of the IMU for a set of three gyroscopes and three accelerometers are presented in each figure. Similarly, Figures D-10 through D-15 in Appendix D depict six designs for the case where the base of the IMU is mounted in a vertical plane in the vehicle. Restrictions such as limitation of that design to pendulous accelerometers are noted on the figures.

As an example of the procedure used to determine the dimensions of the IMU, horizontal design 1 shown in Figure 12 can be analyzed as follows. The critical paths which must be evaluated to determine the dimension are

$$A = W(1) + D(3) + D(6) + 2 \times S2 + 2 \times XBSE,$$

$$A = W(1) + W(4) + D(6) + 2 \times S2 + 2 \times XBSE,$$

$$A = FL(2) + W(5) + D(3) + 3 \times SEP + 2 \times XBSE, \text{ and}$$

$$A = FL(2) + W(5) + W(4) + 3 \times SEP + 2 \times XBSE,$$

where:

A	= Dimension along one side of the base
W(1)	= Dimension perpendicular to the input axis of accelerometer 1
W(4)	= Dimension perpendicular to the input axis of gyro 4 (roll)
W(5)	= Dimension perpendicular to the input axis of gyro 5 (yaw)
D(3)	= Dimension along the input axis of accelerometer 3
D(6)	= Dimension along the input axis of gyro 6 (pitch)
FL(2)	= Dimension along the output axis of accelerometer 2
S2	= Twice the separation between sensors
XBSE	= Clearance between the edge of the SAB and the edge of the base
SEP	= Separation between sensors in the assembled block.

The critical paths which must be evaluated to determine the B dimension are

$$B = FL(1) + D(2) + S2 + 2 \times XBSE,$$

$$B = W(6) + D(5) + 3 \times SEP + 2 \times XBSE,$$

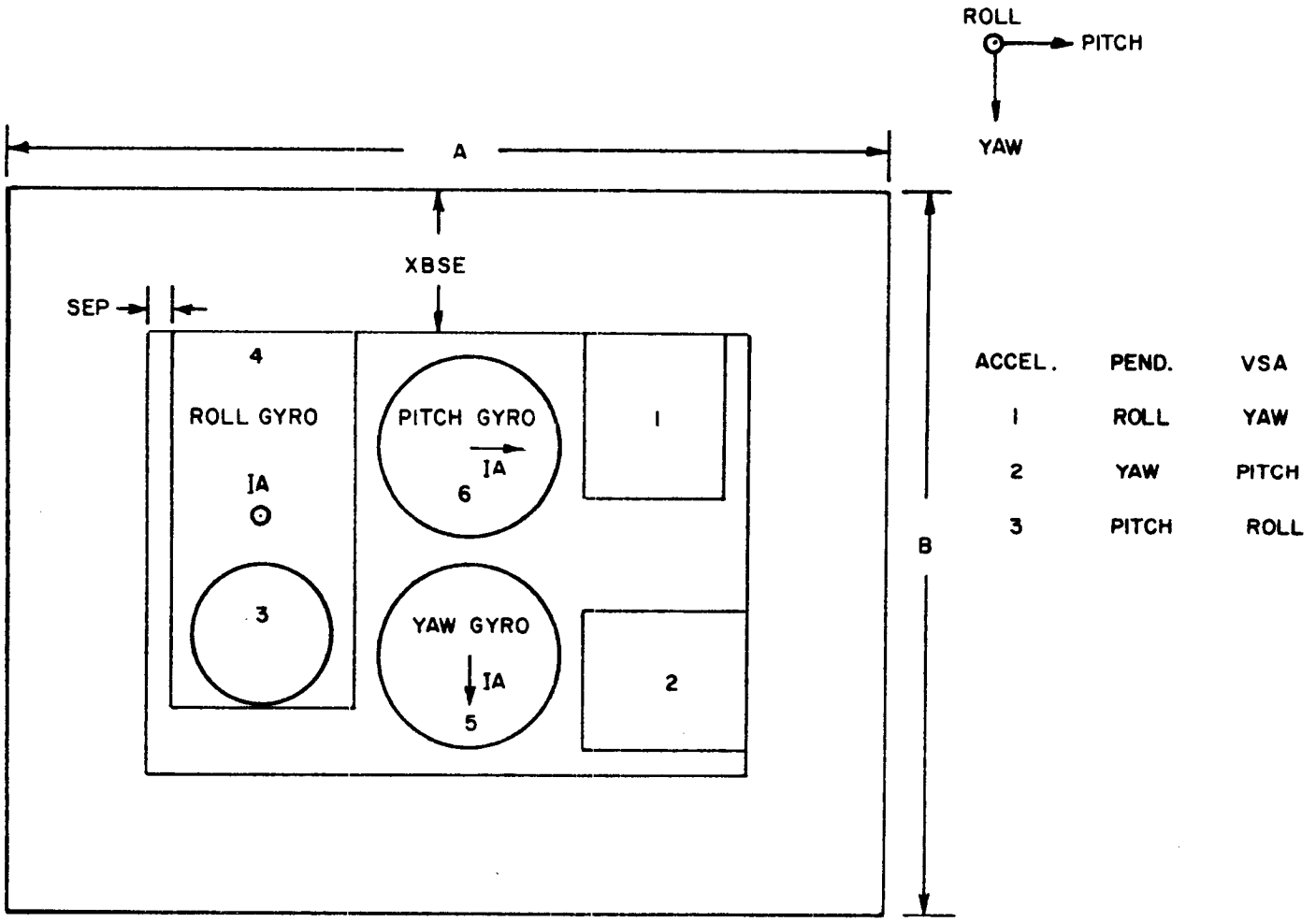

FIGURE 12. TOP VIEW OF IMU BASE AND SAB, HORIZONTAL DESIGN 1

$$B = FL(4) + SEP + 2 \times XBSE, \text{ and}$$

$$B = W(3) + S2 + 2 \times XBSE,$$

where

B = Dimension along other side of the base
FL(1) = Dimension along the output axis of accelerometer 1
FL(4) = Dimension along the output axis of gyro 4 (roll)
D(2) = Dimension along the input axis of accelerometer 2
D(5) = Dimension along the input axis of gyro 5 (yaw)
W(6) = Dimension along the spin axis of gyro 6 (pitch).

The critical paths which must be evaluated to determine the C (height) dimension are

$$C = D(1) + S2 + XCOV,$$

$$C = W(2) + S2 + XCOV,$$

$$C = FL(5) + SEP + XCOV,$$

$$C = FL(6) + SEP + XCOV, \text{ and}$$

$$C = D(4) + FL(3) + S2 + XCOV,$$

where

C = Height dimension of IMU
D(1) = Dimension along the input axis of accelerometer 1
D(4) = Dimension along the input axis of gyro 4 (roll)
W(2) = Dimension perpendicular to the input axis of accelerometer 2
FL(5) = Dimension along the output axis of gyro 5 (yaw)
FL(6) = Dimension along the output axis of gyro 6 (pitch)
FL(3) = Dimension along the output axis of accelerometer 3
XCOV = Separation between cover and highest point on SAB.

The longest critical path in each direction, A, B, and C, is determined from dimensions of the inertial sensors selected for the IMU and the specified clearances.

The volume and weight of the base are calculated as follows:

$$VBSE = A \times B \times TBSE, \text{ and}$$

$$WBSE = VBSE \times RHOBSE,$$

where

VBSE = Volume of the base,
TBSE = Thickness of the base,
WBSE = Weight of the base, and
RHOBSE = Density of the material comprising the base.

The volume and weight of the cover are calculated as follows:

$$VCOV = (2 \times C \times [A + B] + A \times B) \times TCOV, \text{ and}$$

$$WCOV = VCOV \times RHOCOV,$$

where

VCOV = Volume of the cover,
TCOV = Thickness of the cover,
WCOV = Weight of the cover, and
RHOCOV = Density of the material comprising the cover.

The volume and weight of the insulation are calculated as follows:

$$VINS = (2 \times C \times [A \times B] + A \times B) \times TINS, \text{ and}$$

$$WINS = VINS \times RHOINS,$$

where

VINS = Volume of the insulation ,
TINS = Thickness of the insulation,
WINS = Weight of the insulation, and
RHOINS = Density of the insulation material.

The total inertial measurement unit (IMU) weight is estimated by summing the weight of (1) the inertial sensors in the IMU (three gyroscopes and three accelerometers), (2) the sensor assembly block (SAB), (3) the base, (4) the cover, (5) the insulation, and (6) the electronics plus any other weight which may be considered constant such as vibration isolators. In designing a SAB, access to the inertial sensors and center of gravity considerations must be

kept in mind. The conceptual designs in Appendix D are by no means firm designs and are for illustrative purposes only.

Computer Weight.--The suggested means of estimating the strapdown inertial guidance system computer weight was determined by analyzing state-of-the-art computers such as the UNIVAC 1824, Honeywell, Inc. SIGN III, CDC 5360, and Nortronics NDC-1051. The computer was broken down into major components and a weight factor estimated for each of the components. Table X contains the computer component breakdown and preliminary weight factors.

TABLE X
STRAPDOWN IGS COMPUTER COMPONENTS
AND PRELIMINARY WEIGHT FACTORS

Component	Preliminary Weight Factor
Input/Output (I/O) Logic Modules	4.0 lb/tray
Input/Out Tray Structure	1.5 lb/tray
Memory Module(s)--Memory Stack and Electronics	5.0 lb/tray of 4,096 words, 18-24 bit Fe Core 4.0 lb/tray of 2,048 words, 18-24 bit Fe Core 2.0 lb/tray of 1,024 words, 18-24 bit Fe Core
Memory Tray Structure	1.0 lb/tray
Processor Module(s)--Control Logic and Arithmetic Register	4.0 lb/tray
Processor Tray Structure	1.5 lb/tray
Power Supply and Timing Assembly Module	5.0 lb/tray assuming 80-120 watts required
Power Supply Tray Structure	1.0 lb/tray
Computer Base	2.0 lb
Computer Cover	2.0 lb
Wiring	2.0 lb/2,048 to 4,096 words
Other	?

The preliminary weight factors were estimated based upon a computer organized in a modular fashion in which the tray structure of the modules are assumed to form four sides of the computer case. The trays containing the modules would be fastened together with the base and cover completing the computer case. For an 8,192 word computer memory capacity, two memory trays would be required and possibly an additional one pound allowed for wiring. It is emphasized that the data in Table X is an estimate and based upon ferrite core memories.

Using the weight factors presented in Table X, an estimate of the weight of an 8,192 word computer was made and is shown in Table XI.

TABLE XI
WEIGHT ESTIMATE FOR 8,192 WORD SRT COMPUTER

Component	Preliminary Weight Est. (lb)
I/O Modules	4.0
I/O Tray Structure	1.5
Memory Module(s)	10.0
Memory Tray Structure	2.0
Central Processor	4.0
Central Processor Tray	1.5
Power Supply	5.0
Power Supply Tray	1.0
Base	2.0
Cover	2.0
Wiring	3.0
EST. TOTAL WEIGHT	36.0 lb

Since this technique is quite simple and the computer requirements vary little from one strapdown IMU to another for the same interplanetary mission, it was felt that this weight calculation did not require a computer subroutine. If a particular change in one of the computer modules such as the memory stack and electronics is to be evaluated, the user should substitute his weight estimate for that module in place of the weight factor in Table X. Since the primary objective of this contract was not to develop a computer weight estimating technique, development of a more sophisticated weight estimation technique based on density of materials, type of memory, number of bits, etc., was not investigated further.

System Power.--Estimation of the system power requirements is dependent upon the thermal design of the IMU as well as the computer. The guidance system operating sequence also is a factor in the total system power requirements. After determining the power requirements, consideration must be given to the energy source which will supply this power. This section discusses

the techniques developed to determine the system power.

IMU Power.--The inertial sensors can be maintained at their designed operating temperature by two methods. These are (1) use of the heater windings on each sensor with the appropriate temperature control electronics duplicated for each instrument, or (2) use of a sensor assembly block (SAB) heater with its associated temperature control amplifier, bridge circuit, thermistor, etc. If the former method is used, it is desirable to have a high thermal resistance between each inertial sensor and the SAB. Use of the latter method requires high thermal conductance between the inertial sensors and the SAB. Many of the present-day strapdown guidance systems are heated by the latter method (References 11 and 12).

Heating of the SAB alone with no fine control of the temperature of each inertial component is likely to cause some degradation in the accuracy of floated instruments since it is probable no two instruments will float at neutral buoyancy at exactly the same temperature. This degradation in accuracy is offset somewhat by a slight reliability gain and weight decrease achieved by elimination of temperature control electronics for each sensor.

The primary concern in thermal control of the IMU should be to minimize the total system power required. The power (heat) flow of the IMU can be expressed by the equation

$$Q_R + Q_C + Q_{exc} = Q_S + Q_L$$

where:

Q_R -- is the summation of direct and reflected solar radiations, direct and reflected earth albedo radiation, and direct and reflected earth thermal radiation on the IMU,

Q_C -- is the power to the IMU from the temperature controller,

Q_{exc} -- is the power into the IMU from the excitation of the wheels, signal and torque generators, electronics, etc.,

Q_S -- is the rate at which heat is stored in the IMU, and

Q_L -- is the lost or dissipated power due to radiation and conduction from the IMU.

Furthermore,

$$Q_L = K_1(T - T_a)$$

where $(T - T_a)$ is the difference between the temperature of the inertial sensors on the SAB, T, and the ambient temperature, T_a. K_1, the thermal conductance between the IMU and the vehicle, can be calculated for $Q_C = 0$ when T_a is at its maximum value, $T_{a_{max}}$. In this case,

$$K_1 = \frac{Q_{exc}}{T - T_{a_{max}}} \text{ (watts/}^{o}\text{ F)} \quad .$$

If a material with such a value of thermal conductance could be found and used, no cooling of the IMU would be required. If the average ambient temperature is much lower than the maximum ambient and if the maximum ambient occurs for only a short time period, consideration should be given to setting the thermal impedance to minimize the total temperature controller power. This involves a tradeoff between the heat sink weight (thermal impedance set for less than maximum ambient temperature) and the extra power source weight (thermal impedance set for no cooling at maximum ambient temperature) when the average ambient temperature is much lower than the maximum. The computer program containing this IMU power estimation technique allows the user to load a user selected value for K_1 or will calculate K_1 for $Q_C = 0$ as in the previous equation. Also,

$$Q_S = K_2 \frac{dT}{dt}$$

where K_2 is the thermal storage constant and has units of watts/(^{o}F/sec). It is presently assumed that dT/dt, the rate of change of the sensor operating temperature with time, is zero. Further discussion of temperature control problems for inertial components can be found in References 13 and 14. K_1 and K_2 can be found experimentally for an existing system.

Data on T_a as a function of time along the trajectory are needed to perform a precise thermal (power) analysis of the IMU. If these data are not available, an estimate of the average T_a can be made by the user as was done in the exercising of this program. Of course, Q_R and T_a depend upon the location of the IMU on the vehicle. Since many possible tradeoffs exist in thermal control of the IMU, this should by no means be considered as other than a tool for estimating the IMU power. The user should keep in mind that the value of K_1 he selects, should he elect not to have $Q_C = 0$ at $T_{a_{max}}$, is quite important.

In summary, the IMU power is currently estimated by (1) calculating or specifying a thermal conductance, K_1, (2) assuming an average ambient temperature, $T_{a_{ave}}$, and (3) assuming an IMU operating temperature, T_{op}. Expressed analytically, the IMU power is

$$P_{IMU} = K_1(T_{op} - T_{a_{ave}}) \quad .$$

Computer Power.--The power being supplied to the computer is that power required to operate the various modules such as input/output plus that dissipated in the power supply. The computer does not usually require maintenance of a constant temperature. From a thermal viewpoint, the designer is principally concerned with dissipating enough of the heat to prevent a temperature rise over the designed operating temperature range of the computer. Since a precise power and thermal analysis depends upon the design of a specific computer which depends upon its use, we are principally concerned only with estimating the power required to operate the computer. Therefore, the logical approach is to sum the estimates of the power required by each of the modules making up the computer. These are shown below in Table XII. For example, if a change from one type of memory to another is made, the power estimates should be checked and revised as required to reflect the requirements of the new memory type. Similar practice should be followed for the other modules.

TABLE XII
STRAPDOWN IGS COMPUTER MODULES AND POWER REQUIRED

Module	Example of Preliminary Power Estimate
Input/Output (I/0) Logic Module(s)	20 watts
Memory Module(s) - Ferrite Core, 8K Stack and Electronics	20 watts
Processor Module(s)	15 watts
Σ Power	55 watts

To find the total computer prime power, divide the summation of the power of the three functional modules in Table XII by the efficiency of the computer power supply module. That is:

$$\text{Computer Prime Power} = \frac{\Sigma(\text{I/O + Memory + Processor) Power}}{\text{Efficiency Power Supply}} \quad .$$

For the example above, a typical efficiency of 60% would give:

$$\text{Computer Prime Power} = \frac{55}{0.60} \cong 92 \text{ watts} \quad .$$

Since the I/O module power depends upon the electrical interfaces of the IMU, telemetry, etc., with the computer, precise power estimates cannot be made until this information is available. Therefore, a subroutine to calculate computer power was not written. Instead, the user is required to input actual or user estimated computer power as data. If the user of these techniques does estimate the computer power required from the guidance power source, he must keep in mind the significance of the I/O interfaces.

Estimated Power.--The guidance system power required from the power source is simply the summation of the IMU power and the computer power. As currently used in the computer program implementing these techniques, the average system power is found by assuming that the system operates continuously from launch to the midcourse correction burn in an average ambient temperature. Expressed analytically, we have

$$P_{IC} = P_C + K_1(T_{op} - T_{a_{ave}})$$

where:

P_{IC} = Average power required by the IMU and computer,

P_C = Average power required by the computer,

K_1 = Thermal conductance,

T_{op} = Operating temperature of the IMU, and

$T_{a_{ave}}$ = Average ambient temperature over the trajectory.

Guidance Power Subsystems.--At present, there are four power subsystems available for production of raw electrical power: chemical fuels, solar energy, radioisotope thermal energy, and nuclear fission energy (References 15 through 22). Chemical subsystems (hydrogen-oxygen, hydrazine and solid propellants, fuel cells, batteries) provide energy limited sources whose performances are time dependent. Primary batteries, for example, serve quite well for relatively low power requirements (up to about 100 watts) for around one to three day mission. Chemical dynamic systems using storable propellants (H_2-O_2, hydrazine) can produce higher power than primary batteries but show about the same time dependency characteristic. Fuel cells using hydrogen and oxygen as reactants extend the duration period to three or four weeks for power levels up to about 1-2 KW (e.g., Apollo Command and Service Module). When the energy conversion unit limits the available power (as opposed to energy source limitation) the subsystem is categorized as power limited. Solar energy conversion is an example of a power limited subsystem and has been utilized through the application of single-crystal silicon cells since 1960 (Tiros). As of today, the solar cell is the dominant source of power in long-lived spacecraft (i.e., in excess of one year in space) requiring 0.5-1 KW. Radioisotopes

are another example of power limited sources. Power levels of a few kilowatts lasting in excess of a year are available through proper use of the radioisotope. Its big advantage over the silicon solar cell is that its output does not vary with distance to the sun. Nuclear reactors with varying conversion units are being produced under the SNAP (Space Nuclear Axiliary Power program to provide higher levels (i.e., 10-100 KW or more) for durations well over a year.

Between the source and the load there is a power conversion device described as a cell, dynamic, thermoelectric, or thermionic type. These converters are applicable to the various sources (except for the chemical direct conversion) so that the choice of system concepts for a given requirement is quite broad. However, performances of the different combinations are not separated by thin, well-defined lines found on a plot of power levels versus mission duration. The problem of this "overlapping" effect is that the choice of a suitable power subsystem is often far from obvious, and, as one would begin to suspect, details of the specific application are needed for a satisfactory solution.

When the details of the specific application are known, a suitable power subsystem can be selected. Factors such as the time of operation of the power subsystem, its specific power or specific energy, i.e., watts/lb or watt-hours/lb, and any constant weight factor are used in determination of the principal item of concern, the guidance system power subsystem weight. It is this weight which is dependent upon the guidance system power requirements and is used in the penalty functions as a factor in the total effective guidance system weight.

An example of the guidance power subsystem weight determination result is given in a subsequent section of this report. In this example, the selection of the power subsystem was based upon mission analysis. The weight in this specific case was determined by solving the following equation:

$$W_P = K_{P1} + K_{P2} P_{IC}$$

where K_{P1} is power source constant weight, K_{P2} is the reciprocal of power source specific power density, and P_{IC} is the average power required by the IMU and computer.

Reliability.--Several possible reliability descriptions were examined. The Weibull distribution was chosen to allow more realistic estimation of failure probabilities without the large amounts of data needed for more complex distributions such as the Markovian. The Weibull distribution is especially attractive as it contains the more commonly used exponential model as a special case (References 23 and 24).

The Weibull distribution assumes a hazard function with a failure rate proportional to a power of time or,

$$\dot{P}_s(t)/P_s(t) = -\alpha\lambda t^{\alpha-1}$$

which yields the probability of success,

$$P_s(t) = e^{-\lambda t^{\alpha}}$$

which for $\alpha = 1$ is identical to the exponential distribution.

The expected life or mean time to failure (MTTF) is obtained by

$$MTTF = \int_0^{\infty} tP_s(t)dt$$

which for the Weibull distribution gives

$$MTTF = \int_0^{\infty} te^{-\lambda t^{\alpha}} dt = \left(\frac{1}{\lambda}\right)^{1/\alpha} \Gamma(1 + 1/\alpha)$$

where $\Gamma(x)$ is the Gamma function. Since MTTF is a more meaningful parameter than the arbitrary λ, the following substitutions will be made.

Let $\Phi(\alpha) = \Gamma(1 + 1/\alpha)$,

$T = MTTF$,

$\lambda = (\Phi(\alpha)/T)^{\alpha}$

$P_s(t) = e^{-(\Phi(\alpha)t/T)^{\alpha}}$, and

$P_F(t) = 1 - P_s(t)$.

The form of the equation for $P_s(t)$ is convenient as it contains time normalized to MTTF. The function $\Phi(\alpha)$ is between approximately 0.88 and 1.0 for all α greater than 1.0. Figure 13 shows t/T for several values of probability and α.

Figure 14 shows the effect of increasing α. For α larger than 1.0, failures are more likely to occur near the MTTF. In the limit, as α approaches infinity, all units would fail at exactly their MTTF. Obtaining data for α will involve special test procedures. However, as stated above, assuming α

ALPHA	PHI(ALPHA)	PROBABILITY OF FAILURE											
		.9990	.9950	.9900	.9500	.9000	.7000	.5000	.3000	.1000	.0500	.0100	.0050	.0010
1.0	1.000000	6.9078	5.2983	4.6052	2.9957	2.3026	1.2040	.6931	.3567	.1054	.0513	.0101	.0050	.0010
1.1	.965245	6.0034	4.7170	4.1525	2.8040	2.2113	1.2265	.7424	.4058	.1339	.0696	.0158	.0084	.0019
1.2	.941510	5.3165	4.2621	3.7921	2.6501	2.1282	1.2398	.7826	.4449	.1628	.0894	.0230	.0129	.0034
1.3	.924383	4.7840	3.9010	3.5022	2.5159	2.0548	1.2478	.8160	.4895	.1918	.1101	.0314	.0184	.0053
1.4	.911889	4.3510	3.6083	3.2644	2.4011	1.9897	1.2521	.8440	.5251	.2198	.1314	.0410	.0250	.0076
1.5	.903600	4.0140	3.3634	3.0633	2.2998	1.9297	1.2525	.8668	.5566	.2469	.1528	.0515	.0324	.0111
1.6	.897300	3.7295	3.1597	2.8946	2.2125	1.8769	1.2515	.8863	.5851	.2730	.1741	.0629	.0407	.0148
1.7	.892662	3.4917	2.9873	2.7508	2.1390	1.8297	1.2495	.9030	.6109	.2981	.1952	.0746	.0497	.0193
1.8	.890280	3.2868	2.8364	2.6239	2.0663	1.7853	1.2453	.9163	.6335	.3217	.2157	.0872	.0593	.0242
1.9	.888148	3.1137	2.7079	2.5153	2.0059	1.7464	1.2415	.9284	.6544	.3445	.2358	.1000	.0693	.0297
2.0	.886230	2.9657	2.5973	2.4215	1.9530	1.7122	1.2381	.9394	.6739	.3663	.2556	.1131	.0799	.0357
2.2	.886698	2.7148	2.4065	2.2579	1.8570	1.6477	1.2271	.9547	.7058	.4055	.2923	.1394	.1016	.0488
2.4	.887088	2.5221	2.2582	2.1300	1.7806	1.5957	1.2179	.9676	.7336	.4414	.3270	.1656	.1241	.0634
2.6	.888831	2.3659	2.1345	2.0243	1.7157	1.5506	1.2083	.9771	.7568	.4735	.3590	.1918	.1468	.0790
2.8	.891636	2.2365	2.0344	1.9350	1.6596	1.5107	1.1984	.9839	.7761	.5021	.3883	.2169	.1692	.0952
3.0	.894067	2.1301	1.9499	1.8609	1.6124	1.4770	1.1899	.9899	.7932	.5283	.4156	.2414	.1914	.1119
4.0	.907820	1.7858	1.6712	1.6137	1.4492	1.3569	1.1539	1.0051	.8513	.6276	.5242	.3488	.2931	.1959
5.0	.918170	1.6030	1.5202	1.4782	1.3564	1.2868	1.1303	1.0121	.8862	.6944	.6013	.4340	.3775	.2736
6.0	.929230	1.4851	1.4209	1.3881	1.2921	1.2366	1.1100	1.0124	.9063	.7396	.6560	.4999	.4452	.3402
7.0	.937130	1.4064	1.3541	1.3272	1.2452	1.2021	1.0958	1.0127	.9210	.7737	.6981	.5531	.5008	.3974
8.0	.943055	1.3501	1.3061	1.2834	1.2103	1.1769	1.0853	1.0129	.9322	.8004	.7315	.5957	.5470	.4472
9.0	.947663	1.3040	1.2700	1.2504	1.1920	1.1577	1.0772	1.0131	.9410	.8218	.7586	.6329	.5859	.4898
10.0	.951350	1.2752	1.2419	1.2246	1.1730	1.1426	1.0708	1.0133	.9482	.8393	.7810	.6636	.6190	.5268
12.0	.959458	1.2244	1.1976	1.1837	1.1420	1.1173	1.0585	1.0109	.9565	.8640	.8137	.7104	.6704	.5861
14.0	.965250	1.1894	1.1670	1.1554	1.1205	1.0996	1.0498	1.0092	.9625	.8822	.8380	.7459	.7097	.6325
16.0	.969594	1.1638	1.1446	1.1347	1.1046	1.0865	1.0434	1.0080	.9670	.8960	.8566	.7737	.7407	.6648
18.0	.972972	1.1443	1.1275	1.1188	1.0924	1.0765	1.0384	1.0071	.9706	.9070	.8714	.7960	.7658	.7002
20.0	.975675	1.1289	1.1140	1.1063	1.0827	1.0686	1.0345	1.0063	.9734	.9159	.8835	.8143	.7865	.7254
25.0	.980540	1.1018	1.0902	1.0841	1.0656	1.0544	1.0274	1.0050	.9786	.9321	.9056	.8484	.8252	.7736
30.0	.983783	1.0841	1.0746	1.0696	1.0543	1.0451	1.0228	1.0041	.9821	.9430	.9207	.8720	.8520	.8074
35.0	.986100	1.0717	1.0636	1.0593	1.0464	1.0386	1.0195	1.0035	.9847	.9509	.9316	.8892	.8717	.8325
40.0	.987837	1.0624	1.0554	1.0517	1.0405	1.0336	1.0170	1.0031	.9866	.9569	.9399	.9023	.8868	.8518
45.0	.989189	1.0553	1.0491	1.0458	1.0359	1.0298	1.0151	1.0027	.9880	.9616	.9464	.9127	.8997	.8671
50.0	.990270	1.0496	1.0441	1.0411	1.0322	1.0268	1.0136	1.0025	.9892	.9654	.9516	.9211	.9083	.8795
55.0	.991155	1.0450	1.0400	1.0373	1.0293	1.0243	1.0123	1.0022	.9902	.9685	.9559	.9280	.9163	.8899
60.0	.991892	1.0412	1.0366	1.0342	1.0268	1.0223	1.0113	1.0020	.9910	.9711	.9595	.9338	.9230	.8985
65.0	.992515	1.0379	1.0337	1.0315	1.0247	1.0206	1.0104	1.0019	.9917	.9733	.9625	.9387	.9287	.9060
70.0	.993050	1.0352	1.0313	1.0292	1.0229	1.0191	1.0097	1.0017	.9923	.9751	.9652	.9429	.9336	.9124
75.0	.993513	1.0328	1.0292	1.0272	1.0214	1.0178	1.0090	1.0016	.9928	.9768	.9674	.9466	.9379	.9180
80.0	.993919	1.0307	1.0273	1.0255	1.0200	1.0167	1.0085	1.0015	.9932	.9782	.9694	.9499	.9417	.9229
85.0	.994276	1.0289	1.0257	1.0240	1.0188	1.0157	1.0080	1.0014	.9936	.9795	.9712	.9528	.9450	.9273
90.0	.994594	1.0273	1.0242	1.0226	1.0178	1.0148	1.0075	1.0013	.9940	.9806	.9728	.9553	.9480	.9312
95.0	.994879	1.0258	1.0229	1.0214	1.0168	1.0140	1.0071	1.0013	.9943	.9816	.9742	.9576	.9506	.9347
100.0	.995135	1.0245	1.0218	1.0204	1.0160	1.0133	1.0068	1.0012	.9946	.9825	.9755	.9597	.9531	.9378

OPERATING TIME DIVIDED BY MEAN TIME TO FAIL

FIGURE 13. WEIBULL TABLE

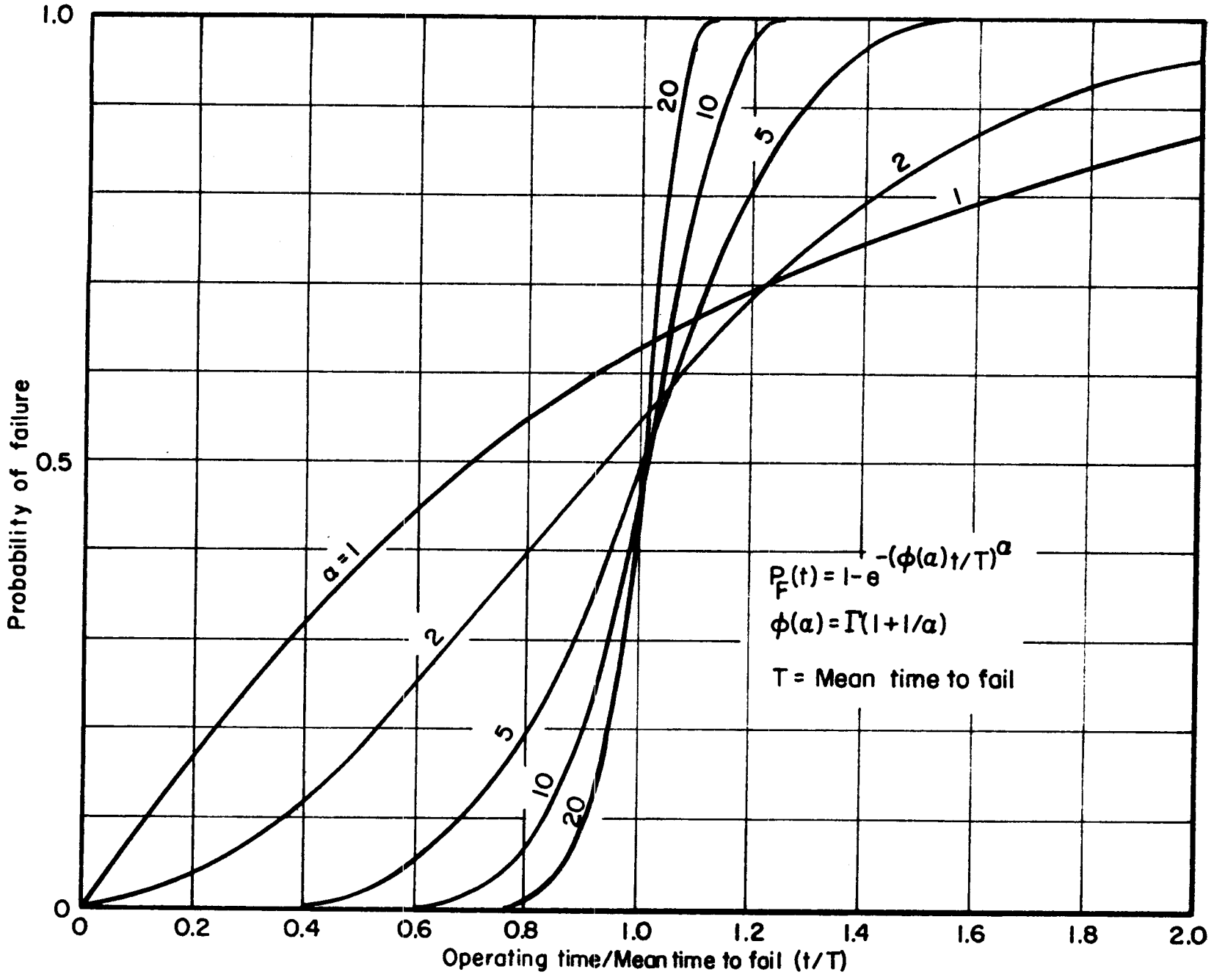

FIGURE 14. THE WEIBULL DISTRIBUTION

equals 1.0 yields the more familiar exponential distribution. This assumption should be made when better knowledge of α is not available.

The probability of failure due to reliability for the entire guidance system is computed with the distributions and operating times shown in Table XIII.

TABLE XIII
RELIABILITY ESTIMATION

Component	Distribution	Operating Time
Accelerometers	Weibull	Time of thrust(s)
Gyroscopes	Weibull	Time to midcourse
Computer	Weibull	Time to midcourse
Electronics	Exponential	Time to midcourse
Energy Source	Exponential	Time to midcourse
Midcourse System	-------- Fixed probability of failure ----------	

Accuracy Analysis.--In the evaluation of any of the three penalty functions, four system parameters related to accuracy are needed. These are the square root of the trace and the degrees of freedom for each covariance matrix describing midcourse delta-V and errors at the target. Additional information in the form of standard deviations or covariance matrices of other error quantities may be of interest but are not needed for penalty evaluation.

Nine components of error are of interest. In general these are split into a set of six position-velocity errors and a set of three attitude errors. All errors are described in the local vertical coordinate system defined in Figure 15. Attitude error components are small angles about each axis.

Injection Errors.--The injection errors are obtained by multiplying the vector representing hardware (accelerometers, gyroscopes, and the computer) errors by a matrix produced by the Strapdown Error Analysis Program (SEAP) supplied by NASA/ERC. SEAP obtains the injection error sensitivities for each source by integrating the navigation error equations with the appropriate forcing function for the error model.

IMU Error Models.--Appendix E of this report contains a derivation of the error model for the single-degree-of-freedom gyroscope, and Appendix F contains a similar derivation for the pendulous accelerometer. Of the error sources

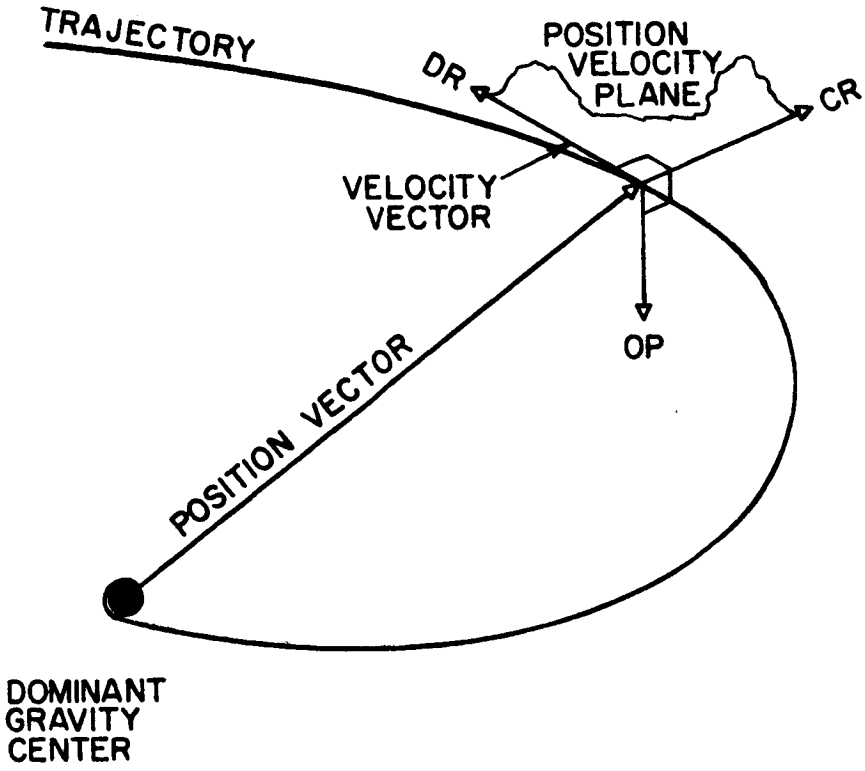

THE THREE ORTHONORMAL COMPONENTS ARE:

DR DOWN RANGE (THE DIRECTION OF VELOCITY)

CR CROSS RANGE (NORMAL TO VELOCITY, IN THE P-V PLANE)

OP OUT-OF-PLANE (COMPLETES THE SET).

FIGURE 15. LOCAL VERTICAL COORDINATE SYSTEM

listed in Table E-1 of Appendix E, those listed in Table XIV are not presently contained in SEAP.

For error analysis we are primarily concerned with the uncertainty in each of the error coefficients. If the error coefficient is a deterministic value that can be compensated with zero uncertainty, then it could be considered to make no contribution to the navigation errors.

TABLE XIV
SINGLE-DEGREE-OF-FREEDOM GYROSCOPE
ERROR SOURCES TO BE ADDED TO SEAP

Symbol	Forcing Excitation	Nomenclature
$\frac{S_{loop}}{H}[\theta;M]$	θ or ω_{IA}	Rebalance loop scale factor - includes signal and torque generator, loop transfer function, and wheel speed modulation errors
D_{KSI}	a_I^2	Spin axis compliance drift
D_{KIS}	a_S^2	Input axis compliance drift
D_{KSO}	$a_O a_I$	Spin axis compliance drift
D_{KIO}	$a_O a_S$	Input axis compliance drift
D_{UO}	a_O	Dump term per MIT Instrumentation Lab.
$\frac{I_{OA}}{H}$	$\dot{\omega}_{OA}$	Output axis inertia (OA angular acceleration error)
$\frac{(I_{IA} - I_{SA})}{H}$	$\omega_{IA}\omega_{SA}$	Anisoinertia
ω_{SA}	θ or ω_{IA}	Spin axis cross coupling (kinematic rectification)
E	θ	Elastic restraint Coning Quantization

Table XV lists those pendulous accelerometer errors sources in Table F-1 of Appendix F which are not presently contained in SEAP.

System errors can exist due to the effects discussed below:

(1) Gyro loops with different gains and phase shifts (time constants) at a specific vibration frequency cause errors in the computation process. If the net drift from this effect is expressed as

$$\omega_{d_j} = \omega_{r,j+1}\,\omega_{r,j+2}\,(\tau_{g_{j+2}} - \tau_{g_{j+1}}) \qquad j = 1,2,3,1,2, \ldots$$

then the effect of instrument quantization, $\Delta\theta$, can be evaluated by substituting the best estimate for the time of occurrence of $\Delta\theta$, $\frac{\Delta\theta}{2\omega_{r_j}}$, for τ_{g_j}. This error has been referred to as pseudo coning (Reference 25), fictitious coning, or commutation error (Reference 26).

(2) Angular vibration about the input axis of one gyro is also an angular vibration about the output axis of another gyro. A pseudo coning effect results when the computer processes the signals due to this effect (Reference 25).

(3) Accelerometer and gyro loop with different gain and phase shift characteristics at the same vibration freqency cause the computational process to introduce an acceleration error when subjected to a coherent linear and angular vibration. This error has been called pseudo sculling.(Reference 25).

(4) The separation of the accelerometer axes in a system produces a system size effect error which could be partially compensated. The uncertainty in the computed velocity and position due to this effect should be considered in the system error analysis.

Computer Error Models.--The errors due to computer parameters (computation frequency, number of bits, and integration scheme) were studied. Reference 27 formulates the problem as shown in Figure 16. This is the same approach that is applied to hardware error models in computer programs such as SEAP. The problem is reduced to describing instantaneous generated error rates $\vec{\epsilon}$ as a function of $\vec{U}$ and $\vec{X}$ where $\vec{U}$ is the vector of sensor inputs and $\vec{X}$ the state of the system.

Reference 27 solves for $\vec{e}(t)$ by defining a matrix function Z by the differential equation

$$\left[\frac{dZ(t,s)}{dt}\right] = \left[\frac{\partial f}{\partial x}\right]\left[Z(t,s)\right] \quad (t \geq s); \quad \left[Z(t,s)\right] = \left[I\right] \quad (t = s)$$

TABLE XV
TORQUED PENDULUM ACCELEROMETER
ERROR SOURCES TO BE ADDED TO SEAP

Symbol	Forcing Excitation	Nomenclature
$\frac{I_{OA}}{P}$	$\dot{\omega}_{OA}$	Output axis angular acceleration error
$\frac{I_{IA} - I_{PA}}{P}$	$\omega_{IA}\omega_{PA}$	Anisoinertia
$\frac{1}{P}$	$a_{PA}A_{ca,p}, a_{OA}A_{m_{OA}}, a_{PA}A_{m_{PA}}$	Vibropendulous
$\frac{I_{IA} - I_{PA}}{P}$	$\begin{bmatrix} (\omega_{IA}^2 + \omega_{PA}^2)\, A_{m_{PA}} + (\omega_{IA}^2 - \omega_{PA}^2)\, A_{ca,P} \\ - (\omega_{IA}\, \omega_{OA})\, A_{m_{OA}} \end{bmatrix}$	Rotational cross coupling
	$(\omega_{OA}^2 + \omega_{PA}^2)\, R_{(cg_{veh} - cg_{TPA})}$	Size effect
	$\frac{a_{PA}A_{ca,p}}{2} \cos A$	Sculling effect Quantization Rebalance loop dynamics

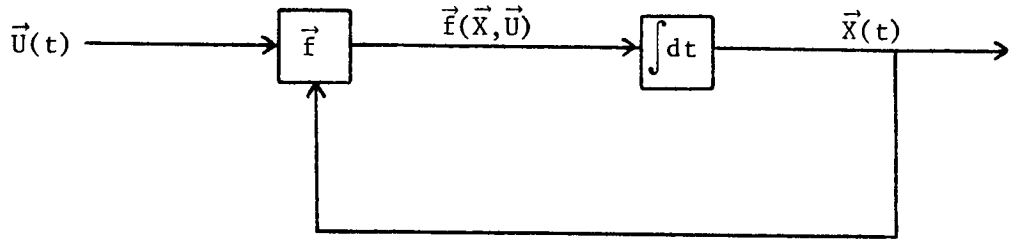

$\dot{\vec{X}} = \vec{f}(\vec{X},\vec{U})$

(a) Ideal System

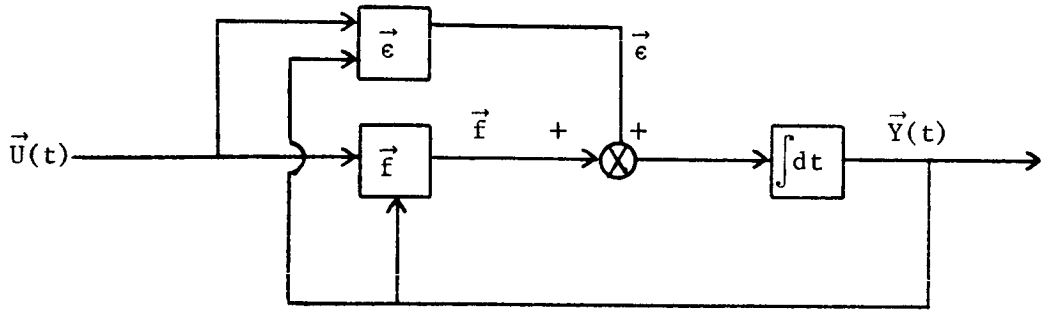

$\dot{\vec{Y}} = \vec{f}(\vec{Y},\vec{U}) + \vec{\epsilon}(\vec{Y},\vec{U})$ where ϵ = Generated Errors

(b) Real System

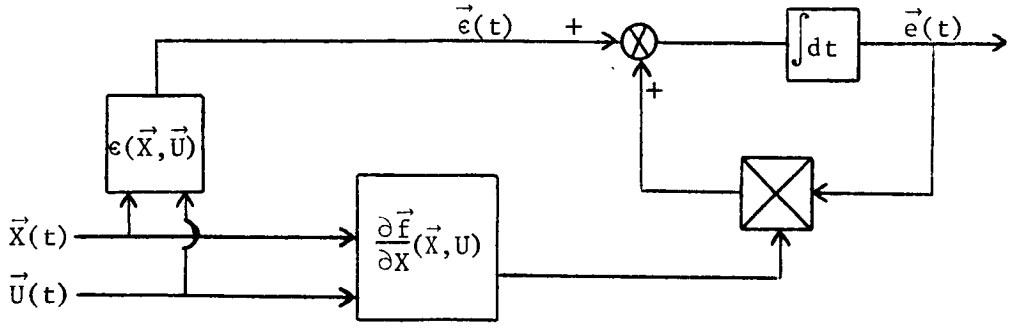

$\dot{\vec{e}} = \vec{\epsilon}(\vec{X},\vec{U}) + \frac{\partial \vec{f}}{\partial \vec{X}}(\vec{X},\vec{U}) \cdot \vec{e}$

(c) Error Model

FIGURE 16. FORMULATION OF COMPUTER ERROR MODEL

then

$$\vec{e}(t) = \left[Z(t,o)\right] \vec{e}(0) + \int_o^t \left[Z(t,s)\right] \epsilon(s)\, ds$$

where $Z(t,s)$ is the state transition matrix mapping errors at time = s to time = t.

To maintain compatibility with SEAP, the instantaneous error generation rate $\vec{\epsilon}(\vec{X},\vec{U})$ must be expanded into the form

$$\epsilon_i = \Sigma S_{ij} K_j$$

where

ϵ_i = i^{th} generated error rate component,

S_{ij} = SEAP sensitivity, and

K_j = j^{th} error coefficient.

The SEAP sensitivity is a function of the instantaneous environment, $\vec{X}$, $\vec{U}$, supplied to SEAP as trajectory information, and the error coefficients are functions of the computer parameters.

Simulation of several integration schemes were made to investigate possible methods for expressing S_{ij} and K_j for both GP and DDA computers. The formulation of Reference 28 is as good as possible while maintaining compatability with SEAP. Computer errors due to three sources are included in the model:

(1) Constant rate truncation

(2) Round off

(3) Vibration.

Constant rate truncation results in an equivalent instantaneous drift rate in degrees per hour of

(a) $36.5\ \omega_i^2/f_c$ (Rectangular Algorithm)

(b) $0.133\ \omega_i^3/f_c^{\,2}$ (Runge-Kutta - 2nd Order Algorithm)

(c) $4.62 \times 10^{-6}\ \omega_i^5/f_c^{\,4}$ (Runge-Kutta - 4th Order Algorithm)

where f_c is the attitude update computation frequency and ω_i is each component of body angular rate.

These equations have been separated into the time variation of ω to the proper power as a forcing function on attitude errors in SEAP. This handles the generation and propagation as described above, on a per unit basis. The proper SEAP sensitivity is then multiplied by the proper $1/f_c^N$ as an error coefficient where N is the power dependent upon the integration scheme as shown on the previous page.

Round off is expressed as a drift uncertainty in deg/hour of

$$2.1 \times 10^5 \, f_c / 2^{NB}$$

where NB is the number of bits in the computer word or words (if multiple precision is used) used to store the attitude matrix. Since the drift rate is not a function of time, it is treated as three identical additional error coefficients to be multiplied by the three drift sensitivities generated by SEAP for gyro fixed drift.

Vibration is treated in a similar fashion in Reference 28 with the drift uncertainty for angular vibration given as

$$\frac{117}{4\pi} \int_o^{\frac{\pi f_o}{2f_c}} \Phi \left(\frac{2f_c T}{\pi}\right) \frac{\sin^2(T)}{T^2} \, dT \qquad \text{(Rectangular Algorithm)}$$

$$\frac{0.0985}{16\pi^2 f_c} \int_o^{\frac{\pi f_o}{2f_c}} \Phi^2 \left(\frac{2f_c T}{\pi}\right) \frac{\sin^4(T)}{T^4} \, dT \qquad \text{(Runge-Kutta - 2nd Order Algorithm)}$$

$$\frac{0.0503}{16\pi^2 f_c} \int_o^{\frac{\pi f_o}{2f_c}} \Phi^2 \left(\frac{2f_c T}{\pi}\right) \frac{\sin^6(T)}{T^4} \, dT \qquad \text{(Runge-Kutta - 4th Order Algorithm)}$$

where Φ is the spectral vibration density passed to the computer by the gyro. It has been assumed that $\Phi(f)$ is a constant spectrum Φ for $0 \leq f \leq f_o$.

A summary of the computer error contributions is shown in Table XVI.

TABLE XVI
COMPUTER ERROR MODEL

Error Type	Error Coefficient Associated with a Computer	Sensitivity Mapping to Pos., Vel., or Attitude Errors	
Roundoff X	$2.1 \times 10^5 \, f_c/2^{NB}$	R_X	Repeated Gyro Fixed Drift Terms
Roundoff Y		R_Y	
Roundoff Z		R_Z	
Vibration X	Equation 14 a, b, or c	R_X	
Vibration Y		R_Y	
Vibration Z		R_Z	
Truncation*:	$1/f_c$	RECT	
	$1/f_c^2$	RUK2	New SEAP Terms
	$1/f_c^4$	RUK4	

NB = # of bits

f_c = Attitude computation frequency

* A single computer is given only the appropriate integration scheme dependent truncation coefficient. The other two are zero.

State Transition Matrices.--The state transition matrices necessary to propagate the velocity and position errors from injection to other points in the flight were obtained from a modification to an n-body integration program supplied by NASA/Lewis Research Center. The Lewis n-body program was modified to produce the state transition matrices by the following technique. After integration of the nominal trajectory, six additional trajectories are integrated, each with one of the six initial conditions perturbed by a small amount. The perturbations were set to 10^{-6} times the radius magnitude for position components and 10^{-6} times the velocity magnitude for the velocity components. Matrices are then obtained for many points along the trajectory by subtracting the nominal trajectory state vector from the perturbed trajectory.

$$T_{ij}(t) = X_{ij}(t) - X_{io}(t)$$

where

$T_{ij}(t)$ = an element of the state transition matrix from time = 0 to time = t,

$X_{ij}(t)$ = the i^{th} component of the state vector at time t with the j^{th} component of the initial vector X(0), perturbed, and

$X_{io}(t)$ = the i^{th} component of the nominal state vector at time = t.

Other perturbation ratios ranging from 10^{-4} to 10^{-7} were tried and the resultant matrices were equivalent out to the sixth decimal place. The perturbation of 10^{-6} is small enough to avoid errors due to nonlinearities and large enough to avoid noise due to finite computer word length. The program uses two 60 bit words for each state variable when run on a CDC 6400 computer.

A state transition matrix between any two points may then be found by

$$\left[T(a,b)\right] = \left[T(0,b)\right]\left[T(0,a)\right]^{-1}$$

where

$\left[T(a,b)\right]$ = state transition matrix from time = a to time = b,

$\left[T(0,a)\right]$ = state transition matrix from time = 0 to time = a, and

$\left[T(0,b)\right]$ = state transition matrix from time = 0 to time = b.

Attitude errors are propagated by the identity matrix. However, during coasting portions of the flight (e.g., injection cutoff to midcourse correction) additional attitude errors are generated due to gyro fixed drift and computer errors. Under the assumption of small angle attitude errors, the generated errors are approximated by multiplying the drift rates by the elapsed time. The resultant attitude transformation becomes

$$\vec{e}_a(t_b) = \vec{e}_a(t_a) + (t_b - t_a)\,\vec{d}$$

where

$\vec{e}_a(t_i)$ = attitude error vector at time t_i, and

$\vec{d}$ = fixed drift error vector.

When handled statistically, the attitude propagation becomes

$$\left[\mathrm{Cov}_a(t_b)\right] = \left[\mathrm{Cov}_a(t_a)\right] + (t_b - t_a)^2 \left[D\right]\left[D\right]^T$$

where

$\left[\mathrm{Cov}_a(t_i)\right]$ = the three by three covariance of attitude errors at time = t_i, and

$\left[D\right]$ = the three by n matrix describing n fixed drift gyroscope and computer error sources.

Midcourse Correction Determination.--Midcourse correction delta-V may be determined from the position and velocity errors at midcourse and the state transition matrix mapping errors at midcourse to errors at the target. The errors and matrices of interest are defined in Table XVII.

TABLE XVII
MIDCOURSE CORRECTION DEFINITIONS

Symbol	Definition
$[A]$	The 6 by 6 state transition matrix from midcourse to the target
$\vec{e}_m$	The 6 element error vector prior to midcourse correction
$\vec{e}_t$	The 6 element error vector at the target
$\vec{e}_m'$	The 6 element error vector after midcourse correction
$\vec{e}_{xp}$	The 3 element position error vector subset of any 6 element error vector e_x
$\vec{e}_{xv}$	The 3 element velocity subset of e_x
$\vec{\Delta V}$	The midcourse correction vector

Midcourse correction velocity is obtained by determining the required velocity (for desired target miss) after midcourse ($\vec{e}_{mv}'$) in terms of the errors at midcourse ($\vec{e}_m$) and computing the difference,

$$\vec{\Delta V} = \vec{e}_{mv}' - \vec{e}_{mv} .$$

Since errors have been assumed linear and zero errors produce zero midcourse delta-V, the required velocity just after midcourse may be expressed by

$$\vec{e}_{mv}' = [C]\ \vec{e}_m$$

and the correction becomes

$$\vec{\Delta V} = \left[[C] - [0|I]\right]\ \vec{e}_m$$

where

[C] - is the 3 by 6 matrix mapping position-velocity errors prior to midcourse to required velocity after midcourse,

I - is the 3 by 3 identity matrix, and

0 - is the 3 by 3 zero matrix.

A matrix [F] (3 by 6) may be defined to be the matrix yielding $\vec{\Delta V}$ from errors prior to midcourse by

$$[F] = [C] - [0|I]$$

The problem is then to obtain [F] in terms of [A] to meet miss requirements at the target.

Two types of target miss requirements have been studied. They are:

(1) Zero all position errors at the target, and

(2) Zero one position or velocity component error at the target.

When making a midcourse correction, three variables may be specified (three components of delta-V). Thus, three conditions may be met at the target. Zeroing all position errors specifies three conditions. However, zeroing any one component at the target specifies only one condition. In other words, there are an infinite number of possible corrections which will zero one component of error at the target. In this case, it is desirable to make the correction that uses the least fuel (minimum magnitude of delta-V).

Zeroing All Position Errors.--The state transition matrix, [A], may be partitioned into four 3 by 3 submatrices giving

$$\begin{bmatrix} \vec{e}_{tp} \\ \vec{e}_{tv} \end{bmatrix} = \begin{bmatrix} A_{11} & A_{12} \\ A_{21} & A_{22} \end{bmatrix} \begin{bmatrix} \vec{e}'_{mp} \\ \vec{e}'_{mv} \end{bmatrix} .$$

For zero position errors at the target

$$0 = [A_{11}]\, \vec{e}'_{mp} + [A_{12}]\, \vec{e}'_{mv}$$

or expressing $\vec{e}'_{mv}$ in terms of $\vec{e}'_{mp}$

$$\vec{e}'_{mv} = -[A_{12}]^{-1}[A_{11}]\, \vec{e}'_{mp} .$$

Thus, $\vec{e}'_{mp} = \vec{e}_{mp}$

$$\vec{e}'_{mv} = \left[-[A_{12}]^{-1}\, [A_{11}] \;\middle|\; 0 \right] \begin{bmatrix} \vec{e}_{mp} \\ \vec{e}_{mv} \end{bmatrix}$$

or

$$[C] = \left[-[A_{12}]^{-1}[A_{11}] \;\middle|\; 0 \right]$$

The matrix [F] mapping $\vec{e}_m$ to $\vec{\Delta V}$ is then

$$[F] = [C] - [0 \,|\, I]$$

or

$$[F] = \left[-[A_{12}]^{-1}\, [A_{11}] \;\middle|\; -I \right]$$

yielding the $\vec{\Delta V}$ in terms of error prior to midcourse.

The required midcourse delta-V is then obtained by multiplying the errors at midcourse by the matrix F.

Zeroing One Component of Error.--The state transition matrix A may be partitioned into a set of six row vectors, each vector representing a row of A. Thus,

$$\vec{e}_t = \begin{bmatrix} \vec{a}_1 \\ \vdots \\ \vec{a}_6 \end{bmatrix} \vec{e}'_m$$

and any component of target error becomes

$$e_{ti} = \vec{a}_i \cdot \vec{e}'_m \quad .$$

To zero the i^{th} component of error at the target

$$0 = \vec{a}_i \cdot \vec{e}'_m \quad .$$

Breaking the 6 element vector $\vec{a}_i$ into its position and velocity subsets and substituting for $\vec{e}'_m$ the error prior to midcourse and delta-V yields

$$0 = \vec{a}_{ip} \cdot \vec{e}_{mp} + \vec{a}_{iv} \cdot \vec{e}_{mv} + \vec{a}_{iv} \cdot \vec{\Delta V}$$

or

$$0 = \vec{a}_i \cdot \vec{e}_m + \vec{a}_{iv} \cdot \vec{\Delta V}$$

which defines delta-V to lie in a plane as shown in Figure 17. The problem is now to find the $\vec{\Delta V}$ with minimum magnitude which is the normal to the plane that passes through the origin, or

$$\vec{\Delta V} = \frac{\vec{a}_{iv} (\vec{a}_i \cdot \vec{e}_m)}{(\vec{a}_{iv} \cdot \vec{a}_{iv})}$$

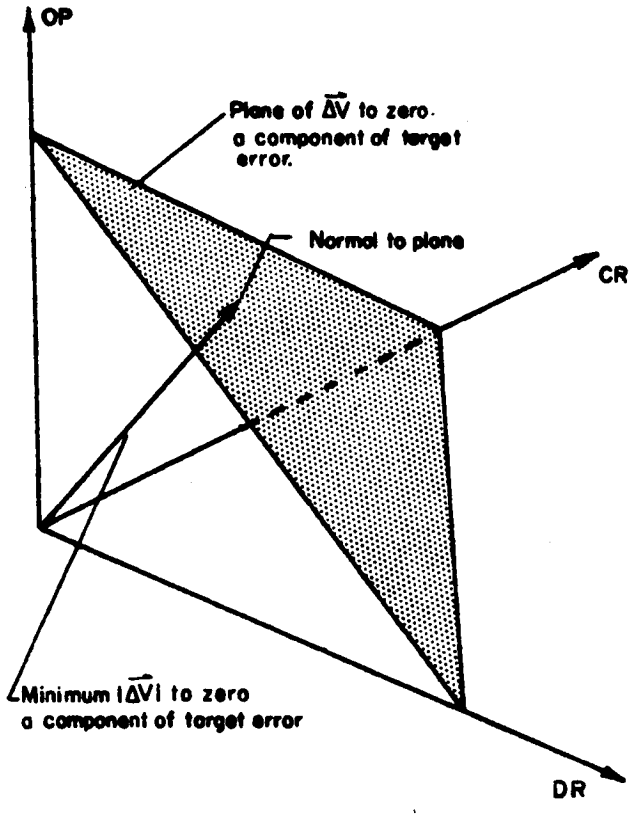

FIGURE 17. MINIMUM FUEL DELTA-V TO ZERO ONE COMPONENT OF TARGET ERROR

which when expressed as a matrix becomes

$$\vec{\Delta V} = [F]\ \vec{e}_m$$

where an element of F, f_{jk}, is given by

$$f_{jk} = \frac{a_{i,j+3}\ a_{i,k}}{(a_{i4}^2 + a_{i5}^2 + a_{i6}^2)}$$

with i equal to the index of the component to be zeroed and a_{ik} equal to the components of $\vec{a}_{ip}$ (k = 1 to 3) or $\vec{a}_{iv}$ (k = 4 to 6). It should be noted that the zeroing of any one target miss component is completely general and any position or velocity component may be zeroed. However, zeroing of the cross range (CR) position error is of the greatest interest. At a time of nominal periapsis the nominal position and velocity errors are perpendicular. The CR component of error is in the direction of the periapsis vector, and zeroing this component is equivalent to zeroing the error in periapsis magnitude.

Uncertainty in Midcourse Correction.--If a perfect impulsive delta-V correction is made according to either scheme discussed above, no target error occurs. That is, either all three position errors will be zero or the desired component will be zero. However, the midcourse correction cannot be made perfectly. Errors will occur in aiming the vehicle for the midcourse burn and the magnitude of the correction will be in error due to imperfections in its measurement. The inaccuracy in making the midcourse is calculated by the techniques described in Reference 29 and shown below.

$$\left[\mathrm{Cov}\ (\vec{e}_{vc})\right] = (U_m^2 - \frac{U_a^2}{2})\ \left[\mathrm{Cov}\ (\vec{e}_{dv})\right] + \mathrm{tr}\left\{\left[\mathrm{Cov}\ (\vec{e}_{dv})\right]\right\} \frac{U_a^2}{2}\ [I]$$

where

$\left[\mathrm{Cov}\ (\vec{e}_{vc})\right]$ = the covariance matrix of the corrected velocity,

$\left[\mathrm{Cov}\ (\vec{e}_{dv})\right]$ = the covariance matrix of the midcourse correction delta-V,

U_m = the relative uncertainty in midcourse correction magnitude,

U_a = the uncertainty in midcourse angle,

tr = the trace of a matrix, and

I = the identity matrix.

The relative uncertainty in midcourse correction magnitude and angle are either loaded as data or calculated by the program.

The uncertainty in midcourse magnitude (U_m) may be approximated by assuming the roll axis accelerometer is used to measure the thrust acceleration of the midcourse correction and terminate the thrusting when the integrated acceleration equals the desired velocity magnitude. The bias, scale factor, and nonlinearity error terms for the roll axis accelerometer are used in this calculation as shown below.

$$U_m^2 = \left| \frac{\vec{e}_{dv}}{\vec{\Delta V}} \right|^2 = (K_0/a)^2 + (K_1)^2 + (K_2 a)^2$$

where

a = midcourse correction acceleration = $\frac{\text{Thrust}}{\text{Mass}}$ and assumed constant,

K_0 = bias uncertainty,

K_1 = scale factor uncertainty, and

K_2 = nonlinearity uncertainty.

The midcourse correction angle uncertainty (U_a) may be approximated by the square root of the trace of the propagated attitude angle covariance at the time of the midcourse, or U_a may be arbitrarily set to reflect an attitude error update.

Errors at the target may be obtained by propagating the errors in making the midcourse delta-V correction to the target.

Digital Computer Programs

The calculation of the three penalty functions and the necessary estimation of the system parameters have been coded into a deck of FORTRAN subroutines. The subroutines, with a short, simple, user written main program may be used to evaluate an arbitrary guidance system using specified hardware components. Also, an optimum system (minimum penalty) may be found from a catalog of possible components.

Program Data.--Data needed to run the program consist of the following:

(1) Injection error sensitivities as computed by the Strapdown Error Analysis Program (SEAP)

(2) A set of state transition matrices as generated by the Lewis n-body Program

(3) Data describing the hardware components (accelerometers, gyroscopes, and computers).

(4) Data describing the mission and spacecraft subsystems.

Accelerometer and gyro data needed are:

(1) Weight

(2) Excitation power

(3) Mean time to failure (MTTF)

(4) Alpha (Weibull constant)

(5) Length

(6) Diameter or height

(7) Width (rectangular components only)

(8) Error coefficient uncertainties

(9) Temperature dependent error coefficients.

Computer data required is similar to that for gyros and accelerometers except the number of bits used to store each element of the attitude matrix, attitude update frequency, and integration scheme (rectangular, Runge-Kutta 2nd order, or Runge-Kutta 4th order) are used in the error model. The spacecraft and mission parameters needed for penalty function analysis are set internally to standard values unless the user specifies an alternate value.

A guidance system is defined in the subroutines by indicating the seven components (three accelerometers, three gyros, and a computer) by seven indices. The indices refer to the components location in the candidate hardware catalog. A report such as the one shown in Figure 1 is printed under any of the three penalty modes.

Additional output in the form of tables or graphs of penalty variation with any hardware, spacecraft, or mission parameter may be obtained. Examples of these tables and graphs are shown in Figures 2, 3, and 4.

Options are provided to allow specification of the type of midcourse correction (zeroing all position or any one component of miss at the target), mechanical orientation (horizontal or vertical), mechanical configuration

(one of the stored designs or the one yielding minimum weight), midcourse correction accuracy (specified or computed), thermal conductance (specified or computed), and an optimization option indicating if the gyros and accelerometers must be identical or be of differing types in the three axes.

Optimizing Algorithm.--Optimum systems are found by a method similar to a steepest descent technique. The search algorithm makes a step from one system to another by making the single substitution that produces the least penalty. If identical components are required, all three gyros are changed together and likewise for all three accelerometers. Table XVIII is an example of a hypothetical case of one step in the search algorithm, with three candidate accelerometers (numbered 1-3), three candidate gyros (numbered 21-23), and three candidate computers (numbered 41-43).

TABLE XVIII
EXAMPLE OF SEARCH ALGORITHM

Remarks	System			Penalty	
	Accelerometers	Gyros	Computers		
Present System	1	21	41	100	
Changing Accelerometers	2	21	41	95	Best New Accelerometer
	3	21	41	97	
Changing Gyros	1	22	41	96	Best New Gyro
	1	23	41	98	
Changing Computers	1	21	42	96	
	1	21	43	94	Best New Computer
New System	1	21	43	94	

There is no better system that differs from the original system by only one substitution. Each step requires many evaluations of the penalty function. For identical components

$$\text{Number of Penalty Evaluations} = N_a + N_g + N_c \quad ,$$

and for mixed components

$$\text{Number of Penalty Evaluations} = 3N_a + 3N_g + N_c,$$

where

N_a = the number of candidate accelerometers,

N_g = the number of candidate gyroscopes, and

N_c = the number of candidate computers.

This is similar to a search in three dimensional space (seven dimensional if mixed gyros and accelerometers are permitted). However, the dimensions are arbitrary catalog indices and only discrete points exist in the hyperspace. Changing a component represents motion in one spatial direction. However, since the indices are arbitrary, any number of steps in a direction are of equal interest. Steepest descent usually involves testing one step in each direction, then moving in some direction combining the results of the tests. In this technique all possible steps in each direction are tried, then the change is made in only the one direction to the new point with the least penalty. In summary, this algorithm changes only one component, never moves to an untried location, and never moves to a location with a larger penalty value. Other search algorithms have been tried but either failed to converge or resulted in long running times. Finite enumeration (trying all possible combinations) showed some promise. This approach would find the absolute optimum in the following number of evaluations of the penalty:

$$\text{Number of Penalty Evaluations} = N_a N_g N_c$$

for identical components, and

$$\text{Number of Penalty Evaluations} = N_a^3 N_g^3 N_c$$

for mixed components. For most searches the algorithm must be applied about ten times. For equal numbers of candidate accelerometers, gyroscopes, and computers, Table XIX gives a comparison of the number of penalty evaluations for the algorithm and finite enumeration. This shows that finite enumeration results in excessive running time for more than simple problems.

TABLE XIX
COMPARISON OF THE SEARCH ALGORITHM
TO FINITE ENUMERATION

Number of Components $N_a = N_g = N_c$	Mixed		Identical	
	Algorithm*	Enumeration	Algorithm*	Enumeration
5	350	78,125	150	125
10	700	10,000,000	300	1,000
15	1,050	$(15)^7$	450	3,375

* Assumes ten iterations to find optimum.

The algorithm has been coded into a separate subroutine (SYSNEW) so it may be easily replaced with any other algorithm that finds a new seven element set of component indices from a given set.

Search Housekeeping.--Another subroutine (SYSOPT) initiates the search, repetitively calls the algorithm, checks for convergence, and prints a history of the search. The search for a mode 3 optimum system, nominal data, is shown in Figure 18, and a report on the optimum system is shown in Figure 19. Actually, two independent searches are made. The first starts with the lowest numbered components (accelerometers = 1, gyroscopes = 21, and computer = 41). The second starts with the highest numbered components (accelerometers = N_a, gyroscopes = $20 + N_g$, and computer = $40 + N_c$). Each search is terminated by one of three conditions:

(1) The algorithm returns its present system as the best system. This indicates a local minima in the penalty.

(2) The algorithm returns a previously tried system. This indicates the start of an unending limit cycle, impossible with the present algorithm but included should a new algorithm be tried.

(3) More than one hundred iterations have been made and terminations 1 or 2 have not occurred.

Termination number 1 is the only one encountered in the exercising of the program. It represents a local optimum and is used as the optimum for that search. Terminations 2 and 3 are not local optima. The system tried during these searches that had the least penalty is used at the end point of the search.

The results of the two searches are compared, and if equal, a message indicating identical convergence is printed and the result assumed to be optimum. If the searches have unequal end points, a message is printed, and the one with least penalty is used as the optimum.

```
SEARCH HISTORY, MODE 3

CONVERGENCE

 1  1  1 21 21 21 41      0.10061346E+07
 1  1  1 21 21 21 42      0.22969038E+03
 1  1  1 23 23 23 42      0.21244637E+03
 2  2  2 23 23 23 42      0.20880400E+03

CONVERGENCE

 5  5  5 27 27 27 49      0.23947505E+03
 5  5  5 23 23 23 49      0.22307513E+03
 2  2  2 23 23 23 49      0.20905134E+03
 2  2  2 23 23 23 42      0.20880400E+03
CONVERGENCE IDENTICAL
```

FIGURE 18. ILLUSTRATION OF A SEARCH FOR A MODE 3 OPTIMUM SYSTEM

PENALTY(MODE 3)= 208.80400 PAGE 1

ZERO CR POS. ERRORS AT TARGET
WITH MID COURSE AT 25.0 HOURS

260/5-IVB/CENTAUR-I/KICK JUPITER FLY BY
ZERO ALL ERRORS BEFORE SECOND BURN

HARDWARE DATA (OPTIMUM,IDENT.)

ACCELEROMETERS	WEIGHT	POWER	MTTF	ALPHA	LENGTH	DIAMETER	WIDTH	AXIS
GG-177	.30	1.00	50000.00	1.00	1.80	1.50	-0.00	YAW
CONSTANT	4.20E-05	5.10E-05	9.40E-06	1.04E-06	-0.	-0.	5.00E-06	5.00E-06	2.00E+01	2.00E+01
PER DEG-F	-0.	-0.	-0.	-0.	-0.	-0.	-0.	-0.	-0.	-0.
	K0	K1	K2	K3	M0	N0	M1	N1	IP	IN
	G	G/G	G/G**2	G/G**3	G/G	G/G	G/G**2	G/G**2	ARC SEC	ARC SEC
GG-177	.30	1.00	50000.00	1.00	1.80	1.50	-0.00	PITCH
CONSTANT	4.20E-05	5.10E-05	9.40E-06	1.04E-06	-0.	-0.	5.00E-06	5.00E-06	2.00E+01	2.00E+01
PER DEG-F	-0.	-0.	-0.	-0.	-0.	-0.	-0.	-0.	-0.	-0.
	K0	K1	K2	K3	M0	N0	M1	N1	IP	IN
	G	G/G	G/G**2	G/G**3	G/G	G/G	G/G**2	G/G**2	ARC SEC	ARC SEC
GG-177	.30	1.00	50000.00	1.00	1.80	1.50	-0.00	ROLL
CONSTANT	4.20E-05	5.10E-05	9.40E-06	1.04E-06	-0.	-0.	5.00E-06	5.00E-06	2.00E+01	2.00E+01
PER DEG-F	-0.	-0.	-0.	-0.	-0.	-0.	-0.	-0.	-0.	-0.
	K0	K1	K2	K3	M0	N0	M1	N1	IP	IN
	G	G/G	G/G**2	G/G**3	G/G	G/G	G/G**2	G/G**2	ARC SEC	ARC SEC

GYROSCOPES	WEIGHT	POWER	MTTF	ALPHA	LENGTH	DIAMETER	WIDTH	AXIS
18-IRIG-B	1.20	3.30	35000.00	1.00	3.86	2.00	-0.00	YAW
CONSTANT	1.50E-02	3.00E-02	3.00E-02	3.00E-02	5.00E+00	1.00E+00	3.00E-05	-0.	-0.	-0.
PER DEG-F	-0.	-0.	-0.	-0.	-0.	-0.	-0.	-0.	-0.	-0.
	R	UI	US	S	IS	IO	T			
	DEG/HOUR	DEG/HR/G	DEG/HR/G	DEG/H/G**2	ARC-SEC	ARC-SEC	UNITY			
18-IRIG-B	1.20	3.30	35000.00	1.00	3.86	2.00	-0.00	PITCH
CONSTANT	1.50E-02	3.00E-02	3.00E-02	3.00E-02	5.00E+00	1.00E+00	3.00E-05	-0.	-0.	-0.
PER DEG-F	-0.	-0.	-0.	-0.	-0.	-0.	-0.	-0.	-0.	-0.
	R	UI	US	S	IS	IO	T			
	DEG/HOUR	DEG/HR/G	DEG/HR/G	DEG/H/G**2	ARC-SEC	ARC-SEC	UNITY			
18-IRIG-B	1.20	3.30	35000.00	1.00	3.86	2.00	-0.00	ROLL
CONSTANT	1.50E-02	3.00E-02	3.00E-02	3.00E-02	5.00E+00	1.00E+00	3.00E-05	-0.	-0.	-0.
PER DEG-F	-0.	-0.	-0.	-0.	-0.	-0.	-0.	-0.	-0.	-0.
	R	UI	US	S	IS	IO	T			
	DEG/HOUR	DEG/HR/G	DEG/HR/G	DEG/H/G**2	ARC-SEC	ARC-SEC	UNITY			

COMPUTER	WEIGHT	POWER	MTTF	ALPHA	BITS	COMP.FREQ.	INT.SCH.
SIGN III	27.00	115.00	5582.00	1.00	40	50	1

FIGURE 19a. PENALTY, MODE 3, REPORT ON AN OPTIMUM SYSTEM

IMU MECHANICAL DATA(HORIZONTAL DESIGN NUMBER 5 OPTIMUM)

OUTSIDE DIMENSIONS		WEIGHT	
LENGTH=	10.20000	BLOCK=	5.40681
WIDTH=	7.50000	BASE=	3.54050
HEIGHT=	4.61000	COVER=	2.17140
		INSULATION=	1.01854
		ELECTRONICS=	10.00000
		COMPONENTS=	31.50000

TOTAL(IMU+COMPUTER)WEIGHT= 53.63725

THERMAL ANALYSIS

AVERAGE WATTS = 329.5 MIN.HEATER WATTS = -.0
PEAK WATTS = 393.8 THERMAL COND. = 2.14(W/D-F)

ENERGY SOURCE WEIGHT= 126.87750

ERROR ANALYSIS

		DR	CR	OP	RMS	DOF
INJECTION	POSITION	9.5157E+02	2.1932E+03	1.9120E+03	3.0613E+03	2.319119
	VELOCITY	1.9429E+00	4.8259E+00	3.9753E+00	6.5473E+00	2.275595
	ATTITUDE	1.5727E-04	9.3196E-05	9.3255E-05	2.0522E-04	2.289238
MID COURSE	POSITION	1.9678E+05	5.0793E+05	3.2899E+05	6.3636E+05	1.762408
	VELOCITY	2.1949E+00	5.7316E+00	3.6675E+00	7.1498E+00	1.730978
	ATTITUDE	8.7449E-03	8.5654E-03	8.5632E-03	1.4939E-02	2.998805
CORRECTION	DELTA VEL.	2.6489E+00	5.0447E+00	1.6405E+00	5.9294E+00	1.000000
AT TARGET						
NO MID COR	POSITION	4.3589E+07	7.1718E+08	6.0438E+07	7.2104E+08	1.008142
	VELOCITY	1.0873E+03	9.1179E+02	1.2729E+04	1.2807E+04	1.011989
PERFECT MC	POSITION	3.8167E+07	1.9614E-06	3.8180E+07	5.3985E+07	1.976512
	VELOCITY	7.3183E+02	8.3140E+02	5.0050E+02	1.2154E+03	1.845622
IMPERFECT	POSITION	3.8168E+07	3.2567E+06	3.8181E+07	5.4085E+07	1.990887
	VELOCITY	7.3185E+02	8.3141E+02	5.0394E+02	1.2169E+03	1.851653

MIDCOURSE SYSTEM

RELATIVE ACCURACY		WEIGHT			
MAGNITUDE=	.00454102	FUEL=	7.28946	DELTA-V CAPABILITY=	10.11586
ANGLE=	.00291000	TANKAGE=	.69979	EXPECTED BURN TIME=	19.92409
		CONSTANT=	20.30000		

TOTAL MIDCOURSE WEIGHT= 28.28925

PENALTY ANALYSIS

PROBABILITIES OF FAILURE		WEIGHT		
RELIABILITY=	.01255456	NON-GUIDANCE=	5201.20	
SUFFICIENT FUEL=	.08855723	GUIDANCE=	208.80	(PENALTY)
MISS AT TARGET=	.00000000			
SYSTEM=	.10000000 (FIXED)	TOTAL=	5410.00	(FIXED)

FIGURE 19b. PENALTY, MODE 3, REPORT ON AN OPTIMUM SYSTEM

MISSION AND SPACE CRAFT DATA

IC=0

	ID	DESCRIPTION		VALUE	SENSITIVITY		ID	DESCRIPTION		VALUE	SENSITIVITY
	1	TIME TO MID COURSE	(HOURS)	25.00000	.0011824		20	VIBRATION UPPER FREQ.	(CPS)	100.00000	0.0000000
	2	PROBABILITY OF GUIDANCE FAIL.		.10000	-.0122878		21	INSULATION THICKNESS	(IN)	.05000	.0048780
	3	MID COURSE SYSTEM CON.	(LB/LB)	1.09600	.0382619		22	INSULATION DENSITY	(IN)	.09100	.0048780
	4	SPECIFIC IMPULSE	(SEC.)	233.00000	-.0378578		23	ELECTRONICS POWER	(WATTS)	30.00000	.2478401
C	5	NONGUIDANCE WEIGHT	(LB)	5000.00000	0.0000000		24	MID COURSE SYSTEM	(LB)	20.30000	.0972204
	6	TOTAL WEIGHT	(LB)	5410.00000	.0382619		25	BOOST TIME	(HOURS)	.20000	.0000013
	7	ENERGY SOURCE CONSTANT	(LB)	13.20000	.0632172		26	OPERATING TEMPERATURE	(DEG-F)	160.00000	-2.1002152
	8	ENERGY SOURCE CONSTANT	(LB/W)	.34500	.5444220		27	MAX.AMBIENT TEMPERATURE	(DEG-F)	140.00000	2.6676120
	9	BLOCK DENSITY	(LB/IN**3)	.09700	.0258942		28	AVE.AMBIENT TEMPERATURE	(DEG-F)	60.00000	-.2126468
	10	BASE DENSITY	(LB/IN**3)	.09700	.0169561		29	MIN.AMBIENT TEMPERATURE	(DEG-F)	30.00000	0.0000000
	11	COVER DENSITY	(LB/IN**3)	.09700	.0103992		30	OPERATING TEMP.UNCER.	(DEG-F)	.10000	0.0000000
	12	IMU COMPONENT SEPARATION	(IN)	.25000	.0288235	A	31	THERMAL CONDUCTIVITY	(W/DEG-F)	0.00000	0.0000000
	13	BASE OFFSET	(IN)	1.50000	.0191947	B	32	REL.UNC.IN MID COURSE MAG.		-1.00000	0.0000000
	14	BASE THICKNESS	(IN)	.50000	.0169561	B	33	REL.UNC.IN MID COURSE ANGLE		.00291	0.0000000
	15	COVER CLEARANCE	(IN)	.25000	.0005903		34	TARGET MISS DISTANCE	(FT)	100000000.00000	0.0000000
	16	COVER THICKNESS	(IN)	.10000	.0103992		35	MID COURSE THRUST	(LB)	50.00000	0.0000000
	17	ELECTRONICS WEIGHT	(LB)	10.00000	.0478918		36	MIDCOURSE ENGINE RELIABILTY		.00100	.0001112
	18	ELECTRONICS MTBF	(HR)	10000.00000	-.0002748		37	ENERGY SOURCE MTBF	(HRS)	10000.00000	-.0002748
	19	VIBRATION(MILLARAD/SEC)**2/CPS		.30457	0.0000000		38			0.00000	0.0000000

NOTES A=COMPUTED BY PROGRAM IF DATA SET TO ZERO
B=COMPUTED BY PROGRAM IF DATA SET TO LESS THAN ZERO
C=NOT USED BY THIS PENALTY FUNCTION

SENSITIVITY = PERCENT CHANGE IN PENALTY / PERCENT CHANGE IN DATA

FIGURE 19c. PENALTY, MODE 3, REPORT ON AN OPTIMUM SYSTEM

HARDWARE SENSITIVITY

ID		GG-177 YAW ACC. IC= 2	GG-177 PITCH ACC. 2	GG-177 ROLL ACC. 2		18-IRIG-B YAW GYRO 23	18-IRIG-B PITCH GYRO 23	18-IRIG-B ROLL GYRO 23
1	WEIGHT	.0014368	.0014368	.0014368		.0057470	.0057470	.0057470
2	POWER	.0082613	.0082613	.0082613		.0272624	.0272624	.0272624
3	MTTF	-.0000004	-.0000004	-.0000004		-.0000785	-.0000785	-.0000785
4	ALPHA	-.0000053	-.0000053	-.0000053		-.0005823	-.0005823	-.0005823
5	LENGTH	.0083477	.0018671	.0083477		.0055739	.0146885	.0146885
6	DIAMETER	.0027653	.0027653	.0027653		.0134241	.0206367	.0206367
7	WIDTH	0.0000000	0.0000000	0.0000000		0.0000000	0.0000000	0.0000000
	CONSTANT				CONSTANT			
8	K0	.0025847	.0002963	.0016863	R	.0001617	.0014101	.0000076
9	K1	0.0000000	0.0000000	.0023451	UI	0.0000000	0.0000000	0.0000000
10	K2	0.0000000	0.0000000	.0001090	US	0.0000000	0.0000000	.0000302
11	K3	0.0000000	0.0000000	.0000027	S	0.0000000	0.0000000	0.0000000
12	M0	0.0000000	0.0000000	0.0000000	IS	.0000106	.0000001	.0000007
13	N0	0.0000000	0.0000000	0.0000000	I0	.0000000	.0000000	.0000000
14	M1	0.0000000	0.0000000	0.0000000	T	.0000000	.0001481	.0000000
15	N1	0.0000000	0.0000000	0.0000000		0.0000000	0.0000000	0.0000000
16	IP	.0127243	.0014483	.0014483		0.0000000	0.0000000	0.0000000
17	IN	0.0000000	0.0000000	.0127243		0.0000000	0.0000000	0.0000000
	PER DEG-F				PER DEG-F			
18	K0	0.0000000	0.0000000	0.0000000	R	0.0000000	0.0000000	0.0000000
19	K1	0.0000000	0.0000000	0.0000000	UI	0.0000000	0.0000000	0.0000000
20	K2	0.0000000	0.0000000	0.0000000	US	0.0000000	0.0000000	0.0000000
21	K3	0.0000000	0.0000000	0.0000000	S	0.0000000	0.0000000	0.0000000
22	M0	0.0000000	0.0000000	0.0000000	IS	0.0000000	0.0000000	0.0000000
23	N0	0.0000000	0.0000000	0.0000000	I0	0.0000000	0.0000000	0.0000000
24	M1	0.0000000	0.0000000	0.0000000	T	0.0000000	0.0000000	0.0000000
25	N1	0.0000000	0.0000000	0.0000000		0.0000000	0.0000000	0.0000000
26	IP	0.0000000	0.0000000	0.0000000		0.0000000	0.0000000	0.0000000
27	IN	0.0000000	0.0000000	0.0000000		0.0000000	0.0000000	0.0000000

COMPUTER SENSITIVITY
SIGN III
IC= 42

ID			ID			
1	WEIGHT	.1293079	8	NO.OF BITS	-.0000000	PER BIT
2	POWER	.1900107	9	COMP.FREQ.	-.0000909	
3	MTTF	-.0004923	10	INT.SCHEME	-.0623826	CHANGE TO RUK-2
4	ALPHA	-.0027954	10	INT.SCHEME	-.0623826	CHANGE TO RUK-4

SENSITIVITY = PERCENT CHANGE IN PENALTY / PERCENT CHANGE IN DATA
EXCEPT AS NOTED FOR COMPUTER BITS AND INTEGRATION SCHEME

FIGURE 19d. PENALTY, MODE 3, REPORT ON AN OPTIMUM SYSTEM

Unequal end points occurred occasionally in the exercising of the program. However, in every case one of the endpoints was a system that was saturated. Saturation occurs when the system fails an implied constraint such as one with a P_{FR} greater than P_{FC} (probability of failure due to reliability greater than the required probability of total system failure). When a system is saturated, the penalty function coding arbitrarily adds one million to the penalty. This number was chosen to be a ridiculously large penalty (spacecraft weight or probability of failure).

Although not strictly a steepest descent technique, this search routine and its algorithm are vulnerable to the usual pitfalls of steepest descent. The most obvious danger is that the local minima is not the global minima. However, the use of two separate searches and comparison of the end points helps check for this problem. In any case, it should be remembered that there is no system that differs by one substitution from the indicated end point with a smaller penalty.

Application of Study Techniques to a Jupiter Flyby Mission

The techniques developed in this study were applied to a Jupiter flyby mission. The data required for exercising the computer programs implementing these techniques were compiled or derived in a cooperative effort with NASA/ERC, personnel of the NASA Launch Vehicle Planning (NLVP) Project at Battelle, and those Battelle staff members assigned to this study. Much of the hardware data, particularly the reliability and error coefficient data, is assumed based on manufacturers' data and are not to be used conclusively.

Data Required.--For the purpose of exercising the computer programs, trajectory, mission, spacecraft, and candidate components data are required. These are listed and discussed in the following section.

Boost Trajectory and SEAP Data.--Curves were fitted to the non-zero body rates and accelerations of the simulated boost trajectory discussed in detail in Appendix A of this report. These curves were of the form $a_o + a_1 t + \ldots + a_n t^n$ for the body rates and $\frac{C}{1-t/T} + b_0 + b_1 t + \ldots + b_n t^n$ for the accelerations where T is the time when the stage, if it were all fuel, would be burned up (see Table XX). The coefficients in Table XX for Stages 3 and 4 i.e., the curves expressing the body rates and accelerations as a function of time, were used as the trajectory input data for the Strapdown Error Analysis Program (SEAP). The error sensitivity coefficients output from SEAP are shown in Figures 20a, 20b, and 20c for the trajectory used. The first column in the figures denotes the error coefficient whose sensitivity is listed and the last symbol in that column denotes whether the sensitivity is position, xxxP, velocity, xxxV, or attitude, xxxA. The columns headed by X, Y, and Z are shown in Figure 21. The columns headed by DR (down range along the velocity vector, $\vec{V}$), CR (in the plane determined by the radius and velocity vectors and normal to DR), and OP (out of plane) are the sensitivities after rotation through the angle defined in Figure 22, in this case -29.3°.

TABLE XX. TRAJECTORY COEFFICIENTS FOR 260(3.7)/SIVB/CI/K *

		$\frac{1}{1 - t/T}$	1	t	t^2	t^3	t^4	t^5	t^6	RSS Error
STAGE 1 $0 \le t \le 142.5$ T = 165.5	ω_x	-	- 0.654249	3.85261E-2	-7.02324E-4	5.57232E-6	-1.55967E-8			0.02
	ω_y	-	4.15842E-2	-1.93747E-3	3.48060E-5	-2.65408E-7	7.24123E-10			7E-4
	ω_z	-	- 0.288183	6.85073E-2	-1.31632E-3	9.14747E-6	-2.19875E-8			8E-3
	A_x	-606.185	696.759	-4.50569	0.588758	-1.71753E-2	2.62512E-4	-1.89115E-6	5.37136E-9	4.5
	A_y	0.0								-
	A_z	0.0								-
STAGE 2 $142.5 \le t \le 608.25$ T = 766	ω_x**	-	3.37874E-5	-4.04684E-7	1.72864E-9	-3.14130E-12	2.06151E-15			7E-7
	ω_y**	-	- 1.88514E-4	2.25798E-6	-9.64540E-9	1.75281E-11	-1.15021E-14			3E-6
	ω_z**	-	2.35846E-2	7.17176E-6	1.65414E-7	-2.50892E-10	2.85586E-13			2E-5
	A_x	12.3901	2.40770	3.22325E-2	-7.94327E-5	1.09332E-7				0.052
	A_y	0.0								-
	A_z	0.0								-
STAGE 3 $608.25 \le t \le 1145$ T = 1270	ω_x	-	- 1.16238E-3	6.40612E-6	-1.64724E-8	1.25573E-11	-3.58665E-15			2E-7
	ω_y	-	1.88787E-3	1.55663E-6	-3.74653E-9	1.88027E-12	-1.83568E-16			3E-7
	ω_z	-	0.119060	-2.83942E-4	3.59370E-7	-2.96584E-10	-7.99250E-14			9E-6
	A_x	1.67796	-19.69842	0.127302	-1.71167E-4	9.20000E-8				0.032
	A_y	0.0								-
	A_z	0.0								-
STAGE 4 $1145 \le t \le 1505.5$ T = 1671.3	ω_x	-	- 2.71249E-3	1.28980E-5	-2.44277E-8	1.57486E-11	-3.73124E-15			8E-7
	ω_y	-	9.25705E-4	4.54954E-6	-7.69401E-9	4.47188E-12	-8.70072E-16			2E-7
	ω_z	-	- 0.360981	1.31842E-3	-1.53795E-6	7.46341E-10	-1.31948E-13			7E-6
	A_x	7.23879	- 2.03476	7.05516E-3	-6.23020E-6	2.14803E-9				6E-4
	A_y	0.0								-
	A_z	0.0								-

* This simulated trajectory contains a 7° increment in pitch angle between stages 1 and 2. If used for Earth launch, add an impulse in ω_z between stages 1 and 2 to change the pitch angle by 7°.

** For $565 \le t \le 608.25$ use ω_x, ω_y, ω_z from third stage.

SEAP AFTER ROTATION BY -29.3 DEG.

		X	Y	Z	DR	CR	OP
K0XP	1	-0.1626892E+06	-0.3030607E+04	-0.4494894E+06	0.7773467E+05	-0.4716628E+06	0.3030607E+04
K0XV	1	-0.4860069E+03	-0.1110136E+02	-0.9060854E+03	0.1880295E+02	-0.1028027E+04	0.1110136E+02
K0YP	11	0.2627004E+04	0.4154988E+06	-0.4470865E+04	0.4476889E+04	-0.2616726E+04	-0.4154988E+06
K0YV	11	0.6139231E+01	0.8473178E+03	-0.1607975E+02	0.1321454E+02	-0.1102835E+02	-0.8473178E+03
K0ZP	21	0.4306283E+06	-0.4329325E+04	-0.8181363E+05	0.4156826E+06	0.1390764E+06	0.4329325E+04
K0ZV	21	0.9377635E+03	-0.1354473E+02	-0.2182127E+03	0.9247897E+03	0.2679200E+03	0.1354473E+02
K1XP	2	0.	0.	0.	0.	0.	-0.
K1XV	2	0.	0.	0.	0.	0.	-0.
K1YP	12	0.	0.	0.	0.	0.	-0.
K1YV	12	0.	0.	0.	0.	0.	-0.
K1ZP	22	0.1349608E+08	-0.1318971E+06	-0.2392115E+07	0.1294363E+08	0.4508738E+07	0.1318971E+06
K1ZV	22	0.2904818E+05	-0.4132134E+03	-0.6459580E+04	0.2849979E+05	0.8560632E+04	0.4132134E+03
K2XP	3	0.	0.	0.	0.	0.	-0.
K2XV	3	0.	0.	0.	0.	0.	-0.
K2YP	13	0.	0.	0.	0.	0.	-0.
K2YV	13	0.	0.	0.	0.	0.	-0.
K2ZP	23	0.5188258E+09	-0.4462123E+07	-0.6892975E+08	0.4863334E+09	0.1934201E+09	0.4462123E+07
K2ZV	23	0.1051932E+07	-0.1371586E+05	-0.1836854E+06	0.1007521E+07	0.3538387E+06	0.1371586E+05
K3XP	4	0.	0.	0.	0.	0.	-0.
K3XV	4	0.	0.	0.	0.	0.	-0.
K3YP	14	0.	0.	0.	0.	0.	-0.
K3YV	14	0.	0.	0.	0.	0.	-0.
K3ZP	24	0.2455069E+11	-0.1686334E+09	-0.1711936E+10	0.2225575E+11	0.1050470E+11	0.1686334E+09
K3ZV	24	0.4531768E+08	-0.4991903E+06	-0.4250143E+07	0.4161424E+08	0.1843938E+08	0.4991903E+06
M0XP	5	0.	0.	0.	0.	0.	-0.
M0XV	5	0.	0.	0.	0.	0.	-0.
M0YP	15	0.7919797E+05	0.1297614E+08	-0.1370695E+06	0.1360836E+06	-0.8088032E+05	-0.1297614E+08
M0YV	15	0.1862094E+03	0.2605536E+05	-0.4904060E+03	0.4021256E+03	-0.3368485E+03	-0.2605536E+05
M0ZP	25	0.	0.	0.	0.	0.	-0.
M0ZV	25	0.	0.	0.	0.	0.	-0.
N0XP	6	-0.5018268E+07	-0.9219351E+05	-0.1414694E+08	0.2535653E+07	-0.1479491E+08	0.9219351E+05
N0XV	6	-0.1500550E+05	-0.3372034E+03	-0.2806982E+05	0.6266603E+03	-0.3182275E+05	0.3372034E+03
N0YP	16	0.	0.	0.	0.	0.	-0.
N0YV	16	0.	0.	0.	0.	0.	-0.
N0ZP	26	0.	0.	0.	0.	0.	-0.
N0ZV	26	0.	0.	0.	0.	0.	-0.
M1XP	7	0.	0.	0.	0.	0.	-0.
M1XV	7	0.	0.	0.	0.	0.	-0.
M1YP	17	0.	0.	0.	0.	0.	-0.
M1YV	17	0.	0.	0.	0.	0.	-0.
M1ZP	27	0.	0.	0.	0.	0.	-0.
M1ZV	27	0.	0.	0.	0.	0.	-0.
N1XP	8	0.	0.	0.	0.	0.	-0.
N1XV	8	0.	0.	0.	0.	0.	-0.
N1YP	18	0.	0.	0.	0.	0.	-0.
N1YV	18	0.	0.	0.	0.	0.	-0.
N1ZP	28	0.	0.	0.	0.	0.	-0.
N1ZV	28	0.	0.	0.	0.	0.	-0.
RXP	31	0.5186452E+08	0.4015737E+10	-0.3325842E+08	0.6150275E+08	-0.3669178E+07	-0.4015737E+10
RXV	31	0.2006051E+06	0.1256224E+08	-0.1545652E+06	0.2505549E+06	-0.3681088E+05	-0.1256224E+08
RXA	1	-0.3351593E+03	-0.1190791E+02	-0.8680075E+03	0.1317998E+03	-0.9210850E+03	0.1190791E+02
RYP	41	0.1849338E+10	0.1633751E+08	0.4003009E+10	-0.3428827E+09	0.4396199E+10	-0.1633751E+08

FIGURE 20a. ERROR COEFFICIENT SENSITIVITIES FROM SEAP

RYV	41	0.7036609E+07	0.7628391E+05	0.1218704E+08	0.1830691E+06	0.1407140E+08	-0.7628391E+05
RYA	11	0.6757395E+01	0.9438819E+03	-0.1657920E+02	0.1399794E+02	-0.1116199E+02	-0.9438819E+03
RZP	51	0.2917069E+07	-0.7043666E+09	0.3203655E+08	-0.1311174E+08	0.2937571E+08	0.7043666E+09
RZV	51	0.1650558E+05	-0.2458759E+07	0.1284315E+06	-0.4836611E+05	0.1201158E+06	0.2458759E+07
RZA	21	0.8681148E+03	-0.1381040E+02	-0.3349423E+03	0.9210726E+03	0.1320416E+03	0.1381040E+02
UIXP	32	0.	0.	0.	0.	0.	-0.
UIXV	32	0.	0.	0.	0.	0.	-0.
UIXA	2	0.	0.	0.	0.	0.	-0.
UIYP	42	0.	0.	0.	0.	0.	-0.
UIYV	42	0.	0.	0.	0.	0.	-0.
UIYA	12	0.	0.	0.	0.	0.	-0.
UIZP	52	0.	0.	0.	0.	0.	-0.
UIZV	52	0.	0.	0.	0.	0.	-0.
UIZA	22	0.	0.	0.	0.	0.	-0.
USXP	33	0.	0.	0.	0.	0.	-0.
USXV	33	0.	0.	0.	0.	0.	-0.
USXA	3	0.	0.	0.	0.	0.	-0.
USYP	43	0.	0.	0.	0.	0.	-0.
USYV	43	0.	0.	0.	0.	0.	-0.
USYA	13	0.	0.	0.	0.	0.	-0.
USZP	53	0.9106924E+08	-0.2297363E+11	0.1031423E+10	-0.4246182E+09	0.9443657E+09	0.2297363E+11
USZV	53	0.5142576E+06	-0.7870696E+03	0.4072733E+07	-0.1541741E+07	0.3804556E+07	0.7870696E+08
USZA	23	0.2682269E+05	-0.4201874E+03	-0.1019528E+05	0.2838387E+05	0.4213822E+04	0.4201874E+03
SXP	34	0.	0.	0.	0.	0.	-0.
SXV	34	0.	0.	0.	0.	0.	-0.
SXA	4	0.	0.	0.	0.	0.	-0.
SYP	44	0.	0.	0.	0.	0.	-0.
SYV	44	0.	0.	0.	0.	0.	-0.
SYA	14	0.	0.	0.	0.	0.	-0.
SZP	54	0.	0.	0.	0.	0.	-0.
SZV	54	0.	0.	0.	0.	0.	-0.
SZA	24	0.	0.	0.	0.	0.	-0.
ISXP	35	0.4464410E+05	0.3436580E+07	-0.2297237E+05	0.5017640E+05	0.1776098E+04	-0.3436580E+07
ISXV	35	0.1614727E+03	0.9620328E+04	-0.8869950E+02	0.1842246E+03	0.1528663E+01	-0.9620328E+04
ISXA	5	-0.1586765E+00	-0.4526596E-02	-0.5395489E+00	0.1252488E+00	-0.5482737E+00	0.4526596E-02
ISYP	45	0.5160725E+05	0.4023703E+03	0.1131413E+06	-0.1026932E+05	0.1239306E+06	-0.4023703E+03
ISYV	45	0.1892685E+03	0.1740060E+01	0.3296399E+03	0.4026443E+01	0.3800905E+03	-0.1740060E+01
ISYA	15	0.1596074E-03	0.2325400E-01	-0.3616990E-03	0.3160159E-03	-0.2375597E-03	-0.2325400E-01
ISZP	55	0.2470805E+04	-0.6626159E+05	0.2950859E+05	-0.1226562E+05	0.2695211E+05	0.6626159E+06
ISZV	55	0.1288056E+02	-0.2227537E+04	0.1121537E+03	-0.4357353E+02	0.1041427E+03	0.2227537E+04
ISZA	25	0.5395718E+00	-0.6040514E-02	-0.1586035E+00	0.5482580E+00	0.1253237E+00	0.6040514E-02
I0XP	36	-0.1479129E+04	-0.1153317E+05	0.1250126E+04	-0.1901412E+04	0.3677940E+03	0.1153317E+06
I0XV	36	-0.6297086E+01	-0.4199163E+03	0.6716922E+01	-0.8776509E+01	0.2782663E+01	0.4199163E+03
I0XA	6	0.1638839E-01	0.6423673E-03	0.3563549E-01	-0.3117611E-02	0.3909921E-01	-0.6423673E-03
I0YP	46	0.5410493E+05	0.6565807E+03	0.1119952E+06	-0.7530114E+04	0.1241514E+06	-0.6565807E+03
I0YV	46	0.2313647E+03	0.3632626E+01	0.3941344E+03	0.9233678E+01	0.4569314E+03	-0.3632626E+01
I0YA	16	0.3054066E-03	0.3962623E-01	-0.8882553E-03	0.7005531E-03	-0.6256965E-03	-0.3962623E-01
I0ZP	56	-0.8141493E+02	0.2076886E+05	-0.9340522E+03	0.3854546E+03	-0.8546969E+03	-0.2076886E+05
I0ZV	56	-0.4439131E+00	0.7108792E+02	-0.3645306E+01	0.1394223E+01	-0.3397272E+01	-0.7108792E+02
I0ZA	26	-0.2159157E-01	0.3095247E-03	0.7647400E-02	-0.2257482E-01	-0.3880175E-02	-0.3095247E-03
TXP	37	0.1459731E+04	0.1126555E+06	-0.8454078E+03	0.1686696E+04	-0.2417970E+02	-0.1126555E+06
TXV	37	0.5479245E+01	0.3359161E+03	-0.3697351E+01	0.6587282E+01	-0.5479469E+00	-0.3359161E+03
TXA	7	-0.7652011E-02	-0.2592695E-03	-0.2158942E-01	0.3875101E-02	-0.2257520E-01	0.2592695E-03
TYP	47	0.1564697E+07	0.1043267E+05	0.3478514E+07	-0.3348882E+06	0.3799498E+07	-0.1043267E+05
TYV	47	0.5459295E+04	0.3749376E+02	0.9579629E+04	0.8122882E+02	0.1102572E+05	-0.3749376E+02
TYA	17	0.3664116E-02	0.5700848E+01	-0.6402496E-02	0.6329727E-02	-0.3795113E-02	-0.5700848E+00

FIGURE 20b. ERROR COEFFICIENT SENSITIVITIES FROM SEAP (Continued)

TZP	57	-0.8531442E+02	0.1693719E+05	-0.8058982E+03	0.3194218E+03	-0.7447954E+03	-0.1693719E+05
TZV	57	-0.5395394E+00	0.6387000E+02	-0.3562765E+01	0.1270456E+01	-0.3371994E+01	-0.6387000E+02
TZA	27	-0.3564228E-01	0.7019543E-03	0.1637619E-01	-0.3909917E-01	-0.3131581E-02	-0.7019543E-03
RECT P	67	0.8115220E+03	0.5906542E+01	0.1840077E+04	-0.1912641E+03	0.2001966E+04	-0.5906542E+01
RECT V	67	0.2709112E+01	0.1705704E-01	0.4792677E+01	0.2129921E-01	0.5505324E+01	-0.1705704E-01
RECT A	37	0.2293720E-05	0.2502710E-03	-0.2762537E-05	0.3351233E-05	-0.1289185E-05	-0.2502710E-03
RUK2 P	68	0.1572570E+00	0.6960624E-03	0.3620852E+00	-0.3975821E-01	0.3927528E+00	-0.6960624E-03
RUK2 V	68	0.5121371E-03	0.1812225E-05	0.9110402E-03	0.1572655E-05	0.1045120E-02	-0.1812225E-05
RUK2 A	38	0.2125435E-09	0.4440954E-07	-0.2567970E-09	0.3109327E-09	-0.1201680E-09	-0.4440954E-07
RUK4 P	69	0.5670635E-08	0.1775380E-10	0.1335885E-07	-0.1581347E-08	0.1442617E-07	-0.1775380E-10
RUK4 V	69	0.1799575E-10	0.3753399E-13	0.3224158E-10	-0.5663569E-13	0.3692375E-10	-0.3753399E-13
RUK4 A	39	0.6066420E-17	0.1466236E-14	-0.5900430E-17	0.8176235E-17	-0.2183050E-17	-0.1466236E-14
PXY0P	0	0.	0.	0.	0.	0.	-0.
PXY0V	0	0.	0.	0.	0.	0.	-0.
PYZ0P	0	0.7919797E+05	0.1297614E+08	-0.1370695E+06	0.1360836E+06	-0.8088032E+05	-0.1297614E+08
PYZ0V	0	0.1862094E+03	0.2605536E+05	-0.4904060E+03	0.4021256E+03	-0.3368485E+03	-0.2605536E+05
PZX0P	0	0.5018268E+07	0.9219351E+05	0.1414694E+08	-0.2535653E+07	0.1479491E+08	-0.9219351E+05
PZX0V	0	0.1500550E+05	0.3372034E+03	0.2806982E+05	-0.6266603E+03	0.3182275E+05	-0.3372034E+03

0 BAD CARDS

FIGURE 20c. ERROR COEFFICIENT SENSITIVITIES FROM SEAP (Continued)

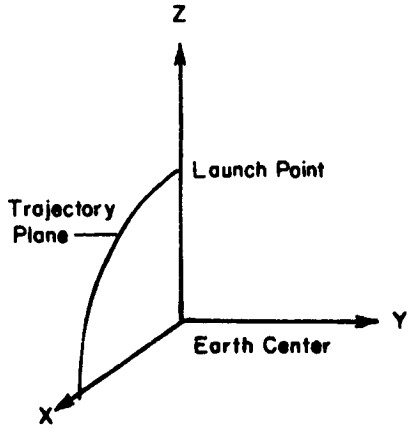

FIGURE 21. INERTIAL FRAME

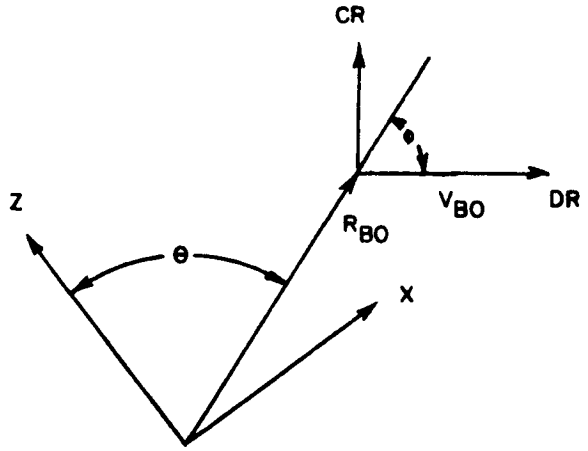

Rotation Angle = $90° - (\theta + \phi)$

where: θ = angle from SEAP origin to burnout

ϕ = angle between radius, R_{BO} and velocity, V_{BO}, at burnout.

FIGURE 22. DEFINITION OF ROTATION ANGLE

State Transition Matrices Data.--The Lewis Research Center n-body computer program was modified to calculate n-body state transition matrices. The state transition matrices used in exercising of these computer programs were obtained by running the Lewis n-body program for the trajectory previously summarized in Table III. Figure 23 summarizes the n-body trajectory from which the state transition matrices were calculated.

As a check on the compatibility of the three trajectory integration programs (three degree of freedom, SEAP, and Lewis n-body), the program reading the SEAP and Lewis decks prints the velocity and flight path angle of each trajectory at booster burnout. This information and the error in the matching is also presented in Figure 23.

Figure 23 also presents the state transition matrix which propagates injection errors to the target. This matrix is presented for information only and serves as a check point in using the program.

Midcourse Propulsion System Data.--The midcourse propulsion system data required for exercising the computer programs, the fixed weight, specific impulse, thrust, and tankage constant were extracted from Reference 1. This system is a constant gas-pressure-regulated monopropellant hydrazine unit using a Shell 405-type catalyst. It was selected because this type of system is applicable to accelerometer and burn timer shutoff mechanisms.

N-BODY TRAJECTORY (FT-SEC)

```
TIME= 0.                        POSITION                                MAG.                    VELOCITY                        MAG.
SEGMENT  1  NO.  1  -0.199892E+08 0.726959E+07 0.331325E+07 0.215266E+08-0.205654E+05-0.447736E+05-0.217279E+05 0.538490E+05

CROSS 0.75102315E+05            POSITION                                MAG.                    VELOCITY                        MAG.
SEGMENT  1  NO. 40  -0.331217E+09-0.271726E+10-0.131021E+10 0.303478E+10-0.398537E+04-0.358615E+05-0.172882E+05 0.400102E+05
SEGMENT  2  NO.  0  -0.468297E+12 0.120442E+12 0.521024E+11 0.486337E+12-0.325321E+05-0.122364E+06-0.548028E+05 0.137966E+06

TIME= 0.76000001E+05            POSITION                                MAG.                    VELOCITY                        MAG.
SEGMENT  2  NO.  1  -0.468327E+12 0.120332E+12 0.520532E+11 0.486333E+12-0.325148E+05-0.122367E+06-0.548041E+05 0.137965E+06

CROSS 0.32775357E+08            POSITION                                MAG.                    VELOCITY                        MAG.
SEGMENT  2  NO. 40   0.104615E+13-0.194289E+13-0.864314E+12 0.236987E+13 0.491936E+05-0.330656E+05-0.145800E+05 0.610403E+05
SEGMENT  3  NO.  0  -0.294012E+11 0.144041E+12 0.573688E+11 0.157808E+12 0.108673E+05-0.520925E+05-0.218054E+05 0.575083E+05

TIME= 0.32832000E+08            POSITION                                MAG.                    VELOCITY                        MAG.
SEGMENT  3  NO.  1  -0.287857E+11 0.141091E+12 0.561335E+11 0.154551E+12 0.108662E+05-0.520978E+05-0.218073E+05 0.575135E+05

      SEGMENTS       0.              39      0.75102315E+05   39      0.32775357E+08    8      0.10000000E+21


        MATCH WITH N-BODY AT    543 SECONDS,  0.33600000E+08 FT.

                                        SEAP            N-BODY          ERROR
                VELOCITY MATCH          49155           49359           -204
                  ANGLE  MATCH          45.06           44.65           .40


        TARGET CONDITIONS
             TIME  0.35458262E+08 SECONDS
           RADIUS  0.16798330E+10 FEET
         VELOCITY  0.92543645E+05 FT/SEC
            ANGLE           90.00 DEG.

        STATE TRANSITION MATRIX INJ. TO TARGET

         0.13115555E+04 0.34894063E+04 0.17125866E+04    0.16252011E+08 0.36079133E+07 0.17266233E+07
         0.30651284E+05 0.24225283E+05 0.14378768E+05    0.65296170E+08 0.12686759E+09 0.47406636E+08
        -0.16692923E+04-0.51908288E+03-0.23676823E+04   -0.35858477E+07-0.11241996E+08 0.66711760E+07

        -0.33027808E-01-0.94317766E-01-0.35920940E-01   -0.42454521E+03-0.57188888E+02-0.89143551E+02
        -0.36759363E-01-0.38860486E-01 0.99667614E-02   -0.71169168E+02-0.65027921E+02-0.20738060E+03
        -0.53835451E+00-0.42947263E+00-0.27700012E+00   -0.12191936E+04-0.22704400E+04-0.72451338E+03
```

FIGURE 23. N-BODY TRAJECTORY SUMMARY

Bipropellant midcourse propulsion systems are competitive with monopropellant systems when the total impulse requirement is 50,000 lb-sec or greater (Reference 2). Assuming the maximum delta velocity required is 20 ft/sec for example, the total impulse requirement for the 5,410 lb spacecraft is approximately

$$I_t = \frac{5410}{32.2} \times 20 = 336 \text{ lb-sec} \quad .$$

Since in none of the exercise runs was the delta velocity required as great as 20 ft/sec, a monopropellant system should be used for the midcourse propulsion system for the payload and mission considered.

The choice between the pressure regulated and blowdown monopropellant systems (References 1 and 2) was not considered to be of major importance for the purpose of exercising the computer programs. Therefore, the midcourse propulsion system data used in the exercising was based upon the pressure regulated system. This data is presented in Table XXI. For the purpose of the exercising, it was assumed that the probability that the midcourse engine would not ignite upon command was 0.001.

TABLE XXI
MIDCOURSE PROPULSION SYSTEM VALUES

Midcourse System Fixed Weight	20.30 lb
Midcourse System Tankage Factor	1.096 lb/lb of fuel
Specific Impulse	233 sec
Midcourse System Thrust	50 lb

Guidance System Electrical Power Source Data.--The guidance system power source was assumed to be a radioisotope thermoelectric generator (RTG) for the purpose of exercising the computer programs. Mission durations restrict power source consideration to solar, nuclear reactors, or an RTG. Due to the extreme distance from the sun, solar power sources were ruled out due to size and weight considerations. Solar thermal energy intensity at Jupiter's orbit is approximately 4 percent of that at a near Earth orbit according to Reference 1. This low level prohibits use of any currently envisioned solar energy collection system. Nuclear reactors have a minimum critical size and weight required to maintain a controlled nuclear reaction (Reference 1). The minimum weight is currently approximately 250 lbs, and therefore the only practical choice of power at this time is the RTG.

The major components of an RTG are: (1) an isotope heat source, (2) thermoelectric converters, and (3) a heat rejection system (Reference 2). A power conditioning and distribution system is also required. These components weights can be estimated by assuming the weight to be made up of a fixed weight plus a specific power factor expressed in lb/watt required. Table XXII lists the values assumed for the RTG data used in the exercising.

TABLE XXII
ASSUMED RTG POWER SOURCE VALUES

Fixed Weight, K_{P1}	13.20 lb
Specific Power Factor, K_{P2}	0.345 lb/watt

These values are quite optimistic but suffice for exercising of the program.

It was assumed throughout the power source weight estimation that the power source required at the target planet for the experiments could be used in the earlier phases of the mission for the guidance system. Should one assume guidance only through the first midcourse, a lower power source weight might result if a different source were selected. Since the power needed for experiments on a Jupiter flyby mission will require use of an RTG (References 1 and 2), it was decided to make use of the same power source to keep the total scientific experiment payload as large as possible.

Candidate Component Hardware Data.--Figures 24a and 24b present the candidate component hardware data used in the exercising of the program. As previously noted, the MTTF (mean time to failure) data of the components were assumed for the purpose of exercising the computer programs and are not to be used conclusively. Data on the uncertainty in the gyroscope and accelerometer error coefficients per ^{o}F (DEG-F in figure) was generally incomplete, so no values are given. When these data are available, they should be included since temperature uncertainty effects are included in the accuracy analysis. A zero value for width of the inertial sensors denotes the sensor is cylindrical. The SIGN III computer is listed with a 40 bit word length and integration scheme (INT. SCH.) 1, a 20 bit word length and integration scheme 2, and a 20 bit word length and integration scheme 3. These word lengths and integration schemes were assumed for purposes of exercising the programs and do not necessarily correspond to actual hardware. Integration scheme 1 uses a rectangular algorithm to update the direction cosine matrix. Integration scheme 2 uses a Runge-Kutta second order algorithm to update the direction cosine matrix. Computation frequency (COMP. FREQ. in Figure 24b) is the algorithm integration frequency.

HARDWARE DATA

IC	ACCELEROMETERS	WEIGHT	POWER	MTTF	ALPHA	LENGTH	DIAMETER	WIDTH			
1	ARMA D-4E	.35	1.50	100000.00	1.00	1.30	2.70	-0.00			
	CONSTANT	6.70E-06	1.00E-05	9.00E-07	1.00E-07	-0.	-0.	5.60E-06	5.60E-06	2.00E+01	2.00E+01
	PER DEG-F	-0.	-0.	-0.	-0.	-0.	-0.	-0.	-0.	-0.	-0.
		K0	K1	K2	K3	M0	N0	M1	N1	IP	IN
		G	G/G	G/G**2	G/G**3	G/G	G/G	G/G**2	G/G**2	ARC SEC	ARC SEC
2	GG-177	.30	1.00	50000.00	1.00	1.80	1.50	-0.00			
	CONSTANT	4.20E-05	5.10E-05	9.40E-06	1.04E-06	-0.	-0.	5.00E-06	5.00E-06	2.00E+01	2.00E+01
	PER DEG-F	-0.	-0.	-0.	-0.	-0.	-0.	-0.	-0.	-0.	-0.
		K0	K1	K2	K3	M0	N0	M1	N1	IP	IN
		G	G/G	G/G**2	G/G**3	G/G	G/G	G/G**2	G/G**2	ARC SEC	ARC SEC
3	2401-005	.20	8.00	188217.00	1.00	2.00	1.00	1.13			
	CONSTANT	2.00E-05	1.00E-05	1.00E-06	2.00E-07	1.00E-07	1.00E-05	-0.	-0.	5.00E+00	5.00E+00
	PER DEG-F	-0.	-0.	-0.	-0.	-0.	-0.	-0.	-0.	-0.	-0.
		K0	K1	K2	K3	M0	N0	M1	N1	IP	IN
		G	G/G	G/G**2	G/G**3	G/G	G/G	G/G**2	G/G**2	ARC SEC	ARC SEC
4	BELL-7	.40	3.50	40000.00	1.00	1.15	1.75	-0.00			
	CONSTANT	4.00E-06	8.00E-05	2.00E-06	1.60E-07	1.00E-05	1.00E-05	2.00E-06	2.00E-06	1.50E+01	1.50E+01
	PER DEG-F	-0.	-0.	-0.	-0.	-0.	-0.	-0.	-0.	-0.	-0.
		K0	K1	K2	K3	M0	N0	M1	N1	IP	IN
		G	G/G	G/G**2	G/G**3	G/G	G/G	G/G**2	G/G**2	ARC SEC	ARC SEC
5	PERT-ACC	.35	1.50	100000.00	1.00	1.30	2.70	-0.00			
	CONSTANT	1.68E-04	3.00E-04	9.00E-07	1.00E-07	-0.	-0.	5.60E-06	5.60E-06	2.00E+01	2.00E+01
	PER DEG-F	-0.	-0.	-0.	-0.	-0.	-0.	-0.	-0.	-0.	-0.
		K0	K1	K2	K3	M0	N0	M1	N1	IP	IN
		G	G/G	G/G**2	G/G**3	G/G	G/G	G/G**2	G/G**2	ARC SEC	ARC SEC

IC	GYROS	WEIGHT	POWER	MTTF	ALPHA	LENGTH	DIAMETER	WIDTH			
21	RI-1139	1.45	3.32	18000.00	1.00	2.60	3.50	-0.00			
	CONSTANT	1.50E-01	5.00E-02	7.00E-02	1.40E-02	1.50E+01	1.50E+01	8.50E-05	-0.	-0.	-0.
	PER DEG-F	-0.	-0.	-0.	-0.	-0.	-0.	-0.	-0.	-0.	-0.
		R	UI	US	S	IS	I0	T			
		DEG/HOUR	DEG/HR/G	DEG/HR/G	DEG/H/G**2	ARC-SEC	ARC-SEC	UNITY			
22	GG 334-A	1.65	3.00	25000.00	1.00	4.70	2.50	-0.00			
	CONSTANT	1.00E-01	1.50E-01	1.50E-01	4.00E-02	6.00E+00	7.00E+00	1.00E-04	-0.	-0.	-0.
	PER DEG-F	-0.	-0.	-0.	-0.	-0.	-0.	-0.	-0.	-0.	-0.
		R	UI	US	S	IS	I0	T			
		DEG/HOUR	DEG/HR/G	DEG/HR/G	DEG/H/G**2	ARC-SEC	ARC-SEC	UNITY			
23	18-IRIG-B	1.20	3.30	35000.00	1.00	3.86	2.00	-0.00			
	CONSTANT	1.50E-02	3.00E-02	3.00E-02	3.00E-02	5.00E+00	1.00E+00	3.00E-05	-0.	-0.	-0.
	PER DEG-F	-0.	-0.	-0.	-0.	-0.	-0.	-0.	-0.	-0.	-0.

FIGURE 24a. CANDIDATE HARDWARE DATA

		R DEG/HOUR	UI DEG/HR/G	US DEG/HR/G	S DEG/H/G**2	IS ARC-SEC	IO ARC-SEC	T UNITY			
24	GG 334-C	1.00	3.00	20000.00	1.00	3.50	2.15	-0.00			
	CONSTANT	1.50E-01	3.00E-01	3.00E-01	4.00E-02	5.00E+00	5.00E+00	1.00E-04	-0.	-0.	-0.
	PER DEG-F	-0.	-0.	-0.	-0.	-0.	-0.	-0.	-0.	-0.	-0.
		R DEG/HOUR	UI DEG/HR/G	US DEG/HR/G	S DEG/H/G**2	IS ARC-SEC	IO ARC-SEC	T UNITY			
25	SYG-1440	1.40	4.00	50000.00	1.00	3.86	2.00	-0.00			
	CONSTANT	5.00E-02	1.00E-01	1.00E-01	2.00E-02	5.00E+00	5.00E+00	5.00E-05	-0.	-0.	-0.
	PER DEG-F	-0.	-0.	-0.	-0.	-0.	-0.	-0.	-0.	-0.	-0.
		R DEG/HOUR	UI DEG/HR/G	US DEG/HR/G	S DEG/H/G**2	IS ARC-SEC	IO ARC-SEC	T UNITY			
26	SYG-1000	.92	3.00	25000.00	1.00	2.76	1.83	-0.00			
	CONSTANT	1.00E-01	1.00E+00	1.00E+00	1.00E-02	3.00E+01	3.00E+01	1.00E-04	-0.	-0.	-0.
	PER DEG-F	-0.	-0.	-0.	-0.	-0.	-0.	-0.	-0.	-0.	-0.
		R DEG/HOUR	UI DEG/HR/G	US DEG/HR/G	S DEG/H/G**2	IS ARC-SEC	IO ARC-SEC	T UNITY			
27	PERT-GYRO	1.65	3.00	25000.00	1.00	4.70	2.50	-0.00			
	CONSTANT	2.00E-01	1.50E-01	1.50E-01	4.00E-02	6.00E+00	7.00E+00	1.00E-04	-0.	-0.	-0.
	PER DEG-F	-0.	-0.	-0.	-0.	-0.	-0.	-0.	-0.	-0.	-0.
		R DEG/HOUR	UI DEG/HR/G	US DEG/HR/G	S DEG/H/G**2	IS ARC-SEC	IO ARC-SEC	T UNITY			

IC	COMPUTERS	WEIGHT	POWER	MTTF	ALPHA	BITS	COMP.FREQ.	INT.SCH.
41	LEM AEA	32.50	80.00	3200.00	1.00	18	50	1
42	SIGN III	27.00	115.00	5582.00	1.00	40	50	1
43	SIGN III	27.00	115.00	5582.00	1.00	20	50	2
44	SIGN III	27.00	115.00	5582.00	1.00	20	50	3
45	1824	34.14	92.90	2949.00	1.00	24	50	1
46	GPK-33	65.00	160.00	400.00	1.00	24	50	1
47	D210B	24.24	125.00	500.00	1.00	24	50	1
48	4PI-CUSTOM	50.00	85.00	2500.00	1.00	32	50	1
49	SRT RUK-2	36.00	90.00	6000.00	1.00	32	128	2

FIGURE 24b. CANDIDATA HARDWARE DATA (Continued)

Typical Output Listing.--Figures 25a, 25b, 25c, and 25d make up a typical four-page report for mode 2 using system A components and nominal mission data. Similar reports for mode 3 were presented in Figures 1a through 1d in the summary section of this report for system A and Figures 19 a through 19d for an optimum system. Figure 25a presents the penalty mode 2, 0.01309 probability of mission failure due to guidance, lists descriptive information about the launch vehicle and mission, and presents the hardware data for each instrument used in the conceptual system A IMU. In addition, data describing the conceptual SRT computer are presented. The notation RUK-2 denotes that a Runge-Kutta second order algorithm was used to update the direction cosine matrix.

IMU mechanical data is presented in Figure 25b. Horizontal design number 4 (see Appendix D for sketch of design) was found to be optimum (yields minimum weight) for the specified instruments. The dimensions of the case of the IMU, the calculated weights of the block, base, cover, and insulation, and the summation of the components (inertial sensors and computer) weights are presented. The electronics weight was a specified value. The total estimated weight for the system A IMU and computer is 69.46 lb for IMU design number 4.

The thermal analysis presented indicates that the thermal conductance for the IMU was calculated to be 2.17 watts/^{o}F on the basis that no heater power or cooling was to be required at the maximum ambient temperature, 140^{o} F. The peak watts, 372.7, are the total power (IMU plus computer) required at the minimum ambient temperature, 30^{o} F, for the calculated thermal conductance. The average watts, 307.5, are the total power required at the average ambient temperature, 60^{o} F, for the calculated thermal conductance. The energy source weight is the weight of the RTG needed to supply the average power required. This assumes that the peak power is required for a short time and would be drawn from a small secondary energy source as well as the RTG.

Figure 25b also presents the results of the navigation error analysis at various times along the trajectory. The velocity errors at injection are given in down range (DR), cross range (CR), and out of plane (OP) components. The root mean square (RMS) of these components is 11.03 ft/sec at injection with the degree of freedom (DOF) of 1.984. The injection errors propagated to the target with no midcourse correction are seen to result in a CR position error of 11.645 x 10^{8} ft. If a single perfect midcourse delta-velocity correction is made to null the CR position error, the correction delta-velocity required has an RMS value of 9.6276 ft/sec. If an imperfect midcourse is made with the relative accuracy shown, 0.07% error in magnitude and angular aiming error of 0.00291 radians, the CR position error would be 84.3593 x 10^{4} ft. Data describing the midcourse propulsion system is also presented. Under this penalty, mode 2, the total guidance weight is fixed, and the total midcourse propulsion system weight is calculated to be the difference between the total guidance weight and the sum of the IMU, computer, and energy source weight. For this example, the total guidance weight was fixed at 410 lbs and the resultant midcourse propulsion system weight after subtracting the weights of the IMU, computer, and energy source was calculated to be 221.249 lbs. The fuel weight of 183.34773 lbs gives a delta-velocity capability of 258.68 ft/sec. From this capability, the calculated probability of failure due to lack of

88

PENALTY(MODE 2) = .01309

ZERO CR POS. ERRORS AT TARGET
WITH MID COURSE AT 25.0 HOURS

260/S-IVB/CENTAUR-I/KICK JUPITER FLY BY
ZERO ALL ERRORS BEFORE SECOND BURN

HARDWARE DATA (ARBITRARY)

ACCELEROMETERS	WEIGHT	POWER	MTTF	ALPHA	LENGTH	DIAMETER	WIDTH	AXIS
ARMA D-4E	.35	1.50	100000.00	1.00	1.30	2.70	-0.00	YAW
CONSTANT	6.70E-06	1.00E-05	9.00E-07	1.00E-07	-0.	-0.	5.60E-06	5.60E-06	2.00E+01	2.00E+01
PER DEG-F	-0.	-0.	-0.	-0.	-0.	-0.	-0.	-0.	-0.	-0.
	K0	K1	K2	K3	M0	N0	M1	N1	IP	IN
	G	G/G	G/G**2	G/G**3	G/G	G/G	G/G**2	G/G**2	ARC SEC	ARC SEC
ARMA D-4E	.35	1.50	100000.00	1.00	1.30	2.70	-0.00	PITCH
CONSTANT	6.70E-06	1.00E-05	9.00E-07	1.00E-07	-0.	-0.	5.60E-06	5.60E-06	2.00E+01	2.00E+01
PER DEG-F	-0.	-0.	-0.	-0.	-0.	-0.	-0.	-0.	-0.	-0.
	K0	K1	K2	K3	M0	N0	M1	N1	IP	IN
	G	G/G	G/G**2	G/G**3	G/G	G/G	G/G**2	G/G**2	ARC SEC	ARC SEC
ARMA D-4E	.35	1.50	100000.00	1.00	1.30	2.70	-0.00	ROLL
CONSTANT	6.70E-06	1.00E-05	9.00E-07	1.00E-07	-0.	-0.	5.60E-06	5.60E-06	2.00E+01	2.00E+01
PER DEG-F	-0.	-0.	-0.	-0.	-0.	-0.	-0.	-0.	-0.	-0.
	K0	K1	K2	K3	M0	N0	M1	N1	IP	IN
	G	G/G	G/G**2	G/G**3	G/G	G/G	G/G**2	G/G**2	ARC SEC	ARC SEC

GYROSCOPES	WEIGHT	POWER	MTTF	ALPHA	LENGTH	DIAMETER	WIDTH	AXIS
GG 334-A	1.65	3.00	25000.00	1.00	4.70	2.50	-0.00	YAW
CONSTANT	1.00E-01	1.50E-01	1.50E-01	4.00E-02	6.00E+00	7.00E+00	1.00E-04	-0.	-0.	-0.
PER DEG-F	-0.	-0.	-0.	-0.	-0.	-0.	-0.	-0.	-0.	-0.
	R	UI	US	S	IS	I0	T			
	DEG/HOUR	DEG/HR/G	DEG/HR/G	DEG/H/G**2	ARC-SEC	ARC-SEC	UNITY			
GG 334-A	1.65	3.00	25000.00	1.00	4.70	2.50	-0.00	PITCH
CONSTANT	1.00E-01	1.50E-01	1.50E-01	4.00E-02	6.00E+00	7.00E+00	1.00E-04	-0.	-0.	-0.
PER DEG-F	-0.	-0.	-0.	-0.	-0.	-0.	-0.	-0.	-0.	-0.
	R	UI	US	S	IS	I0	T			
	DEG/HOUR	DEG/HR/G	DEG/HR/G	DEG/H/G**2	ARC-SEC	ARC-SEC	UNITY			
GG 334-A	1.65	3.00	25000.00	1.00	4.70	2.50	-0.00	ROLL
CONSTANT	1.00E-01	1.50E-01	1.50E-01	4.00E-02	6.00E+00	7.00E+00	1.00E-04	-0.	-0.	-0.
PER DEG-F	-0.	-0.	-0.	-0.	-0.	-0.	-0.	-0.	-0.	-0.
	R	UI	US	S	IS	I0	T			
	DEG/HOUR	DEG/HR/G	DEG/HR/G	DEG/H/G**2	ARC-SEC	ARC-SEC	UNITY			

COMPUTER	WEIGHT	POWER	MTTF	ALPHA	BITS	COMP.FREQ.	INT.SCH.
SRT RUK-2	36.00	90.00	6000.00	1.00	32	128	2

FIGURE 25a. PENALTY, MODE 2, REPORT ON SYSTEM A

IMU MECHANICAL DATA(HORIZONTAL DESIGN NUMBER 4 OPTIMUM)

OUTSIDE DIMENSIONS		WEIGHT	
LENGTH=	9.35000	BLOCK=	8.70314
WIDTH=	10.45000	BASE=	4.54869
HEIGHT=	5.45000	COVER=	2.86681
		INSULATION=	1.34474
		ELECTRONICS=	10.00000
		COMPONENTS=	42.00000

TOTAL(IMU+COMPUTER)WEIGHT= 69.46339

THERMAL ANALYSIS

AVERAGE WATTS = 307.5 MIN.HEATER WATTS = -.0
PEAK WATTS = 372.7 THERMAL COND. = 2.17(W/D-F)

ENERGY SOURCE WEIGHT= 119.28750

ERROR ANALYSIS

		DR	CR	OP	RMS	DOF
INJECTION	POSITION	4.1990E+02	2.9703E+03	2.7140E+03	4.0454E+03	1.992334
	VELOCITY	3.9591E-01	8.1812E+00	7.3895E+00	1.1031E+01	1.984135
	ATTITUDE	7.8376E-04	4.6165E-04	4.6163E-04	1.0201E-03	2.276002
MID COURSE	POSITION	1.3815E+05	8.5126E+05	6.1261E+05	1.0578E+06	1.680602
	VELOCITY	1.5805E+00	9.6111E+00	6.8329E+00	1.1898E+01	1.658041
	ATTITUDE	4.3764E-02	4.2866E-02	4.2855E-02	7.4762E-02	2.998805
CORRECTION DELTA VEL.		4.3011E+00	8.1912E+00	2.6637E+00	9.6276E+00	1.000000
AT TARGET						
NO MID COR	POSITION	4.2965E+07	1.1645E+09	1.0277E+08	1.1698E+09	1.007496
	VELOCITY	1.0307E+03	1.6246E+03	2.0568E+04	2.0657E+04	1.008347
PERFECT MC	POSITION	6.0252E+07	3.2808E-06	7.1496E+07	9.3498E+07	1.937559
	VELOCITY	5.8238E+02	1.5016E+03	9.3774E+02	1.8637E+03	1.210988
IMPERFECT	POSITION	6.0252E+07	8.4359E+05	7.1496E+07	9.3503E+07	1.937878
	VELOCITY	5.8242E+02	1.5016E+03	9.3787E+02	1.8638E+03	1.211131

MIDCOURSE SYSTEM

RELATIVE ACCURACY		WEIGHT		
MAGNITUDE=	.00072442	FUEL=	183.34773	DELTA-V CAPABILITY= 258.67555
ANGLE=	.00291000	TANKAGE=	17.60138	EXPECTED BURN TIME= 32.35117
		CONSTANT=	20.30000	

TOTAL MIDCOURSE WEIGHT= 221.24911

PENALTY ANALYSIS

PROBABILITIES OF FAILURE		WEIGHT		
RELIABILITY=	.01308678	NON-GUIDANCE=	5000.00	(FIXED)
SUFFICIENT FUEL=	.00000000	GUIDANCE=	410.00	(FIXED)
MISS AT TARGET=0	00000000			
SYSTEM=	.01308678 (PENALTY)	TOTAL=	5410.00	(FIXED)

FIGURE 25b. PENALTY, MODE 2, REPORT ON SYSTEM A (Continued)

06

MISSION AND SPACE CRAFT DATA

IC=0

	ID	DESCRIPTION		VALUE	SENSITIVITY		ID	DESCRIPTION		VALUE	SENSITIVITY
	1	TIME TO MID COURSE	(HOURS)	25.00000	.9174689		20	VIBRATION UPPER FREQ.	(CPS)	100.00000	0.0000000
C	2	PROBABILITY OF GUIDANCE FAIL.		.10000	0.0000000		21	INSULATION THICKNESS	(IN)	.05000	0.0000000
	3	MID COURSE SYSTEM CON.	(LB/LB)	1.09600	0.0000000		22	INSULATION DENSITY	(IN)	.09100	0.0000000
	4	SPECIFIC IMPULSE	(SEC.)	233.00000	0.0000000		23	ELECTRONICS POWER	(WATTS)	30.00000	0.0000000
	5	NONGUIDANCE WEIGHT	(LB)	5000.00000	0.0000000		24	MID COURSE SYSTEM	(LB)	20.30000	0.0000000
	6	TOTAL WEIGHT	(LB)	5410.00000	0.0000000		25	BOOST TIME	(HOURS)	.20000	.0004525
	7	ENERGY SOURCE CONSTANT	(LB)	13.20000	0.0000000		26	OPERATING TEMPERATURE	(DEG-F)	160.00000	0.0000000
	8	ENERGY SOURCE CONSTANT	(LB/W)	.34500	0.0000000		27	MAX.AMBIENT TEMPERATURE	(DEG-F)	140.00000	0.0000000
	9	BLOCK DENSITY	(LB/IN**3)	.09700	0.0000000		28	AVE.AMBIENT TEMPERATURE	(DEG-F)	60.00000	0.0000000
	10	BASE DENSITY	(LB/IN**3)	.09700	0.0000000		29	MIN.AMBIENT TEMPERATURE	(DEG-F)	30.00000	0.0000000
	11	COVER DENSITY	(LB/IN**3)	.09700	0.0000000		30	OPERATING TEMP.UNCER.	(DEG-F)	.10000	0.0000000
	12	IMU COMPONENT SEPARATION	(IN)	.25000	0.0000000	A	31	THERMAL CONDUCTIVITY	(W/DEG-F)	0.00000	0.0000000
	13	BASE OFFSET	(IN)	1.50000	0.0000000	B	32	REL.UNC.IN MID COURSE MAG.		-1.00000	0.0000000
	14	BASE THICKNESS	(IN)	.50000	0.0000000	B	33	REL.UNC.IN MID COURSE ANGLE		.00291	0.0000000
	15	COVER CLEARANCE	(IN)	.25000	0.0000000		34	TARGET MISS DISTANCE	(FT)	100000000.00000	0.0000000
	16	COVER THICKNESS	(IN)	.10000	0.0000000		35	MID COURSE THRUST	(LB)	50.00000	0.0000000
	17	ELECTRONICS WEIGHT	(LB)	10.00000	0.0000000		36	MIDCOURSE ENGINE RELIABILTY		.00100	.0754885
	18	ELECTRONICS MTBF	(HR)	10000.00000	-.1866681		37	ENERGY SOURCE MTBF	(HRS)	10000.00000	-.1866681
	19	VIBRATION(MILLARAD/SEC)**2/CPS		.30457	0.0000000		38			0.00000	0.0000000

NOTES A=COMPUTED BY PROGRAM IF DATA SET TO ZERO
B=COMPUTED BY PROGRAM IF DATA SET TO LESS THAN ZERO
C=NOT USED BY THIS PENALTY FUNCTION

SENSITIVITY = PERCENT CHANGE IN PENALTY / PERCENT CHANGE IN DATA

FIGURE 25c. PENALTY, MODE 2, REPORT ON SYSTEM A (Continued)

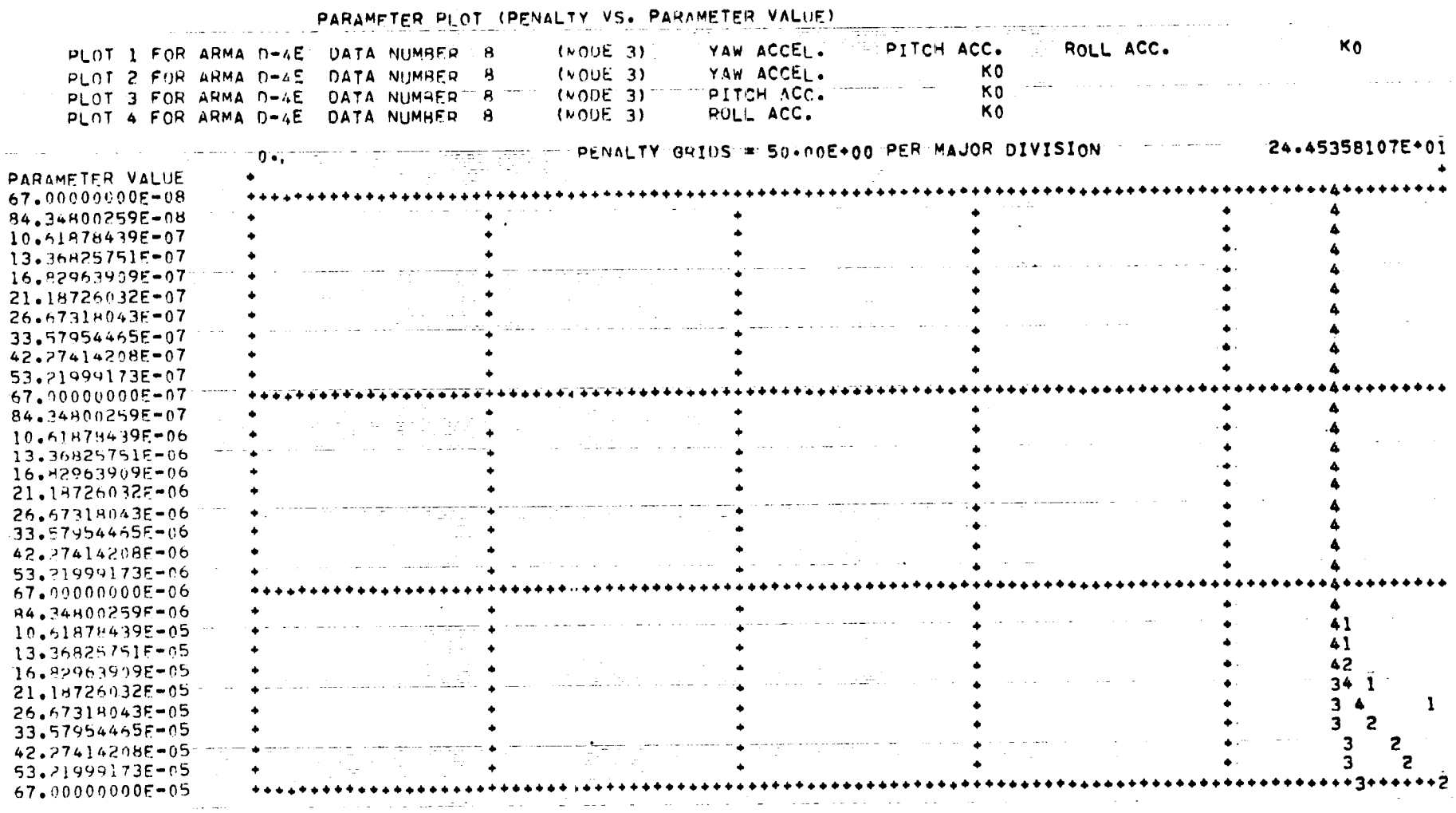

FIGURE 3. PLOTS OF PENALTY, MODE 3, VARIATION WITH SYSTEM A ACCELEROMETER BIAS SWEEPS

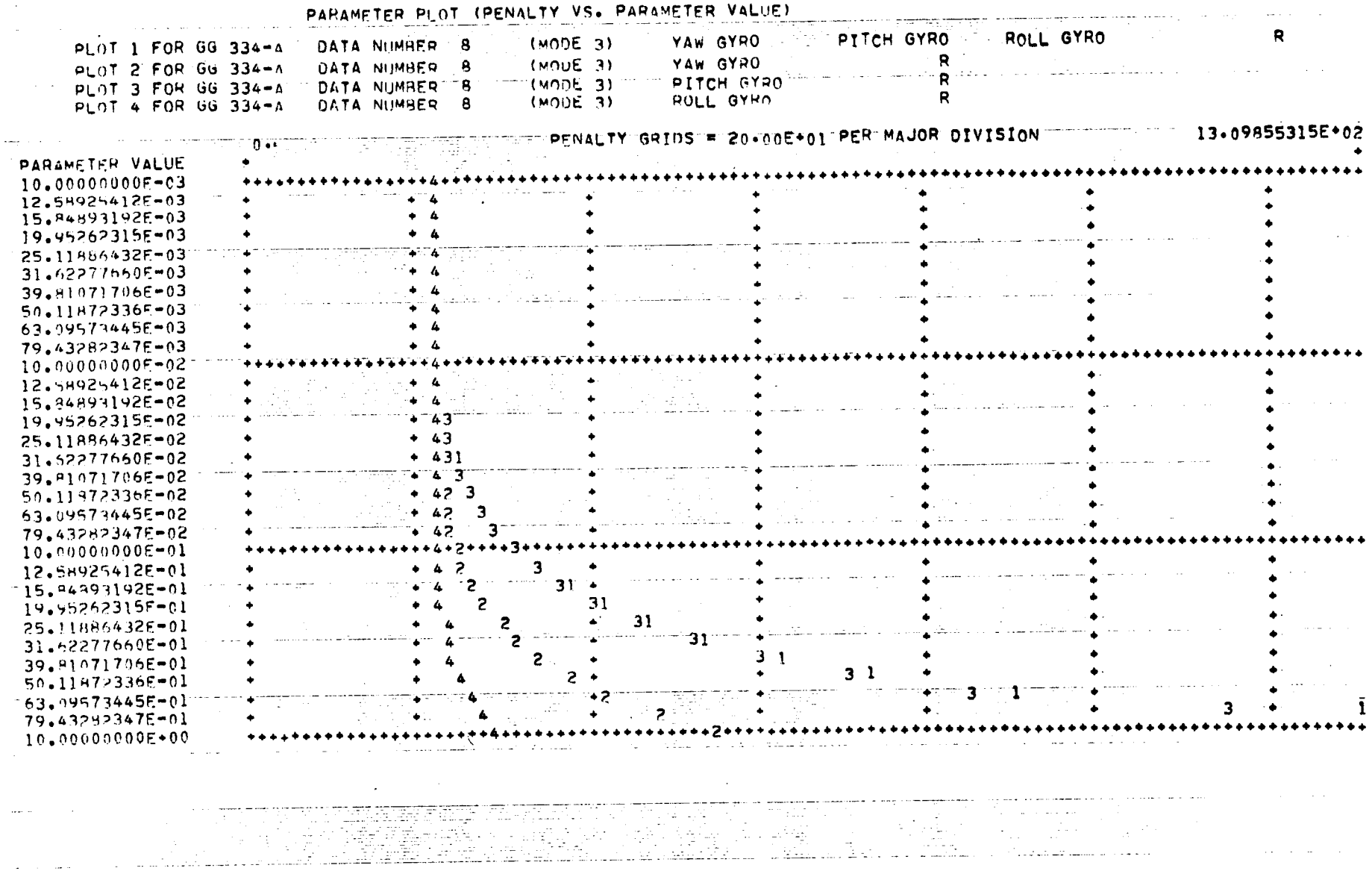

FIGURE 4. PLOTS OF PENALTY, MODE 3, VARIATION WITH SYSTEM A GYRO FIXED DRIFT SWEEPS

HARDWARE SENSITIVITY

ID		ARMA D-4E YAW ACC. IC= 1	ARMA D-4E PITCH ACC. 1	ARMA D-4E ROLL ACC. 1		GG 334-A YAW GYRO 22	GG 334-A PITCH GYRO 22	GG 334-A ROLL GYRO 22
1	WEIGHT	0.0000000	0.0000000	0.0000000		0.0000000	0.0000000	0.0000000
2	POWER	0.0000000	0.0000000	0.0000000		0.0000000	0.0000000	0.0000000
3	MTTF	-.0001493	-.0001493	-.0001493		-.0746667	-.0746667	-.0746667
4	ALPHA	-.0019054	-.0019054	-.0019054		-.5302735	-.5302735	-.5302735
5	LENGTH	0.0000000	0.0000000	0.0000000		0.0000000	0.0000000	0.0000000
6	DIAMETER	0.0000000	0.0000000	0.0000000		0.0000000	0.0000000	0.0000000
7	WIDTH	0.0000000	0.0000000	0.0000000		0.0000000	0.0000000	0.0000000
	CONSTANT				CONSTANT			
8	K0	0.0000000	0.0000000	0.0000000	R	0.0000000	0.0000000	0.0000000
9	K1	0.0000000	0.0000000	0.0000000	UI	0.0000000	0.0000000	0.0000000
10	K2	0.0000000	0.0000000	0.0000000	US	0.0000000	0.0000000	0.0000000
11	K3	0.0000000	0.0000000	0.0000000	S	0.0000000	0.0000000	0.0000000
12	M0	0.0000000	0.0000000	0.0000000	IS	0.0000000	0.0000000	0.0000000
13	N0	0.0000000	0.0000000	0.0000000	I0	0.0000000	0.0000000	0.0000000
14	M1	0.0000000	0.0000000	0.0000000	T	0.0000000	0.0000000	0.0000000
15	N1	0.0000000	0.0000000	0.0000000		0.0000000	0.0000000	0.0000000
16	IP	0.0000000	0.0000000	0.0000000		0.0000000	0.0000000	0.0000000
17	IN	0.0000000	0.0000000	0.0000000		0.0000000	0.0000000	0.0000000
	PER DEG-F				PER DEG-F			
18	K0	0.0000000	0.0000000	0.0000000	R	0.0000000	0.0000000	0.0000000
19	K1	0.0000000	0.0000000	0.0000000	UI	0.0000000	0.0000000	0.0000000
20	K2	0.0000000	0.0000000	0.0000000	US	0.0000000	0.0000000	0.0000000
21	K3	0.0000000	0.0000000	0.0000000	S	0.0000000	0.0000000	0.0000000
22	M0	0.0000000	0.0000000	0.0000000	IS	0.0000000	0.0000000	0.0000000
23	N0	0.0000000	0.0000000	0.0000000	I0	0.0000000	0.0000000	0.0000000
24	M1	0.0000000	0.0000000	0.0000000	T	0.0000000	0.0000000	0.0000000
25	N1	0.0000000	0.0000000	0.0000000		0.0000000	0.0000000	0.0000000
26	IP	0.0000000	0.0000000	0.0000000		0.0000000	0.0000000	0.0000000
27	IN	0.0000000	0.0000000	0.0000000		0.0000000	0.0000000	0.0000000

COMPUTER SENSITIVITY

SRT RUK-2
IC= 49

ID			ID			
1	WEIGHT	0.0000000	8	NO.OF BITS	0.0000000	PER BIT
2	POWER	0.0000000	9	COMP.FREQ.	0.0000000	
3	MTTF	-.3111161	10	INT.SCHEME	0.0000000	CHANGE TO RECT.
4	ALPHA	-1.7897195	10	INT.SCHEME	0.0000000	CHANGE TO RUK-4

SENSITIVITY = PERCENT CHANGE IN PENALTY / PERCENT CHANGE IN DATA
EXCEPT AS NOTED FOR COMPUTER BITS AND INTEGRATION SCHEME

FIGURE 25d. PENALTY, MODE 2, REPORT ON SYSTEM A (Continued)

sufficient fuel was zero. Therefore, the total penalty, probability of mission failure due to guidance, is equal to the probability of failure due to hardware reliability, 0.01309.

Mission and spacecraft data used in the computation of the results presented in Figure 25b are listed in Figure 25c. A short phrase describing the item of data and the value used in the computation is followed by the sensitivity of the penalty to that value. This sensitivity, as noted in Figure 25c, is the percent change in the penalty to a one percent change in the data value. For example, a one percent change in ID 1, the time to midcourse correction, would result in a 0.917 percent change in the penalty for this case. A negative value of sensitivity indicates that the penalty will decrease if the data value is increased and vice versa. It should be noted that even though the mission and spacecraft data values listed in Figure 25c are the same as those listed earlier in Figure 1c, the sensitivity of the penalty to these values is quite different for the two different modes.

Sensitivity of the penalty to inertial sensor and computer data is presented in Figure 25d. A zero value of sensitivity indicates that a one percent change in the data value presented in Figure 25d for the item of interest results in no change in the penalty out to the number of significant figures printed, or that the data value was zero. The sensitivity to the number of bits of the computer and integration scheme is not the sensitivity to a percent change in the data value, but is the percent change in penalty to the change noted for these items. Under mode 2, the principal data affecting the penalty are seen to be the mean time to failure, MTTF, and the Weibull constant, α.

IMU Mechanical Weight Estimation Results.--The system A IMU components, the GG 334A and the D4E, were used to evaluate horizontal mechanical designs 1 through 6 and the six vertical designs illustrated in Appendix D. The same material densities, component separation, base offset and thickness, cover clearance and thickness, and insulation thickness were used for each design. These data values are listed in Figure 25c. Table XXIII lists the results of this evaluation.

TABLE XXIII
IMU WEIGHT ESTIMATION RESULTS FOR SYSTEM A

	Item Weight (lbs)					
Design No.	Block	Base	Cover	Insulation	Sensors + Electronics	Total IMU
Horizontal 1	8.70	5.05	3.09	1.45	16.00	34.29
Horizontal 2	8.70	4.97	3.06	1.43	16.00	34.16
Horizontal 3	8.70	4.59	2.92	1.37	16.00	33.58
Horizontal 4	8.70	4.55	2.87	1.34	16.00	33.46
Horizontal 5	8.70	5.17	3.14	1.47	16.00	34.48
Horizontal 6	8.70	5.19	3.14	1.47	16.00	34.50
Vertical 1	8.70	4.73	3.33	1.56	16.00	34.32
Vertical 2	8.70	5.49	3.28	1.54	16.00	35.01
Vertical 3	8.70	6.07	2.71	1.27	16.00	34.75
Vertical 4	8.70	6.75	2.93	1.37	16.00	35.75
Vertical 5	8.70	6.07	3.47	1.63	16.00	35.87
Vertical 6	8.70	5.17	3.62	1.70	16.00	35.19

In reality, horizontal designs three through six are for pendulous accelerometers, and therefore, the results are not strictly true since the D4E is a vibrating string accelerometer. Similarly, vertical designs two through four are for pendulous accelerometers only. The above results do illustrate that the mechanical design variations make little difference for these conceptual designs for the system A components. The total weight variation is seen to be 1.29 lbs from the lightest to the heaviest.

Although horizontal design 4 yields minimum weight for system A, another design may yield minimum weight for another set of components as shown previously for an optimum system, Figure 19b.

System B.-- Results for system A, penalty mode 3, nominal conditions, as shown in Figures 1 through 5 indicate that the inertial components have more than sufficient accuracy. When gyro fixed drift (R) and accelerometer bias (K_0) are swept in Figures 2, 3, and 4, the curves show that increases in these values should not increase the penalty significantly. It was decided to investigate a system similar to system A with components identical to the system A components except for increased gyro fixed drift (R), accelerometer bias (K_0), and accelerometer scale factor (K_1) error coefficients.

The new components are labeled Pert-ACC and Pert-GYRO, and the system is referred to as system B.

System B Components.--The sweeps and sensitivities shown in Figures 1, 2, 3, and 4 indicate changes in penalty for changing only one parameter. It was decided to increase the error coefficients in such a way that the three become equally important (nearly equal sensitivities) and that the combined penalty increase be about ten percent by allotting a five percent penalty change to gyros and five percent to accelerometers.

A sweep of gyro drift for all three gyros (Plot 1 of Figure 4) shows that a penalty increase of five percent occurs when fixed drift is increased from 0.1 to about 0.2 deg/hr. The Pert-GYRO was defined to be identical to the GG 334-A except for a 0.2 deg/hr fixed drift uncertainty.

A sweep of accelerometer bias for all three accelerometers (Plot 1 of Figure 3 and the table in Figure 2) show that bias may be increased from 6.7×10^{-6} to about 2.2×10^{-4} g's (a factor of about 30) before penalty is increased by about five percent. Rather than allocate the entire increase to K_0, however, it was decided to increase both K_0 and K_1. No sweep was made for K_1. However, its effect may also be estimated from the sensitivities shown in Figure 1d.

Since only the sensitivities per single component are shown, the sensitivities for changing all three accelerometers are calculated by adding as shown in Table XXIV.

TABLE XXIV
SUMMING ACCELEROMETER SENSITIVITIES

Error Source	Yaw	Pitch	Roll	Total
K_0	0.0000381	0.0000044	0.0000249	0.0000674
K_1	0.0	0.0	0.0000523	0.0000523

Thus, for changing all three accelerometer K_0's and K_1's, the sensitivity is about the same. The five percent increase was split to a two percent increase in penalty for both K_0 and K_1. From the table in Figure 2 a two percent increase (to 226 lbs) in the penalty occurs at about 1.6×10^{-4} g's or a factor of 30. Since the sensitivities are about the same, it was decided to increase K_1 by a factor of 30 also. The Pert-ACC was defined to be identical to the D-4E except for 1.68×10^{-4} g bias and 3.0×10^{-4} scale factor uncertainties.

System B Results.--The penalty, mode 3, for system B under nominal conditions is 239.5 lbs, an increase of about 8% over system A. The sensitivities are shown in Table XXV.

TABLE XXV
ERROR SOURCE SENSITIVITIES FOR SYSTEM B

Error Source	Yaw	Pitch	Roll	Total
R	0.01238	0.10839	0.00058	0.12135
K_0	0.01782	0.00204	0.08662	0.10648
K_1	0.0	0.0	0.03501	0.03501
K_0+K_1				0.14149

Plots of the penalty vs the error coefficients are shown in Figures 26, 27, and 28. Circles have been drawn to indicate the plot points closest to the values for the system B components. It can be seen that these values represent a tight condition where any further increase will result in large increases in the penalty.

This technique of loosening specifications will work equally well on any component data. Care should be used when applying this approach to certain error coefficients, however. The SEAP coefficients for sensitivity to yaw and pitch accelerometer scale factor are zero. This would indicate unlimited increase in these error coefficients and would not change the penalty, or in fact that these accelerometers are not needed. This is an obvious fallacy in that, although this nominal trajectory does not have acceleration components in these body coordinates, an actual flight would due to wind disturbances, etc. Any trajectory which involves yaw steering or a plane change such as synchronous equatorial orbital missions would have non-zero sensitivities for these terms due to the additional accelerations appearing in the nominal trajectories. In general, however, any term with small sensitivity should be considered one for which an easing of specifications would not seriously change the penalty.

Summary of Systems Exercised.--Additional studies of system A, system B, and optimum systems were made for variations of the nominal conditions and under different penalty modes. These results are summarized in Table XXVI.

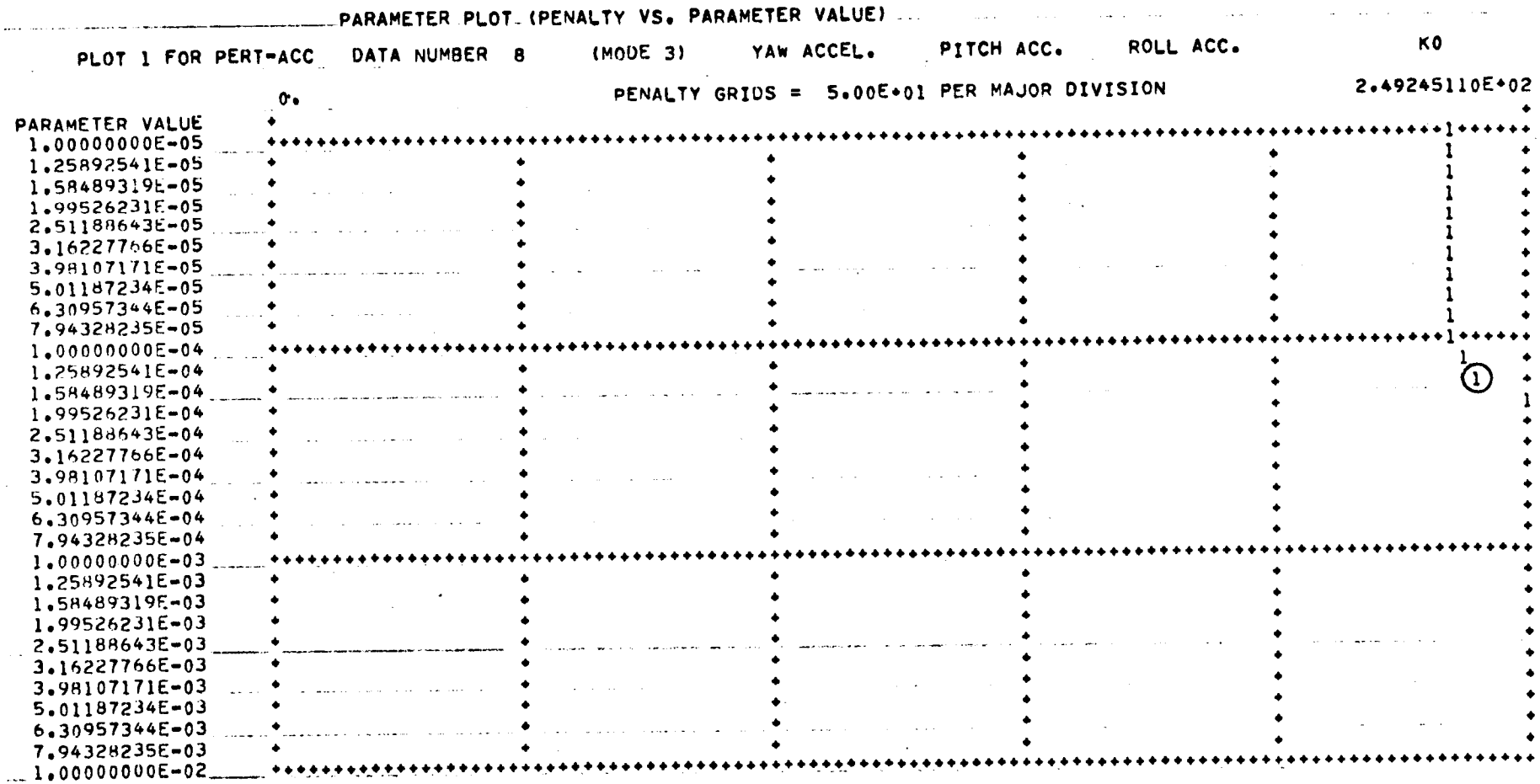

FIGURE 26. PENALTY, MODE 3, VARIATION WITH SYSTEM B ACCELEROMETER BIAS SWEEP

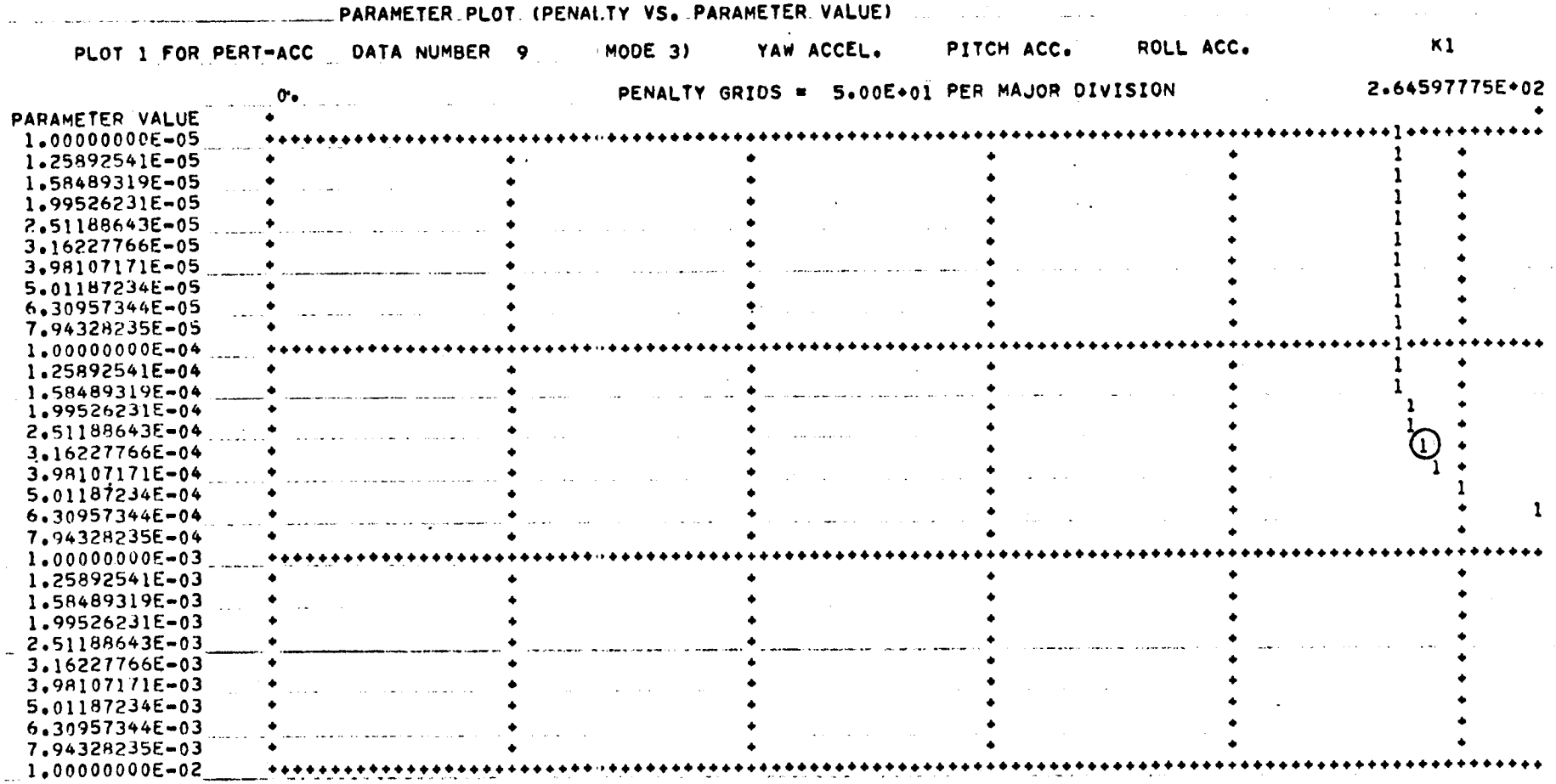

FIGURE 27. PLOT OF PENALTY, MODE 3, VARIATION WITH SYSTEM B ACCELEROMETER SCALE FACTOR SWEEP

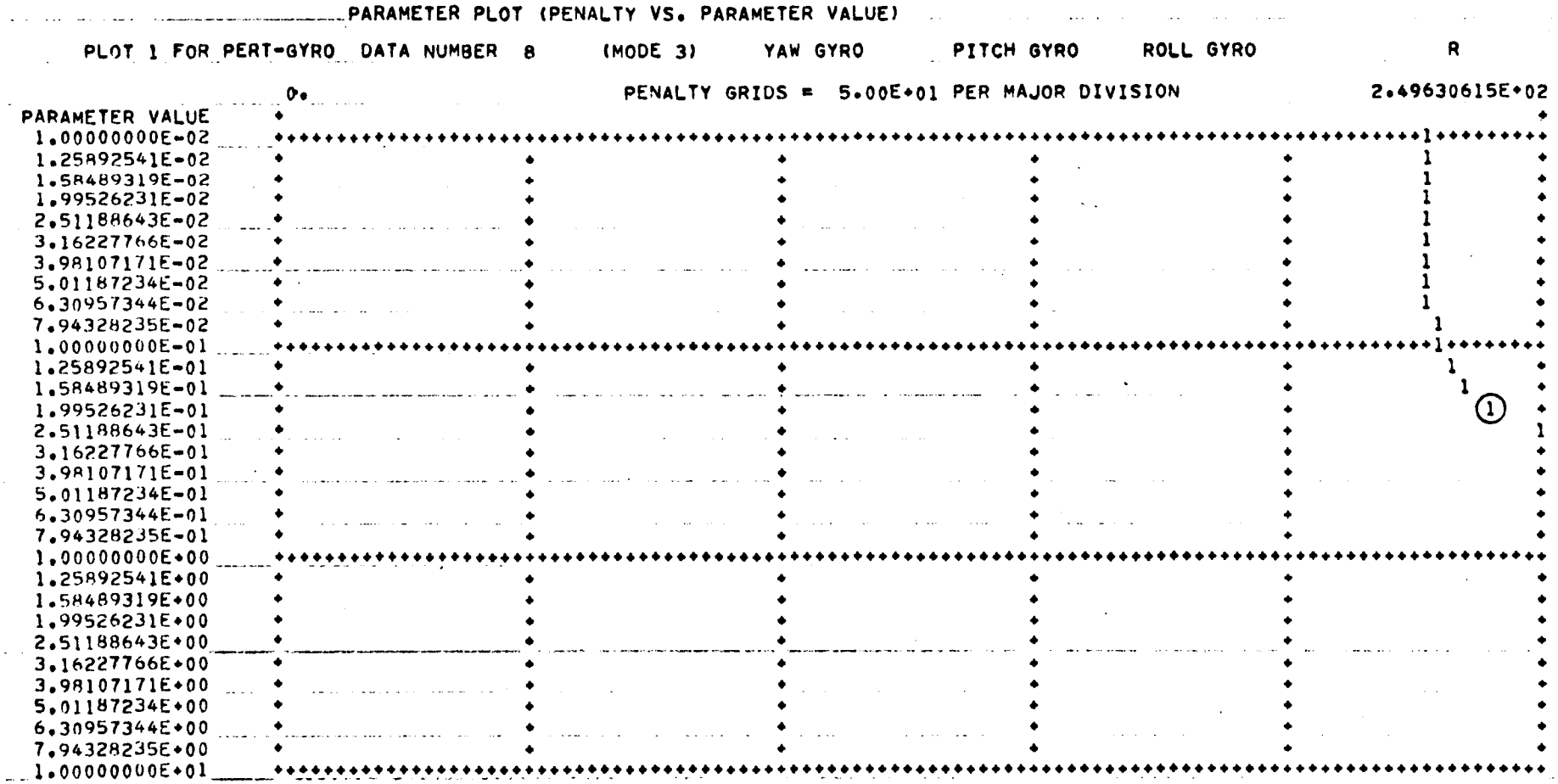

FIGURE 28. PLOT OF PENALTY, MODE 3, VARIATION WITH SYSTEM B GYRO FIXED DRIFT SWEEP

TABLE XXVI
ADDITIONAL PENALTY RESULTS

Penalty Mode	System (Optimum defined below)	Probability of Guidance Failure	Time to Midcourse 25 hours	Time to Midcourse 240 hours
2	A	Calculated	0.01309	0.11113
2	B	Calculated	0.04042	0.13575
2	Optimum	Calculated	0.01160[1]	0.09824[1]
3	A	0.1	222.04	Fails
3	B	0.1	239.47	Fails
3	Optimum	0.1	208.80[2]	222.08[3]
3	A	0.05	224.89	Fails
3	B	0.05	250.96	Fails
3	Optimum	0.05	210.55[4]	None

Notes: Fails = Probability of hardware failure exceeds P_{FG}

None = No system was found with sufficient reliability

Optimum Systems:

	Accelerometers	Gyroscopes	Computer	
(1)	2401-005	SYG-1440	SRT RUK-2	
(2)	GG-177	18-IRIG-B	SIGN-III	(Full report shown in Figures 19a-19d)
(3)	GG-177	SYG-1440	SIGN-III	
(4)	2401-005	SYG-1440	SRT-RUK-2	

Parameter Sweeps.--During the exercise of the computer programs selected parameters were swept, and the results are shown in Figures 29 through 36. Time to midcourse correction was swept from zero to 240 hours in linear steps of ten hours as shown in Figure 29 for penalty mode 2 and Figure 30 for penalty mode 3. For the mission data used, the penalty mode 2 is essentially the probability of failure due to reliability; thus, the plot of penalty mode 2 vs time to midcourse increases due to increased gyro and computer operating time. The similar plot for penalty mode 3 shows very little change between 10 and 200 hours. Above 200 hours the penalty increases rapidly, and above 220 hours

the penalty is saturated. This is because the probability of failure due to reliability exceeds the required probability of guidance failure (P_{FG} = 0.1). This can be confirmed by noting that penalty mode 2, essentially P_{FG}, crosses the 0.1 value at 220 hours.

Probability of guidance failure (P_{FG}) was swept in linear steps of 0.002 from 0.05 to 0.10, and the results for penalty mode 3 are shown in Figure 31. This plot, with the time of midcourse at the nominal value of 25 hours, shows little change. However, had the sweep included values lower than 0.050, the penalty would increase greatly when P_{FG} became close to the probability of failure due to reliability (P_{FR} = 0.013 for 25 hours to midcourse).

A plot of penalty, mode 3, vs operating temperature from 150 to 180° F is shown in Figure 32. Note the increase in penalty for lower operating temperature. This is easily understood when the effect of designing the thermal conductance is considered. The thermal conductance is designed to dissipate the exciting power through a drop from operating temperature to maximum ambient temperature. The nominal data includes a maximum ambient temperature of 140° F. Therefore, operating temperatures near 140° F result in very high conductance and a corresponding increase in heater power for portions of the mission when the ambient temperature is below its maximum. In fact, if the operating temperature were equal to the maximum ambient temperature, zero conductance would be used and infinite heater power would be needed during the colder portions of the mission.

Figure 33 presents four parameter plots of logarithmic sweeps of the parameter versus the penalty for system A. Plot 1 is a sweep of excitation power to all three gyros versus the penalty for mode 3. Plots 2, 3, and 4 coincide and are shown as plot 4. In this case, the excitation power to each gyro was swept while the other two gyros' power remained at the original value for the GG 334A.

Plots of logarithmic sweeps of gyro weight versus the penalty for system A are presented in Figure 34. Plot 1 is a sweep of the weight of all three gyroscopes simultaneously. Plots 2, 3, and 4 coincide and are shown as plot 4. In this case, the weight of each gyro was swept while the other two gyros' weight remained at the original value for the GG 334A.

Figure 35 presents a plot of a linear sweep of IMU component separation versus the penalty for system A for mode 3. Increasing the component separation from the nominal value of 0.25 inch to 1.00 inch increases the penalty from 222.04 lbs to 256.38 lbs as shown in the figure.

A plot of the penalty versus a logarithmic sweep of the computation frequency (frequency at which the direction cosine matrix is updated) is presented in Figure 36 for the system A computer, SRT RUK-2.

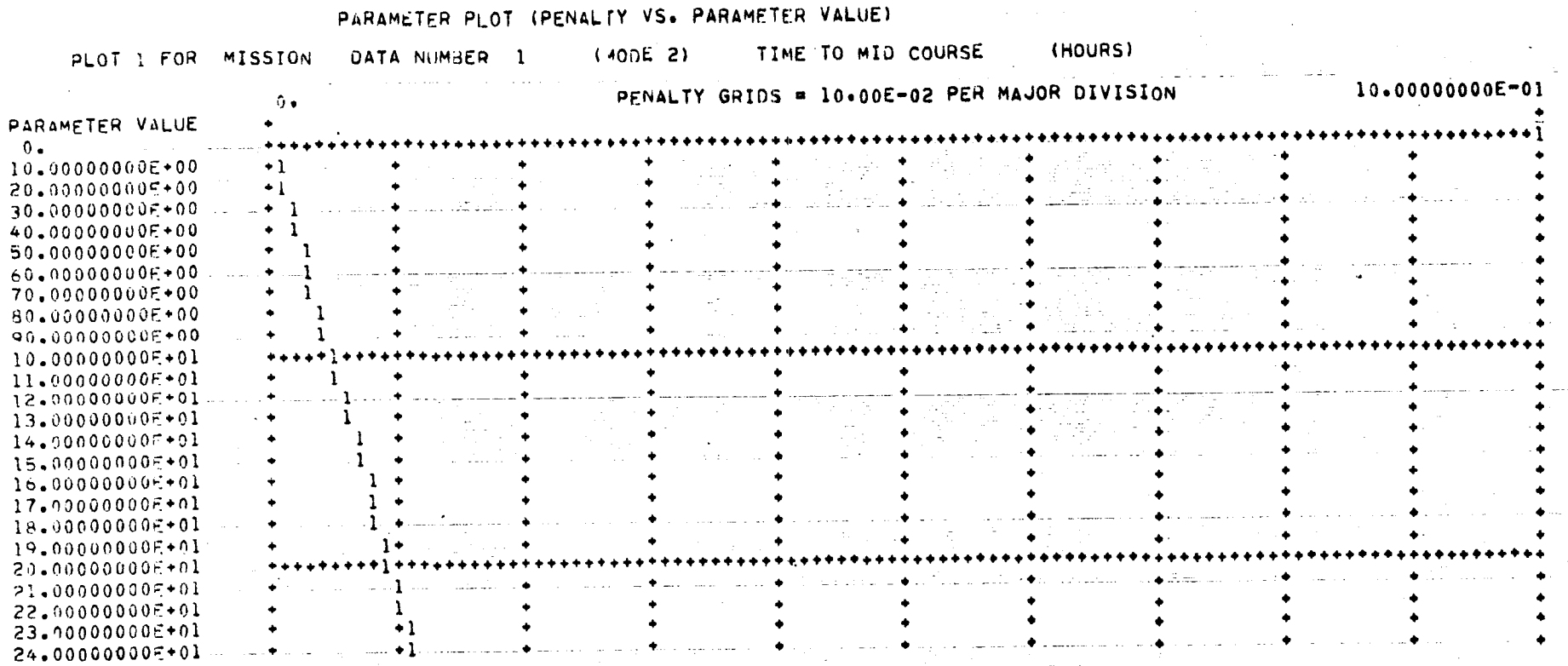

FIGURE 29. PLOT OF PENALTY, MODE 2, (SYSTEM A)
VARIATION WITH TIME TO MIDCOURSE SWEEP

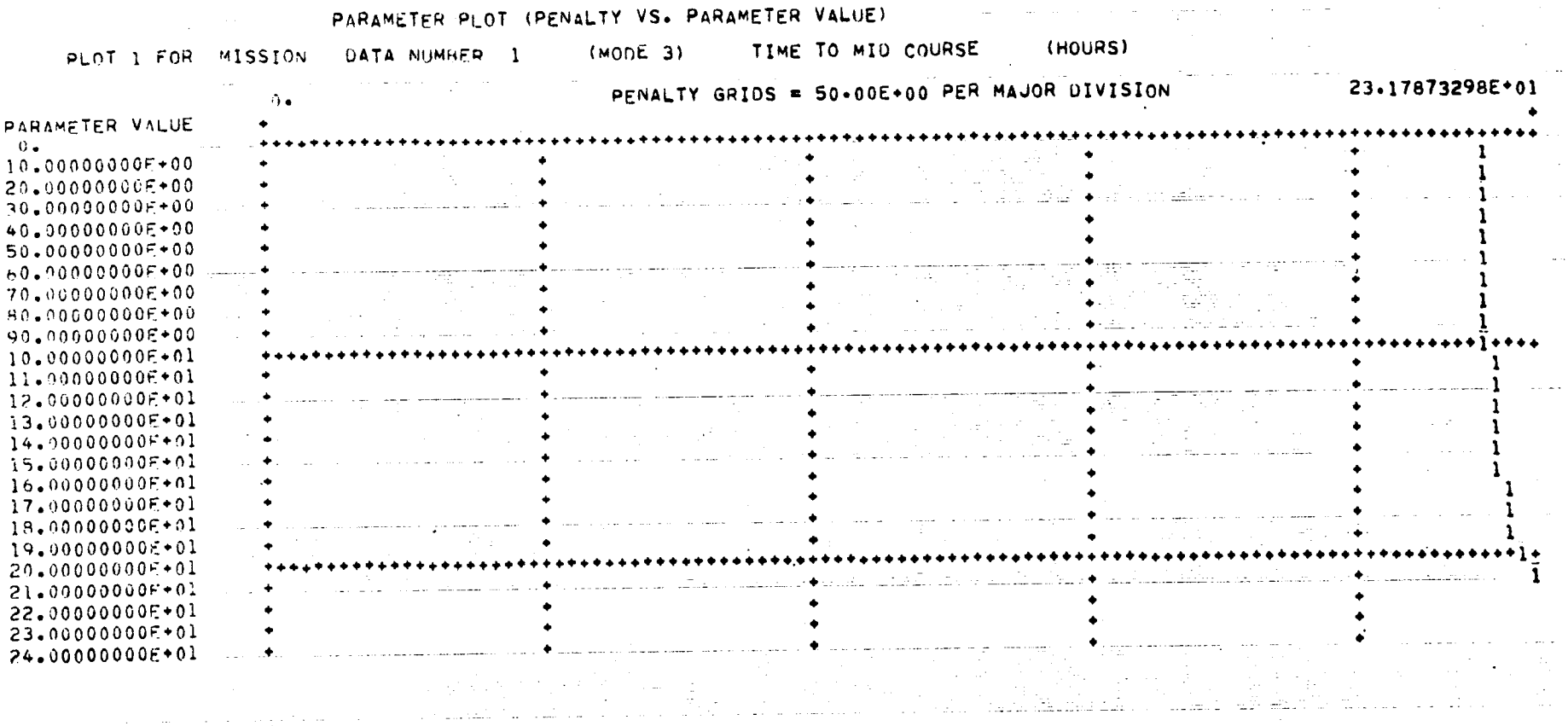

FIGURE 30. PLOT OF PENALTY, MODE 3, (SYSTEM A)
VARIATION WITH TIME TO MIDCOURSE SWEEP

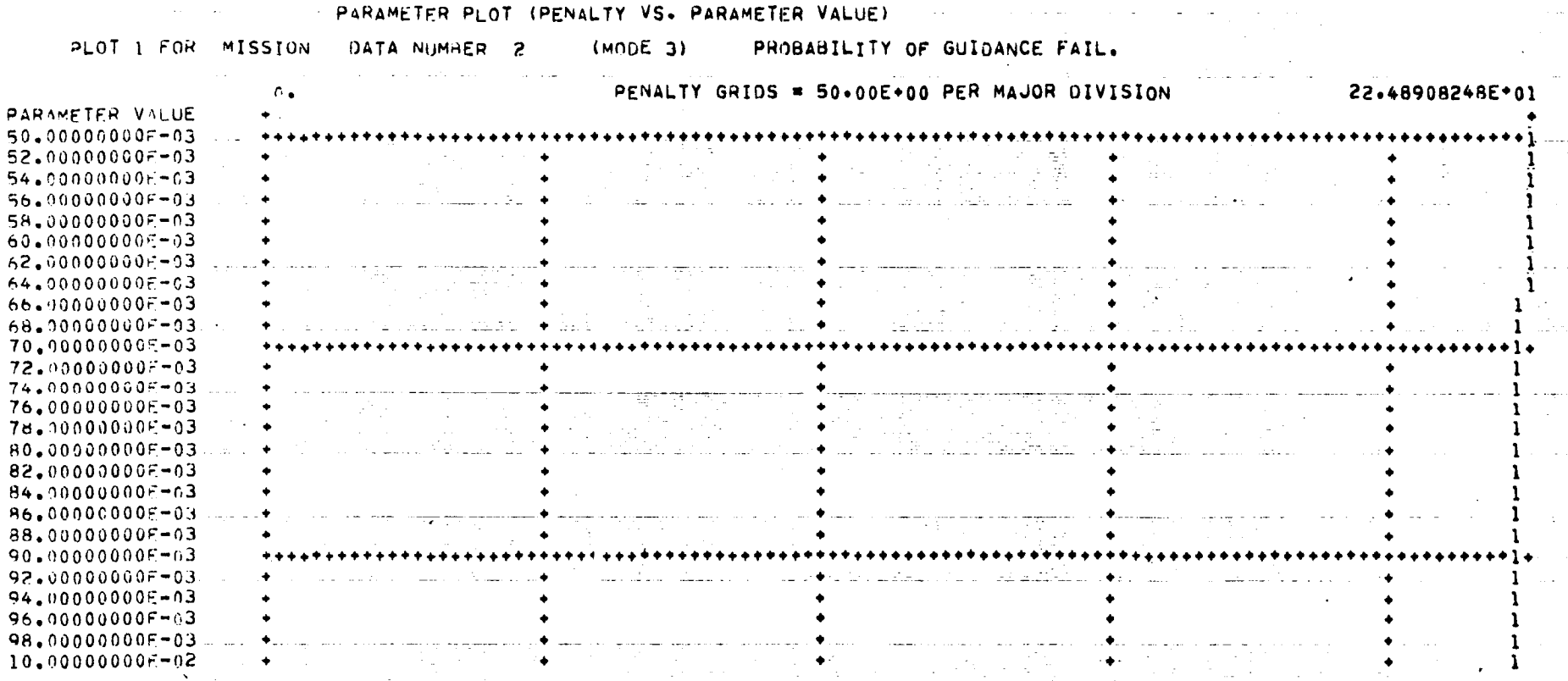

FIGURE 31. PLOT OF PENALTY, MODE 3, (SYSTEM A) VARIATION WITH PROBABILITY OF GUIDANCE FAILURE SWEEP

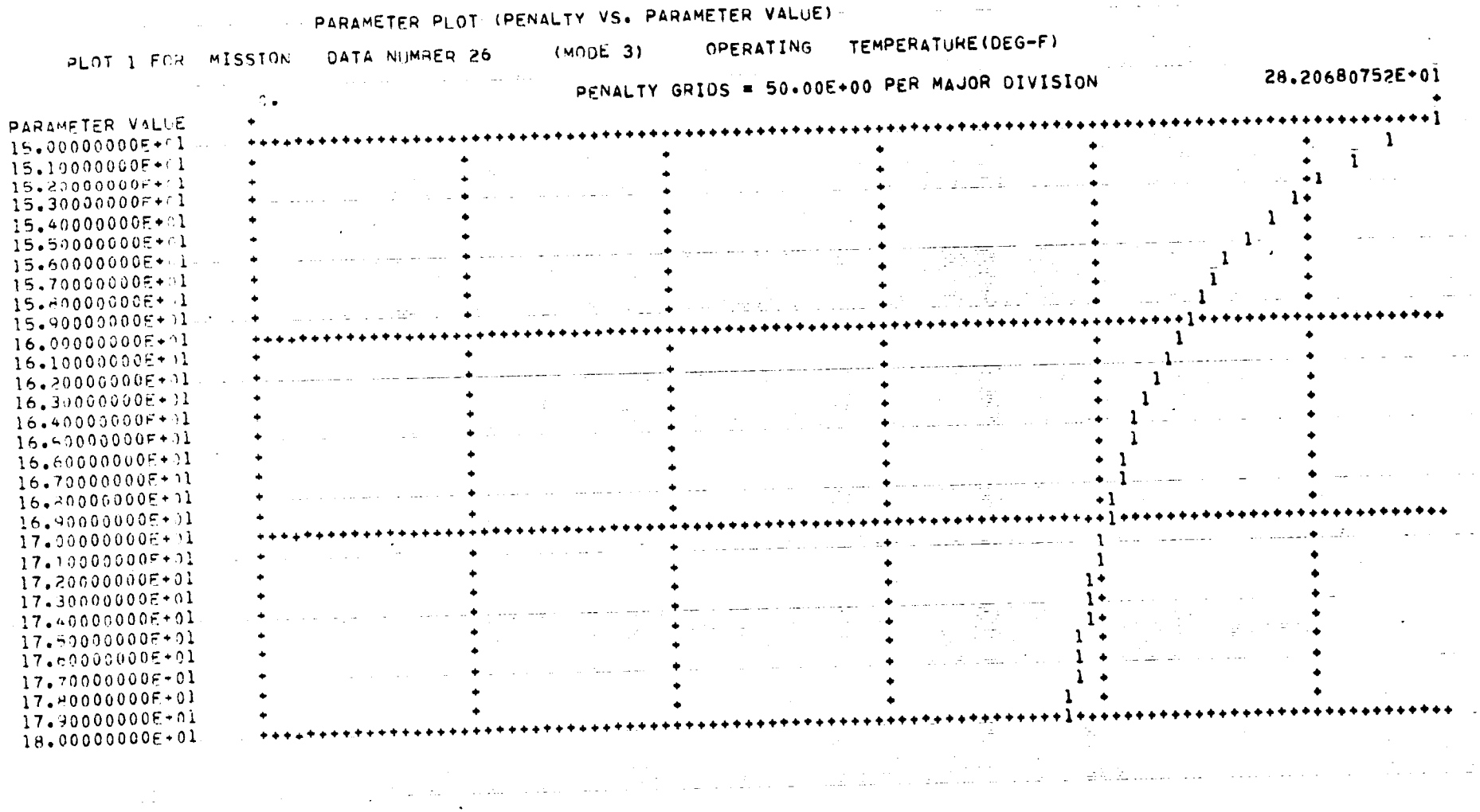

FIGURE 32. PLOT OF PENALTY, MODE 3, (SYSTEM A) VARIATION WITH OPERATING TEMPERATURE SWEEP

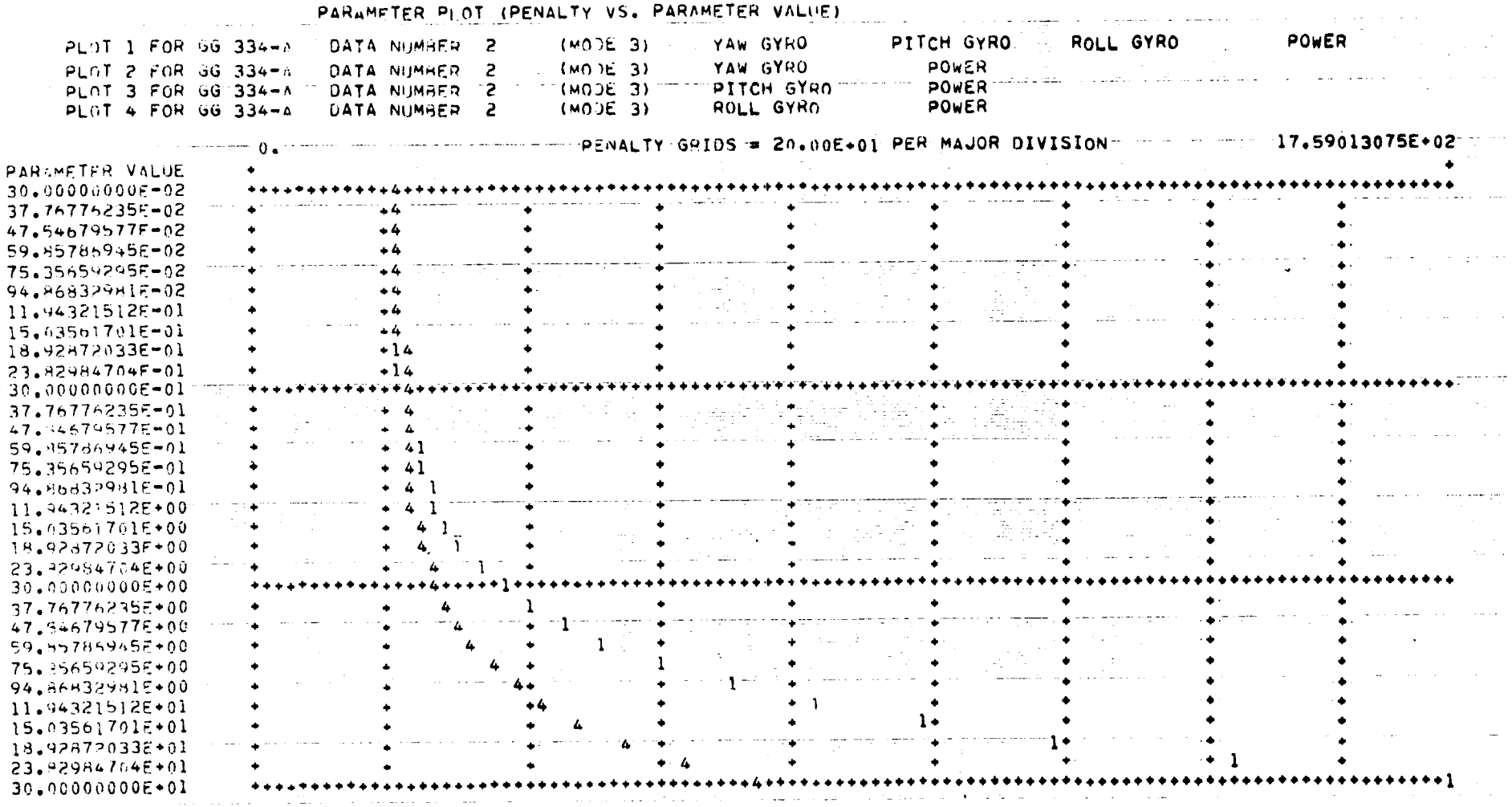

FIGURE 33. PLOTS OF PENALTY, MODE 3, (SYSTEM A) VARIATION WITH GYRO EXCITATION POWER SWEEPS

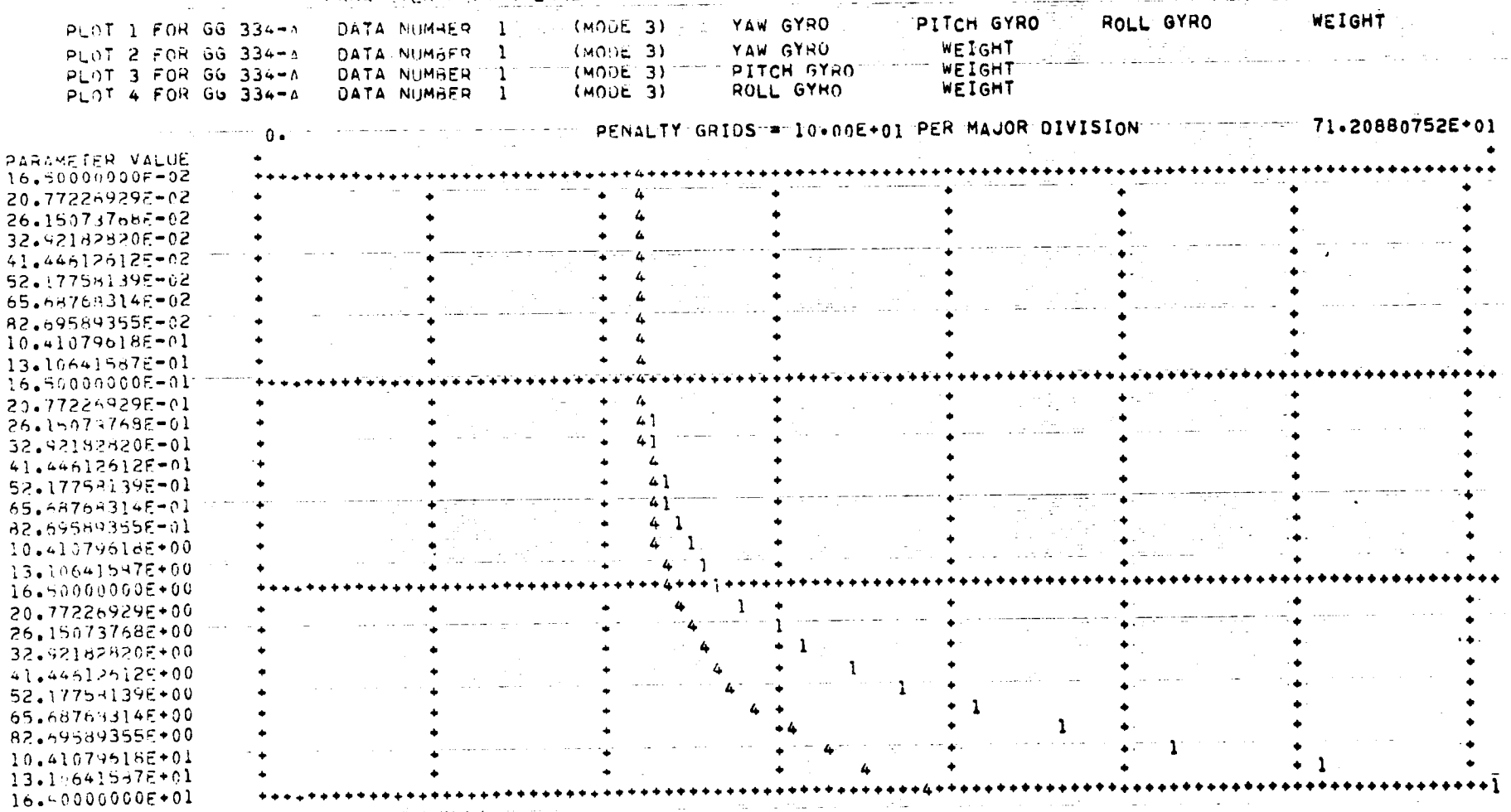

FIGURE 34. PLOTS OF PENALTY, MODE 3, (SYSTEM A) VARIATION WITH GYRO WEIGHT SWEEPS

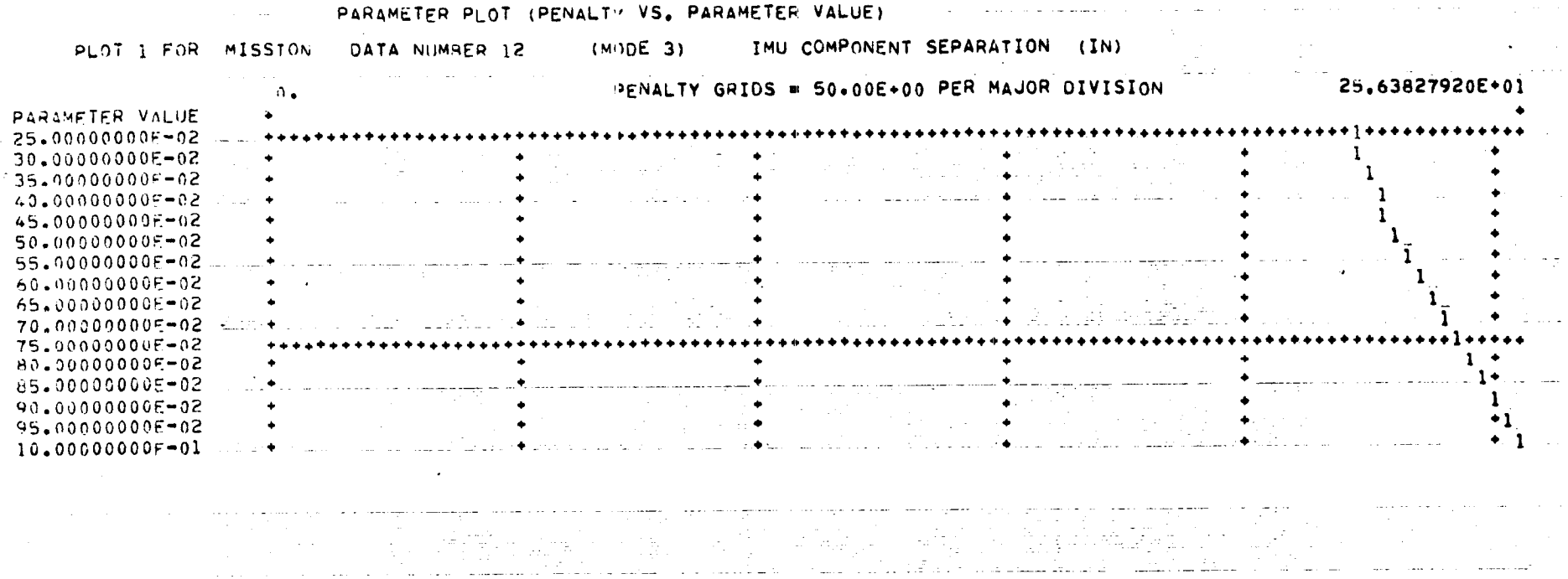

FIGURE 35. PLOT OF PENALTY, MODE 3, (SYSTEM A) VARIATION WITH IMU COMPONENT SEPARATION SWEEP

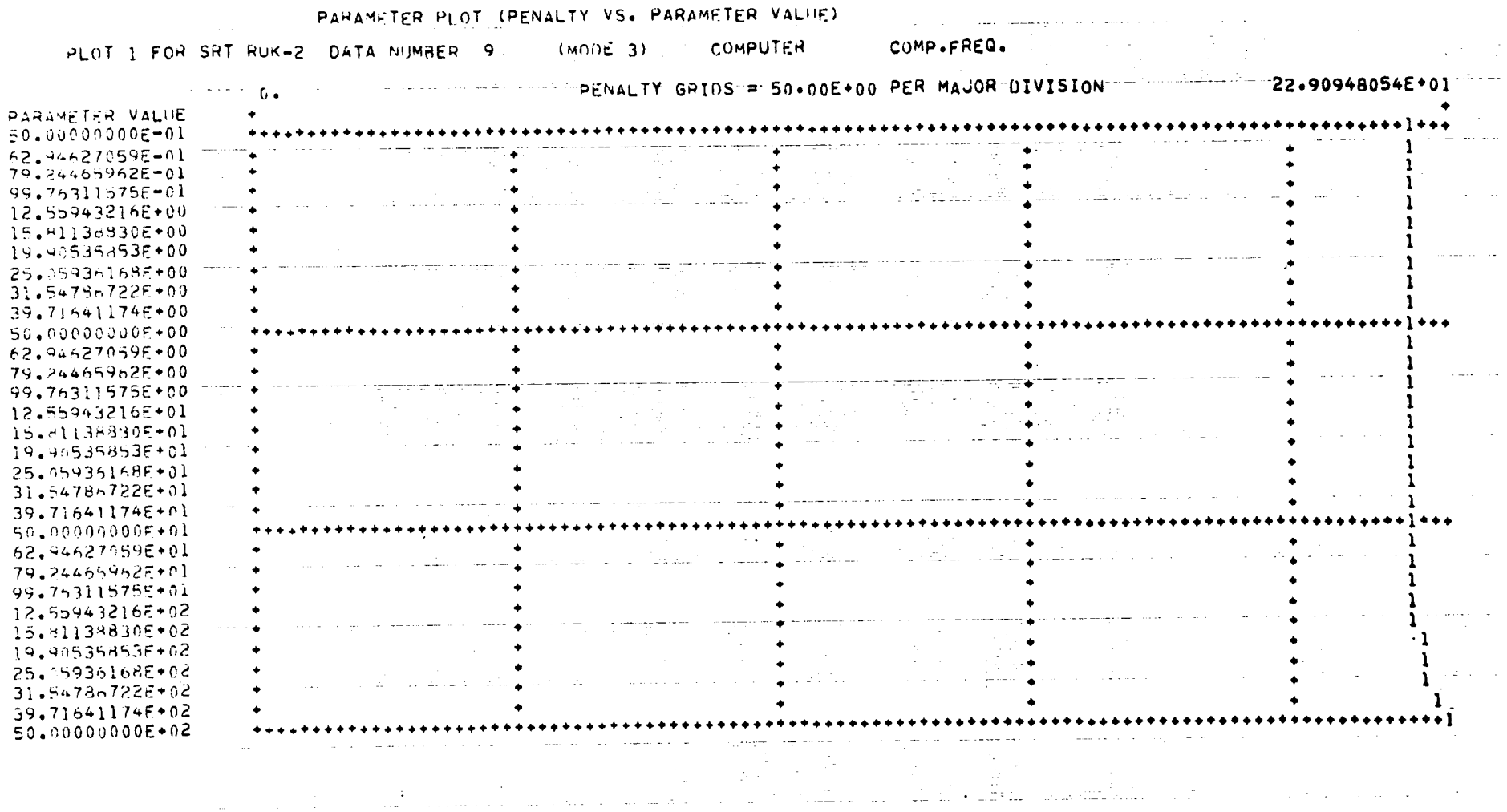

FIGURE 36. PLOT OF PENALTY, MODE 3, (SYSTEM A) VARIATION WITH COMPUTATION FREQUENCY SWEEP

CONCLUSIONS

An evaluation technique was developed for pure inertial strapdown guidance systems designed for interplanetary missions. This technique is useful in evaluating competitive systems, in determination of research needed to improve system performance, as an aid in preliminary design of conceptual systems, and provides a measure of system performance on each mission being examined. The technique assumes a perfect update of velocity, position, and attitude occurs prior to the burn from the parking orbit.

The system parameters used in the evaluation technique can be estimated using techniques that are relatively unsophisticated but are of sufficient accuracy to accomplish the desired result.

These techniques were implemented in computer programs now in use at NASA/ERC. The computer programs were exercised on a Jupiter flyby mission. For this mission and the assumptions made, it can be concluded that the accuracy of the strapdown guidance systems evaluated is more than sufficient to accomplish the guidance and navigation of the first spacecraft to flyby Jupiter.

If the first midcourse correction is made 10 days after launch and the required probability of mission failure attributable to guidance is 0.05, the reliability (mean time to failure) of the pure inertial strapdown guidance systems considered is such that no system examined would succeed if operated continuously from launch to midcourse. If the probability of mission failure attributable to guidance is relaxed to 0.1, the two specified systems still fail if midcourse correction is made 10 days after launch. An optimum system which will succeed was found.

Concentrated attention to reduction of system power requirements would yield a significant reduction in the weight attributable to guidance for this specific mission. This might be achieved by development of a lightweight variable thermal impedance for the IMU.

RECOMMENDATIONS

The techniques developed, the computer programs implementing these techniques, and the results from exercising these computer programs on a Jupiter flyby mission lead to the following recommendations.

It is recommended that NASA/ERC consider extension of the work which led to the present parameter estimation techniques to more sophisticated techniques that could eventually result in computer-aided design of strapdown guidance systems.

For the Jupiter flyby mission studied, a concentrated effort on reduction of system power, and hence power source weight, is recommended. The direction to be followed in this research depends upon cost and other factors such as the likelihood of success of each research approach to power (or power source weight) reduction.

It is recommended that attention be directed toward improving the reliability of strapdown guidance systems which might be used for a Jupiter flyby mission. This effort should consider not only improvement in the mean time to failure (MTTF) of the hardware, but also investigate reliability models for strapdown guidance systems and methods of testing to verify these models. As shown in the exercise cases previously discussed, an improvement in the MTTF of the strapdown guidance system hardware must be made if the system is to operate continuously from launch until midcourse correction ten days later, or the probability of mission failure attributable to guidance must be relaxed.

If the reliability of the system can be increased, a decrease in accuracy could be considered on acceptable tradeoff. Such a relaxed accuracy system (system B) was used in the exercise runs.

REFERENCES

(1) "A Study of Jupiter Flyby Missions, Final Technical Report", General Dynamics, Fort Worth Division, FZM-4625, May 17, 1966.

(2) "Advanced Planetary Probe Study, Final Technical Report", TRW Systems, Reports 4547-6004-R000 to 4547-6007-R000, Volumes 1-4, July 27, 1966.

(3) "Final Report for the Study of Simplified Navigation and Guidance Schemes", Volume I-Technical Analysis, United Aircraft Corporate Systems Center, SCR 290-I, October 31, 1966.

(4) "Application of the Saturn V Launch Vehicle to Unmanned Scientific Exploration of the Solar System, Jupiter Orbiter/Solar Probe Mission Study, Advanced Mission Investigations", Northrop Space Laboratories, TM-29213-6-075, September, 1966.

(5) Porter, R. F., "Preliminary Trajectory Analysis of the 260(0.75) and 260(FL) Stacks", Battelle Memorial Institute, BMI-NLVP-IM-66-64, May 26, 1966.

(6) Porter, R. F., "Examination of a 'Dog-Leg' Trajectory for the 260(3.7)-SIVB Launch Vehicle", Battelle Memorial Institute, BMI-NLVP-IM-66-81, August 15, 1966.

(7) "Saturn IB Improvement Study (Solid First Stage) Phase II, Final Detailed Report", Douglas Missile and Space Systems Division, Report SM-51896, Volume II, March 30, 1966.

(8) "Launch Vehicle Estimating Factors for Generating OSSA Prospectus 1968", Launch Vehicle and Propulsion Programs, Office of Space Science and Applications, National Aeronautics and Space Administration, December, 1967.

(9) "Final Report for the Centaur Phase II Guidance System Study, Volume I-Technical", United Aircraft Corporate Systems Center, SCR 264-1, April 15, 1966.

(10) Borland, L. D., Honeywell Aerospace Division, St. Petersburg, Florida, July, 1967, Note to Ellis F. Hitt, Battelle Memorial Institute.

(11) "Final Report for the Centaur Phase II Guidance Systems Study, Volume I-Technical Appendices", Appendix A, United Aircraft Corporate Systems Center, SCR 264-I, April 15, 1966.

(12) "Proposal for a Strapdown Inertial Sensing Unit Subassembly, Volume I-Technical", Honeywell Aerospace Division, St. Petersburg, Florida, R-ED 24644, July 25, 1967.

(13) McKinley, Howard L, Jr., "An Analysis of Temperature Control Problems for Inertial Components and Experimental Results", Guidance and Control Division, Central Inertial Guidance Test Facility, Air Force Missile Development Center, Technical Report GL-2, June, 1963.

(14) Mednick, Ralph, "GE-E-3 Temperature Controller", Instrumentation Laboratory, Massachusetts Institute of Technology, September, 1960.

(15) Stafford, G. B., "Space Power Subsystem Capabilities", AF Aero Propulsion Laboratory, WPAFB, Ohio, AIAA Paper No. 65-468, dtd., July, 1965.

(16) Electrical Power Generation Systems for Space Applications, NASA SP-79, 1965.

(17) Shair, Lerner, Joyner, and Evans, "A Review of Batteries and Fuel Cells for Space Power Systems", Journal of Spacecraft and Rockets, July, 1967, pp 833-838, Vol 4, No. 7.

(18) "Space Power Systems Engineering", Edited by G. C. Azego and J. E. Taylor, Academic Press, 1966, AIAA Series - Vol 16.

(19) Corliss, W. R., and Harver, D. G., "Radioisotopic Power Generation", Prentice-Hall Series, 1964.

(20) "Final Report for the Study of Simplified Navigation and Guidance Schemes", Vol I-Technical Analysis, Contract NAS 12-40, UACSC, October 31, 1966.

(21) "Advanced Planetary Probe", Final Technical Report, Vol 2, Spin-Stabilized Spacecraft for the Basic Mission, TRW Systems, July 27, 1966.

(22) "Application of the Saturn V Launch Vehicle to Unmanned Scientific Exploration of the Solar System", Contract NAS 8-20082, September, 1966.

(23) Lloyd, David K., and Lipow, Myron, "Reliability: Management, Methods, and Mathematics", Prentice Hall, 1962, Englewood Cliffs, New Jersey.

(24) Hayre, H. S., Schrader, G. F., Daruvalla, S. R., and Hearn, N. K., "Accelerated Life-Testing and Reliability Prediction of Missile Control Systems", Air Force Missile Development Center, AFMDC-TR-65-25, August, 1965.

(25) Roantree, J., and Kormanik, N., "A Generalized Design Criterion for Strapped-Down Inertial Sensor Loops", AIAA/JACC Guidance and Control Conference, August, 1966.

(26) Farrell, J. L., "Performance of Strapdown Inertial Attitude Reference Systems", AIAA/JACC Guidance and Control Conference, August, 1966.

(27) Vichnevetsky, Robert, "Error Analysis in the Computer Simulation of Dynamic Systems: Variational Aspects of the Problem", IEEE Transactions on Electronic Computers, Vol EC-16, No. 4, August, 1967.

(28) A Study of the Critical Computational Problems Associated with Strapdown Inertial Navigation Systems, Volumes I and II", United Aircraft Corporate Systems Center, SCR 328-I and SCR 328-II, February 23, 1967.

(29) Battin, Richard H., "Astronautical Guidance", McGraw Hill Book Company, 1964.

APPENDIX A

SIMULATION OF THE 260(3.7)/SIVB/CENTAUR I/KICK LAUNCHING A 5,410 LB PAYLOAD ONTO A JUPITER FLYBY TRAJECTORY

APPENDIX A

SIMULATION OF THE 260(3.7)/SIVB/CENTAUR I/KICK LAUNCHING A 5,410 LB PAYLOAD ONTO A JUPITER FLYBY TRAJECTORY

INTRODUCTION

This appendix discusses the simulated performance of the 260(3.7)/SIVB/Centaur I/Kick launch vehicle launching a 5,410 lb payload onto a Jupiter flyby interplanetary trajectory. The simulation was for a due east launch from the Eastern Test Range (ETR). The SIVB/CI/K plus payload was injected into a 100.2 by 100 nm parking orbit at 420.22 seconds into the SIBV burn. It was assumed that the SIVB was restarted at the correct time to begin the final injection phase of the launch trajectory.

GROUND RULES

To provide the most meaningful results, the thrust shaping of the first stage and the kick angle were chosen to meet criteria established by NASA/MSFC for this type of vehicle. Specifically, these constraints are:

(1) Maximum dynamic pressure ≤ 950 lb/ft^2

(2) Maximum axial load factor ≤ 6 g's

(3) Dynamic pressure at first stage burnout ≤ 10 lb/ft^2

DESCRIPTION OF VEHICLE

Weights, thrust, propellant weight flow, and other selected characteristics of the vehicle were obtained from References A1 and A2. Table A-I contains pertinent data for this vehicle. Representative aerodynamic data were obtained from Reference A2 and are presented in Figure A-1.

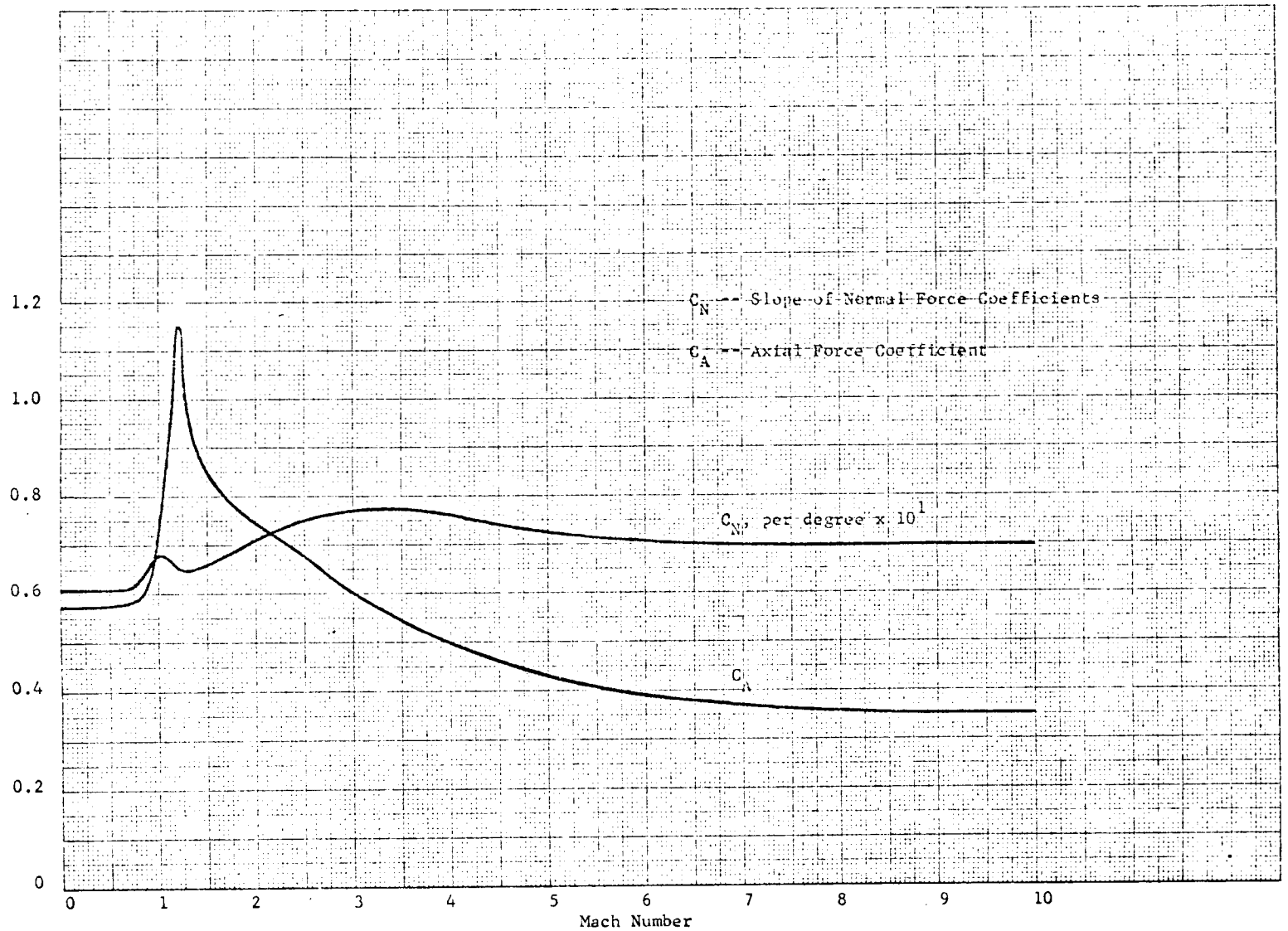

FIGURE A-1. ASSUMED AERODYNAMIC CHARACTERISTICS OF 260(3.7)/SIVB/CI/K

TABLE A-I.
SELECTED CHARACTERISTICS OF 260(3.7)/
SIVB/CENTAUR I/KICK LAUNCH VEHICLE

Stage	260(3.7)	SIVB	Centaur I	Kick
Initial Total* Gross Weight (lb)	4,019,302	315,303***	54,202	12,410
Final Total* Gross Weight (lb)	720,302	85,303	17,602	6,460
Vacuum Thrust (lb)	6,430,000**	205,000	31,000	7,500
Propellant Weight Flow (lb/sec)	24,300**	482	68.20	16.47
Exit Area (ft^2)	376	35.8	16.58	4.14

* All weights include 5,410 lb payload
** Initial value only: for time history, see Figure A-2
*** Includes 5,600 lb shroud which is ejected 26 seconds after SIVB ignition.

ANALYSIS

All simulations were performed using the Battelle three-degree-of-freedom computer program. The pitch steering program for the SIVB burn was computed using a linear steering technique (Reference A3).

The first stage trajectory consisted of a vertical rise until a relative velocity of 150 ft/sec was attained. The vehicle was then subjected to an instantaneous deflection of the flight path through a selected kick angle of 1.83 degrees from the vertical along an initial azimuth of 90 degrees from true North. The vehicle then flew a gravity turn until first stage burnout. Figure A-2 is a time history from liftoff of selected stage and trajectory parameters during the first stage, 260(3.7), burn. The thrust shaping shown was necessary to keep the dynamic pressure below 950 lb/ft^2. Acceleration along the roll axis of the vehicle (axial load factor) is quite nonlinear during first stage burn due to this thrust shaping. Also displayed in Figure A-2 are the velocity relative to Earth, the flight path angle from the local vertical, and the vehicle altitude as functions of time from liftoff.

The final conditions at first stage burnout were used in determining a linear pitch steering program for the SIVB stage. The steering used is depicted in Figure A-3 with the altitude, inertial velocity, flight path angle, and roll axis acceleration plotted as functions of time from liftoff. At 563 seconds into the mission (420.22 seconds from first SIVB ignition), the SIVB/CI/K plus

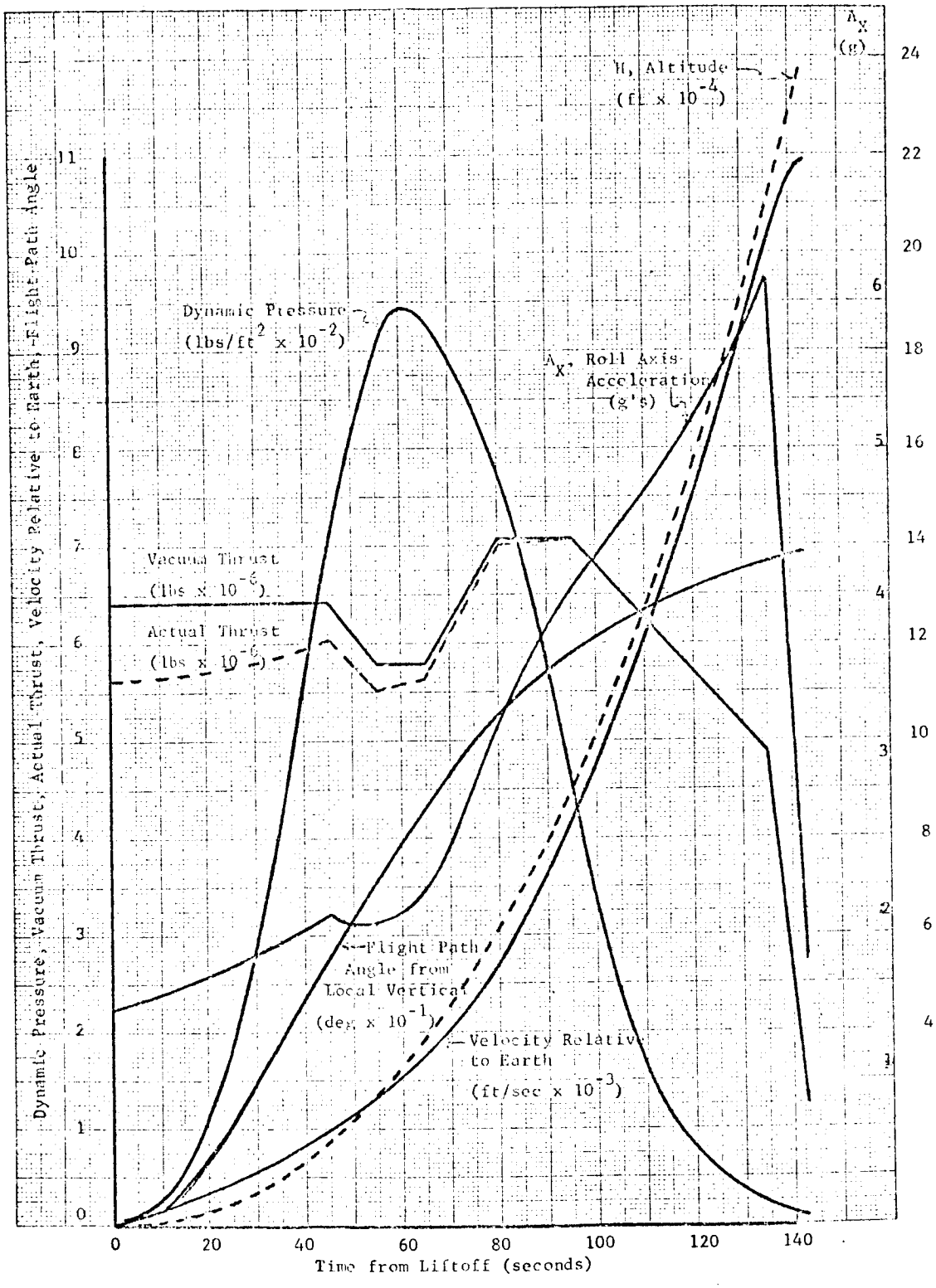

FIGURE A-2. TIME HISTORY OF 260(3.7) STAGE TRAJECTORY PARAMETERS

payload was injected into a 100.2 by 100 nm parking orbit. It was assumed that the SIVB thrust was terminated and the vehicle was then oriented such that the pitch angle and flight path angle were equal. It was further assumed that the SIVB was restarted at the correct time to begin the final injection phase of the launch trajectory as shown in Figure A-3. The SIVB was burned to fuel depletion in its second burn. At that time, the SIVB was jettisoned and the Centaur I ignited.

Figure A-4 depicts the inertial velocity, roll axis acceleration, and hyperbolic excess velocity as functions of total burn time from liftoff for the Centaur I burn. Figure A-5 depicts the same information for the Kick stage burn.

The hyperbolic excess velocity at injection was 39,728 ft/sec. This is equivalent to a characteristic velocity of 53,732 ft/sec.

CONCLUSIONS

Based upon this simulation, it appears that the 260(3.7)/SIVB/CI/K launch vehicle is capable of launching a 5,410 pound payload onto an interplanetary trajectory to Jupiter with an expected time of flight of 410 days. This simulation was made assuming the guidance system was part of the payload. If one is forced to use the present Saturn Instrument Unit to provide guidance to the SIVB and 260(3.7), the results of this simulation will not be applicable. This simulation was performed to generate the boost trajectory data needed for the Strapdown Error Analysis Program (SEAP).

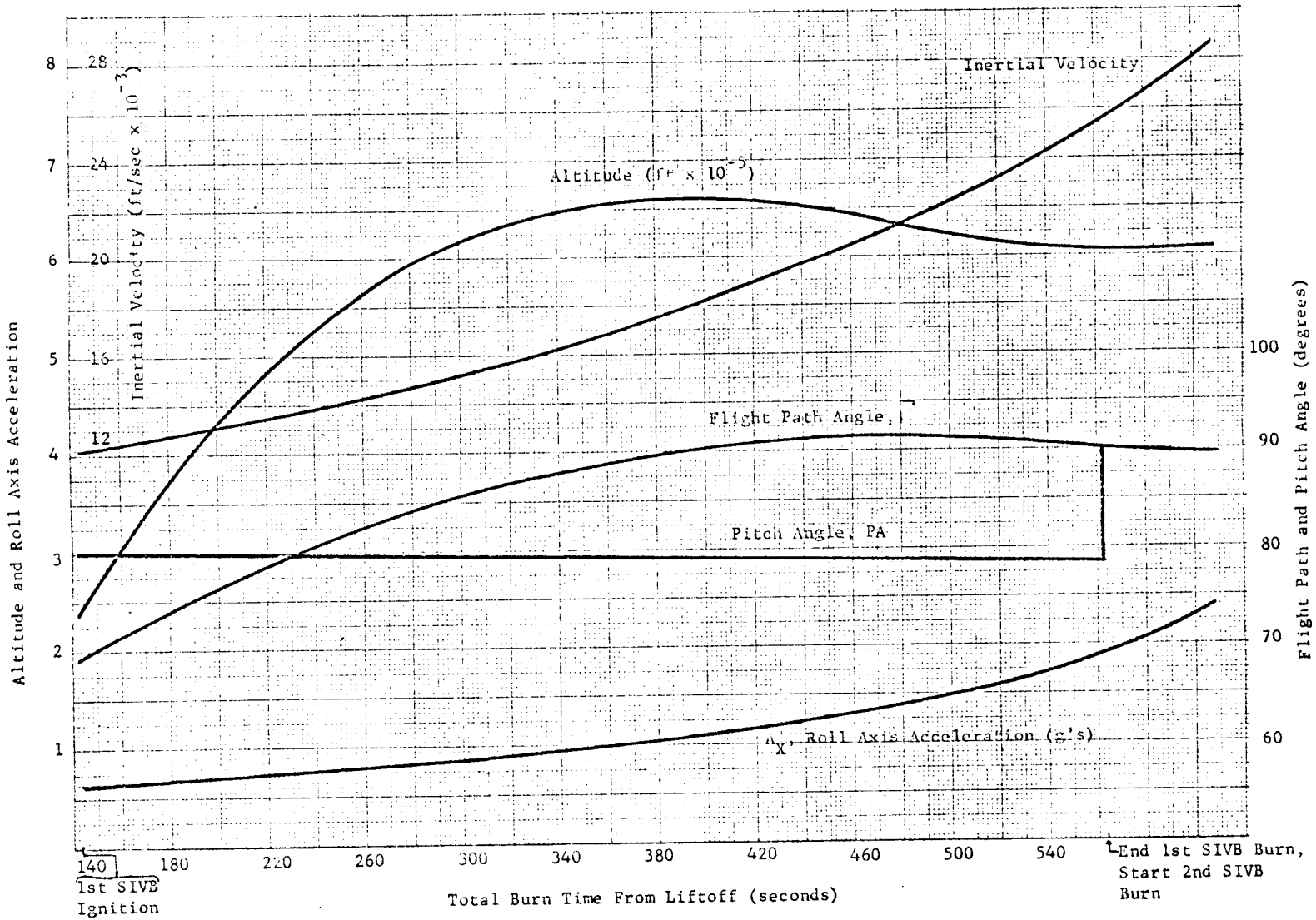

FIGURE A-3. SECOND STAGE TRAJECTORY FOR SIVB/CI/K PLUS 5,410 POUND PAYLOAD ON JUPITER FLYBY MISSION

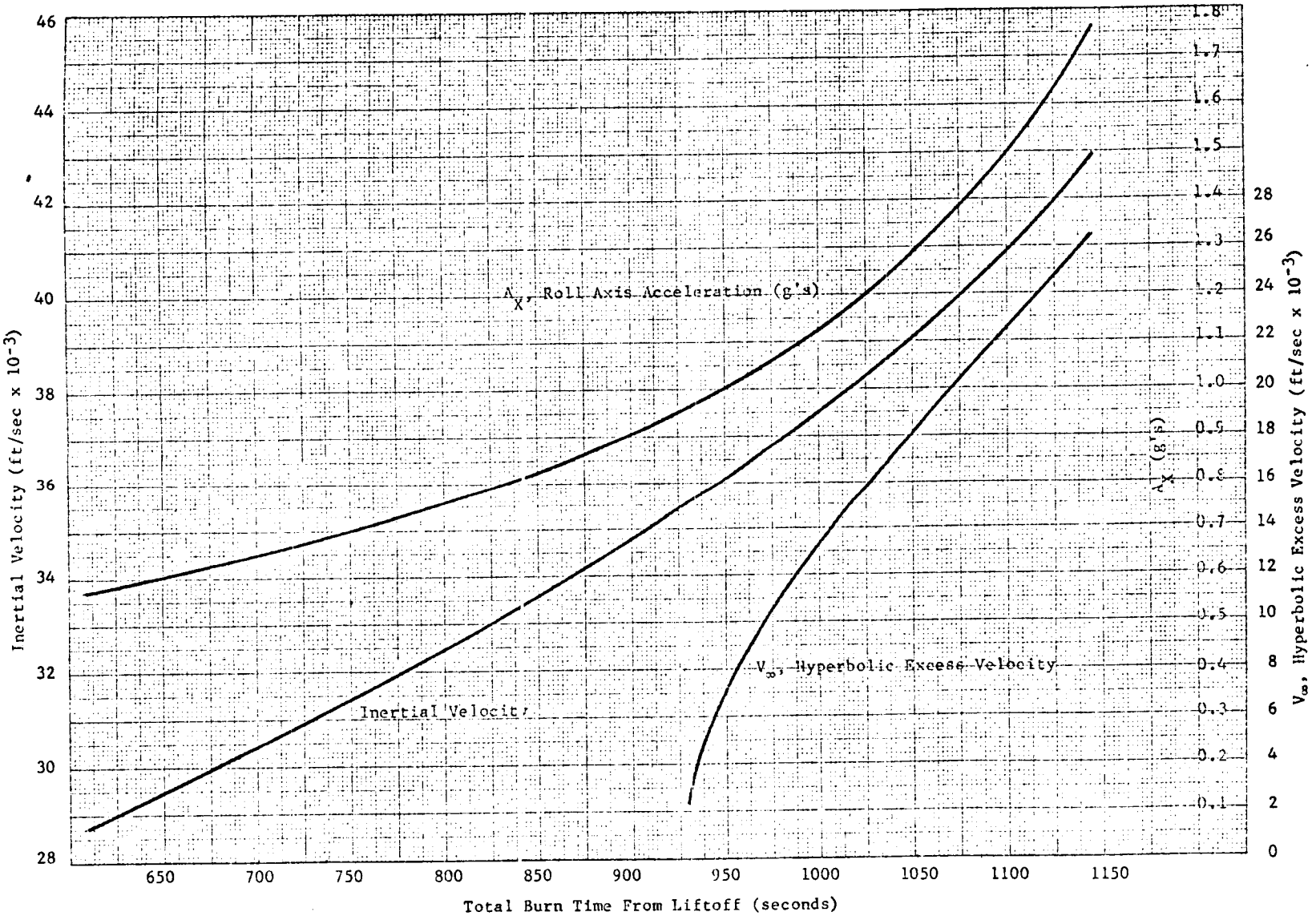

FIGURE A-4. THIRD STAGE TRAJECTORY FOR CI/K PLUS 5,410 POUND PAYLOAD ON JUPITER FLYBY MISSION

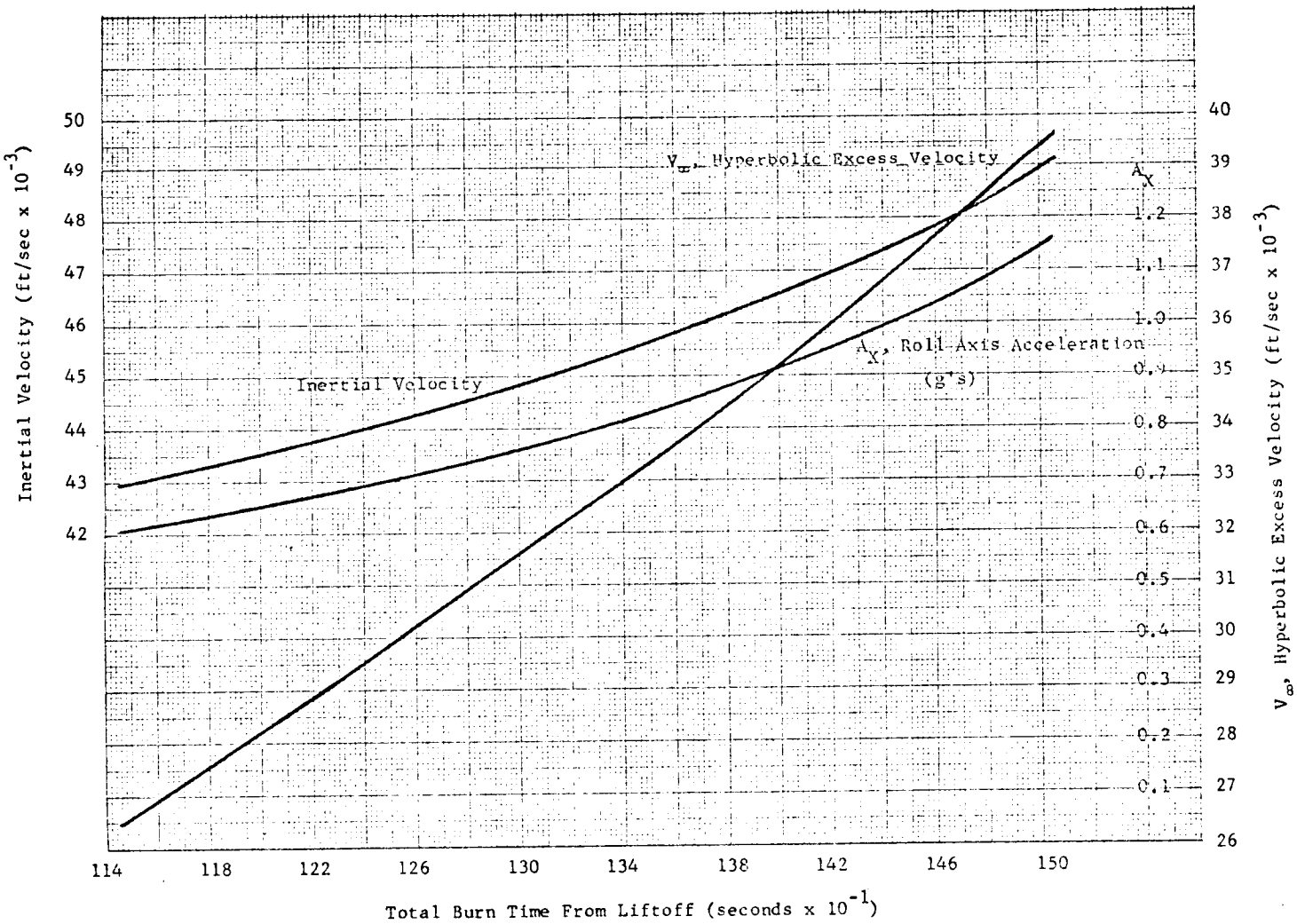

FIGURE A-5. FOURTH STAGE TRAJECTORY FOR K PLUS 5,410 POUND PAYLOAD ON JUPITER FLYBY MISSION

APPENDIX A

REFERENCES

(A1) Porter, R. F., "Preliminary Trajectory Analysis of the 260(0.75) and 260(FL) Stacks", Battelle Memorial Institute, BMI-NLVP-IM-66-64, May 26, 1966.

(A2) Porter, R. F., "Examination of a 'Dog-Leg' Trajectory for the 260(3.7)-SIVB Launch Vehicle", Battelle Memorial Institute, BMI-NLVP-IM-66-81, August 15, 1966.

(A3) Duty, R. L., "Trajectory Determination by Linear Steering", Journal of Spacecraft and Rockets, Vol 3, No. 1, January, 1966.

APPENDIX B

SYNOPSIS OF STANDARDIZED SPACE GUIDANCE SYSTEM COST-EFFECTIVENESS MODELS

APPENDIX B

SYNOPSIS OF STANDARDIZED SPACE GUIDANCE SYSTEM COST-EFFECTIVENESS MODELS

Prior to defining a performance index for use in evaluating strapdown guidance systems, existing "cost-effectiveness" models for space guidance systems were reviewed. This appendix presents a review and evaluation of four existing models developed by contractors for the USAF Space Systems Division (now Space and Missile Systems Organization) "Standardized Space Guidance System (SSGS) Study". The input data required and fundamental figure of merit of each model is followed by an evaluation of the applicability of the four models discussed.

(I) IBM Federal Systems Division, Space Guidance Center, developed a "cost-effectiveness" model (Reference B1) as part of their work on the Standardized Space Guidance System (SSGS). Input data required for the effectiveness analysis for each configuration is tabulated in Table B-I.

TABLE B-I
IBM EFFECTIVENESS ANALYSIS INPUT DATA

(i)	Navigation accuracy requirements for each mission
(ii)	Guidance error analysis for each candidate guidance system configuration
(iii)	Mission time profile broken into specific periods, "t"
(iv)	Constant guidance system failure rate for each period, "t"
(v)	Average repair time duration
(vi)	Probability that a spare is available
(vii)	Additional logistic delay time

Table B-II contains a listing of cost data required for each candidate guidance system.

TABLE B-II
IBM "COST-EFFECTIVENESS" ANALYSIS
COST INPUT DATA

(i)	Research and Development Cost - all expenditures for research development, test, and engineering of all subsystems.
(ii)	Investment Cost - purchase price per developed subsystem in quantity buys.
(iii)	Operating Expense - one-time other operating costs (technical manuals, training, field engineering, etc.) for each mission plus spares cost.
(iv)	All non-guidance costs associated with mission - includes launch vehicle spacecraft, etc.

This model requires that a fixed number of missions be accomplished. Therefore, the user must estimate the number of attempts required per mission.

To determine the "best" guidance system configuration, the user performs the analysis for each configuration and that configuration with the lowest total cost of ownership is the best for the mission considered.

(II) The model developed by Sperry Gyroscope Company during their SSGS work (References B2 and B3) also requires that a fixed number of successful missions be accomplished. Table B-III tabulates some of the input data required for each candidate system to determine the probability of mission success for the candidate.

TABLE B-III
SPERRY EFFECTIVENESS ANALYSIS INPUT DATA

(i)	Probability of successful operation of guidance AGE
(ii)	Probability of successful guidance countdown - failure rate, repair rate, launch window duration, time between launch windows, abort probability

TABLE B-III (Continued)

(iii)	Probability that systems other than guidance operate reliably
(iv)	Probability of guidance system operating reliably during ascent
(v)	Probability of guidance system operating reliably during subsequent phases of mission
(vi)	Navigation accuracy requirements for each mission
(vii)	Probability that candidate guidance system configuration satisfies prescribed accuracy requirement
(viii)	Total useful payload weight
(ix)	Guidance system weight (burdened for power and cooling requirements)

Some of the cost input data required for the Sperry model is tabulated in Table B-IV.

TABLE B-IV
SPERRY "COST-EFFECTIVENESS"
ANALYSIS COST INPUT DATA

(i)	Production cost of each candidate guidance system required for each mission type
(ii)	Cost of all other systems (launch vehicle services, etc.) required for each mission type
(iii)	Research, development, test, and engineering cost for each candidate guidance system

As with the IBM model, the user must estimate the number of attempts (systems) required to accomplish the mission with a specified probability of success.

The basic figure of merit resulting from the manipulation of the input data is an "assurance cost", A/C. This cost is

$$(A/C) = \frac{N(G + C)}{P(MS)} \quad ,$$

where

N = Number of attempts

G = Cost of candidate guidance system

C = Launch vehicle and other system costs

P(MS) = Probability of mission success.

A subordinate measure of guidance system worth which brings into effect weight is the assurance cost per pound of useful payload. The candidate guidance system with the lowest assurance cost is the preferred system according to Sperry.

(III) Autonetics subcontracted development of the cost-effectiveness model to Planning Research Corporation (PRC). This model (Reference B4) was also designed on the assumption that a fixed number of missions must be accomplished successfully. Accuracy and reliability were treated as the measures of probability of success of the candidate guidance system. The probability of mission success was defined as the product of the probability of vehicle-payload success and the probability of guidance success. The number of launches required to achieve a specified fixed effectiveness level is found by dividing the fixed number of successful missions by the probability of mission success.

The parameters weight and power are not considered either explicitly or implicitly in the PRC cost model. Autonetics did include them by converting power required to an equivalent power source weight which was added to the guidance system weight. The sum of these weights was converted to cost by a dollar/lb factor and added to the guidance hardware cost.

Some of the non-cost input data and calculations required for the PRC developed model are tabulated in Table B-V.

TABLE B-V
AUTONETICS AND PLANNING RESEARCH CORPORATIONS
EFFECTIVENESS ANALYSIS INPUT DATA

(i)	Estimated Gross National Product
(ii)	Estimated Air Force Budget
(iii)	Forecast Air Force Astronautics Budget
(iv)	Estimate mission types and number of launches required for each mission (iterative comparison with astronautics budget)
(v)	Perform mission analysis to determine navigation accuracy requirements, guidance reliability requirements, etc.
(vi)	Perform navigation error analysis and reliability for each candidate guidance system on each mission
(vii)	Determine probability of vehicle and payload success
(viii)	Determine probability of guidance success
(ix)	Number of R&D flights
(x)	Number of operational launches per year
(xi)	Number of years in the operational program
(xii)	Number of payloads to be used per year
(xiii)	Number of guidance systems required per year
(xiv)	Number of men to be trained initially
(xv)	Number of launch vehicles
(xvi)	Number of guidance and control readout stations
(xvii)	Launch vehicle spares factor
(xviii)	Payload spares factor
(xix)	Guidance spares factor
(xx)	Number of circuit miles of land line communications network per station

Cost data required for the PRC developed model is tabulated in Table B-VI. These costs are (1) research, development, test, and engineering (RDT&E), (2) investment, and (3) operating costs.

TABLE B-VI
COST DATA INPUT TO PLANNING RESEARCH CORPORATION MODEL

(i)	Initial unit cost for launch vehicle hardware
(ii)	Guidance research, development, test, and engineering (RTD&E) cost
(iii)	Initial investment for ground facilities
(iv)	Payload development
(v)	Initial cost of guidance and control readout station
(vi)	Unit cost for launch vehicles used in flight test
(vii)	Payload prototype cost
(viii)	Flight test unit cost of guidance system
(ix)	Per-launch cost of engineering backup support for flight test
(x)	Per-launch cost for refurbishment of test units and facilities
(xi)	Investment cost per booster
(xii)	Cost per payload
(xiii)	Cost per guidance system
(xiv)	Ground environment equipment cost
(xv)	Cost of payload AGE
(xvi)	Cost of guidance system AGE
(xvii)	Training cost per man of average skill
(xviii)	Pay and allowances
(xix)	Data reduction and analysis cost per launch
(xx)	Operational cost per readout station per year
(xxi)	Cost of land communication network
(xxii)	Contractor support cost

In addition, cost data on booster, payload, guidance, and AGE modifications are inputs for this model. Other miscellaneous cost data are also required but will not be listed in this report.

Basically, this model searches for the candidate guidance system which satisfies a specified fixed effectiveness (determined by analysis of reliability and system accuracy) and has minimum cost. The program computes cost first on the basis of the probability of mission success, P_{sm}, equal to the probability of vehicle and payload success, P_{sv}. It then computes cost with

$$P_{sm} = P_{sv} \cdot P_{sg} \quad ,$$

where P_{sg} = probability of candidate guidance system success. P_{sg} is the product of the probabilities of reliability and accuracy success. The difference between the two costs represents the cost of additional launch vehicles, etc., due to imperfect guidance. Autonetics contends this cost difference could be spent justifiably for designing and constructing an essentially perfect guidance system.

(IV) TRW Space Technology Laboratories (now TRW Systems) developed another cost-effectiveness model in their SSGS study (Reference B5). This model is based on optimizing the dollar cost added to a family of missions by the guidance system. Optimization may be made assuming a fixed number of launches with varying success or variable number of launches for a fixed number of successes. For a system to be considered, it must satisfy some admissibility criteria established for performance and cost. A summary of the data required is listed in Table B-VII.

TABLE B-VII
TRW MODEL INPUT DATA

(i)	Number of flights
(ii)	Average reliability over N flights (product of individual reliabilities of system elements)
(iii)	Change in number of flights due to alternative systems
(iv)	Unit cost for one flight including all non-guidance equipment and operating costs
(v)	Change in nonrecurring cost due to alternative guidance systems

TABLE B-VII (Continued)

(vi)	Change in guidance equipment weight due to alternative systems
(vii)	Change in guidance power due to alternative systems
(viii)	Launch vehicle unit cost (dollars/lb payload)
(ix)	Power source cost (dollars/watt)
(x)	Power source weight (lb/watt)
(xi)	Change in unit recurring costs for alternative guidance systems
(xii)	Change in performance (accuracy) of alternative guidance systems

This trade off approach optimizes total space program costs for alternative guidance systems and requires detailed launch vehicle dollar costs. The fundamental measure of competing candidate guidance systems is seen to be dollars/payload pound. That system with minimum dollars/payload pound would be optimum.

Applicability of SSGS Models

Each of the "cost-effectiveness" models developed for evaluating competing guidance systems for the SSGS may be useful if given the same requirement, i.e., determine for the national space mission model that standardized space guidance system which is most cost-effective. It can be stated that this was not the problem for which NASA/ERC was seeking a solution. NASA/ERC was concerned with development of a performance index which will trade off the system parameters of accuracy, weight, power, and reliability, and thereby serve as a design aid for selection of component subsystems of a strapdown guidance system.

Each of the SSGS models require some of the same input data. Table B-VIII lists some of the common input data.

TABLE B-VIII
COMMON INPUT DATA FOR SSGS
COST-EFFECTIVENESS MODELS

(i)	Mission model
(ii)	Navigation accuracy requirement of each mission
(iii)	Probability of mission success
(iv)	Candidate guidance system error analysis
(v)	Candidate guidance system reliability
(vi)	Nonrecurring cost for launch vehicle and all other non-guidance items
(vii)	Recurring cost for launch vehicle and all other non-guidance items
(viii)	Nonrecurring guidance cost
(ix)	Recurring guidance cost

Some of the models required weight and power of the guidance systems. Others did not.

All of the models are heavily cost oriented. The cost data required is generally subject to doubt or not available. Two of the models make use of a figure of merit which can be expressed as dollars/pound of payload. For missions with quite heavy payloads, the figure of merit would appear much less sensitive to an increase in guidance system weight than a mission utilizing the same guidance system with a low payload weight. The IBM and Autonetics models are very much total mission cost oriented.

Greater length could be added to this appendix in providing additional rationale for non-use of the four SSGS models. It was apparent that a less complex and different type of cost function or performance index was required to aid in the design of a strapdown guidance system. This model should be much less mission and cost oriented than the SSGS models.

APPENDIX B

REFERENCES

(B1) "Standardized Space Guidance System (SSGS), Program Definition Studies, Phase 1A Final Report, Volume VI, Cost Effectiveness (U)", SSD-TDR-64-130(VI), May, 1964 (SECRET), IBM Federal Systems Division, Space Guidance Center.

(B2) "Standardized Space Guidance Study (SSGS), Program Definition Study - Phase 1A, Volume 3, Sections 4 and 5 (U)", SSD-TDR-64-131, Vol. 3 of 13, May, 1964 (SECRET), Sperry Gyroscope Company.

(B3) "Standardized Space Guidance Study (SSGS), Program Definition Study - Phase 1A, Volume 9, Annexes D through F (U)", SSD-TDR-64-131, Vol. 9 of 13, May, 1964 (SECRET), Sperry Gyroscope Company.

(B4) "Standardized Space Guidance System Phase 1A Study, Section 4 (U)", SSD-TDR-64-129, May 28, 1964 (SECRET), North American Aviation, Autonetics Division.

(B5) "Final Report for Phase 1A Standardized Space Guidance System (SSGS), Volume III: System and Subsystem Studies, Section 8 (U)", SSD-TDR-64-132, May 29, 1964 (SECRET), TRW Space Technology Laboratories.

APPENDIX C

APPROXIMATING THE PROBABILITY DISTRIBUTION OF A VECTOR WITH NORMAL COMPONENTS AND ZERO MEAN

APPENDIX C

APPROXIMATING THE PROBABILITY DISTRIBUTION OF A VECTOR WITH NORMAL COMPONENTS AND ZERO MEAN

An N dimensional random vector with normal components and zero mean is completely described by its N by N covariance matrix. For a vector in three dimensional space N = 3. Since only the magnitude of the vector is of interest, two vectors which differ by an orthonormal rotation will have the same distribution. The covariance matrix is always symmetric and nonsingular with positive real eigenvalues. This implies that for any vector there is an equivalent vector, differing by only an orthonormal rotation which has a diagonal covariance matrix in the form

$$\begin{bmatrix} \lambda_1 & 0 & 0 \\ 0 & \lambda_2 & 0 \\ 0 & 0 & \lambda_3 \end{bmatrix}$$

where the λ's are the eigenvalues of the original covariance matrix. The eigenvalues represent the variances of a vector with normal uncorrelated components.

The problem is then to determine the distribution of

$$\sqrt{\lambda_1 X_1^2 + \lambda_2 X_2^2 + \lambda_3 X_3^2}$$

where $\lambda_1 > 0$, $\lambda_2 > 0$, $\lambda_3 > 0$, and X_1, X_2, and X_3 are independent and all normal (0,1) random variables. This is a specific case of the general problem of determining the distribution of $\lambda_1 s_1^2 + \ldots \lambda_K s_K^2$, where the s_i^2 are independent and $s_i^2 \sim \sigma_i^2 \chi_{f_i}^2 / f_i$ (Chi-Squared of degree f_i). Here $\sigma_i^2 = 1$, $f_i = 1$, and $K = 3$.

In general, this exact distribution is not known, so an approximation must be used.* If $\lambda_1 = \lambda_2 = \lambda_3 = a$, the distribution is that of $a\chi_3^2$, or $3a\chi_3^2/3$. This suggests approximating the distribution of $\lambda_1 X_1^2 + \lambda_2 X_2^2 + \lambda_3 X_3^3$ by the distribution $a\chi_d^2/d$ for some constant a and degree of freedom d. The standard way of doing

* K. A. Brownlee, Statistical Theory and Methodology in Science and Engineering, John Wiley and Sons, New York, 1960.

this is to determine a and d by equating the first two moments of $a\chi^2_d/d$ with those of $\lambda_1 X_1^2 + \lambda_2 X_2^2 + \lambda_3 X_3^2$. For a discussion, see the reference, page 235. It can be shown that the third moment of $a\chi^2_d/d$, with a and d determined as above, is smaller than the third moment of $\lambda_1 X_1^2 + \lambda_2 X_2^2 + \lambda_3 X_3^2$ (if the λ_i's are not equal). Thus, it appears that the tail of $a\chi^2_d/d$ is smaller than that of $\lambda_1 X_1^2 + \lambda_2 X_2^2 + \lambda_3 X_3^2$.

As we are particularly interested in the upper 0.99, 0.999, and 0.9999 points of the distribution, it was thought that a better approximation in this range might be obtained by determining a and d by equating the first and third, or perhaps second and third, moments of $a\chi^2_d/d$ and $\lambda_1 X_1^2 + \lambda_2 X_2^2 + \lambda_3 X_3^2$.

Several sets of λ_i's were chosen, and for each set a Monte Carlo experiment of 1,000,000 random vectors was performed to approximate the distribution of $\lambda_1 X_1^2 + \lambda_2 X_2^2 + \lambda_3 X_3^2$. This distribution was then compared to the three $a\chi^2_d/d$ distributions for a and d chosen by equating the first and second, first and third, and second and third moments. Figures C-1 and C-6 show the Monte Carlo results compared to distributions based on equating first and second moments, first and third, and second and third. Figures C-5 and C-6 are special cases where $\lambda_1 X_1^2 + \lambda_2 X_2^2 + \lambda_3 X_3^2$ is exactly distributed as $a\chi^2_d/d$ and equating any two moments gives the correct a and d and serves as a check on the Monte Carlo technique.

The necessary a's and d's for each approximation are calculated as shown in Table C-I.

TABLE C-I
COMPUTATION OF a AND d FOR EQUATING MOMENTS

Moment	a	d
1 and 2	$\lambda_1 + \lambda_2 + \lambda_3$	$\dfrac{(\lambda_1 + \lambda_2 + \lambda_3)^2}{(\lambda_1^2 + \lambda_2^2 + \lambda_3^2)}$
1 and 3	$\lambda_1 + \lambda_2 + \lambda_3$	$\dfrac{(\lambda_1 + \lambda_2 + \lambda_3)^{3/2}}{(\lambda_1^3 + \lambda_2^3 + \lambda_3^3)^{1/2}}$
2 and 3	$\sqrt{d(\lambda_1^2 + \lambda_2^2 + \lambda_3^2)}$	$\dfrac{(\lambda_1^2 + \lambda_2^2 + \lambda_3^2)^3}{(\lambda_1^3 + \lambda_2^3 + \lambda_3^3)^2}$

It is not necessary to solve the eigenvalue problem since the necessary sums can be calculated directly from any covariance matrix as follows:

$$\sum_{i=1}^{3} \lambda_i = \sum_{i=1}^{3} C_{ii}$$

$$\sum_{i=1}^{3} \lambda_i^2 = \sum_{i=1}^{3} \sum_{j=1}^{3} C_{ij}^2$$

$$\sum_{i=1}^{3} \lambda_i^3 = \sum_{i=1}^{3} \sum_{j=1}^{3} \sum_{k=1}^{3} C_{ij} C_{ik} C_{jk}$$

where the C_{ij} are the elements of the covariance matrix.

Table C-II presents the Chi-Squared distribution for non-integer degrees of freedom ranging from 1 to 3. The approximation technique may be used by obtaining a and d from Table C-I and entering them in Table C-II to obtain the desired probability. It should be noted that for approximations equating moments 1 and 2, or 1 and 3, a is the trace of the covariance matrix.

The significance of d, the degrees of freedom, may be seen by studying the shapes of the surfaces of equal probability. With d = 1 the surface is a line, i.e., all random vectors are constrained to lie on a single line. Likewise, with d = 2, a disk or d = 3, a sphere is obtained for surfaces of equal probability.

The state of the art prior to this study has been to use only the first moment. This assumes the distribution to be normal (d = 1) with a standard deviation equal to the square root of trace of the covariance matrix.* For larger degrees of freedom, this is a conservative assumption as can be seen by comparing Figure C-5 to the other curves.

* "AC-9 Guidance System Accuracy Analysis", GDC-BKM 66-028, September 30, 1966, General Dynamics Corporation, Convair Division.

TABLE C-II. CUMULATIVE PROBABILITY DISTRIBUTION FUNCTION [$Pr(|X|>\psi\sqrt{\text{TRACE}})$] OF A VECTOR WITH NORMAL, ZERO MEAN, COMPONENTS

$$\text{Magnitude}/\sqrt{\text{Trace}} = \psi$$

PROB.	D= 1.0	1.1	1.2	1.3	1.4	1.5	1.6	1.7	1.8	1.9	2.0	2.2	2.4	2.6	2.8	3.0
1.00E+00	0 0000X0	0000X0	0000X0	0000X0	0000X0	0000X0	0000X0	0000X0	0000X0	0000X0	0000X0	0000X0	0000X0	0000X0	0000X0	0000X
9.00E-01	.2072	.2182	.2297	.2358	.2464	.2577	.2696	.2822	.2955	.3097	.3237	.3522	.3770	.4004	.4218	.4398
8.00E-01	.3016	.3146	.3285	.3431	.3585	.3872	.4072	.4252	.4418	.4575	.4608	.4989	.5228	.5431	.5617	.5786
7.00E-01	.3866	.4020	.4180	.4348	.4967	.5102	.5371	.5539	.5695	.5840	.5972	.6209	.6411	.6591	.6746	.6887
6.00E-01	.5251	.5572	.5841	.6067	.6281	.6466	.6629	.6779	.6914	.7036	.7147	.7343	.7511	.7655	.7781	.7892
5.00E-01	.6753	.7026	.7265	.7459	.7631	.7783	.7918	.8036	.8143	.8239	.8326	.8476	.8602	.8708	.8800	.8880
4.00E-01	.8416	.8637	.8812	.8965	.9091	.9202	.9296	.9379	.9451	.9515	.9572	.9669	.9746	.9809	.9863	.9910
3.00E-01	1.0367	1.0500	1.0606	1.0690	1.0756	1.0814	1.0860	1.0897	1.0927	1.0952	1.0973	1.1004	1.1025	1.1039	1.1048	1.1053
2.00E-01	1.2819	1.2836	1.2841	1.2835	1.2822	1.2804	1.2784	1.2761	1.2737	1.2712	1.2686	1.2634	1.2583	1.2532	1.2483	1.2436
1.00E-01	1.6452	1.6284	1.6139	1.5982	1.5845	1.5716	1.5594	1.5480	1.5372	1.5270	1.5174	1.4997	1.4836	1.4689	1.4555	1.4433
9.00E-02	1.6955	1.6784	1.6586	1.6419	1.6263	1.6114	1.5982	1.5855	1.5736	1.5624	1.5518	1.5322	1.5146	1.4986	1.4841	1.4709
8.00E-02	1.7516	1.7288	1.7083	1.6894	1.6721	1.6559	1.6408	1.6267	1.6134	1.6010	1.5893	1.5678	1.5485	1.5312	1.5154	1.5009
7.00E-02	1.8120	1.7868	1.7637	1.7424	1.7228	1.7046	1.6878	1.6721	1.6574	1.6436	1.6307	1.6071	1.5860	1.5670	1.5497	1.5340
6.00E-02	1.8812	1.8522	1.8258	1.8017	1.7796	1.7593	1.7405	1.7230	1.7068	1.6916	1.6773	1.6513	1.6281	1.6073	1.5885	1.5712
5.00E-02	1.9600	1.9269	1.8970	1.8699	1.8456	1.8222	1.8011	1.7816	1.7635	1.7466	1.7308	1.7020	1.6764	1.6534	1.6326	1.6138
4.00E-02	2.0535	2.0157	1.9815	1.9506	1.9225	1.8967	1.8730	1.8511	1.8307	1.8118	1.7941	1.7620	1.7335	1.7081	1.6851	1.6643
3.00E-02	2.1704	2.1261	2.0865	2.0508	2.0185	1.9890	1.9619	1.9370	1.9139	1.8925	1.8726	1.8364	1.8044	1.7758	1.7501	1.7268
2.00E-02	2.3266	2.2740	2.2272	2.1852	2.1474	2.1129	2.0814	2.0529	2.0257	2.0009	1.9779	1.9362	1.8995	1.8668	1.8374	1.8108
1.00E-02	2.5760	2.5101	2.4518	2.3999	2.3531	2.3107	2.2721	2.2367	2.2041	2.1740	2.1460	2.0955	2.0511	2.0117	1.9764	1.9446
9.00E-03	2.6122	2.5444	2.4845	2.4311	2.3830	2.3395	2.2998	2.2635	2.2300	2.1991	2.1704	2.1186	2.0731	2.0327	1.9966	1.9640
8.00E-03	2.6521	2.5822	2.5205	2.4655	2.4160	2.3712	2.3304	2.2931	2.2587	2.2269	2.1973	2.1442	2.0975	2.0560	2.0189	1.9854
7.00E-03	2.6971	2.6247	2.5609	2.5040	2.4529	2.4067	2.3646	2.3261	2.2907	2.2579	2.2275	2.1728	2.1247	2.0821	2.0439	2.0095
6.00E-03	2.7482	2.6731	2.6069	2.5480	2.4951	2.4472	2.4037	2.3638	2.3272	2.2933	2.2619	2.2053	2.1557	2.1116	2.0723	2.0368
5.00E-03	2.8075	2.7295	2.6604	2.5991	2.5441	2.4943	2.4491	2.4077	2.3696	2.3344	2.3018	2.2431	2.1918	2.1460	2.1052	2.0685
4.00E-03	2.8784	2.7965	2.7244	2.6603	2.6027	2.5508	2.5035	2.4603	2.4205	2.3838	2.3498	2.2886	2.2349	2.1874	2.1449	2.1066
3.00E-03	2.9683	2.8812	2.8050	2.7372	2.6765	2.6217	2.5720	2.5264	2.4846	2.4460	2.4102	2.3459	2.2895	2.2395	2.1949	2.1547
2.00E-03	3.0905	2.9973	2.9155	2.8429	2.7778	2.7191	2.6658	2.6171	2.5724	2.5311	2.4929	2.4242	2.3641	2.3110	2.2635	2.2207
1.00E-03	3.2917	3.1671	3.0561	3.0154	2.9433	2.8783	2.8192	2.7654	2.7160	2.6704	2.6283	2.5525	2.4863	2.4277	2.3754	2.3284
9.00E-04	3.3202	3.2150	3.1227	3.0409	2.9677	2.9018	2.8419	2.7873	2.7372	2.6910	2.6482	2.5715	2.5043	2.4450	2.3920	2.3443
8.00E-04	3.3528	3.2466	3.1522	3.0691	2.9948	2.9278	2.8670	2.8116	2.7607	2.7138	2.6704	2.5925	2.5243	2.4641	2.4103	2.3620
7.00E-04	3.3897	3.2867	3.1954	3.1088	3.0252	2.9571	2.8953	2.8389	2.7871	2.7394	2.6953	2.6160	2.5468	2.4856	2.4310	2.3819
6.00E-04	3.4318	3.3306	3.2432	3.1670	3.0599	2.9985	2.9275	2.8700	2.8173	2.7687	2.7237	2.6430	2.5724	2.5101	2.4545	2.4045
5.00E-04	3.4809	3.3873	3.2977	3.1794	3.1006	3.0296	2.9652	2.9065	2.8526	2.8029	2.7570	2.6745	2.6025	2.5368	2.4820	2.4309
4.00E-04	3.5401	3.4535	3.3712	3.2906	3.1497	3.0768	3.0107	2.9505	2.8952	2.8442	2.7972	2.7126	2.6387	2.5734	2.5153	2.4629
3.00E-04	3.6154	3.4946	3.3890	3.2955	3.2120	3.1367	3.0685	3.0063	2.9493	2.8967	2.8481	2.7609	2.6846	2.6175	2.5575	2.5035
2.00E-04	3.7191	3.5931	3.4827	3.3850	3.2978	3.2192	3.1482	3.0833	3.0239	2.9691	2.9184	2.8276	2.7483	2.6782	2.6158	2.5597
1.00E-04	3.8987	3.7556	3.6376	3.5331	3.4399	3.3561	3.2801	3.2108	3.1473	3.0889	3.0348	2.9380	2.8535	2.7787	2.7122	2.6524
9.00E-05	3.9162	3.7800	3.6607	3.5551	3.4610	3.3765	3.2997	3.2296	3.1657	3.1067	3.0522	2.9544	2.8691	2.7936	2.7265	2.6662
8.00E-05	3.9445	3.8068	3.6863	3.5796	3.4845	3.3996	3.3215	3.2508	3.1861	3.1266	3.0714	2.9727	2.8865	2.8102	2.7425	2.6816
7.00E-05	3.9764	3.8376	3.7150	3.6072	3.5109	3.4245	3.3460	3.2745	3.2090	3.1489	3.0931	2.9932	2.9061	2.8290	2.7604	2.6989
6.00E-05	4.0130	3.8717	3.7480	3.6387	3.5412	3.4537	3.3742	3.3017	3.2353	3.1744	3.1179	3.0168	2.9285	2.8504	2.7810	2.7187
5.00E-05	4.0559	3.9123	3.7866	3.6757	3.5767	3.4878	3.4072	3.3336	3.2662	3.2044	3.1470	3.0444	2.9548	2.8756	2.8051	2.7419
4.00E-05	4.1077	3.9615	3.8334	3.7206	3.6196	3.5292	3.4471	3.3722	3.3037	3.2406	3.1822	3.0776	2.9867	2.9061	2.8343	2.7700
3.00E-05	4.1739	4.0240	3.8950	3.7778	3.6745	3.5818	3.4979	3.4213	3.3514	3.2867	3.2271	3.1203	3.0273	2.9449	2.8715	2.8058
2.00E-05	4.2655	4.1106	3.9756	3.8570	3.7505	3.6546	3.5686	3.4894	3.4176	3.3506	3.2893	3.1793	3.0832	2.9987	2.9231	2.8556
1.00E-05	4.4177X4	4.2546X4	4.1136X3	3.9877	3.8765	3.7756	3.6848	3.6028	3.5276	3.4573	3.3925	3.2779	3.1766	3.0884	3.0091	2.9376
9.00E-06	4.4494X4	4.2760X4	4.1342X4	4.0072	3.8950	3.7939	3.7024	3.6197	3.5440	3.4732	3.4079	3.2927	3.1906	3.1018	3.0220	2.9501
8.00E-06	4.4656X4	4.2995X4	4.1570X4	4.0288X3	3.9156	3.8140	3.7219	3.6385	3.5623	3.4909	3.4250	3.3091	3.2062	3.1165	3.0363	2.9638
7.00E-06	4.4940X4	4.3268X4	4.1838X4	4.0533X3	3.9393	3.8368	3.7445	3.6597	3.5829	3.5110	3.4443	3.3277	3.2237	3.1330	3.0525	2.9792
6.00E-06	4.5266X4	4.3577X4	4.2124X4	4.0813X3	3.9662X3	3.8628	3.7692	3.6840	3.6067	3.5342	3.4665	3.3490	3.2439	3.1520	3.0711	2.9969
5.00E-06	4.5648X4	4.3939X4	4.2471X4	4.1142X3	3.9976X3	3.8934X3	3.7989	3.7125	3.6345	3.5614	3.4934	3.3741	3.2675	3.1743	3.0930	3.0184
4.00E-06	4.6112X4	4.4378X4	4.2892X4	4.154144	4.0362X3	3.9305X3	3.8349X3	3.7471	3.6683	3.5945	3.5260	3.4036	3.2963	3.2014	3.1196	3.0446
3.00E-06	4.6703X4	4.4937X4	4.3429X4	4.2049X4	4.0851X3	3.9779X3	3.8809X3	3.7913X3	3.7114X3	3.6367	3.5676	3.4408	3.3326	3.2359	3.1536	3.0779
2.00E-06	4.7524X4	4.5715X4	4.4174X4	4.2756X4	4.1530X4	4.0436X3	3.9447X3	3.8527X3	3.7713X3	3.6954X3	3.6254X3	3.4925	3.3827	3.2840	3.2002	3.1243

X indicates extrapolation from Gamma Function Table

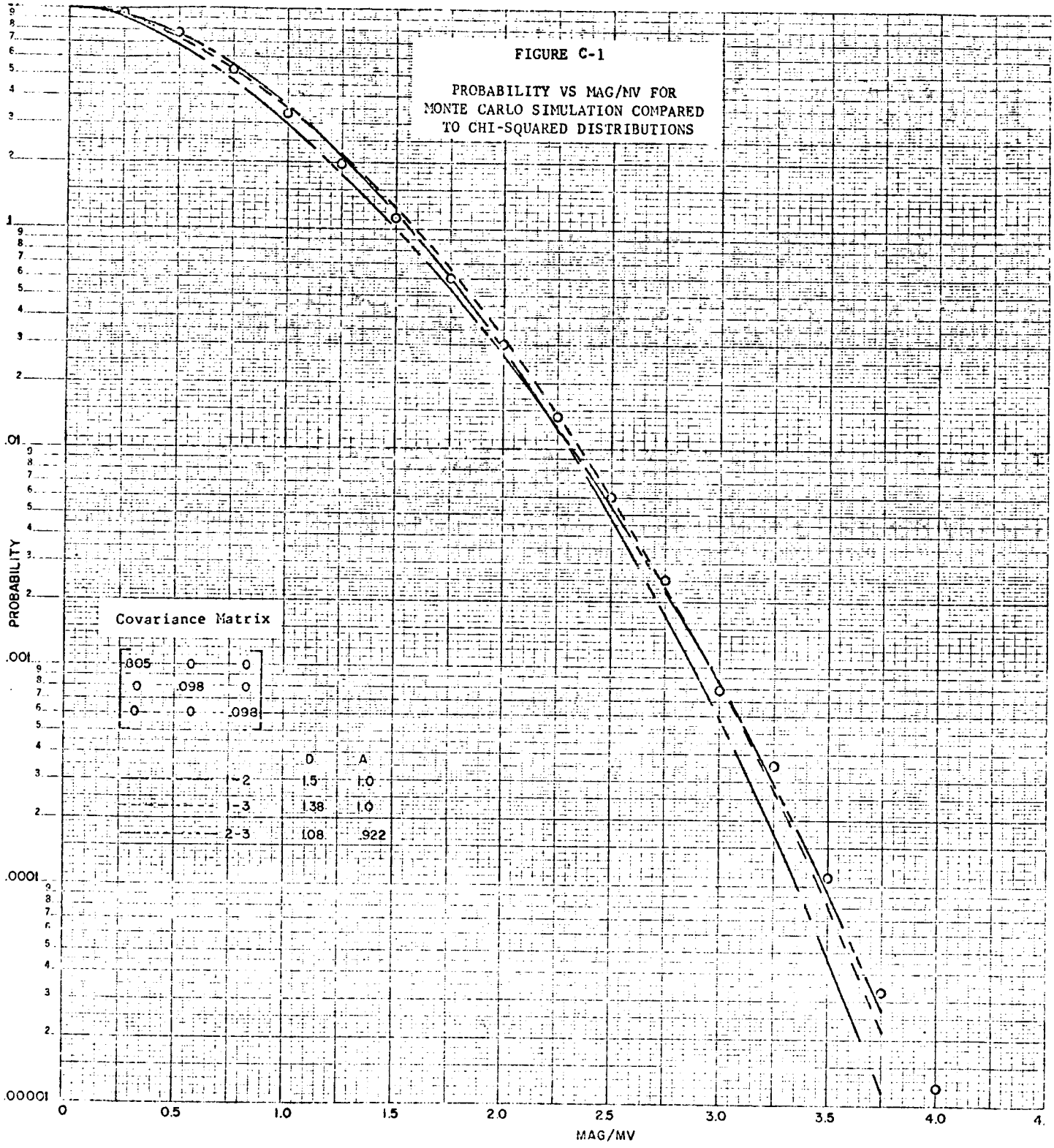
FIGURE C-1
PROBABILITY VS MAG/MV FOR
MONTE CARLO SIMULATION COMPARED
TO CHI-SQUARED DISTRIBUTIONS
PROBABILITY
MAG/MV
Covariance Matrix
.805 0 0
0 .098 0
0 0 .098
D A
1-2 1.5 1.0
1-3 1.38 1.0
2-3 1.08 .922

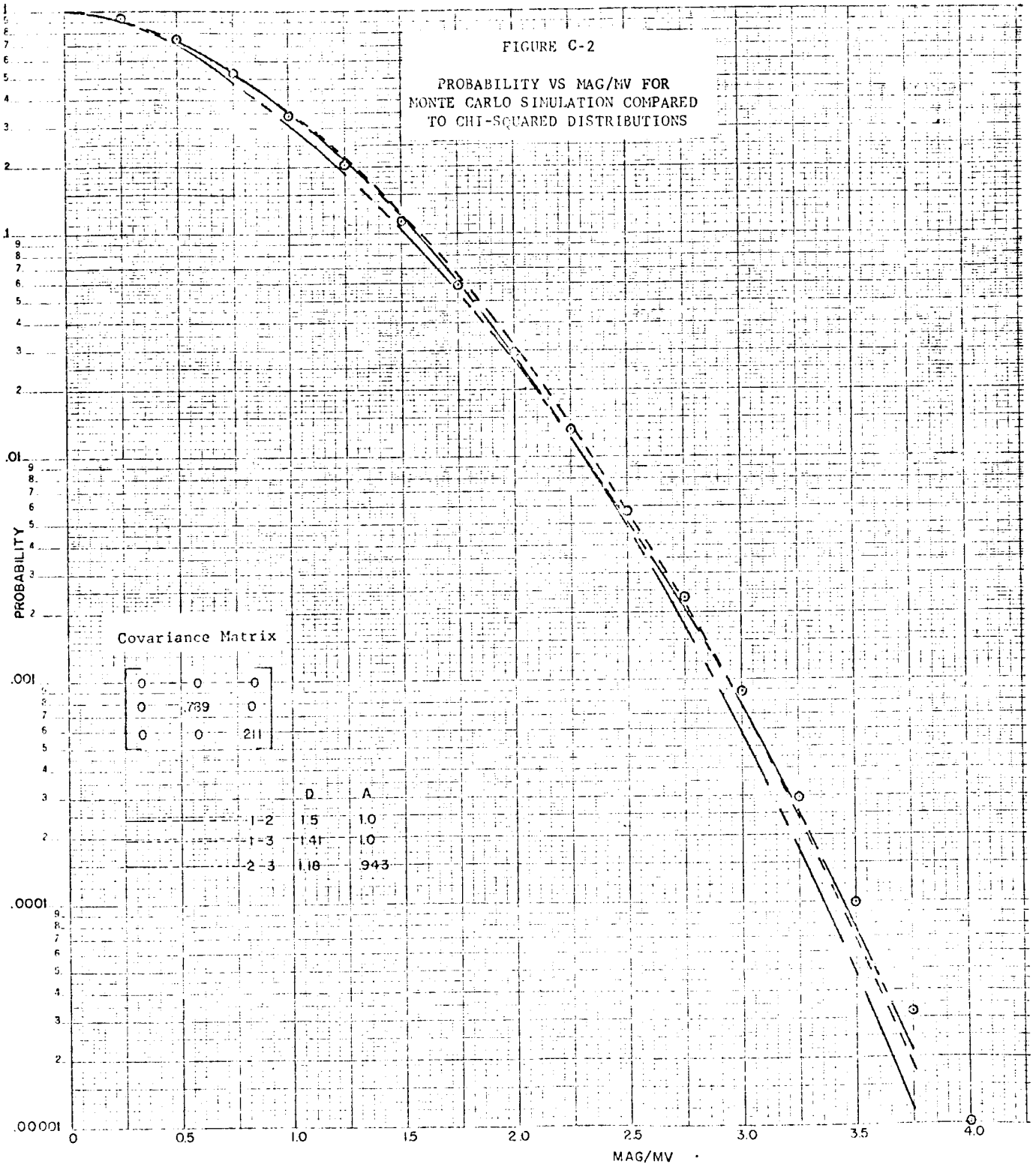
FIGURE C-2
PROBABILITY VS MAG/MV FOR
MONTE CARLO SIMULATION COMPARED
TO CHI-SQUARED DISTRIBUTIONS
PROBABILITY
MAG/MV
0
0.5
1.0
1.5
2.0
2.5
3.0
3.5
4.0
.01
.001
.0001
.00001
Covariance Matrix
0 0 0
0 .789 0
0 0 211
D A
1-2 1.5 1.0
1-3 1.41 1.0
2-3 1.18 .943

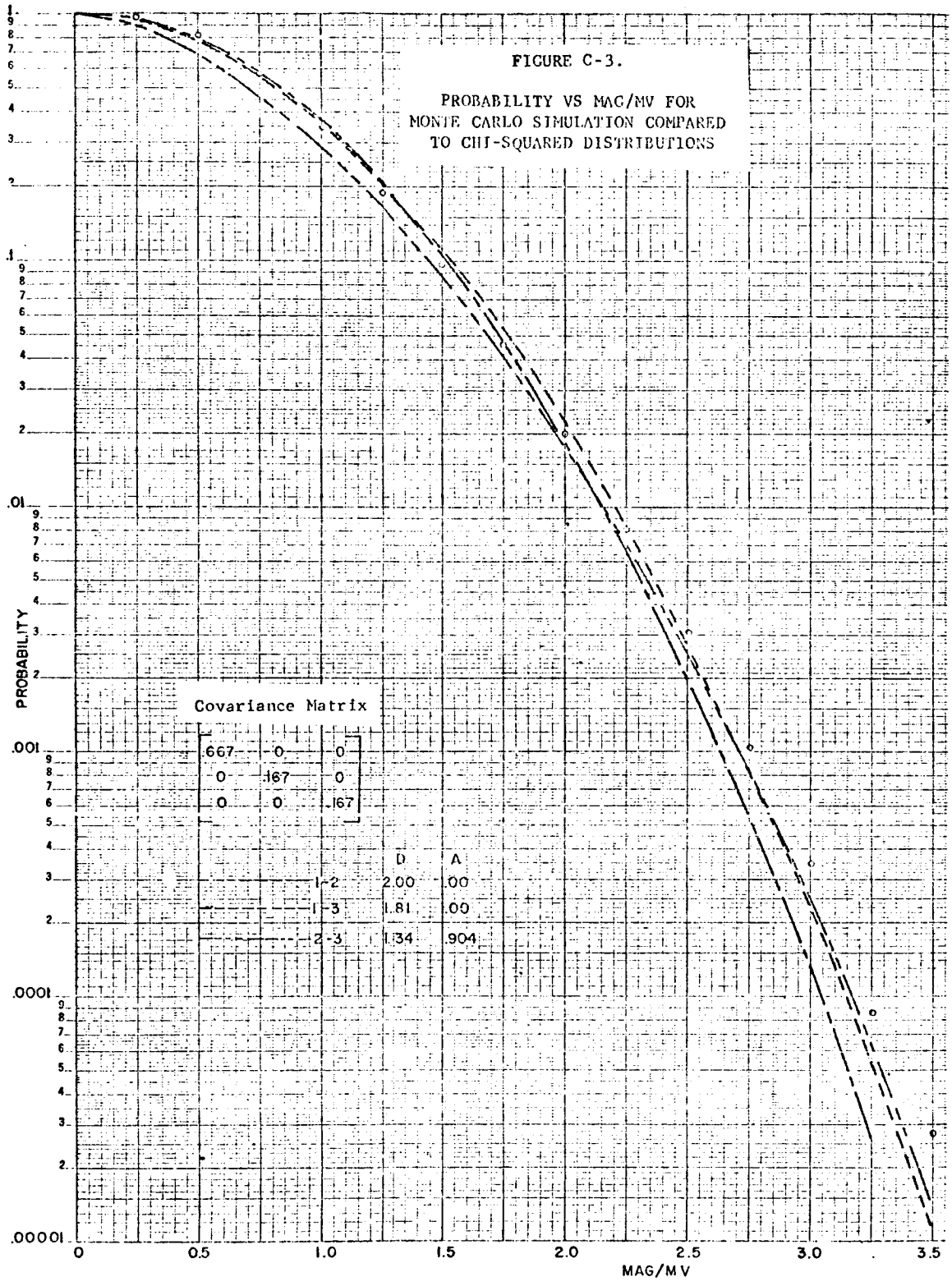

FIGURE C-3.

PROBABILITY VS MAG/MV FOR MONTE CARLO SIMULATION COMPARED TO CHI-SQUARED DISTRIBUTIONS

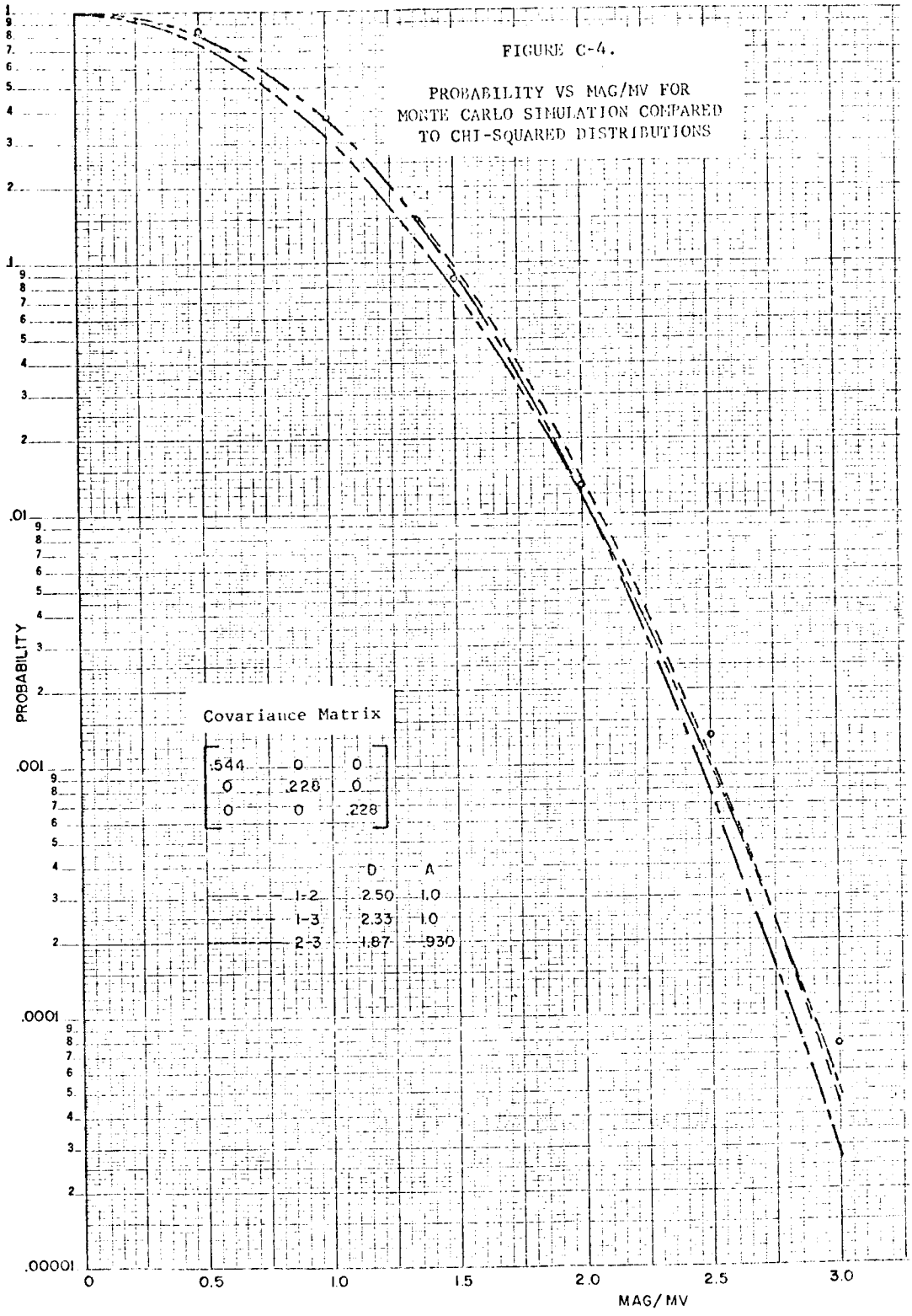
FIGURE C-4.
PROBABILITY VS MAG/MV FOR
MONTE CARLO SIMULATION COMPARED
TO CHI-SQUARED DISTRIBUTIONS
PROBABILITY
MAG/MV
0
0.5
1.0
1.5
2.0
2.5
3.0
.01
.001
.0001
.00001
Covariance Matrix
.544 0 0
0 .228 0
0 0 .228
D A
1-2 2.50 1.0
1-3 2.33 1.0
2-3 1.87 .930

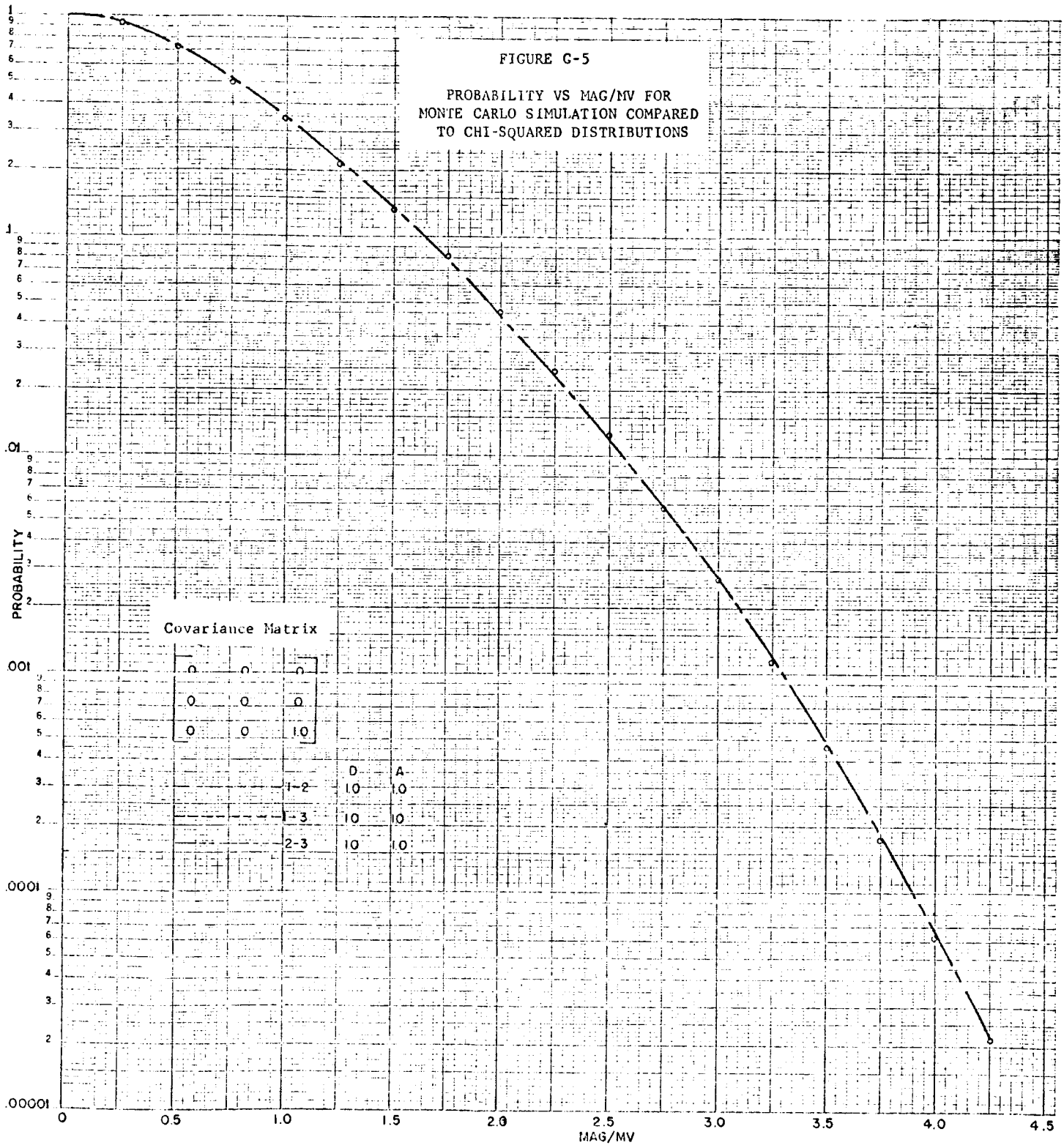
FIGURE C-5
PROBABILITY VS MAG/MV FOR MONTE CARLO SIMULATION COMPARED TO CHI-SQUARED DISTRIBUTIONS
PROBABILITY
MAG/MV
Covariance Matrix
0 0 0
0 0 0
0 0 1.0
D
A
1-2 1.0 1.0
1-3 1.0 1.0
2-3 1.0 1.0

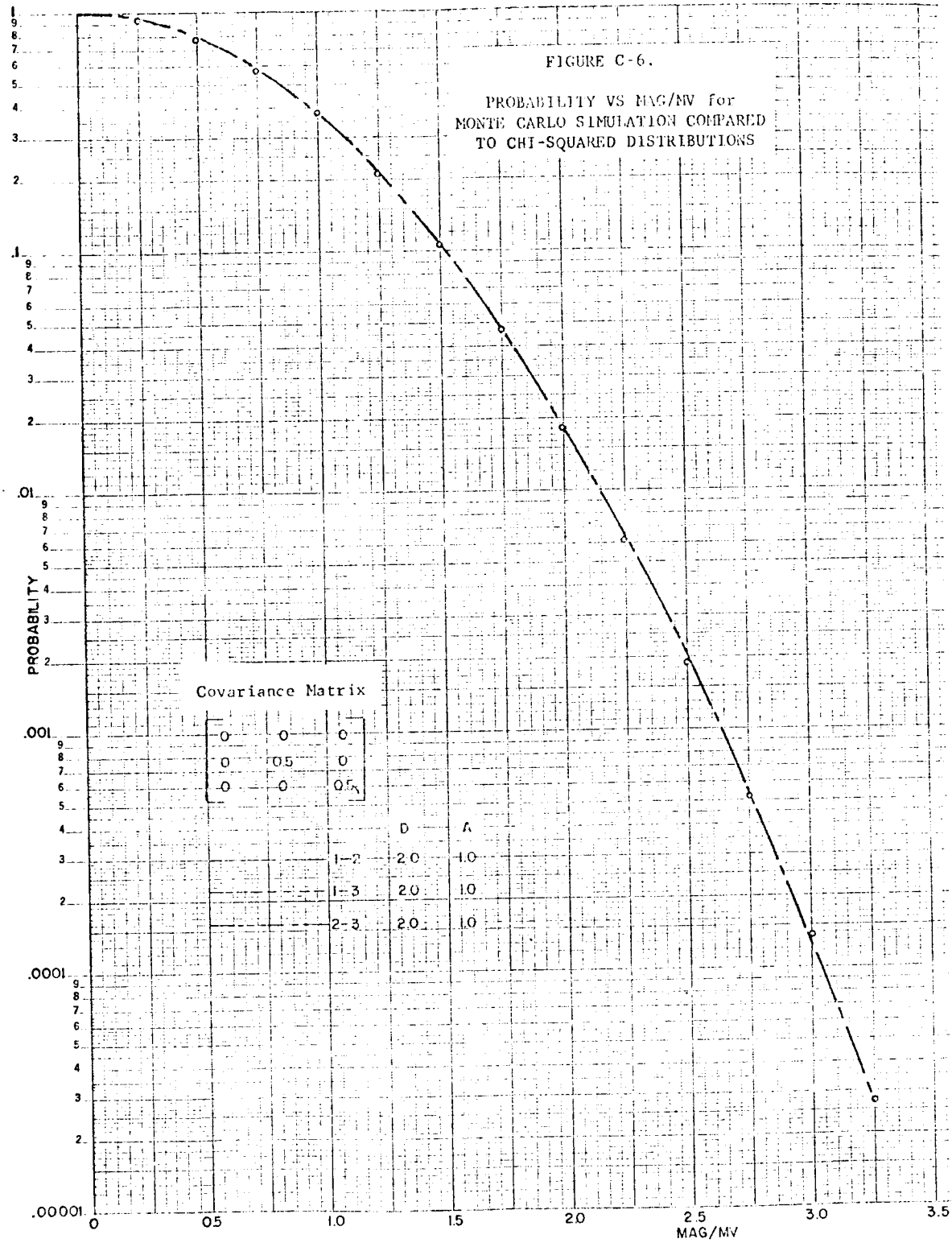
FIGURE C-6.
PROBABILITY VS MAG/MV for
MONTE CARLO SIMULATION COMPARED
TO CHI-SQUARED DISTRIBUTIONS
PROBABILITY
MAG/MV
Covariance Matrix
1 0 0
0 0.5 0
0 0 0.5
D A
1-2 2.0 1.0
1-3 2.0 1.0
2-3 2.0 1.0

APPENDIX D

CONCEPTUAL IMU DESIGNS

APPENDIX D

CONCEPTUAL IMU DESIGNS

This appendix contains sketches of fifteen conceptual strapdown IMU designs. Figures D-1 through D-9 depict nine designs for the case where the base of the IMU is mounted horizontally in the vehicle. The analytic expressions which are solved to determine the dimensions of the IMU for a set of three gyroscopes and three accelerometers are presented on Figures D-1 to D-6. Similarly, Figures D-10 through D-15 depict six designs for the case where the base of the IMU is mounted in a vertical plane in the vehicle. Restrictions such as limitation of that design to pendulous accelerometers are noted on the figures.

A=
AMAX1(W(1)+D(3)+D(6),
W(1)+W(4)+D(6), FL(2)
+W(5)+D(3)-SEP,FL(2)+
W(5)+W(4)-SEP) +
2 * S2 + 2 * XBSE

B=
AMAX1(FL(1)+D(2),
W(6)+D(5)+SEP,FL(4)
-SEP,W(3)) +S2 + 2
* XBSE

C=
AMAX1(D(1), W(2),
FL(5)-SEP,FL(6)-
SEP,D(4)+FL(3)) +
S2

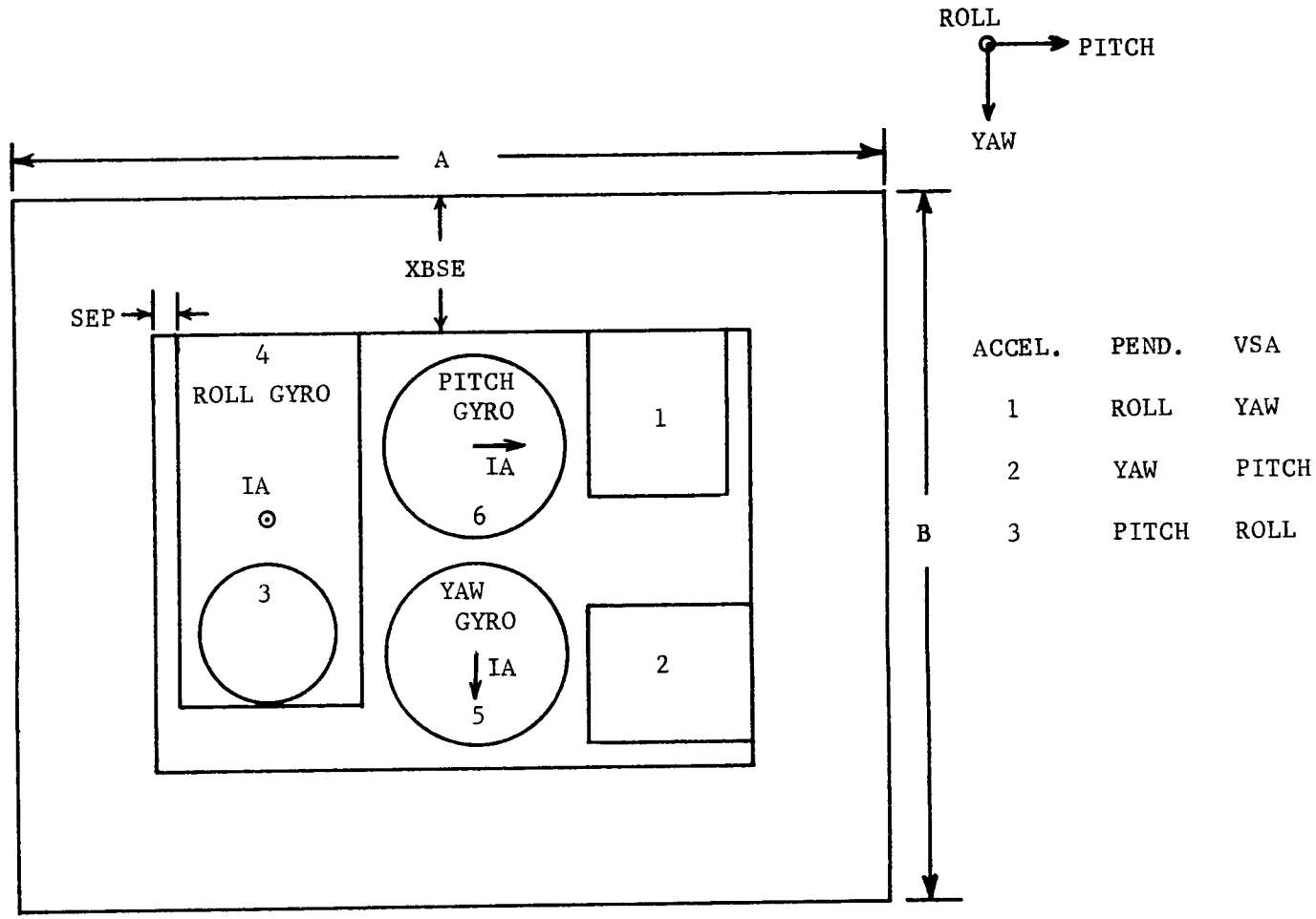

FIGURE D-1. TOP VIEW OF IMU BASE AND SAB, HORIZONTAL DESIGN 1

```
A=
AMAX1(W(1)+FL(2)+
S2,D(3)+S2,W(5)+D(6)
+3 *SEP, FL(4)+SEP)
+ 2 * XBSE

B=
AMAX1(FL(1)+D(5)+
W(4)-SEP,W(3)+D(5)
+W(4),W(3)+W(6)+W(4),
D(2)+W(6)+W(4)) + 2
* XBSE + 2 *S2

C=
AMAX1(D(1)+FL(3),
W(2)+FL(3),FL(5)-
SEP,FL(6)-SEP,D(4))
+ S2
```

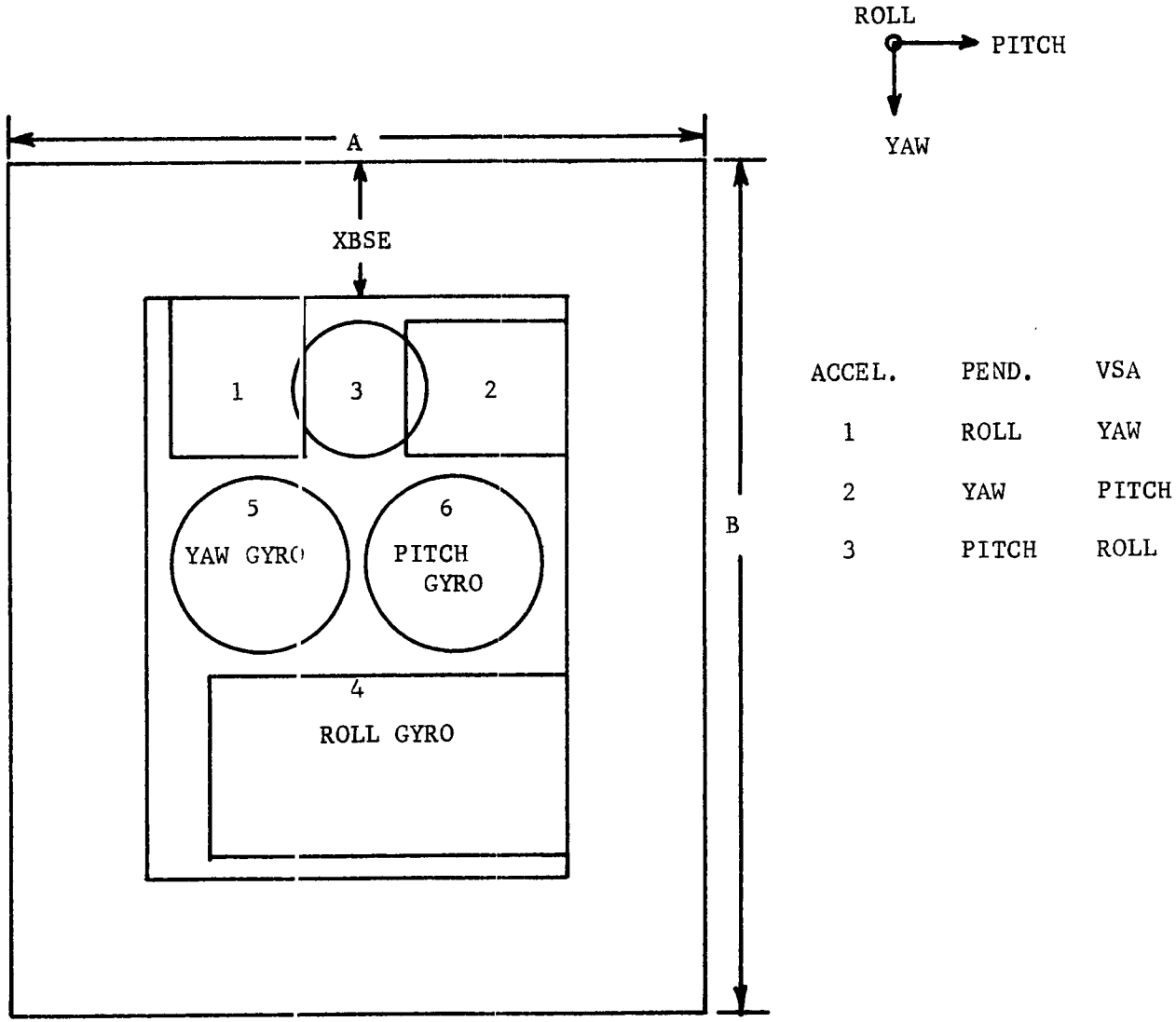

ACCEL.	PEND.	VSA
1	ROLL	YAW
2	YAW	PITCH
3	PITCH	ROLL

FIGURE D-2. TOP VIEW OF IMU BASE AND SAB, HORIZONTAL DESIGN 2

```
A=
AMAX1(W(1)+W(4)+D(3),
W(2)+W(5)+D(6),W(4)+W(5)
+W(5)+D(6)) +4,* SEP
+ 2.0 * XBSE

B=
AMAX1(FL(4),FL(1)+
D(5)+SEP,FL(3)+W(6)
+SEP,W(2)+SEP) +
SEP + 2. * XBSE

C=
AMAX1(D(4)+FL(2)+
SEP,FL(5),FL(6),D(1)
+SEP,W(3)+SEP) + SEP
```

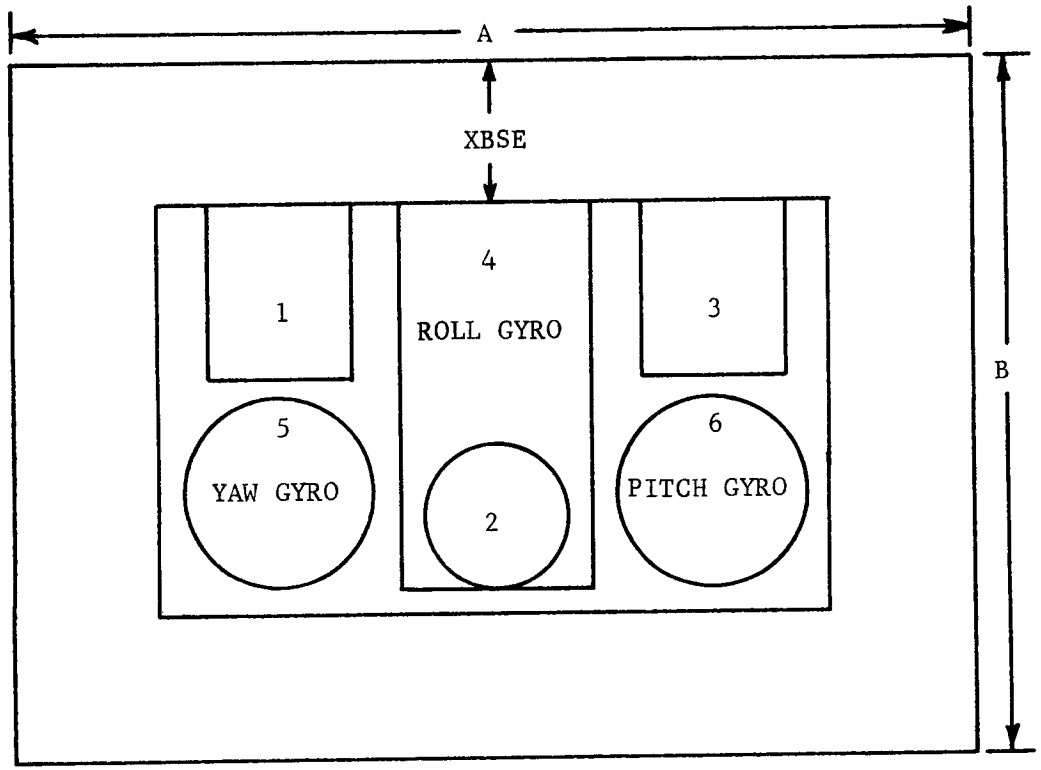

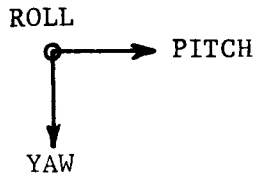

ACCEL.	PEND.
1	ROLL
2	YAW
3	PITCH

FIGURE D-3. TOP VIEW OF IMU BASE AND SAB, HORIZONTAL DESIGN 3 PENDULOUS ONLY

A=
AMAX1(W(1)+D(3)+
S2,W(5)+D(6)+S2,
FL(4),W(2)+SEP) +
SEP + 2 * XBSE

B=
AMAX1(FL(1)+D(5)+
W(4),FL(1)+D(5)+D(2),
FL(3)+W(6)+W(4),
FL(3)+W(6)+D(2)) +
3 * SEP + 2 * XBSE

C=
AMAX1(D(1)+S2,W(3)
+S2,FL(5)+SEP,FL(6)
+SEP,D(4)+FL(2)
+S2)

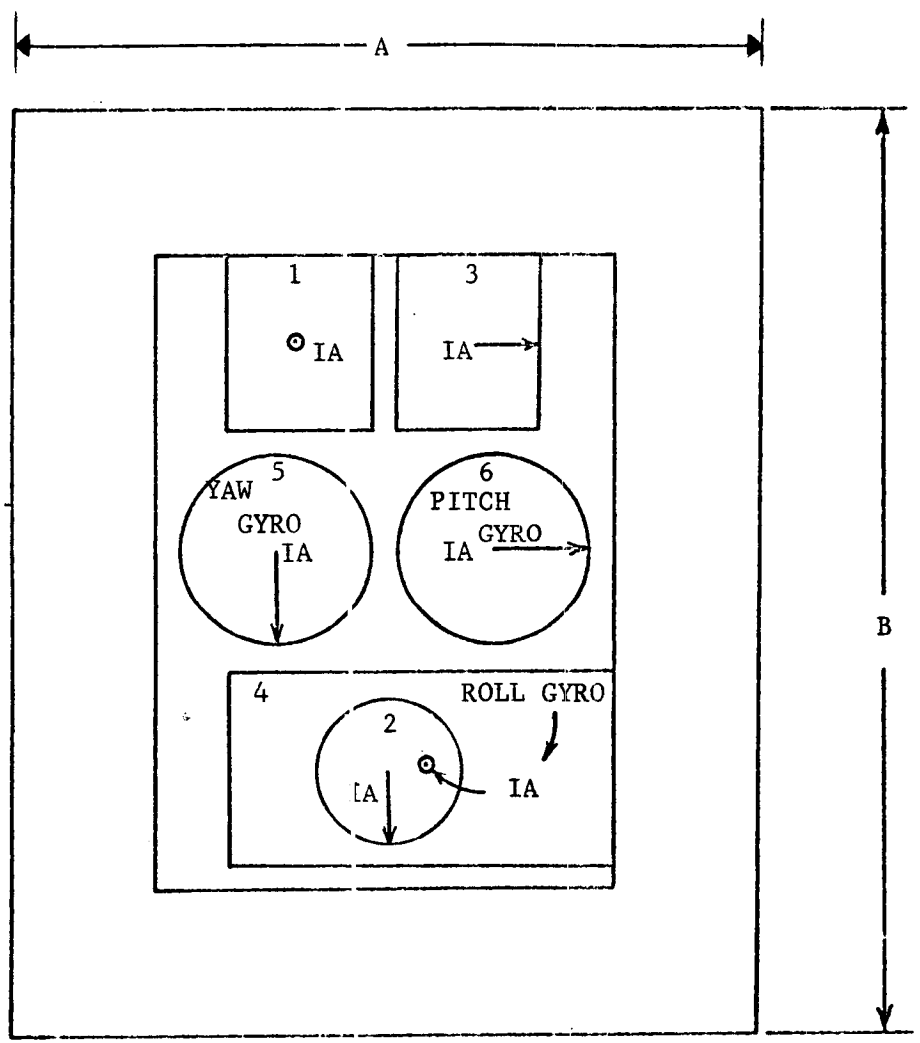

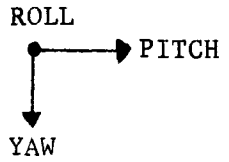

ACCEL.	PEND.
1	ROLL
2	YAW
3	PITCH

FIGURE D-4. TOP VIEW OF IMU BASE AND SAB, HORIZONTAL DESIGN 4 PENDULOUS ONLY

A=
AMAX1(W(1)+W(4)+D(3),
W(2)+W(4)+D(3),W(5)
+W(4)+D(6)) + 2 * S2
+ 2 * XBSE

B=
AMAX1(FL(1)+D(5)+
SEP,D(2)+D(5)+S2,
FL(4),FL(3)+W(6)+
SEP) + SEP + 2 *
XBSE

C=
AMAX1(D(1)+FL(2),
D(4),W(3),FL(5)-
SEP,FL(6)-SEP) +
S2

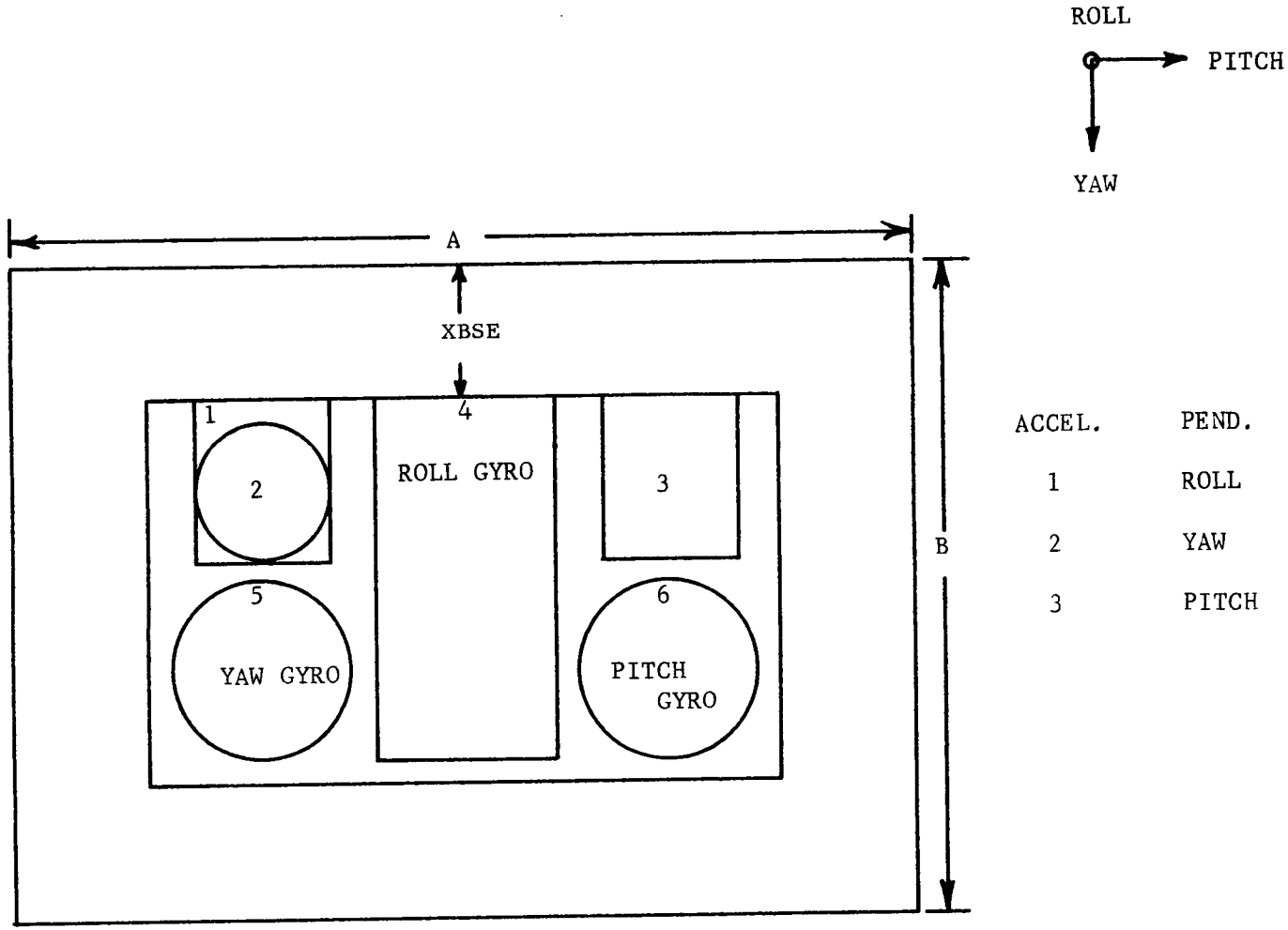

FIGURE D-5. TOP VIEW OF IMU BASE AND SAB, HORIZONTAL DESIGN 5 PENDULOUS ONLY

```
A=
AMAX1(W(1)+D(3)+
S2,W(5)+D(6)+S2,
FL(4),W(2)+SEP) +
SEP + 2 * XBSE

B=
AMAX1(FL(1)+D(5)+
W(4)+SEP,FL(3)+W(6)
+W(4)+SEP,D(2)+
D(5)+W(4)+S2,D(2)+
W(6)+W(4)+S2) +
S2 + 2 * XBSE

C=
AMAX1(D(1)+FL(2)+
S2,W(3)+FL(2)+S2,
FL(5)+SEP,FL(6)+
SEP,D(4)+S2)
```

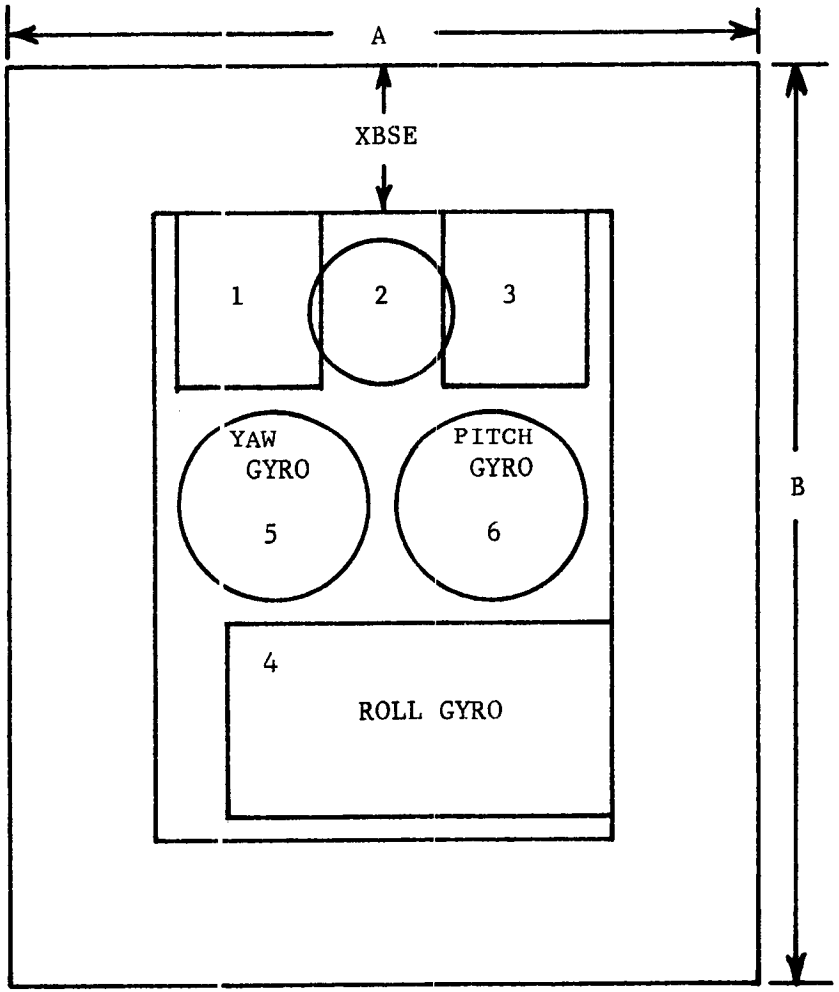

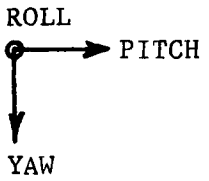

ACCEL.	PEND.
1	ROLL
2	YAW
3	PITCH

FIGURE D-6. TOP VIEW OF IMU BASE AND SAB, HORIZONTAL DESIGN 6 PENDULOUS ONLY

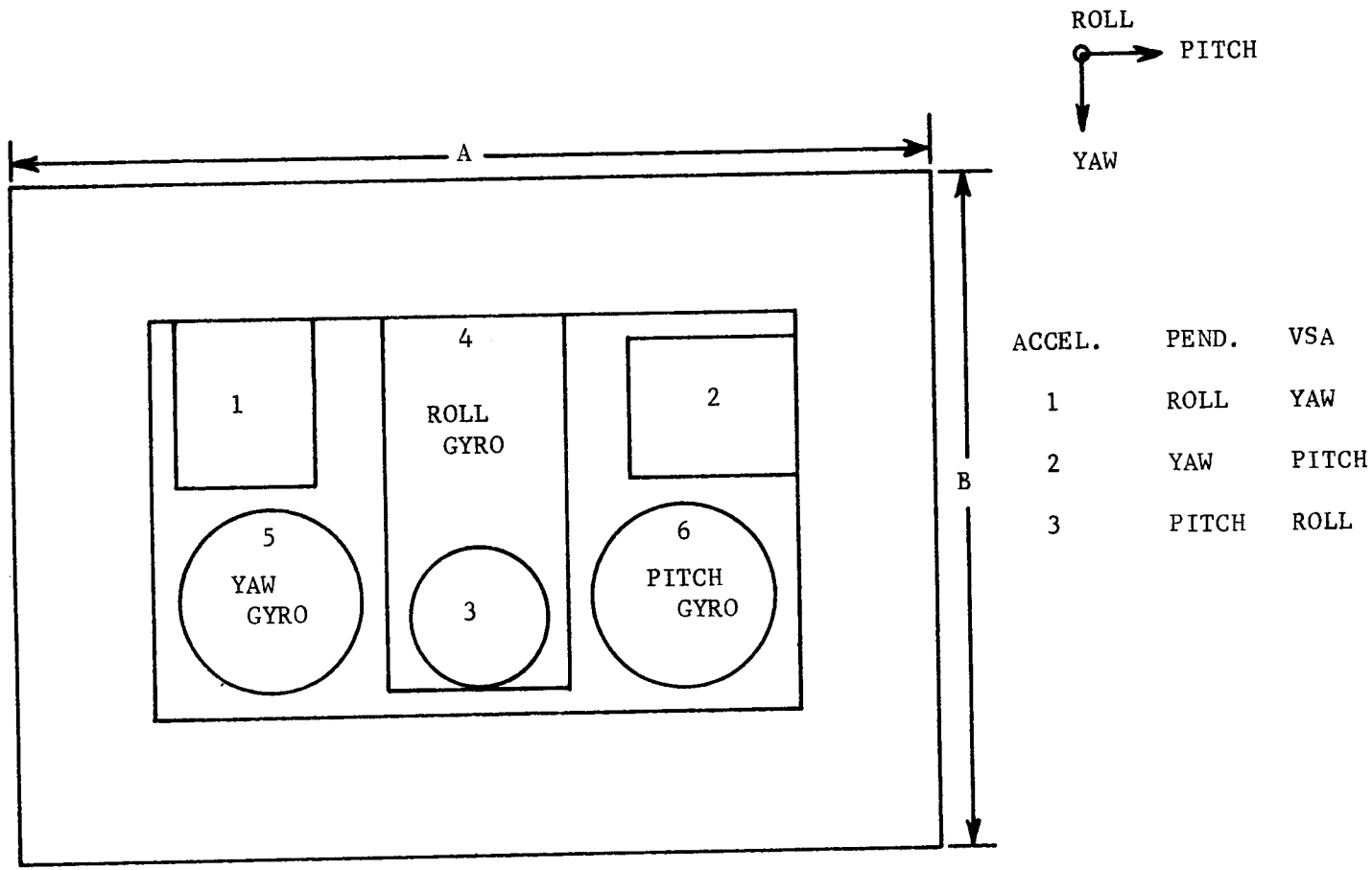

FIGURE D-7. TOP VIEW OF IMU BASE AND SAB, HORIZONTAL DESIGN 7

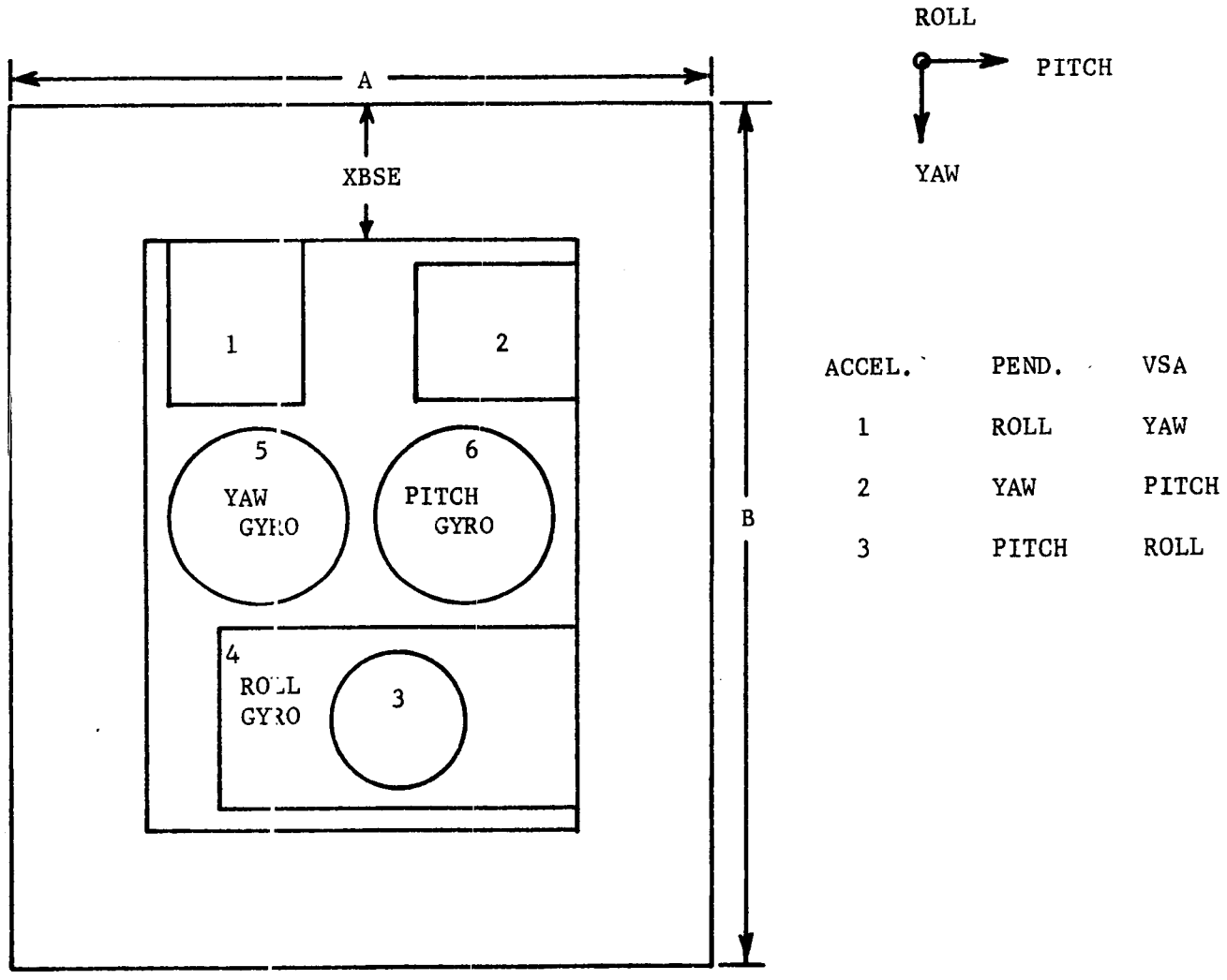

ACCEL.	PEND.	VSA
1	ROLL	YAW
2	YAW	PITCH
3	PITCH	ROLL

FIGURE D-8. TOP VIEW OF IMU BASE AND SAB, HORIZONTAL DESIGN 8

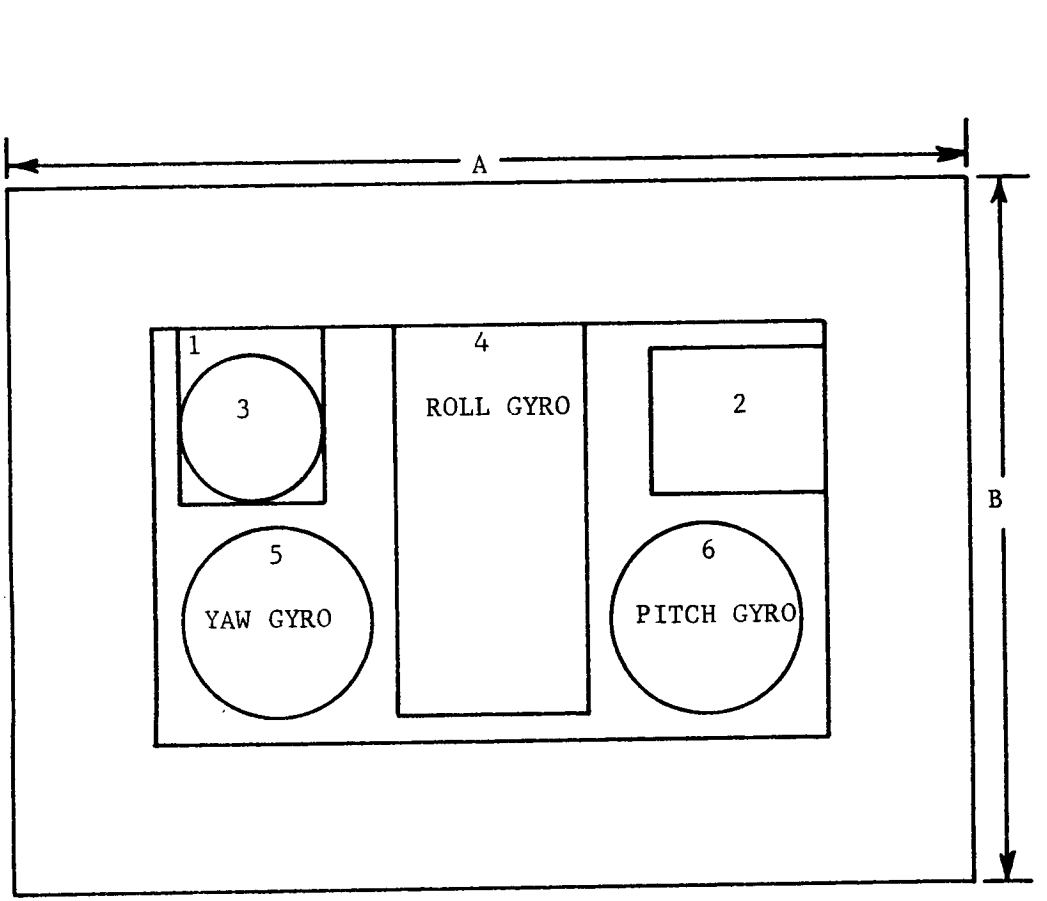

ACCEL.	PEND.	VSA
1	ROLL	YAW
2	YAW	PITCH
3	PITCH	ROLL

FIGURE D-9. TOP VIEW OF IMU BASE AND SAB, HORIZONTAL DESIGN 9

```
A=
AMAX1(D(3)+FL(2)-
SEP,W(5)+D(6),W(4)
+W(1)) + 3 * SEP
+ 2 * XBSE

B=
AMAX1(FL(5)+D(4),
FL(3)+D(4),FL(6)+
D(1), W(2)+D(1)+
SEP) + S2 + 2 * XBSE

C=
AMAX1(FL(4),FL(1),
D(5)+W(3)+S2,W(6)+
D(2)+S2) + SEP
```

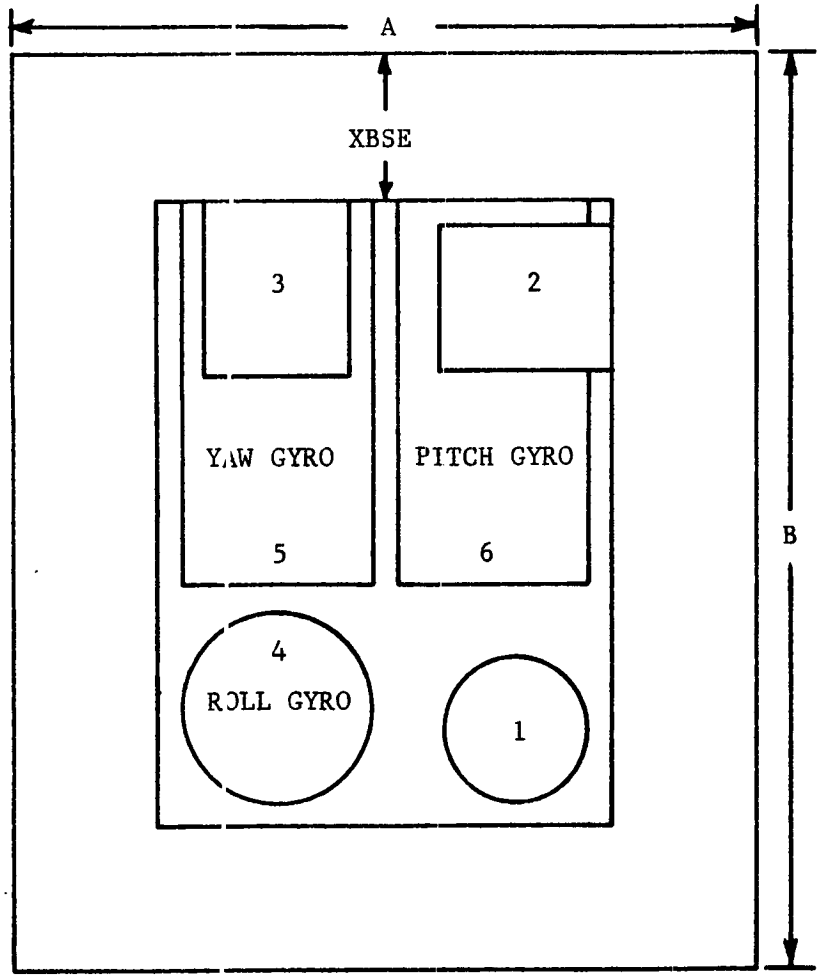

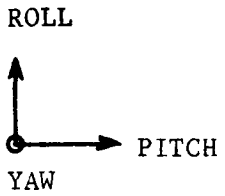

ACCEL.	PEND.	VSA
1	ROLL	YAW
2	YAW	PITCH
3	PITCH	ROLL

FIGURE D-10. TOP VIEW OF IMU BASE AND SAB, VERTICAL DESIGN 1

A=
AMAX1(D(3)+D(6),W(2)
+W(5),W(1)+W(4),
W(5)+W(4),D(6)+W(4))
+ 3 * SEP + 2 * XBSE

B=
AMAX1(FL(5)+FL(6)+
SEP,FL(2)+D(4)+FL(3)
+S2) + 2 * XBSE

C=
AMAX1(FL(4),D(2)+
SEP,W(3)+SEP,D(5)+
FL(1)+SEP,W(6)+FL(1)
+SEP) + SEP

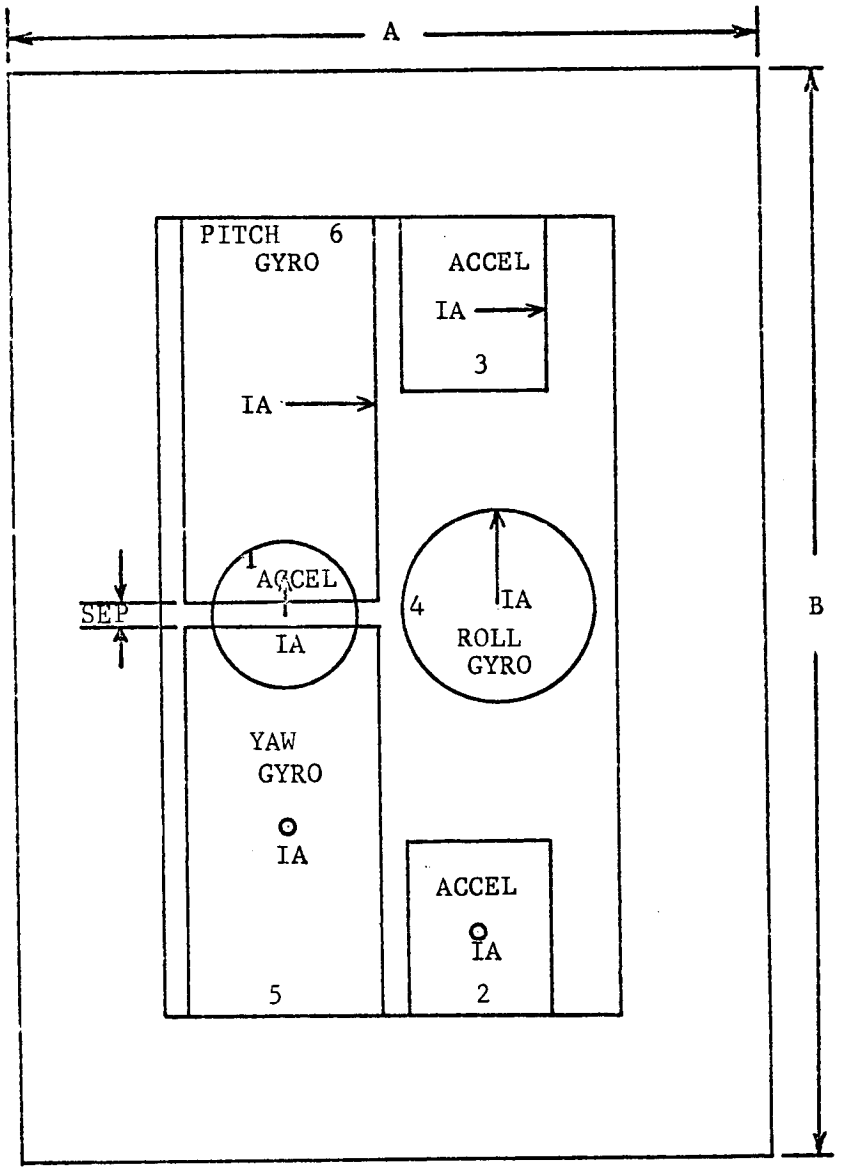

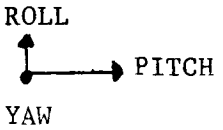

ACCEL.	PEND.
1	ROLL
2	YAW
3	PITCH

FIGURE D-11. TOP VIEW OF IMU BASE AND SAB, VERTICAL DESIGN 2 PENDULOUS ONLY

A=
AMAX1(W(5)+D(6)+W(2),
W(5)+D(6)+W(1),
FL(4)+D(3)-S2) +
2 * S2 + 2 * XBSE

B=
AMAX1(FL(5)+D(4),
FL(6)+D(4),FL(2)+
D(1)+FL(3)) + S2
+ 2 * XBSE

C=
AMAX1(W(4),D(5),W(6),
FL(1)-SEP,D(2),
W(3)) + S2

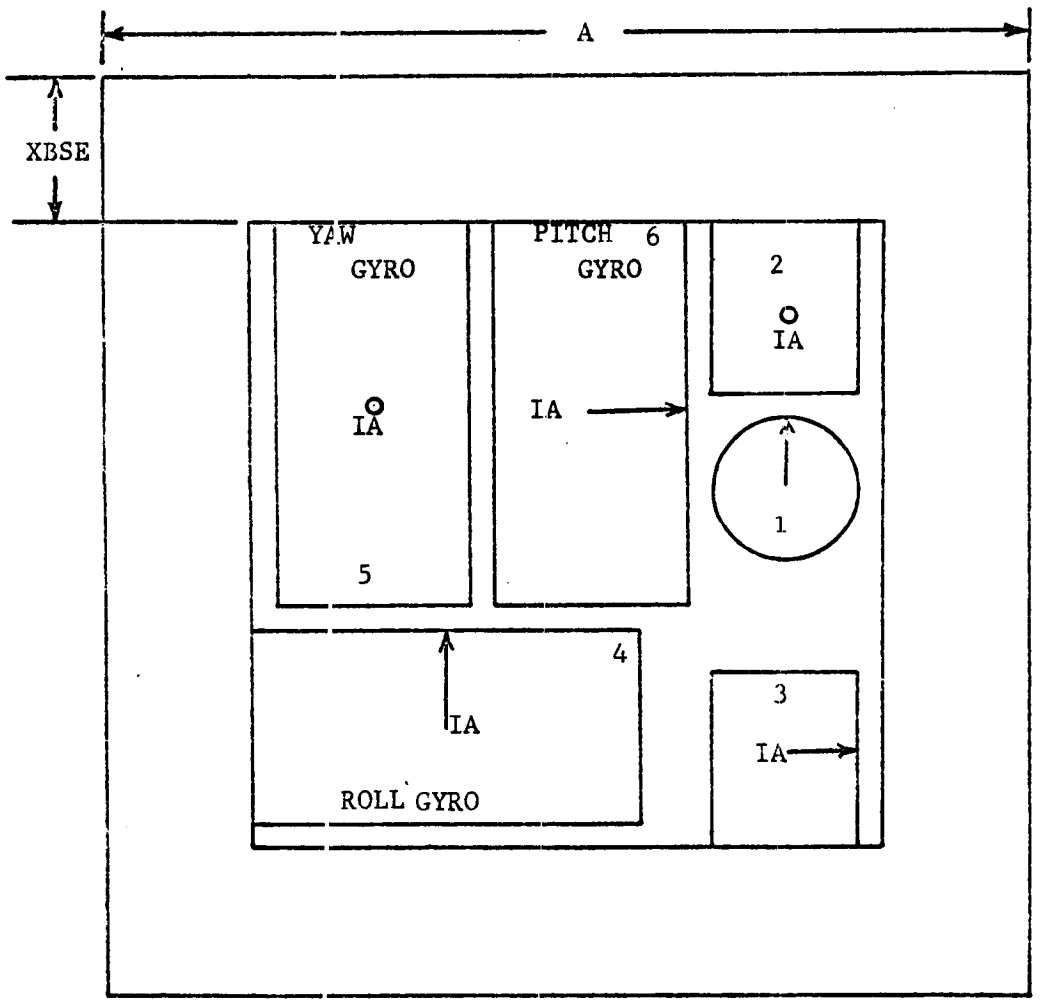

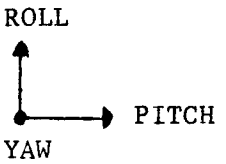

ACCEL.	PEND.
1	ROLL
2	YAW
3	PITCH

FIGURE D- 12 TOP VIEW OF IMU BASE AND SAB, VERTICAL DESIGN 3 PENDULOUS ONLY

```
A=
AMAX1(W(5)+D(6)+D(3),
W(5)+D(6)+W(1),
FL(2)+FL(4)-S2) +
2 * S2 + 2 * XBSE

B=
AMAX1(FL(5)+W(2),
FL(6)+D(4),W(3)+D(1)
+D(4)+S2) + S2 + 2
* XBSE

C=
AMAX1(D(5),D(2),W(6),
W(4),FL(3)-SEP,
FL(1)-SEP) + S2
```

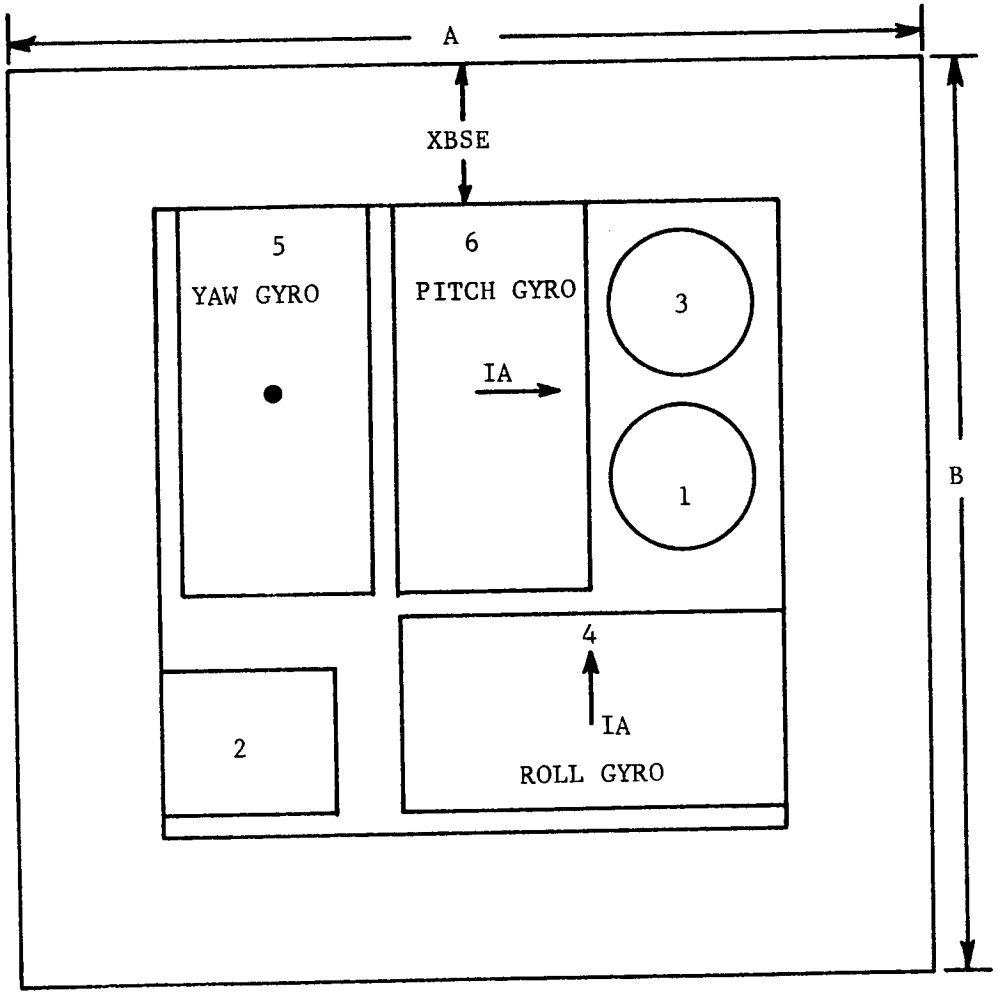

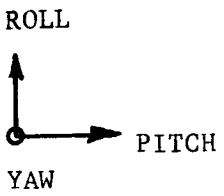

ACCEL.	PEND.
1	ROLL
2	YAW
3	PITCH

FIGURE D-13. TOP VIEW OF IMU BASE AND SAB, VERTICAL DESIGN 4 PENDULOUS ONLY

```
A=
AMAX1(W(5)+D(6)+D(3),
W(5)+D(6)+FL(2)-SEP,
W(5)+D(6)+W(1),
W(5)+D(6)+W(4)) + 2
* S2 + 2 * XBSE

B=
AMAX1(FL(5)-S2,FL(6)
-S2,FL(3)+D(1)+
D(4),FL(3)+W(2)+D(4),
FL(6)+D(4)-SEP) + 3
* SEP +2 * XBSE

C=
AMAX1(D(5),W(6),W(3),
D(2)+FL(1),FL(4)
-SEP) + S2
```

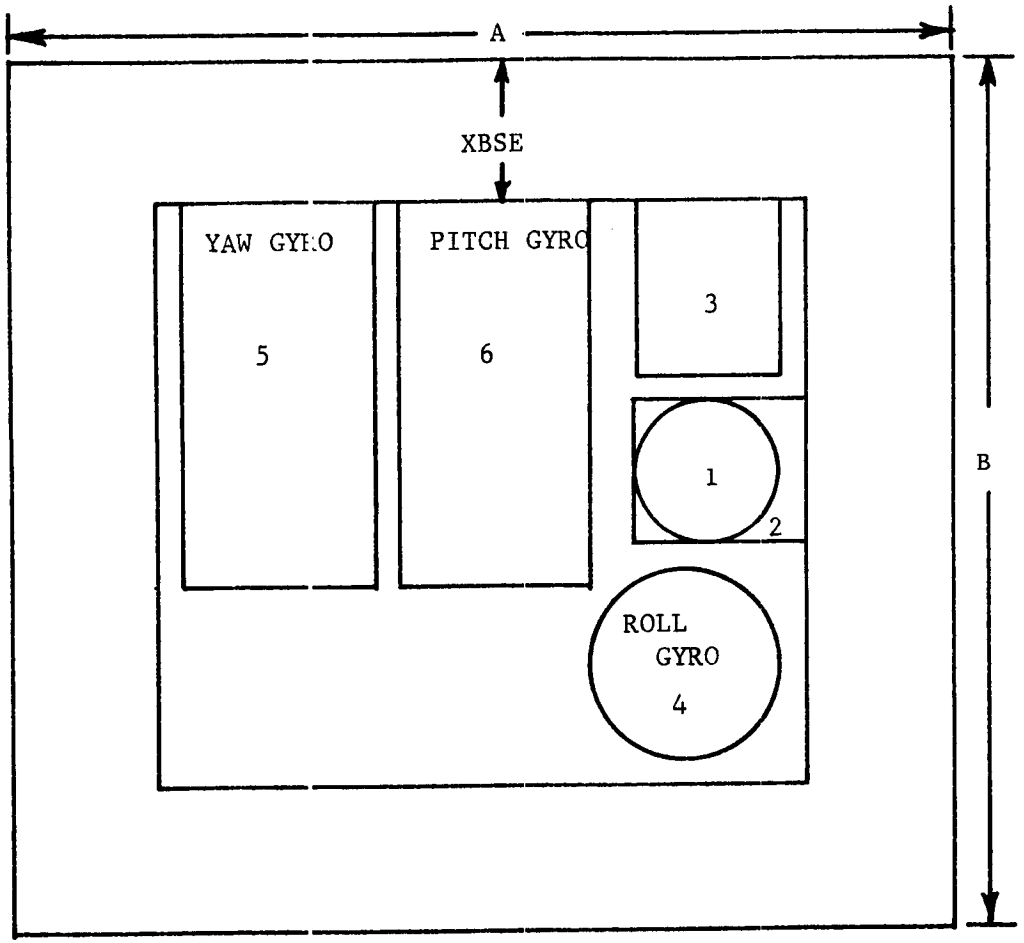

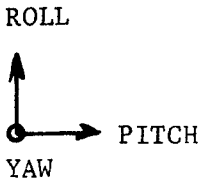

ACCEL.	PEND.	VSA
1	ROLL	YAW
2	YAW	PITCH
3	PITCH	ROLL

FIGURE D-14. TOP VIEW OF IMU BASE AND SAB, VERTICAL DESIGN 5

```
A=
AMAX1(W(5)+D(6)+W(4),
W(5)+D(6)+D(3),
W(5)+D(6)+FL(2)-
SEP,W(5)+W(1)+D(3),
W(5)+W(1)+FL(2)-SEP)
+ 2 * S2 + 2 *XBSE

B=
AMAX1(FL(5)-SEP,
FL(6)-SEP,D(1),FL(3)
+D(4),W(2)+D(4)+SEP)
+ S2 + 2 * XBSE

C=
AMAX1(D(5),W(6)+
FL(1),D(2)+W(3)+
SEP,FL(4)-SEP) +
S2
```

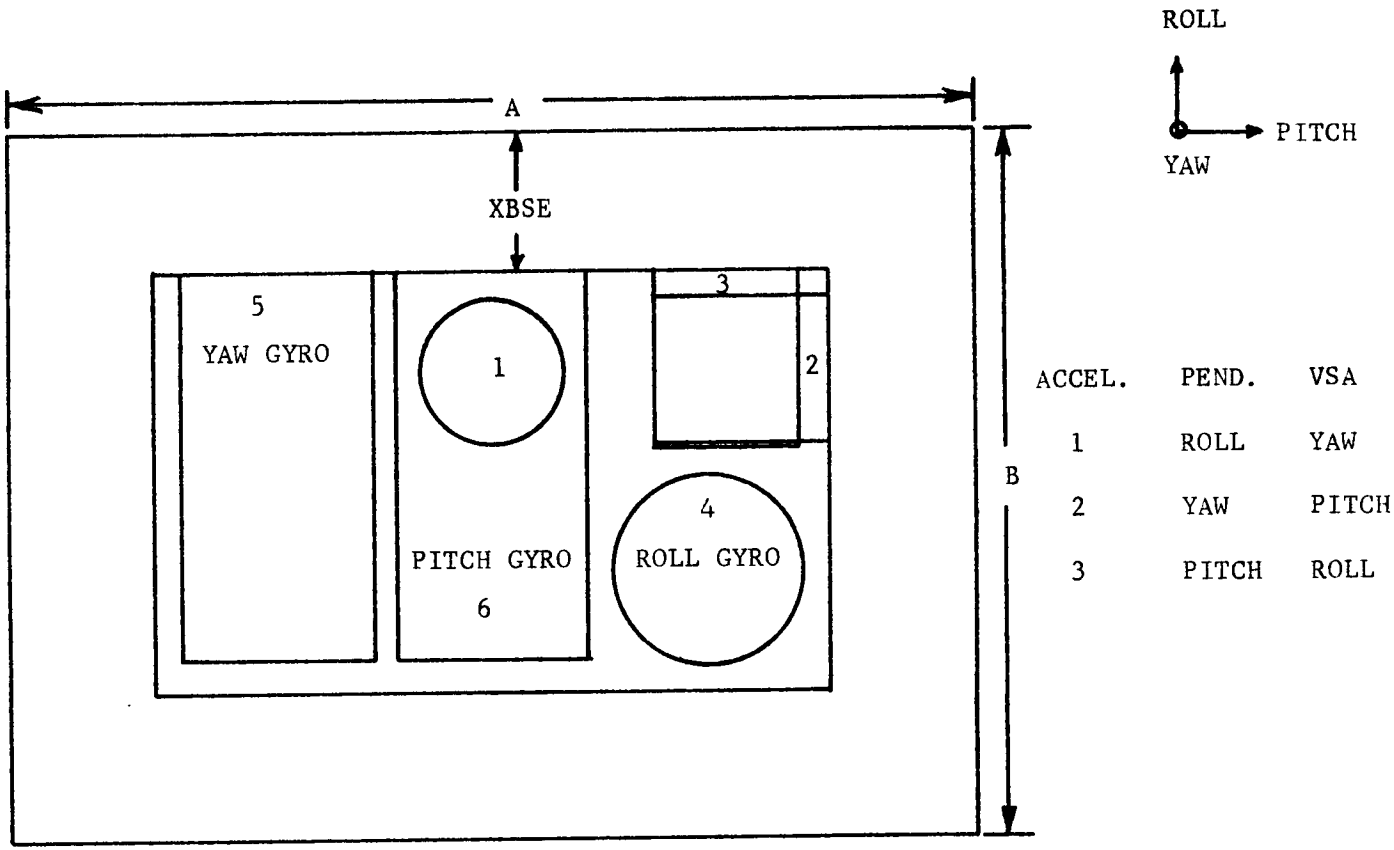

FIGURE D-15. TOP VIEW OF IMU BASE AND SAB, VERTICAL DESIGN 6

APPENDIX E

SINGLE-DEGREE-OF-FREEDOM GYROSCOPE ERROR MODEL

APPENDIX E

SINGLE-DEGREE-OF-FREEDOM GYROSCOPE ERROR MODEL

INTRODUCTION

The error model contained in the ERC provided strapdown error analysis program (SEAP) accounts for only the major steady state error torques of the single-degree-of-freedom (SDF) gyroscope. Recent papers[E1-E4]* have shown that an expansion of the error model to include the effects of vehicle dynamics, gyroscope dynamics, and rebalance loop characteristics should be considered since these effects can increase the total error quite significantly. Of equal importance with the expansion of the SEAP error models is the need for a standard set of symbols denoting the error coefficients for each error source. It is suggested that NASA/ERC give serious consideration to adopting and requiring use by its contractors of a standard error coefficient nomenclature and set of symbols.

DEFINITION OF TERMS

$\bar{M}$	Vector sum of all external torques acting on gyro
$\bar{H}$	Vector angular momentum of gyro (referred to an origin at pivot point and based on inertial velocity)
$\lvert\bar{H}\rvert \cong$	$I_{sp}\omega_{sp}$
g	Gimbal
$\bar{\omega}_{I,g}$	Angular velocity of the gimbal with respect to (wrt) inertial space
x,y,z	Gimbal (moving) axes, where x ‖ IA y ‖ OA z ‖ SA
I_x, I_y, I_z	Moments of inertia of the gimbal about x, y, and z axes
Sp	Spin

* Superscript number denotes references.

$\dot{\omega}$	$d\omega/dt$
$A_{ca,g}$	Angle of gimbal wrt the case
i, j, k	Unit vectors along moving axes x, y, z
i_{ca}, j_{ca}, k_{ca}	Unit vectors along (fixed case axes X_{ca}, Y_{ca}, Z_{ca})
$\bar{\omega}_{I,ca}$	Angular velocity of case wrt inertial space
$\omega_{I,ca_{X_{ca}}}$	The X_{ca} component of case wrt inertial space
M_{TG}	Torque generator applied torque
C_D	Damping coefficient
a_I	Acceleration along Input Axis (IA)
a_S	Acceleration along Spin Axis (SA)
a_O	Acceleration along Output Axis (OA)

DERIVATION

Newton's law in rotational form, applied to a single degree of freedom gyro (rigid body) may be written as

$$\bar{M}_{app} = \frac{d\bar{H}}{dt}\Big]_I \qquad (1)$$

where the angular momentum, $\bar{H}$, is referred to an origin at the body's cg and is based on inertial velocity (cg and pivot point are coincident).

$$\bar{M}_{app} = \frac{d\bar{H}}{dt}\Big]_g + (\bar{\omega}_{I,g} \times \bar{H}) \qquad g \text{ - Gimbal (or float)} \qquad (2)$$

$$\bar{H}_{(body)} = \vec{i}_g I_x \omega_{I,g_x} + \vec{j}_g I_y \omega_{I,g_y} + \vec{k}_g (I_z \omega_{I,g_z} + H_{wh}) \qquad (3)$$

where $H_{wh} \equiv I_{sp} \omega_{sp}$. X, y, z are gimbal axes with x corresponding to (~) IA, y ~ OA, and z ~ SA. From (3)

$$\frac{d\bar{H}}{dt}\Big]_g = \bar{i}_g (I_x \dot{\omega}_{I,g_x}) + \bar{j}_g (I_y \dot{\omega}_{I,g_y}) + \bar{k}_g (I_z \dot{\omega}_{I,g_z}) \qquad (4)$$

(treating H_{wh} as a constant). Then using (3) and (4), (2) becomes

$$\bar{M}_{app} = \begin{vmatrix} \vec{i}_g & \vec{j}_g & \vec{k}_g \\ \omega_{I,g_x} & \omega_{I,g_y} & \omega_{I,g_z} \\ I_x \omega_{I,g_x} & I_y \omega_{I,g_y} & (I_z \omega_{I,g_z} + H_{wh}) \end{vmatrix} + \vec{i}_g (I_x \dot{\omega}_{I,g_x}) + \vec{j}_g (I_y \dot{\omega}_{I,g_y}) + \vec{k}_g (I_z \dot{\omega}_{I,g_z}) \qquad (5)$$

or

$$\begin{aligned} \bar{M}_{app} = {} & \vec{i}_g \left[I_x \dot{\omega}_{I,g_x} - (I_y - I_z)\, \omega_{I,g_y}\, \omega_{I,g_z} + H_{wh}\, \omega_{I,g_y} \right] + \\ & \vec{j}_g \left[I_y \dot{\omega}_{I,g_y} - (I_z - I_x)\, \omega_{I,g_z}\, \omega_{I,g_x} - H_{wh}\, \omega_{I,g_x} \right] + \\ & \vec{k}_g \left[I_x \dot{\omega}_{I,g_y} - (I_x - I_y)\, \omega_{I,g_x}\, \omega_{I,g_y} \right] \end{aligned} \qquad (6)$$

The torque component of interest in this case (SDF gyro) is the one along the OA ($\sim y_g$), so with x ~ IA, y ~ OA, and z ~ SA

$$|\bar{M}_{app}| = I_{OA}\dot{\omega}_{I,g_y} - (I_{SA} - I_{IA})\,\omega_{I,g_z}\omega_{I,g_y} - H_{wh}\,\omega_{I,g_x} \quad . \tag{7}$$

To convert from gimbal motion with respect to (wrt) inertial space to gimbal motion wrt the case (ca), use

$$\bar{\omega}_{I,g} = \bar{\omega}_{I,ca} + \bar{\omega}_{ca,g} = \bar{\omega}_{I,ca} + \dot{\bar{A}}_{ca,g} \quad . \tag{8}$$

Gimbal freedom is about y_g ($\sim$ OA), so the transformation from moving axes to fixed (case) will be through $A_{ca,g}$ as shown in Figure E-1.

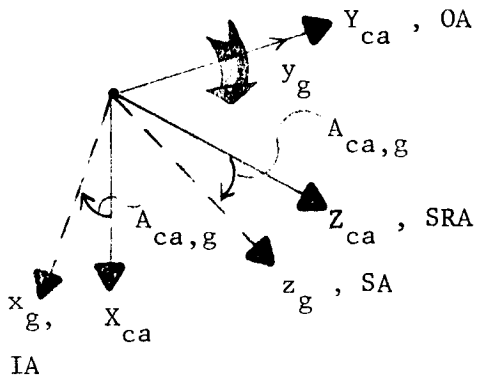

FIGURE E-1. GIMBAL AND CASE AXES

$$\bar{l}_{x_g} = \bar{l}_{X_{ca}} \cos A_{ca,g} + 0 - \bar{l}_{Z_{ca}} \sin A_{ca,g}$$

$$\bar{l}_{y_g} = 0 + \bar{l}_{Y_{ca}} + 0 \tag{9}$$

$$\bar{l}_{z_g} = \bar{l}_{x_g} \sin A_{ca,g} + 0 + \bar{l}_{z_g} \cos A_{ca,g}$$

or

$$\begin{bmatrix} \omega_{I,g_x} \\ \omega_{I,g_y} \\ \omega_{I,g_z} \end{bmatrix} = \begin{bmatrix} \cos A_{ca,g} & 0 & -\sin A_{ca,g} \\ 0 & 1 & 0 \\ \sin A_{ca,g} & 0 & \cos A_{ca,g} \end{bmatrix} \begin{bmatrix} \omega_{I,ca_X} \\ \omega_{I,ca_Y} + \dot{A}_{ca,g} \\ \omega_{I,ca_z} \end{bmatrix} \quad (10)$$

Then by treating $A_{ca,g}$ as "small",

$$\begin{aligned} \omega_{I,g_x} &\cong \omega_{I,ca_X} - \omega_{I,ca_Z} A_{ca,g} \\ \omega_{I,g_y} &\cong \omega_{I,ca_Y} + \dot{A}_{ca,g} \\ \omega_{I,g_z} &\cong \omega_{I,ca_X} A_{ca,g} + \omega_{I,ca_Z} \end{aligned} \quad (11)$$

Before expanding (7) by using (11), we will include the effects of a small misalignment of the gyro's OA and SA with respect to the IA (i.e., the OA and SA are each nonorthogonal with respect to the IA). Symbolize these small angles by $A_{m_{OA}}$ and $A_{m_{SA}}$, and let "t" indicate "true" as shown in Figures E-2 and E-3. The misalignment angles will cause cross-coupling of the components of gimbal rate since the "y" and "z" components are not orthogonal with respect to "x" (consider each rate component singly).

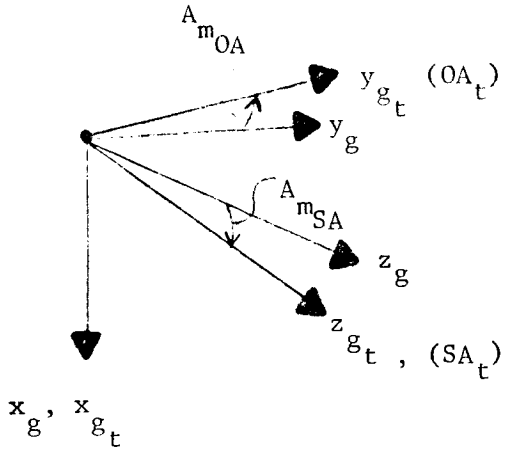

FIGURE E-2. MISALIGNMENT OF IA WITH RESPECT TO SA AND OA

$$\omega_{I,g_{x_t}} = \omega_{I,g_x} + (\text{a component of } \omega_{I,y_y} + \text{a component of } \omega_{I,g_z}) \tag{12}$$

$$\omega_{I,g_{x_t}} = \omega_{I,g_x} - \omega_{I,g_y} A_{m_{OA}} + \omega_{I,g_z} A_{m_{SA}} \tag{13}$$

(letting $\sin A_{m_{OA}} \cong A_{m_{OA}}$) and similarly,

$$\omega_{I,g_{y_t}} = \omega_{I,g_y} + (\text{component of } \omega_{I,g_x}) = \omega_{I,g_y} - \omega_{I,g_x} A_{m_{OA}} \tag{14}$$

and

$$\omega_{I,g_{z_t}} = \omega_{I,g_z} + \omega_{I,g_x} A_{m_{SA}} \tag{15}$$

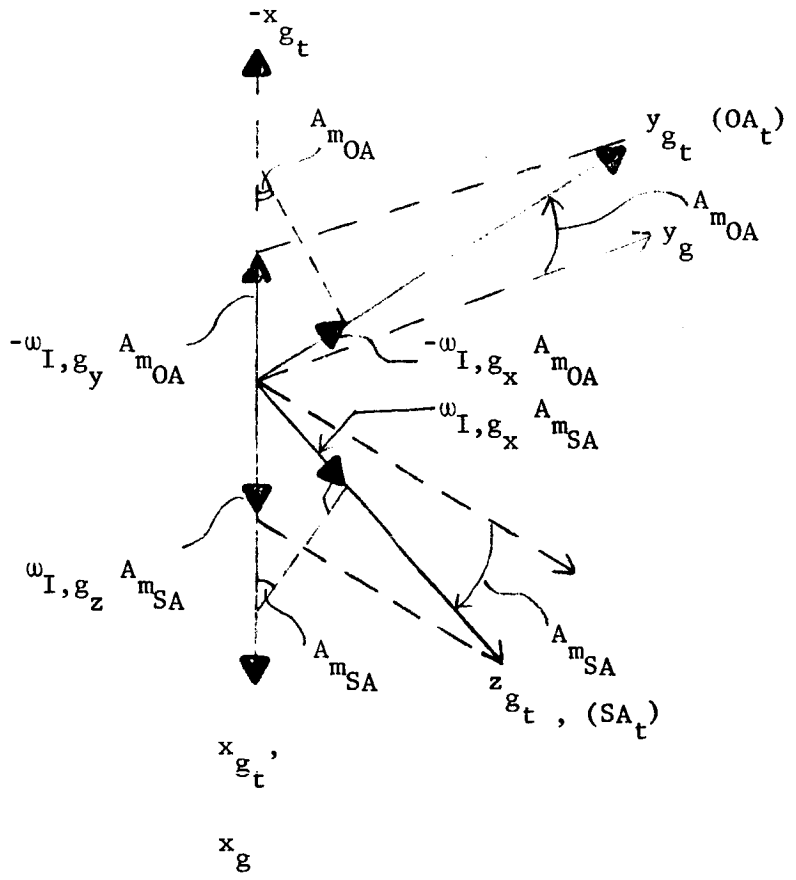

FIGURE E-3. COMPONENTS OF ω VECTOR

Using (13), (14), and (15) to rewrite (11)

$$\text{(a)}\quad \omega_{I,g_{x_t}} = (\omega_{I,ca_X} - \omega_{I,ca_Z} A_{ca,g}) + (\omega_{I,ca_Y} + \dot{A}_{ca,g}) A_{m_{OA}} + (\omega_{I,ca_Z} + \omega_{I,ca_X} A_{ca,g}) A_{m_{SA}}$$

$$\text{(b)}\quad \omega_{I,g_{y_t}} = (\omega_{I,ca_Y} + \dot{A}_{ca,g}) - \omega_{I,ca_Z} A_{m_{OA}} \qquad (16)$$

$$\text{(c)}\quad \omega_{I,g_{z_t}} = (\omega_{I,ca_Z} + \omega_{I,ca_Z} A_{ca,g}) + \omega_{I,ca_X} A_{m_{SA}}$$

From (16) (b), write

$$\dot{\omega}_{I,g_{y_t}} = (\dot{\omega}_{I,ca_Y} + \ddot{A}_{ca,g}) - \dot{\omega}_{I,ca_X} A_{m_{OA}} \tag{17}$$

Now, expanding (7) by using (16) (a,b,c) and (17) (to include effects of misalignment of gyro axes) we have

$$\omega_{I,g_{z_t}} \omega_{I,g_{x_t}} \cong \omega_{I,ca_X} \omega_{I,ca_Z}$$

and

$$- H\omega_{I,g_{x_t}} \cong - H\omega_{I,ca_X} + H\omega_{I,ca_Z} A_{ca,g} + H\omega_{I,ca_Y} A_{m_{OA}} - H\omega_{I,ca_Z} A_{m_{SA}}$$

treating

$$\omega_{I,ca_X} \omega_{I,ca_Z} >> \omega^2_{I,ca_X} A_{ca,g} ,$$

$$\omega_{I,ca_X} \omega_{I,ca_Z} >> \omega_{I,ca_X} \omega_{I,ca_Z} A_{m_{OA}} ,$$

and

$$\omega_{I,ca_X} \omega_{I,ca_Z} >> \omega_{I,ca_Z} A_{ca,g} .$$

Neglecting higher order terms, we then have

$$\left|\bar{M}_{app}\right|_{\perp\!\!\!\perp\ OA} = I_{OA}\,\dot{\omega}_{I,ca_Y} + I_{OA}\,\ddot{A}_{ca,g} + (I_{IA} - I_{SA})(\omega_{I,ca_X}\,\omega_{I,ca_Z})$$

$$- H\omega_{I,ca_X} + H\omega_{I,ca_Z}\,A_{ca,g} + H\omega_{I,ca_Y}\,A_{m_{OA}} - H\omega_{I,ca_Z}\,A_{m_{SA}} . \qquad (18)$$

For an imperfect single-degree-of-freedom (SDF) rate integrating gyroscope operating in a closed loop

$$\left|\bar{M}_{app}\right|_{\perp\!\!\!\perp\ OA} = -C_D\,\dot{A}_{ca,g} + M_{ERROR} + M_{TG} \qquad (19)$$

where:

M_{ERROR} = Error torques

M_{TG} = Applied torque from gyroscope

C_D = Viscous damping coefficient .

Now

$$M_{TG} = -A_{ca,g}\,S_{SG[A;e]}\,S_{EL[e;i]}\,S_{TG[i;M]} \triangleq -A_{ca,g}\,S_{Loop[A;M]} \qquad (20)$$

where:

$S_{SG[A;e]}$ = Sensitivity of the gyro signal generator, volts/degree

$S_{EL[e;i]}$ = Gain of the electronics, amperes/volt

$S_{TG[i;m]}$ = Sensitivity of the torque generator, dyne cm/ampere

$S_{Loop[A;m]}$ = Closed loop scale factor, dyne cm/degree .

The error torques are caused by imperfections in the construction of the gyroscope. The error sources are principally:

(1) Fixed torque due to flex lead and signal and torque generator reaction torques.

(2) Elastic restraint torque due to torque gradient proportional to output angle.

(3) Rigid pendulosity torques caused by the center of mass of the torque summing member being displaced from the gyro output axis.

(4) Elastic compliance torques caused by the deflection of the center of mass of the torque summing member when a specific force is applied.

Treating the compliance torques first, the elastic deflection, Δ, resolved along the principal gyro axes, SRA, IA, and OA, shown in Figure E-1 can be written as

$$\Delta_{SRA} = m[K_{SS}(sf)_{SRA} + K_{SI}(sf)_{IA} + K_{O}(sf)_{OA}] \tag{21}$$

$$\Delta_{IA} = m[K_{IS}(sf)_{SRA} + K_{II}(sf)_{IA} + K_{IO}(sf)_{OA}] \tag{22}$$

$$\Delta_{OA} = m[K_{OS}(sf)_{SRA} + K_{OI}(sf)_{IA} + K_{OO}(sf)_{OA}] \tag{23}$$

where K_{xy} = compliance coefficient due to a displacement along the x axis as a result of a specific force along the y axis.

The torque about OA resulting from the deflection Δ, of a unit mass m, and the specific force, sf, is then given by

$$M_c = m^2 [\Delta_{SRA}(sf)_{IA} - \Delta_{IA}(sf)_{SRA}] . \tag{24}$$

For an SDF gyro, Δ_{OA} should make no contribution to torque about the output axis and is therefore not considered further.

Substituting equations (21) and (22) into (24) one finds after combining terms that

$$M_c = m^2[(K_{SS} - K_{II})(sf)_{IA}(sf)_{SRA} + K_{SI}(sf)^2_{IA} - K_{IS}(sf)^2_{SRA} + K_{SO}(sf)_{OA}(sf)_{IA} - K_{IO}(sf)_{OA}(sf)_{SRA}] . \tag{25}$$

The torques due to mass unbalance along the spin reference and input axes can be expressed as

$$M_U = U_S(sf)_{IA} - U_I(sf)_{SRA} \tag{26}$$

where U_S, U_I = moment of mass unbalance about OA along + SRA and + IA.

With the addition of the fixed torque term R, elastic restraint torque $HEA_{ca,g}$, and a term to account for torque about OA due to the specific force along the output axis, $U_O(sf)_{OA}$, one now has the ten terms that make up the error torques of the SDF gyroscope based upon linear theory. Summing these terms, we have

$$M_{ERROR} = R + HEA_{ca,g} + U_S(sf)_{IA} - U_I(sf)_{SRA} + U_O(sf)_{OA}$$

$$+m^2 \left\{ \begin{array}{l} (K_{SS} - K_{II})(sf)_{IA}(sf)_{SRA} + K_{SI}(sf)^2_{IA} \\ -K_{IS}(sf)^2_{SRA} + K_{SO}(sf)_{OA}(sf)_{IA} - K_{IO}(sf)_{OA}(sf)_{SRA} \end{array} \right\} . \tag{27}$$

In terms of acceleration components (a_S, a_I, a_o) we have

$$M_{ERROR} = R + HEA_{ca,g} - U_S a_{IA} + U_I a_{SA} - U_O a_{OA} + m^2(K_{SS} - K_{II})a_{IA}a_{SA}$$

$$+ m^2 K_{SI} a_{IA}^2 - m^2 K_{IS} a_{SA}^2 + m^2 K_{SO} a_{OS} a_{IA} - m^2 K_{IO} a_{OA} - \tag{28}$$

Substituting for $|M_{app}|_{\perp\perp OA}$ in equating (18) we find that

$$\left\{ \begin{array}{l} -C_D \dot{A}_{ca,g} + HEA_{ca,g} + R - U_S a_{IA} + U_I a_{SA} - U_O a_{OA} \\ +m^2 \left[\begin{array}{l} (K_{SS} - K_{II}) a_{IA} a_{SA} + K_{SI} a_{IA}^2 \\ - K_{IS} a_{SA}^2 + K_{SO} a_{OA} a_{IA} - K_{IO} a_{OA} a_{SA} \end{array} \right] \\ - A_{ca,g} S_{Loop[A;M]} \end{array} \right\} = \left\{ \begin{array}{l} I_{OA} \dot{\omega}_{I,ca_Y} + I_{OA} \ddot{A}_{ca,g} - H\omega_{I,ca_X} \\ + (I_{IA} - I_{SA})(\omega_{I,ca_X} \omega_{I,ca_Z}) \\ + H\omega_{I,ca_Z} A_{ca,g} + H\omega_{I,ca_Y} A_{m_{OA}} \\ - H\omega_{I,ca_Z} A_{m_{SA}} \end{array} \right\} . \tag{29}$$

In guidance error analysis one is interested in the error in the angular rate measurement, so we must divide all terms by H, the angular momentum, to obtain angular rate. To avoid carrying through coefficients involving 1/H, we suggest the following definitions of which many are used by the Central Inertial Guidance Test Facility, Holloman AFB, New Mexico.

$$D_{FR} = \frac{R}{H} \qquad D_{UO} = \frac{U_O}{H} \qquad D_{KIS} = \frac{m^2 K_{IS}}{H}$$

$$D_{UI} = \frac{U_I}{H} \qquad D_{KM} = \frac{m^2 (K_{SS} - K_{II})}{H} \qquad D_{KSO} = \frac{m^2 K_{SO}}{H}$$

$$D_{US} = \frac{U_S}{H} \qquad D_{KSI} = \frac{m^2 K_{SI}}{H} \qquad D_{KIO} = \frac{m^2 K_{IO}}{H}$$

Now

$$\dot{\omega}_{I,ca_Y} = \omega_{OA} \quad , \quad \ddot{A}_{ca,g} = \ddot{\theta} \quad , \quad \dot{\omega}_{I,ca_X} = \omega_{IA} \quad ,$$

$$\omega_{I,ca_Y} = \omega_{OA} \quad , \quad \omega_{I,ca_Z} = \omega_{SA} \quad , \quad \dot{A}_{ca,g} = \dot{\theta} \quad ,$$

$$A_{ca,g} = \theta \quad .$$

Substituting and rearranging terms in Equation (29) we have

$$
\left\{
\begin{array}{l}
\omega_{IA} + E\theta \\
D_{FR} - D_{US}a_I + D_{UI}a_S - D_{UO}a_O \\
+ D_{K_M}a_S a_I + D_{KSI}a_I^2 \\
- D_{KIS}a_S^2 + D_{KSO}a_O a_I - D_{KIO}a_O a_S \\
- \frac{I_{OA}}{H}\dot{\omega}_{OA} - \left(\frac{I_{IA} - I_{SA}}{H}\right)\omega_{IA}\omega_{SA} \\
- \omega_{SA}\theta - \omega_{OA}A_{m_{OA}} + \omega_{SA}A_{m_{SA}}
\end{array}
\right\}
=
\begin{array}{l}
\frac{I_{OA}}{H}\ddot{\theta} + \frac{C_D}{H}\dot{\theta} \\
+ S_{Loop}[\theta;M]\frac{\theta}{H} \quad .
\end{array}
\qquad (30)
$$

As previously stated, we are interested in the error in the angular rate, so it is appropriate to separate those terms which contribute this error from the rate we are trying to measure, ω_{IA}. Table E-1 lists the error term symbols, forcing excitation, and some of the nomenclature associated with the terms. In addition, two errors not in Equation (30), coning and quantization, are listed.

We shall assume that the forcing excitations are made up of trajectory accelerations and angular rates and vibratory excitations. The vibratory excitations are caused by body bending and engine induced vibrations. We assume the angular vibration to be $\omega_{vib} = a\omega \sin \omega t$ and the linear vibration to be $a_{vib} = A\omega^2 \cos \omega t$. The linear vibration may be averaged by integration over one period:

$$\int_o^T A\omega^2 \cos \omega t \, dt = \frac{A\omega^2}{\omega}[\sin \omega t]_o^T = 0 \quad .$$

Similarly, for the linear vibration squared, we have:

$$\frac{1}{T}\int_o^T A^2 \omega^4 \cos^2 \omega t \, dt = \frac{A^2\omega^4}{T\omega}[1/2\ \omega t + 1/4 \sin 2\omega t]_o^T = \frac{A^2\omega^3}{T}[1/2\ \omega T] \quad .$$

Therefore, the following is true for the averages over one cycle

$$\overline{a_{vib}^2} = \frac{A^2\omega^4}{2} \quad , \qquad \overline{a_{vib}} = 0 \quad .$$

TABLE E-I. SINGLE DEGREE OF FREEDOM GYROSCOPES ANGULAR RATE ERROR SOURCES

Symbol	Forcing Excitation	Nomenclature
$S_{\frac{Loop}{H}[\theta;M]}$	θ	Rebalance Loop Scale Factor - includes signal and torque generator, Loop Transfer Function, and Wheel Speed Modulation Errors
D_{FR}	1	Fixed (Bias) Drift
D_{US}	a_I	Mass Unbalance along Spin Axis (SA) Drift
D_{UI}	a_S	Mass Unbalance along Input Axis (IA) Drift
D_{KM}	$a_S a_I$	Major Compliance (Anisoelastic) Drift
D_{KSI}	a_I^2	Spin Axis Compliance Drift
D_{KIS}	a_S^2	Input Axis Compliance Drift
D_{KSO}	$a_O a_I$	Spin Axis Compliance Drift
D_{KIO}	$a_O a_S$	Input Axis Compliance Drift
D_{UO}	a_O	Dump Term as defined by MIT Instrumentation Laboratory
$\frac{I_{OA}}{H}$	$\dot{\omega}_{OA}$	Output Axis Inertia (OA Angular Acceleration Error)
$\frac{(I_{IA} - I_{SA})}{H}$	$\omega_{IA}\omega_{SA}$	Anisoinertia
ω_{SA}	θ	Spin Axis Cross Coupling (Kinematic Rectification)
$A_{m_{OA}}$	ω_{OA}	Misalignment of OA with respect to IA
$A_{m_{SA}}$	ω_{SA}	Misalignment of SA with respect to IA
$\frac{E}{H}$	θ	Elastic Restraint
		Coning
		Quantization

It is easily shown that linear vibration contributes to gyroscope angular rate measurement error through the compliance drifts. Angular vibrations cause rectified drifts for those terms excited by angular rates.

For terms which involve cross coupling or the product of two accelerations such as $a_S a_I$, only those frequencies present in both a_S and a_I will yield a net contribution when averaged over many cycles.

$$\text{Let } a_I = A_I \omega_I^2 \cos(\omega_I t) \text{ and } a_A = A_S \omega_S^2 \cos(\omega_S t + \phi_{IS})$$

$$\overline{a_I a_S} = \frac{1}{T} \int_0^T A_I A_S \omega_I^2 \omega_S^2 \cos(\omega_I t) \cos(\omega_S t + \phi_{IS})\, dt$$

$$\text{Lim } T \to \infty$$

$$\overline{a_I a_S} = 0 \text{ if } \omega_I \neq \omega_S$$

$$\overline{a_I a_S} = \frac{A_I A_S \omega_I^4}{2} \cos \phi_{IS} \quad \text{if } \omega_I = \omega_S \ .$$

A similar procedure would apply for angular vibration. If it is assumed that the angular vibrations remain the same during a particular phase of the flight, then the rectified drift terms can be treated identically to a constant gyro drift.

SEAP presently contains the error in the torque generator scale factor (S_{TG}). The error in the rebalance loop scale factor also consists of the error in the signal generator (S_{GS}) and rebalance loop electronic scale factors (S_{EL}). These two terms' contribution to the loop scale factor error could be treated separately and then the root sum square of the three terms could be formed to find the overall effect of the rebalance loop scale factor errors.

An additional error in the measurement of ω_{IA} which may be included under scale factor error is the error in the gyro angular momentum, ΔH, caused by subjecting the gyro to angular rates about the spin axis. The resultant drift error as a function of time can be expressed as (Reference E5)

$$\frac{I_{sp} \Delta\Omega_s(t)}{H} = \frac{\mathcal{L}^{-1}[G(s)\ \omega_{SA}]}{\omega_{sp}}$$

where G(s) is of the form:

$$G(s) = \frac{s^2}{s^2 + k_1 s + k_2}$$

A constant rate about the spin axis would not cause a steady-state $\Delta\Omega_s$ to occur. Sinusoidal vibrations occurring about the spin axis and at the same frequency but phase shifted about the input axis cause rectified drift effects. This error source, sometimes referred to as spin speed modulation error, can contribute significant drift rates which are forced by the vehicle's angular vibration.

Addition of the four compliance terms as well as the dump term to SEAP poses no problem for the trajectory accelerations. The vehicles linear vibration spectrum must be known to determine the drifts due to effects of the vibration and the five gyroscope compliance coefficients.

For a constant body rate profile, no drift rate due to OA angular acceleration occurs, but a gimbal angle, $\theta = \frac{I_{OA}}{H} \omega_{OA}$, would be interpreted as the integral of a rate about IA. Therefore, compensation might be required. This compensation could be performed in either of two ways.(E5) If we assume the vehicle follows the nominal trajectory, the angular rate about each of the gyroscopes' output axes could be stored as a function of time in the computer and compensation accomplished. Alternatively, the rate about a gyroscope input axis collinear with another gyroscope output axis could be used by the computer to subtract the incorrect output angle due to this error.

The error due to anisoinertia is usually negligible for the nominal rate profile. Sinusoidal vibratory motions about the spin and input axes give rise to a rectified drift. The average value of this drift would be of the form

$$\left(\frac{I_{IA} - I_{SA}}{H}\right) \frac{ab\omega^2 \cos \phi}{2}$$

where $\omega_{IA} = a\omega \sin \omega t$ and $\omega_{SA} = b\omega \sin (\omega t + \phi)$.

Spin axis cross coupling primarily gives rise to kinematic rectification errors. If angular vibrations about IA occur at the same frequency as angular vibrations about SA, the resultant error has been called spin-input rectification. If angular vibrations at the same frequency occur about OA and SA, the resultant error has been called spin-output rectification. In a pulse torqued gyro, the dead zone of the float can also cause a rectified drift of the form $\frac{4}{\pi}\theta_d \frac{\omega a \cos \phi}{2}$ where $\theta = \frac{4}{\pi}\theta_d \sin \omega t$ and $\omega_{SA} = \omega a \sin (\omega t + \phi)$.(E5)

The elastic restraint of a gyroscope is easily measured and can be compensated. Therefore, this term can usually be neglected in navigation error analysis.

Coning has been discussed thoroughly in References E2, E4, E5, and E6. For a strapdown system mounted on a perfectly rigid body with infinitely tight gyro rebalance loops and negligible quantization error, no inherent geometric coning would occur if the data were processed with a perfect computer (infinite speed).

Bending and flexing of the IMU and vehicle structure does give rise to geometric coning errors which are usually neglected. In strapdown, coning motions about IA (ω_{SA} and ω_{OA} are sinusoidal and properly phased, $\omega_{IA} = 0$) and OA (ω_{SA} and ω_{IA} are sinusoidal and properly phased, $\omega_{OA} = 0$) cause cross coupling to occur through the spin axis cross coupling error term. The average drift rate for gyro geometric coning has been given as (Reference E6)

$$\omega_D = -\frac{1}{2} q_o r_o \omega \sin \zeta$$

where

q = amplitude of angular motion of gyro about its OA,

$\dot{q} = q_o \sin \omega t$,

r = amplitude of angular motion of gyro about its SA, and

$\dot{r} = r_o \sin (\omega t - \zeta)$.

Quantization error occurs for pulse rebalanced instruments because the output of the gyroscope is no longer $\theta = \frac{H}{C_D} \int_o^T \omega_{IA} \, dt$ but is the summation of $\Delta\theta$ pulses. This gives rise to errors in the computed direction cosines. Since this error is a system associated error, it will not be discussed further in this appendix.

Sensitivity of the gyroscope to thermal gradients, excitation variation, and external magnetic fields can be treated by preprocessing the appropriate error coefficient sensitivity times the expected magnitude of the variation and then taking the root sum square of the sensitivity terms for each coefficient and the uncertainty of the error coefficient. For example, let us assume that the sensitivity of D_{US} is 0.1 ($^\circ$/hr/g)/$^\circ$F, the uncertainty in D_{US} is 0.01 $^\circ$/hr/g and that the temperature can be controlled to 0.5° F. Therefore, $D_{US} = \sqrt{(0.1 \times 0.5)^2 + (0.01)^2} = 0.051^\circ$/hr/g. This value would be used as the error coefficient in the SEAP analysis.

APPENDIX E

REFERENCES

(E1) Roantree, J., and Kormanik, N., "A Generalized Design Criterion for Strapped-Down Inertial Sensor Loops", AIAA/JACC Guidance and Control Conference, August, 1966.

(E2) Farrell, J. L., "Performance of Strapdown Inertial Attitude Reference Systems", AIAA/JACC Guidance and Control Conference, August, 1966.

(E3) Thompson, J. A., and Unger, F. G., "Inertial Sensor Performance in a Strapped-Down Environment", AIAA/JACC Guidance and Control Conference, August, 1966.

(E4) Alongi, R. E., "Strapdown System Application Studies Related to a Surface to Surface Missile of 100 to 400 Nautical Miles", AIAA/JACC Guidance and Control Conference, August, 1966.

(E5) Levinson, Emanuel, "Aircraft, Missile, and Space Inertial Navigation", Chapter 5, Training Notes, Sperry Gyroscope Company, 1963.

(E6) Macomber, G. R., and Fernandez, M., "Inertial Guidance Engineering" pp 505-507, Prentice Hall, Inc., 1962, Englewood Cliffs, New Jersey.

APPENDIX F

TORQUED PENDULUM ACCELEROMETER ERROR MODEL

APPENDIX F

TORQUED PENDULUM ACCELEROMETER ERROR MODEL

INTRODUCTION

The error model contained in SEAP for accelerometers does not include those errors due to the dynamics of the instrument. A derivation for the torqued pendulum accelerometer (TPA) has been made to determine those terms which are not contained in SEAP.

DERIVATION

Applying Newton's second law of motion in rotational form to the rigid body with mass, m, depicted in Figure F-1, we have

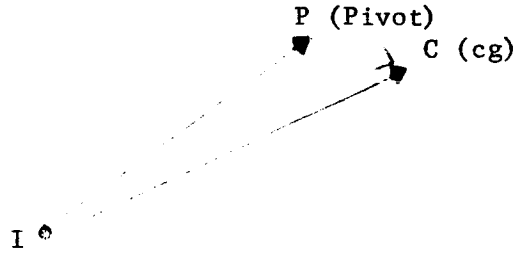

FIGURE F-1. PENDULUM

$$\left(\bar{R}_{PC} \times \bar{F}_{c_{ext}}\right) = \left(m\bar{R}_{PC} \times \ddot{\bar{R}}_{IP}\right) + \frac{d\bar{H}}{dt}\Big]_I \qquad (1)$$

where $\bar{F}_{c_{ext}}$ is an externally applied force at the center of gravity (cg). Now,

$$\bar{M}_{app} = \left(m\bar{R}_{PC} \times \ddot{\bar{R}}_{IP}\right) + \frac{d\bar{H}}{dt}\Big]_p + (\bar{\omega}_{I,P} \times \bar{H}) \quad . \qquad (2)$$

Let x_p, y_p, and z_p denote pendulum axes (chosen to coincide with the principal axes so that products of inertia vanish), and

$$\ddot{m\bar{R}}_{IP} \triangleq \bar{F}_P \Big]_I$$

(force of pivot on the body due to inertial acceleration of pivot). Then

$$\bar{R}_{PC} \times \bar{F}_P = \begin{vmatrix} \bar{i}_p & \bar{j}_p & \bar{z}_p \\ R_{PC_x} & R_{PC_y} & R_{PC_z} \\ F_{P_x} & F_{P_y} & F_{P_z} \end{vmatrix} = \begin{vmatrix} \bar{i}_p \left(R_{PC_y} F_{P_z} - R_{PC_z} F_{P_y}\right) \\ +\bar{j}_p \left(R_{PC_z} F_{P_x} - R_{PC_x} F_{P_z}\right) \\ +\bar{k}_p \left(R_{PC_x} F_{P_y} - R_{PC_y} F_{P_x}\right) \end{vmatrix} . \quad (3)$$

Now

$$\bar{H} = \bar{i}_p \left(I_x \omega_{I,P_x}\right) + \bar{j}_p \left(I_y \omega_{I,P_y}\right) + \bar{k}_p \left(I_z \omega_{I,P_z}\right) \quad (4)$$

and

$$\frac{d\bar{H}}{dt}\Big]_p = \bar{i}_p \left(I_x \dot{\omega}_{I,P_x}\right) + \bar{j}_p \left(I_y \dot{\omega}_{I,P_y}\right) + \bar{k}_p \left(I_z \dot{\omega}_{I,P_z}\right) . \quad (5)$$

Taking the cross product of $\bar{\omega}_{I,P}$ and $\bar{H}$, we have

$$\bar{\omega}_{I,P} \times \bar{H} = \begin{vmatrix} \bar{i}_p & \bar{j}_p & \bar{k}_p \\ \omega_{I,P_x} & \omega_{I,P_y} & \omega_{I,P_z} \\ I_x\omega_{I,P_x} & I_y\omega_{I,P_y} & I_z\omega_{I,P_z} \end{vmatrix} = \begin{vmatrix} \bar{i}_p (-) \left(I_y - I_z\right) \omega_{I,P_y} \omega_{I,P_z} \\ +\bar{j}_p (-) \left(I_z - I_x\right) \omega_{I,P_z} \omega_{I,P_x} \\ +\bar{k}_p (-) \left(I_x - I_y\right) \omega_{I,P_x} \omega_{I,P_y} \end{vmatrix} . \quad (6)$$

Using (3), (5), and (6) to expand (2), treating R_{PC_z} as a principal axis ($R_{PC_x} = R_{PC_y} = 0$), and constraining pendulum motion so that only the OA (y) component of torque is of concern, we have

$$M_{app_y} \equiv M_{app_{OA}} = (R_{PC_z} F_{P_x}) + I_y \dot{\omega}_{I,P} - (I_z - I_x) \omega_{I,P_z} \omega_{I,P_z} \quad (7)$$

Making a coordinate transformation from pendulum axes (x,y,z) to case axes (X,Y,Z) by using a positive displacement angle $A_{ca,P}$ (i.e., rotation about +Y) as shown in Figure F-2, gives

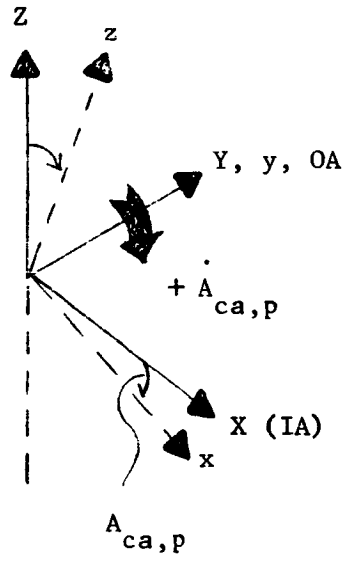

FIGURE F-2. COORDINATE TRANSFORMATION

$$i_x = i_X \cos A_{ca,p} + 0 - k_z \sin A_{ca,p}$$

$$j_y = 0 + j_Y + 0 \quad (8)$$

$$k_y = k_X \sin A_{ca,p} + 0 + k_z \cos A_{ca,p}$$

or

$$\begin{bmatrix} \omega_{I,P_x} \\ \omega_{I,P_y} \\ \omega_{I,P_z} \end{bmatrix} = \begin{bmatrix} \cos A_{ca,p} & 0 & -\sin A_{ca,p} \\ 0 & 1 & 0 \\ \sin A_{ca,p} & 0 & \cos A_{ca,p} \end{bmatrix} \begin{bmatrix} \omega_{I,ca_X} \\ \omega_{I,ca_Y} \\ \omega_{I,ca_Z} \end{bmatrix} .$$

Let us treat $\cos A_{ca,p} \equiv 1$ and $\sin A_{ca,p} \equiv A_{ca,p}$. Then

$$\omega_{I,P_x} \cong (\omega_{I,ca_X} - \omega_{I,ca_Z} A_{ca,p}) ,$$

$$\omega_{I,P_y} \cong (\omega_{I,ca_Y} + \dot{A}_{ca,p}) , \text{ and} \qquad (9)$$

$$\omega_{I,P_z} \cong (\omega_{I,ca_Z} + \omega_{I,ca_X} A_{ca,p}) .$$

Including effects of a "small misalignment angle of the pendulous accelerometer's OA and the pendulum axis, PA (i.e., $A_{m_{OA}}$ and $A_{m_{PA}}$, shown* arbitrarily as angles developed by + rotations) gives

$$\omega_{I,P_{x_t}} = \omega_{I,P_x} - \omega_{I,P_y} A_{m_{OA}} + \omega_{I,P_z} A_{m_{PA}}$$

$$\omega_{I,P_{y_t}} = \omega_{I,P_y} - \omega_{I,P_x} A_{m_{OA}} \qquad (10)$$

$$\omega_{I,P_{z_t}} = \omega_{I,P_z} + \omega_{I,P_x} A_{m_{PA}} .$$

* See Figure E-2, Appendix E, page E-6.

Using (9) in (10) gives

$$\omega_{I,P_{x_t}} \cong (\omega_{I,ca_X} - \omega_{I,_{ca_Z}} A_{ca,p}) - A_{m_{OA}} (\omega_{I,ca_Y}) + A_{m_{PA}} (\omega_{I,ca_Z})$$

$$\omega_{I,P_{y_t}} \cong (\omega_{I,ca_Y} + \dot{A}_{ca,p}) - A_{m_{OA}} (\omega_{I,ca_X}) \tag{11}$$

$$\omega_{I,P_{z_t}} \cong (\omega_{I,ca_Z} + \omega_{I,ca_X} A_{ca,p}) + A_{m_{PA}} (\omega_{I,ca_X}) .$$

Now

$$\dot{\omega}_{I,P_{y_t}} = (\dot{\omega}_{I,ca_Y} + \ddot{A}_{ca,p}) - A_{m_{OA}} \dot{\omega}_{I,ca_X} . \tag{12}$$

Also,

$$F_{P_{x_p}} \equiv (F_{P_X} - F_{P_Z} A_{ca,p}) . \tag{13}$$

So,

$$F_{P_{x_t}} \equiv (F_{P_X} - F_{P_Z} A_{ca,p}) - A_{m_{OA}} (F_{P_Y}) + A_{m_{PA}} (F_{P_Z}) .$$

Furthermore,

$$R_{pc_{z_t}} \cong R_{pc_Z} ,$$

$$\omega_{I,P_{z_t}} \cdot \omega_{I,P_{x_t}} = (\omega_{I,ca_Z} + \omega_{I,ca_Z} A_{ca,p}) + A_{m_{PA}} (\omega_{I,ca_X}) \cdot$$

$$\left[(\omega_{I,ca_X} - \omega_{I,ca_Z} A_{ca,p}) - (A_{m_{OA}} \omega_{I,ca_Y} + A_{m_{PA}} \omega_{I,ca_Z})\right] ,$$

$$\omega_{I,P_{z_t}} \omega_{I,P_{x_t}} \cong \omega_{I,ca_X} \omega_{I,ca_Z} + \omega^2_{I,ca_X} (A_{ca,p} + A_{m_{PA}}) - \omega^2_{I,ca_Z} A_{ca,p}$$

$$- \omega_{I,ca_Y} \omega_{I,ca_Z} A_{m_{OA}} + \omega^2_{I,ca_Z} A_{m_{PA}} , \tag{15}$$

$$\omega_{I,P_{z_t}} \omega_{I,P_{x_t}} \cong \omega_{I,ca_X} \omega_{I,ca_Z} + A_{m_{PA}} (\omega^2_{I,ca_X} + \omega^2_{I,ca_Z})$$

$$- A_{m_{OA}} (\omega_{I,ca_Y} \omega_{I,ca_Z}) + A_{ca,p} (\omega^2_{I,ca_X} - \omega^2_{I,ca_Z}) ,$$

and

$$R_{pc_{z_t}} F_{p_{x_t}} = R_{pc_Z} (F_{p_X} - F_{p_Z} A_{ca,p} - F_{p_Y} A_{m_{OA}} + F_{p_Z} A_{m_{PA}}) . \tag{16}$$

Then, (7) becomes [using (16), (15), and (12)]

$$M_{app_{OA}} = R_{pc_Z} \left[F_{p_X} - F_{p_Z} A_{ca,p} - F_{p_Y} A_{m_{OA}} + F_{p_Z} A_{m_{PA}}\right] + I_{OA} \dot{\omega}_{I,ca_Y} + I_{OA} \ddot{A}_{ca,p}$$

$$+ (I_{IA} - I_{PA}) \left[\omega_{I,ca_X} \omega_{I,ca_Z} + A_{m_{PA}} (\omega^2_{I,ca_X} + \omega^2_{I,ca_Z}) - A_{m_{OA}} (\omega_{I,ca_Y} \omega_{I,ca_Z}) \right. \tag{17}$$

$$\left. + A_{ca,p} (\omega_{I,ca_X} - \omega_{I,ca_Z})\right] .$$

Equation (17) equates externally applied torques to inertia reaction torques arising from inertial acceleration of the pivot and angular motion with respect to inertial space.

Assuming the effects of Earth's gravitational field [$\bar{g} = \bar{G} - \bar{\omega}_{I,E} \times (\bar{\omega}_{I,E} \times \bar{R}_{EC})$], to be included in the $\bar{\bar{F}}_p$ terms, ($F_{p_X} \equiv m\ddot{R}_{IP_X} \equiv ma_{p_X}$) we than have

$$M_{damp} \pm M_{t_g} \pm (I)M = [\text{right hand side of (17)}] \tag{18}$$

or

$$I_{OA}\ddot{A}_{ca,p} + C_d\dot{A}_{ca,p} = mR_{pc_Z}\left[-a_{p_{IA}} + a_{p_{PA}}A_{ca,p} + a_{p_{OA}}A_{m_{OA}} - a_{p_{PA}}A_{m_{PA}}\right]$$

$$-I_{OA}\dot{\omega}_{I,ca_{OA}} - (I_{IA} - I_{PA})\left[\omega_{I,ca_{IA}}\omega_{I,ca_{PA}} + A_{m_{PA}}(\omega^2_{I,ca_{IA}} + \omega^2_{I,ca_{PA}}) \right. \tag{19}$$

$$\left. + A_{ca,p}(\omega^2_{I,ca_{IA}} - \omega^2_{I,ca_{PA}}) - \omega_{I,ca_{PA}}\omega_{I,ca_{OA}}A_{m_{OA}}\right] - M_{t_g} \pm (I)M$$

where:

(I)M - inaccuracy torques

(I)M $\triangleq$ (E)M + (U)M

(E)M - error torques (deterministic or average)

(U)M - uncertainty torques.

Let

$$M_{tg} = \left[S_{tg_{[i;m]}} \cdot S_{sm_{[e:i]}} \cdot S_{sg_{[A;e]}} \cdot A_{ca,p}\right] \tag{20}$$

M - torque
tg - torque generator
S - sensitivity
i - current
sm - signal modifier
sg - signal generator
e - volts
A - angle
ca - case
p - pendulum

Tests which provided an understanding of the error sources within accelerometers were followed by different and improved designs to meet demands for long-term stability, greater accuracy, and wider dynamic ranges. One particular source of difficulty which tends to limit single-axis performance is output-axis friction. A frictionless restraint on the OA is desired, but is most difficult to achieve when cross-axis suspension must be sufficiently stiff. The torqued pendulous accelerometer (TPA) is an example of improved design which forced that difficulty into submission.

Nonlinearities of the restraint torque device (torque generator) can prove troublesome, and require high loop gain so that it functions near a null position (i.e., the pendulous element displacement angle should be very close to zero). Resulting error is a function of "g" since it increases as torque current increases.

Precision balance is a design requirement of the TPA since an uncertainty in balance contributes to instrument error through the scale factor. Also, scale factor instability, while predictable to some extent, can produce an intolerable uncertainty.

Null instability is another source of instrument error which can limit the accelerometer's performance. The uncertainty in output resulting from null shift has long been one of the foremost concerns when greater accuracy was specified since it is very difficult to control or predict. Uncertainty in knowing exactly where the instrument axes are (misalignment) with respect to each other leads to errors in the output when cross-axis acceleration and angular velocity in space occur.

Pendulum inertias about the instrument's input axis and the pendulous-element axis will, if unequal, cause output errors.

The sources of uncertainty in an accelerometer are represented in an empirical equation which assumes them to be sensitive to powers of acceleration (i.e., zero power, 1st power, 2nd power, etc.). Test results, then, showing large and repeatable characteristic values ascribed to definite physical factors within the instrument are used to affect an improved design (i.e., through modification or redesign).

In terms of specific force, to which all accelerometers are designed to respond, with

$x \sim$ input axis (IA)

$y \sim$ output axis (OA)

$z \sim$ pendulous axis (PA), and

(sf) due to acceleration $\triangleq -a \equiv \frac{\text{Force}}{\text{Mass}}$

$$(\text{Output-Input}) \triangleq (E)sf_{ind.} = K_0 + K_1 (sf)_{IA} + K_2 (sf)^2_{IA} + K_3 (sf)^3_{IA}$$
$$+ K_4 (sf)_{OA} + K_5 (sf)_{PA} \qquad (21)$$
$$+ K_6 (sf)_{IA} (sf)_{OA} + K_7 (sf)_{IA} (sf)_{PA} + \ldots$$

The accelerometer unit (au) output varies in form with the design of the instrument, as the units of the coefficients vary accordingly. Let the error coefficients be referred to as "Instrument Output Units", IOU, and be defined as follows:

K_0 - bias (in IOU's)

K_1 - scale factor (in IOU/g)

K_2 - second order nonlinearity effect (in IOU/g^2)

K_3 - third order nonlinearity effect (in IOU/g^3)

K_4, K_5 - cross-axis acceleration sensitivities (in IOU/g)

K_6, K_7 - cross-coupling non-linear effects (in IOU/g^2)

(The model can be expanded to include higher order cross-axis acceleration and cross-coupling nonlinearities if necessary.) The performance function for an ideal TPA [from (19)] is

$$\frac{I_{OA}}{C_d} \ddot{A}_{ca,p} + \dot{A}_{ca,p} = \left(\frac{mR_{pc_Z}}{C_d}\right)\left(-a_{in}\right)_{IA} \equiv M_{app}/C_d \qquad (22)$$

$$A_{ca,p}(s) = \frac{mR_{pc_Z}/C_d}{s\left[\left(\frac{I_{OA}}{C_d}\right) s + 1\right]} (-a_{in}) \qquad (23)$$

As a pendulum displacement, $A_{ca,p}$, develops, it is detected electrically (signal generator), and the signal produced is proportional to the angle's magnitude. To use this signal for actuating a torquer, it is first modified (amplified and conditioned) and then becomes the input current to the torque generator. All are sources of error and uncertainty.

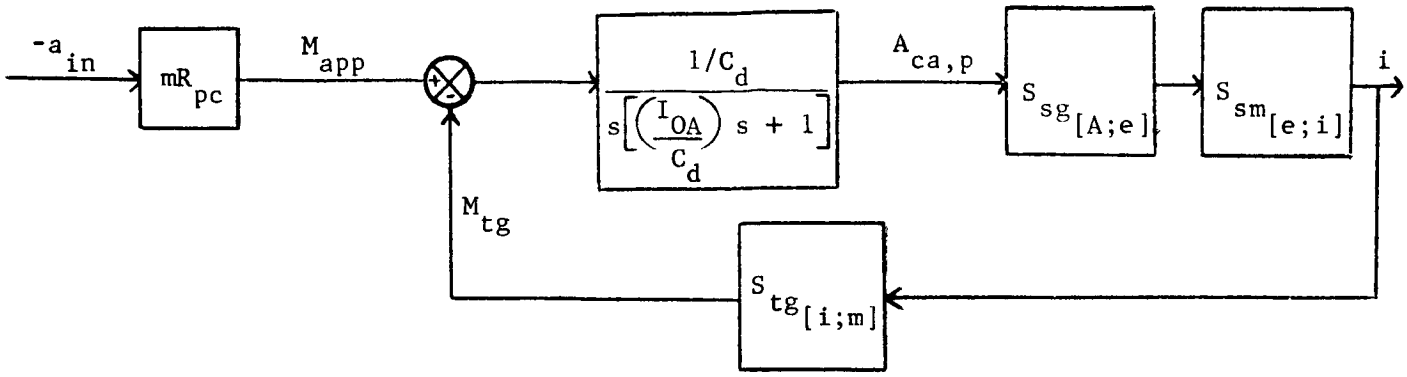

Let: $S_{sg_{[A;e]}} \; S_{sm_{[e;i]}} \; S_{tg} \triangleq S_{pA_{[A;i]}}$ (24)

then

$$i_{tg}(s) = \frac{\left(mR_{pc}/S_{tg}\right)(-a_{in})}{\left(\frac{I_{OA}}{S_{pA}}\right)s^2 + \left(\frac{C_d}{S_{pA}}\right)s + 1} \qquad (25)$$

The kinematic equation of motion for the TPA (Equation 17) shows that false or erroneous contributions to acceleration occur when a pendulous element angle develops, when misalignment of axes is considered, and when case angular motion exists. The errors due to case rotation are likely to be exaggerated (compared with the stabilized platform) for the strapped-down inertial measurement. These error contributors (some of which may be found insignificant) may be termed as follows:

(a) $(mR_{pc_Z})(a_{p_{PA}} A_{ca,p} + a_{p_{OA}} A_{m_{OA}} - a_{p_{PA}} A_{m_{PA}})$ -- these error torques are due to cross-axis (PA and OA) accelerations with the magnitudes being dependent on pendulous element displacement angle and misalignment of instrument axes with respect to the input axis (in this case). It has been shown* that when the forcing acceleration is vibratory, a non-zero average torque results which falsifies the output. This affect is called vibropendulous and has the form

$$\left[\frac{a_{p_{PA}}}{2} A_{ca,p} \cos A_{(\text{Pendulum phase lag angle})}\right]$$

* "Strapdown System Application Studies Related to a Surface to Surface Missile of 100 to 400 Nautical Miles", by R. E. Alongi, AIAA/JACC Guidance and Control Conference, August, 1966.

(The pendulum axis of the TPA should be orthogonal to the thrust axis to help minimize this error effect.)

(b) $I_{OA}\dot{\omega}_{I,ca_{OA}}$ -- this torque contributes error when OA angular velocity is changing. For example, a changing roll rate would cause erroneous outputs in the pitch and yaw accelerometers. Thus, this effect is usually called output-axis coupling error or OA rotation effect.

(c) $(I_{IA} - I_{PA})(\omega_{I,ca_{IA}}\omega_{I,ca_{PA}})$ -- this is known as the anisoinertia effect which occurs for simultaneous angular rates about the IA and PA. The product of angular rates causes a non-zero average error for sinusoidal motion about these axes.

(d) $(I_{IA} - I_{PA})\left[(\omega^2_{I,ca_{IA}} + \omega^2_{I,ca_{PA}})\, A_{m_{PA}} + (\omega^2_{I,ca_{IA}} - \omega^2_{I,ca_{PA}})\, A_{ca,p} - (\omega_{I,ca_{IA}}\omega_{I,ca_{OA}})\, A_{m_{OA}}\right]$

These error torques are due to cross-coupling of angular rates. Their magnitudes depend on pendulous element displacement angle and misalignment of the instrument axes with respect to the input axis. They produce errors called rotational cross-coupling.

In addition to the kinematically derived error sources, other error producing effects are known to be present.

(e) $(\omega^2_{I,ca_{OA}} + \omega^2_{I,ca_{PA}})\, R_{(cg_{veh} - cg_{TPA})}$ -- this error in output acceleration is due to the separation of the cg of the TPA and the cg of the vehicle whose acceleration is being measured. Treating this distance as fixed, angular motion (and vibrations) results in centripetal and tangential acceleration components. The error depends on the separation distance, so it is not a characteristic of instrument imperfection. It is termed a size effect.

(f) $\left(a_{IP_x} A_{(Y_0 - Y_1)} - a_{IP_Y} A_{(X_0 - X_1)}\right)$ or $\left(\frac{a_{P_{PA}}}{2} A_{ca,p} \cos A_{(\text{pendulum phase lag angle})}\right)$

The strapdown platform experiences the same spatial motions as the vehicle, while the computer maintains the space reference coordinates. Thus, for vehicle acceleration (linear vibration) along a given axis, the remaining two reference axes are displaced in accordance with the vibratory input. So far, things are as they should be, but if an angular vibration (of like frequency) occurs about either of the linearly displaced axes, the product of these motions results in rectified acceleration along an axis perpendicular to the two

linearly displaced axes. This effect is called sculling. (Note that it is not attributable to instrument imperfection.)

The complete performance equation becomes

$$
\begin{aligned}
I_{OA}\ddot{A}_{ca,p} + C_d\dot{A}_{ca,p} + kA_{ca,p} = mR_{pc_Z}\Big[-a_{p_{IA}} + a_{p_{PA}}A_{ca,p} + a_{p_{OA}}A_{m_{OA}} - a_{p_{PA}}A_{m_{PA}}\Big] \\
- I_{OA}\dot{\omega}_{I,ca_{OA}} + (I_{PA} - I_{IA})\Big[\omega_{I,ca_{IA}}\omega_{I,ca_{PA}} \\
+ A_{m_{PA}}(\omega^2_{I,ca_{IA}} + \omega^2_{I,ca_{PA}}) + A_{ca,p}(\omega^2_{I,ca_{IA}} - \omega^2_{I,ca_{PA}}) \\
- \omega_{I,ca_{PA}}\omega_{I,ca_{OA}}A_{m_{OA}}\Big] + K_0 + K_1(-a_{IA}) + K_2(-a_{IA})^2 \\
+ K_3(-a_{IA})^3 + K_4(-a_{OA}) + K_5(-a)_{PA} + K_6(-a_{IA})(-a_{OA}) \\
+ K_7(-a_{IA})(-a_{PA})
\end{aligned}
\tag{28}
$$

Table F-I lists the error term symbols, forcing excitation, and some of the nomenclature associated with the terms.

TABLE F-I. SUMMARY OF TORQUED PENDULUM ACCELEROMETER ERROR SOURCES

Symbol	Forcing	Nomenclature
$\frac{1}{P}$	$\left(a_{p_{PA}} A_{ca,p}\right), \left(a_{p_{OA}} A_{m_{OA}}\right), \left(a_{p_{PA}} A_{m_{PA}}\right)$	Error in the indicated acceleration output due to vibropendulous effect. (Vibropendulous Error)
$\frac{I_{OA}}{P}$	$\dot{\omega}_{I,ca_{OA}}$	Error in the indicated acceleration output due to changing case rate about the OA. (Output Axis Coupling Error)
$\frac{I_{IA} - I_{PA}}{P}$	$(\omega_{I,ca_{IA}} \omega_{I,ca_{PA}})$	Error in the indicated acceleration output due to unequal inertias. (Anisoinertia Error)
$\frac{I_{IA} - I_{PA}}{P}$	$\left[(\omega^2_{I,ca_{IA}} + \omega^2_{I,ca_{PA}}) A_{m_{PA}} + (\omega^2_{I,ca_{IA}} - \omega^2_{I,ca_{PA}}) A_{ca,p} - (\omega_{I,ca_{IA}} \omega_{I,ca_{OA}}) A_{m_{OA}}\right]$	Error in the indicated acceleration output due to unequal inertias, pendulous element displacement angle, and misalignment of instrument axes. (Rotational Cross Coupling Error)
	$(\omega^2_{I,ca_{OA}} + \omega^2_{I,ca_{PA}}) R_{(cg_{veh} - cg_{TPA})}$	Error in the indicated acceleration output due to a separation distance between the vehicle cg and the instruments cg. (Size Effect Error)
	$\frac{a_{p_{PA}} A_{ca,p}}{2} \cos A_{(\text{pendulum phase lag angle})}$	Error in the indicated acceleration output due to linear vibration along one axis and angular vibration about an axis perpendicular to that axis. (Sculling Effect Error)
K_0	1	Bias Error (independent of input acceleration). (IOU -- Instrument Output Units)
K_1	$(sf)_{IA}$	Scale Factor Error (varies linearly with acceleration). (IOU/g)

TABLE F-I. SUMMARY OF TORQUED PENDULUM ACCELEROMETER ERROR SOURCES (Continued)

Symbol	Forcing	Nomenclature
K_2	$(sf)^2_{IA}$	Nonlinearity due to second order effects. (IOU/g^2)
K_3	$(sf)^3_{IA}$	Nonlinearity due to third order effects. (IOU/g^3)
K_4	$(sf)_{OA}$	Cross-axis acceleration sensitivity. (IOU/g)
K_5	$(sf)_{PA}$	Cross-axis acceleration sensitivity. (IOU/g)
K_6	$(sf)_{IA}(sf)_{OA}$	Cross coupling nonlinear effect. (IOU/g^2)
K_7	$(sf)_{IA}(sf)_{PA}$	Cross coupling nonlinear effect. (IOU/g^2)

DEFINITION OF TERMS

$\bar{R}_{pc}$	Position vector, from pivot to the cg
$\bar{F}_{c_{ext}}$	Vector resultant of all external forces acting through the cg (center of gravity)
m	Mass of the accelerometer unit
$\ddot{\bar{R}}_{IP}$	The inertial acceleration of the pivot, P
$\bar{F}_p\rfloor_I$	Force of the pivot on the body due to inertial acceleration of the pivot
$\bar{i}_p$, $\bar{j}_p$, $\bar{k}_p$	Represent unit vectors along pendulum axes, x,y, and z, respectively
R_{pc_x},R_{pc_y},R_{pc_z}	Components of $\bar{R}_{pc}$ along pendulum axes
$\bar{H}$	Vector angular momentum of the body referred to the pivot point and based on inertial velocity
I_x, I_y, I_z	Moments of inertia of the pendulous body about pendulum axes, x, y, and z
ω_{I,p_x},ω_{I,p_y},ω_{I,p_z}	Angular velocity components of the pivot with respect to inertial space, in pendulum axes
M_{app}	Applied torque
OA	Output axis
IA	Input axis
PA	Pendulous element axis (or pendulous arm)
a	Acceleration
ca	Case

DEFINITION OF TERMS (Continued)

X,Y,Z	Case fixed axes
$A_{ca,p}$	Angle of the pendulous element displacement with respect to a case reference axis
$\omega_{I,ca_X}, \omega_{I,ca_Y}, \omega_{I,ca_Z}$	Components of angular velocity of the case with respect to inertial space, in case fixed coordinates
$A_{m_{OA}}$	Angle of misalignment of the pendulous body's output axis (with respect to OA reference fixed to the case), arbitrarily represented as a positive rotation about the input axis reference
$A_{m_{PA}}$	Angle of misalignment of the pendulous element axis (with respect to the pendulous axis reference fixed to the case), arbitrarily represented as a position rotation about the OA reference
$\bar{g}$	Vector acceleration due to gravity
$\bar{G}$	Earth's gravitational field vector
$\bar{\omega}_{I,E}$	Earth's angular velocity with respect to inertial space
$\bar{R}_{EC}$	Defined as a position vector from Earth's center to location of pendulous body's cg
M_{damp}	Torque due to viscous damping
M_{tg}	Torque developed by the torque generator
(I)M	Inaccuracy torque
(E)M	Error torque (deterministic or average portion of the total inaccuracy)
(U)M	Uncertainty torque (random portion of the total inaccuracy)
(I)M $\triangleq$ (E)M + (U)M	$\triangleq$ -- Symbol meaning "defined as"

DEFINITION OF TERMS (Continued)

$S_{tg_{[i;m]}}$	Sensitivity of the torque generator for current (i) input and torque (m) output
$S_{sm_{[e;i]}}$	Sensitivity of the signal modifier for volts input and current current output
$S_{sg_{[A;e]}}$	Sensitivity of the signal generator for angle input and volts output
k	An "elastic restraint" coefficient defined as the product $(S_{tg} S_{sm} S_{sg})$
TPA	Torqued Pendulous Accelerometer
(sf)	Specific force, defined as (-a) $\equiv \frac{\text{Force}}{\text{Mass}}$
ind	Indicated
IOU	Instrument Output Units
K_0 through K_7	Accelerometer error coefficients (see Table C-1)
Veh	Vehicle

APPENDIX G

NEW TECHNOLOGY

APPENDIX G

NEW TECHNOLOGY

During the period covered, no new concepts were conceived or first reduced to practice.